



**SOLVENT EXCHANGE AND TRANSFORMATION OF *IN SITU* FORMING  
MICROPARTICLES AND GELS COMPRISING DOXYCYCLINE HYCLATE USING  
SHELLAC AS MATRIX FORMER**



**By  
Miss Pitsiree Praphanwittaya**

**A Thesis Submitted in Partial Fulfillment of the Requirements for the Degree  
Master of Pharmacy Program in Pharmaceutical Sciences  
Graduate School, Silpakorn University  
Academic Year 2015  
Copyright of Graduate School, Silpakorn University**

**SOLVENT EXCHANGE AND TRANSFORMATION OF *IN SITU* FORMING  
MICROPARTICLES AND GELS COMPRISING DOXYCYCLINE HYCLATE USING  
SHELLAC AS MATRIX FORMER**



By  
Miss Pitsiree Praphanwittaya

**A Thesis Submitted in Partial Fulfillment of the Requirements for the Degree  
Master of Pharmacy Program in Pharmaceutical Sciences  
Graduate School, Silpakorn University  
Academic Year 2015  
Copyright of Graduate School, Silpakorn University**

การแลกเปลี่ยนตัวทำละลายและการก่อตัวเป็นไมโครปาร์ติเคิลและเจลชนิดก่อตัวเองที่บรรจุ  
ยาดีออกซีไซคลินไฮโดรคลอไรด์โดยใช้เซลล์เป็นสารก่อเมทริกซ์



วิทยานิพนธ์นี้เป็นส่วนหนึ่งของการศึกษาตามหลักสูตรปริญญาเภสัชศาสตรมหาบัณฑิต  
สาขาวิชาวิทยาการทางเภสัชศาสตร์  
บัณฑิตวิทยาลัย มหาวิทยาลัยศิลปากร  
ปีการศึกษา 2558  
ลิขสิทธิ์ของบัณฑิตวิทยาลัย มหาวิทยาลัยศิลปากร

The Graduate School, Silpakorn University has approved and accredited the Thesis title of “Solvent exchange and transformation of *in situ* forming microparticles and gels comprising doxycycline hyclate using shellac as matrix former” submitted by Miss Pitsiree Praphanwittaya as a partial fulfillment of the requirements for the degree of Master in Pharmaceutical Sciences

.....  
(Associate Professor Panjai Tantatsanawong, Ph.D.)  
Dean of Graduate School  
...../...../.....

The Thesis Advisor

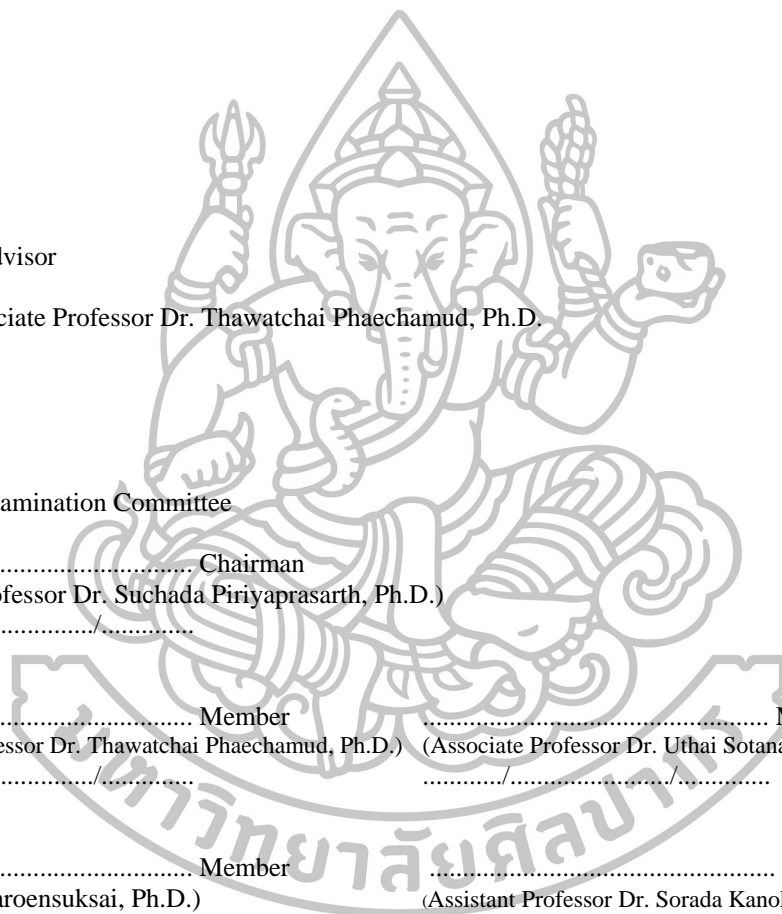
Associate Professor Dr. Thawatchai Phaechamud, Ph.D.

The Thesis Examination Committee

..... Chairman  
(Associate Professor Dr. Suchada Piriyaprasarth, Ph.D.)  
...../...../.....

..... Member ..... Member  
(Associate Professor Dr. Thawatchai Phaechamud, Ph.D.) (Associate Professor Dr. Uthai Sotanaphun, Ph.D.)  
...../...../.....

..... Member ..... Member  
(Dr. Purin Charoensuksai, Ph.D.) (Assistant Professor Dr. Sorada Kanokpanont, Ph.D.)  
...../...../.....



550705: MAJOR: PHARMACEUTICAL SCIENCES

KEY WORD: SOLVENT EXCHANGE / *IN SITU* FORMING GELS / *IN SITU* FORMING  
MICROPARTICLES / BLEACHED SHELLAC

PITSIREE PRAPHANWITTAYA: SOLVENT EXCHANGE AND TRANSFORMATION OF  
*IN SITU* FORMING MICROPARTICLES AND GELS COMPRISING DOXYCYCLINE HYCLATE  
USING SHELLAC AS MATRIX FORMER. THESIS ADVISOR: ASSOC.PROF. THAWATCHAI  
PHAECHAMUD, Ph.D. 156 pp.

Solvent exchange is the diffusion between solvent efflux and water influx at specific site. *In situ* forming gel exhibits a sol-to-gel phase transition after contact with aqueous fluid whereas *in situ* microparticle (ISM) observes transformation of emulsion droplets into the solid particles. Phase separation is the main strategy of these systems, and it undergoes the prompt changes in solubility of polymer in response to solvent exchange. This research purposed to better comprehend the behavior of solvent (e.g. Dimethyl sulfoxide (DMSO), *N*-methyl-2-pyrrolidone (NMP) and 2-pyrrolidone (PYR)) state in bleached shellac from preparation process to the entire phase separation of *in situ* forming microparticles and gel. The formulations employed the *in situ* forming gel as an internal phase of ISM, and emulsion was achieved by mixing the *in situ* forming gel with the external phase made from GMS and olive oil. In preparation process, the parameters such as pH, solubility parameter, density, interfacial tension and phase separation rate of emulsion compositions were investigated. During the phase separation, the physical characteristics were examined for the three phases according to exposure time. 1) Before (morphology of o/o emulsion and its droplet size, viscosities, viscoelasticity and thermal analysis). 2) During (transformation of sol to microparticles, solvent and drug releases, *in vitro* degradation, water diffusion rate and solvent diffusion). 3) After (texture analysis, XRD pattern and SEM microphotograph). Bleached shellac dissolved in solvents via strongly hydrogen bonding and van der Waal forces. *In situ* forming gel using NMP as solvent could not fabricate into an emulsion because NMP was partial miscible with olive oil. The solubility parameter could be in rank of the solvent order as following: NMP > DMSO > PYR. NMP was described as the best “good solvent”. This parameter related to viscosities, viscoelasticity and thermal analysis. Additionally, PYR itself was more viscous than DMSO and NMP, respectively. There are four crucial steps of phase separation. Firstly, water flowed into the system with different rate in rank of the solvent order as following: DMSO > NMP > PYR. This water permeation decreased the solubility of bleached shellac, and it then precipitated. Secondly, solvent and drug diffused out in few minutes later. The diffusion rate of all species was presented in term of solvent applied in formulation as DMSO > NMP > PYR. PYR formula had the slowest release rate of solvent and drug because solvent itself and its systems were higher viscous. Whereas, all diffusion profiles from DMSO and NMP systems were governed by solubility parameter. Thirdly, pores were supplied with water and solvent fluxes. The size and density of pores were increased by time similarly to the release rate of solvent and drug. Bleached shellac matrices prepared using PYR as solvent eventually dissipated due to hydrolysis at ester bond which was accelerated by PYR-induced water accumulation. A higher porous structure collapsed easily and it was more likely plastic but a dense one considerably resisted to a compression and deformed elastically. Finally, the degradation of bleached shellac in aqueous condition actually started after systems completed solidification. At steady state, the total mass loss converted to PYR >> NMP > DMSO similarly to a water content pattern. PYR could gain the high amount of water and pH of doxycycline hyclate solution in matrix was maintained by buffer pH nearly to 7, resulting in the large hydrolysis at polyesters. However, all behaviors of solvent state in ISM was covered by hindrance effect of oil phase. The solvent had no effect on the structure of remained bleached shellac after solvent exchange. PYR was the most appropriated solvent for preparing the *in situ* forming systems because its formulations demonstrated the proper sustained drug release profiles and preferable self-degradation in physiological condition.

---

Program of Pharmaceutical Sciences  
Student's signature.....  
Thesis Advisor's signature.....

---

Graduate School, Silpakorn University  
Academic Year 2015

550705: สาขาวิชาวิทยาการทางเภสัชศาสตร์

คำสำคัญ : การแลกเปลี่ยนตัวทำละลาย / การก่อตัวเป็นเจลชนิดกึ่งตัวเอง / การก่อตัวเป็นไมโครปาร์ติเคิล / เซลล์เล็ก

พินิจสิทธิ์ ประพันธ์วิทยา : การแลกเปลี่ยนตัวทำละลายและการก่อตัวเป็นไมโครปาร์ติเคิลและเจลชนิดกึ่งตัวเองที่บรรจุยาดีออกซีไซคลินไฮโดรคลอไรด์โดยใช้เซลล์เป็นสารก่อเมทริกซ์. อาจารย์ที่ปรึกษาวิทยานิพนธ์: ภ.รศ.ดร.รวิษชัย แพชมัต. 156 หน้า

การแลกเปลี่ยนตัวทำละลายคือการแพร่ระหว่างตัวทำละลายอินทรีย์ที่เคลื่อนที่สู่ภายนอกและตัวกลางที่เป็นน้ำเข้าสู่บริเวณเป้าหมาย เจลชนิดกึ่งตัวเองเป็นระบบที่มีการเปลี่ยนแปลงวัฏภาคจากของเหลวเป็นเจลภายหลังสัมผัสตัวกลางที่เป็นน้ำ และไมโครปาร์ติเคิลชนิดกึ่งตัวเองเป็นระบบที่มีการเปลี่ยนแปลงจากของแข็งเป็นอนุภาคแข็งหลังสัมผัสตัวกลางที่เป็นน้ำ การเปลี่ยนแปลงของทั้งสองระบบนี้เกิดขึ้นผ่านกลไกการแยกวัฏภาคซึ่งเกี่ยวข้องกับการเปลี่ยนแปลงค่าการละลายของพอลิเมอร์อย่างฉับพลันที่ตอบสนองต่อการแลกเปลี่ยนตัวทำละลาย งานวิจัยนี้มีจุดประสงค์เพื่อศึกษาพฤติกรรมของตัวทำละลายอินทรีย์ได้แก่ Dimethyl sulfoxide (DMSO), *N*-methyl-2-pyrrolidone (NMP) และ 2-pyrrolidone (PYR) ภายในเซลล์ตั้งแต่ขั้นตอนการเตรียมจนกระทั่งระบบเกิดการแยกวัฏภาค สูตรตำรับใช้ระบบกึ่งตัวเองเป็นเจลชนิดกึ่งตัวเองเป็นวัฏภาคภายในของระบบกึ่งตัวเองเป็นไมโครปาร์ติเคิลซึ่งมีอิมัลชันที่เกิดจากการผสมระหว่างระบบดังกล่าวกับวัฏภาคภายนอกซึ่งประกอบด้วยน้ำมันมะกอกและ Glyceryl monostearate (GMS) ปัจจัยที่ศึกษาในขั้นตอนการเตรียมได้แก่ ความเป็นกรด-ด่าง ค่าดัชนีการละลาย ความหนาแน่น แรงตึงผิว และอัตราการแยกวัฏภาคของส่วนประกอบอิมัลชัน ในระหว่างการแยกวัฏภาคของระบบกึ่งตัวเองจะศึกษาคุณสมบัติทางกายภาพซึ่งแบ่งเป็น 3 ส่วนตามลำดับการสัมผัสกับตัวกลางที่เป็นน้ำ 1) ก่อนสัมผัส (รูปร่างและขนาดของอิมัลชัน ความหนืด สมบัติหุ่่นหนืด และการวิเคราะห์เชิงความร้อน) 2) ระหว่างสัมผัส (การเปลี่ยนแปลงจากของเหลวไปสู่ไมโครปาร์ติเคิล การปลดปล่อยตัวทำละลายอินทรีย์และขา การสลายตัว อัตราการแพร่ของน้ำ และการแพร่ของตัวทำละลายอินทรีย์) 3) หลังสัมผัส (การวิเคราะห์เนื้อสัมผัส การวิเคราะห์โครงสร้างผลึก และสภาพได้กลิ่นจุลทรรศน์อิเล็กตรอน) ทั้งนี้เซลล์ละลายในตัวทำละลายอินทรีย์ด้วยการเกิดพันธะไฮโดรเจนและแรงวานเดอร์วาลส์ เจลชนิดกึ่งตัวเองที่ใช้ NMP เป็นตัวทำละลายไม่สามารถนำมาเตรียมเป็นอิมัลชันได้เนื่องจาก NMP เข้ากับน้ำมันมะกอกบางส่วน ค่าดัชนีการละลายสามารถเรียงลำดับตามชนิดตัวทำละลายได้ดังนี้  $NMP > DMSO > PYR$  NMP จึงจัดเป็นตัวทำละลายที่ดีที่สุดสำหรับเซลล์ พาราเมเตอร์นี้สอดคล้องกับผลการศึกษาด้านความหนืด สมบัติหุ่่นหนืด และการวิเคราะห์เชิงความร้อน รวมถึง PYR มีความหนืดมากกว่า DMSO และ NMP ตามลำดับ กระบวนการแยกวัฏภาคสามารถแบ่งได้ 4 ขั้นตอนแรกนั้นได้เคลื่อนที่เข้าสู่ระบบด้วยอัตราเร็วต่างกันซึ่งเรียงตามลำดับตามชนิดตัวทำละลายที่ใช้ในระบบดังนี้  $DMSO > NMP > PYR$  น้ำที่เข้าสู่ระบบจะลดค่าการละลายของเซลล์จนเกิดการแยกวัฏภาค ขั้นตอนที่สองตัวทำละลายอินทรีย์และขาแพร่ออกจากระบบออกภายนอก อัตราการแพร่ของสารดังกล่าวเรียงตามลำดับตามชนิดตัวทำละลายในระบบได้ดังนี้  $DMSO > NMP > PYR$  ระบบที่มี PYR มีอัตราการปลดปล่อยสารช้าที่สุดเนื่องจากตัวทำละลายเองและระบบมีความหนืดสูงกว่า สำหรับการแพร่ของระบบที่มี DMSO และ NMP สามารถอธิบายได้จากค่าดัชนีการละลาย ขั้นตอนสามระบบจะเกิดรูพรุนบริเวณที่มีการเคลื่อนที่ของน้ำและตัวทำละลายอินทรีย์ ขนาดและความหนาแน่นของรูพรุนจะเพิ่มขึ้นตามเวลาซึ่งสอดคล้องกับอัตราการปลดปล่อยตัวทำละลายอินทรีย์และขา เมทริกซ์เซลล์ที่เกิดจากระบบที่ใช้ PYR มีการจับขาดในภายหลังเนื่องจากเกิดไฮโดรไลซิสซึ่งถูกเร่งโดย PYR เหนียวน้ำให้มีการสะสมน้ำภายในระบบ โครงสร้างที่มีความพรุนสูงจะเกิดการแตกหักได้ง่ายและมีพฤติกรรมแบบพลาสติก แต่โครงสร้างที่มีความพรุนต่ำจะทนต่อแรงกดและยึดหยุ่นขั้นสุดท้ายเซลล์เริ่มสลายตัวในสภาวะที่มีน้ำหลังจากระบบกลายเป็นของแข็งอย่างสมบูรณ์ เมื่อสภาวะคงที่ปริมาณการสลายตัวทั้งหมดเรียงตามลำดับตัวทำละลายได้ดังนี้  $PYR \gg NMP > DMSO$  ซึ่งมีแนวโน้มคล้ายกับปริมาณน้ำที่สะสมในระบบ ระบบที่เตรียมด้วย PYR สามารถกักเก็บน้ำได้มากและความเป็นกรด-ด่างของสารละลายดีออกซีไซคลินไฮโดรคลอไรด์ที่ควบคุมโดยบัฟเฟอร์มีค่าใกล้เคียง 7 จึงทำให้เกิดไฮโดรไลซิสที่พันธะเอสเทอร์ของเซลล์ได้สูง อย่างไรก็ตามพฤติกรรมของตัวทำละลายอินทรีย์ในระบบกึ่งตัวเองไมโครปาร์ติเคิลถูกบังคับด้วยน้ำมัน ตัวทำละลายดังกล่าวไม่ส่งผลกระทบต่อโครงสร้างเซลล์ที่เหลือหลังจากกระบวนการแลกเปลี่ยนสารละลาย PYR เป็นตัวทำละลายที่เหมาะสมในการเตรียมระบบกึ่งตัวเองที่สุดจากมันทำให้ระบบมีการปลดปล่อยอย่างช้าๆและมีโอกาสสลายตัวได้ในสภาวะร่างกาย

สาขาวิชาเทคโนโลยีเภสัชกรรม

บัณฑิตวิทยาลัย มหาวิทยาลัยศิลปากร

ลายมือชื่อนักศึกษา.....

ปีการศึกษา 2558

ลายมือชื่ออาจารย์ที่ปรึกษาวิทยานิพนธ์ .....

## ACKNOWLEDGEMENTS

After an intensive period of several months, I would like to reflect on all those people who made this thesis possible and a precious experience for me.

First of all, it is an honor for me to express my deepest sense of gratitude to my advisor, Assoc. Prof. Dr. Thawatchai Phaechamud for his guidance, advice and financial support throughout my master studies. He helped me overcome many crisis situations and finally succeed this dissertation.

In particular, I appreciatively acknowledge Faculty of Pharmacy and Graduate School, Silpakorn University, for the laboratory equipment and other facilities to proceed my research and publications.

My grateful gratitude goes to Assoc. Prof. Dr. Suchada Pririyaprasarth, Assoc. Prof. Dr. Uthai Sotanaphun, Asst. Prof. Dr. Sorada Kanokpanont and Dr. Purin Charoensuksai for serving as members of my thesis committee and the creative guidance.

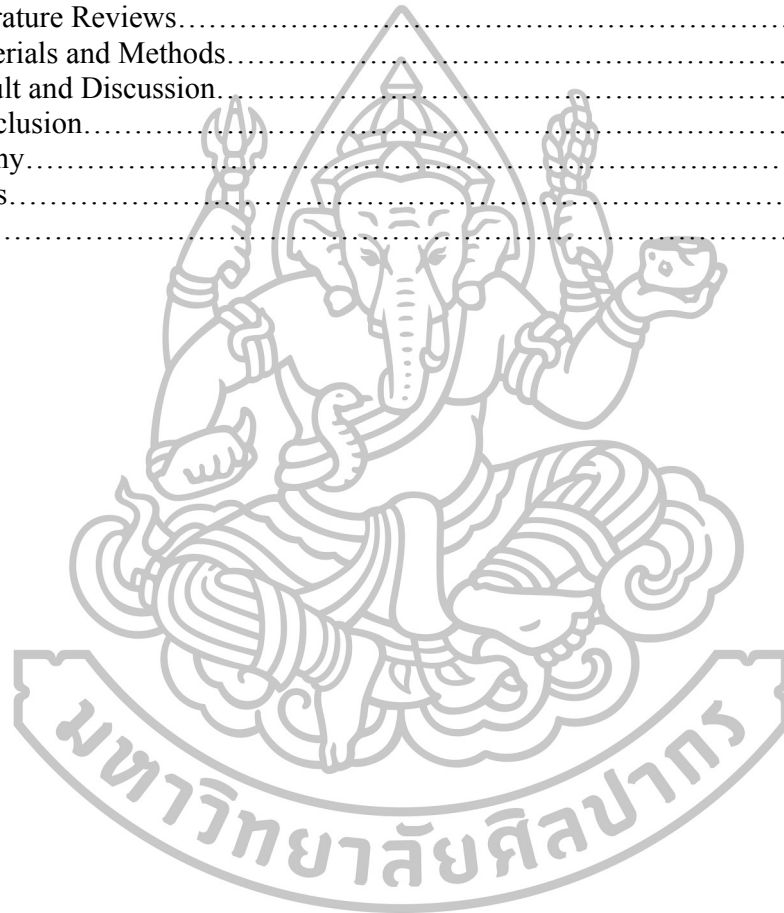
Most of the journeys described in this thesis would not have been achieved without a good collaboration. I owe a great deal of appreciation to lecturers, administrative and technical staff members of the school who have been kind enough to advise and help in their respective roles.

In my daily work I have been blessed with a friendly and cheerful group of fellow students. Many thanks to them for their gorgeous care and helpful suggestions during my progress report presentations. I am indebted to Mr. Kritamorn Jitrangsri who generously shared his time and valuable knowledge, especially HPLC information. Thank you.

Finally, I must express my very profound gratitude to my family for understanding and love during the past few years. Their unfailing motivation and continuous encouragement though the process of coursework and research were the end of this accomplishment.

## Table of Contents

	Page
English Abstract.....	iv
Thai Abstract.....	v
Acknowledgements.....	vi
List of Tables.....	viii
List of Figures.....	x
List of Abbreviation.....	xiv
Chapter	
1 Introduction.....	1
2 Literature Reviews.....	4
3 Materials and Methods.....	21
4 Result and Discussion.....	34
5 Conclusion.....	113
Bibliography.....	116
Appendices.....	136
Biography.....	156





## List of Tables

Tables	Page	
1	Definition of abbreviation in formulation.....	25
2	Composition formula of <i>in situ</i> forming gel.....	25
3	Composition formula of <i>in situ</i> forming microparticles.....	26
4	Solubility parameter of organic solvents, water and oil phase.....	40
5	Flow index and consistency index of prepared solutions at 25°C (n=3), *p≤0.05.....	49
6	Flow index and consistency index of ISMs at 25°C (n=3), *p≤0.05.....	49
7	DTGA peaks of <i>in situ</i> forming gels and their compositions.....	64
8	DTGA peaks of <i>in situ</i> forming microparticles and their compositions.....	66
9	Comparison of degree of goodness-of-fit from curve fitting of solvent release from <i>in situ</i> forming gel systems.....	81
10	Estimate parameter from curve fitting of solvent release from <i>in situ</i> forming gel systems.....	81
11	Comparison of degree of goodness-of-fit from curve fitting of solvent release from ISM.....	82
12	Estimate parameter from curve fitting of solvent release from ISM.....	82
13	Comparison of degree of goodness-of-fit from curve fitting of drug release from <i>in situ</i> gel systems.....	82
14	Estimate parameter from curve fitting of drug release from <i>in situ</i> gel systems.....	82
15	Comparison of degree of goodness-of-fit from curve fitting of drug release from ISM.....	83
16	Estimate parameter from curve fitting of drug release from ISM.....	83
17	Density of liquid compositions at 25°C (n=3).....	140
18	Surface tension of different solvents, olive oil and GMS-dispersed olive oil at 25°C (n=3).....	140
19	Interfacial tension of different solvents in olive oil at 25°C (n=3).....	140
20	Volume of solvent separation during 24 h at 25°C (n=3).....	141
21	pH of organic solvents, PBS 6.8, DI water and their solutions at 25°C (n=3).....	142
22	Relative viscosities of diluted bleached shellac (BS) solution in different solvents (n=3).....	143
23	Droplet size of o/o emulsion with various concentrations of GMS at phase ratio 1:1 (n=3).....	144
24	Droplet size of o/o emulsion at various phase ratios (n=3).....	144
25	Droplet size of o/o emulsion with constant GMS concentration at various phase ratios (n=3).....	144
26	Appearance viscosity of solvents at 25°C (n=3).....	145
27	Appearance viscosity of bleached shellac solutions at 25°C (n=3).....	145

28	Appearance viscosity of ISMs at 25°C (n=3).....	145
29	Release of DMSO, NMP and PYR from <i>in situ</i> forming gels in PBS pH 6.8 within 21 days (n=3).....	146
30	Release of DMSO, NMP and PYR from <i>in situ</i> forming microparticles in PBS pH 6.8 within 21 days (n=3).....	147
31	Release of DMSO, NMP and PYR from <i>in situ</i> forming microparticles in PBS pH 6.8 within 21 days (n=3).....	148
32	Drug release from <i>in situ</i> forming microparticles in PBS pH 6.8 within 21 days (n=3).....	149
33	Dynamic change in total mass of <i>in situ</i> forming gels (n=3).....	149
34	Dynamic change in mass of bleached shellac from <i>in situ</i> forming gels (n=3).....	150
35	Dynamic change in water content of <i>in situ</i> forming gels (n=3).....	150
36	Dynamic change in total mass of <i>in situ</i> forming microparticles (n=3)	150
37	Dynamic change in mass of bleached shellac from <i>in situ</i> forming microparticles (n=3).....	151
38	Dynamic change in water content of <i>in situ</i> forming microparticles (n=3).....	151
39	Water diffusion of <i>in situ</i> forming gels (n=3).....	152
40	Water diffusion of <i>in situ</i> forming microparticles (n=3).....	153
41	Solvent diffusion distance of <i>in situ</i> forming gels prepared with different solvents (n=3).....	153
42	Solvent diffusion rate of <i>in situ</i> forming gels prepared with different solvents (n=3).....	153
43	Solvent diffusion distance of <i>in situ</i> forming microparticles prepared with different solvents (n=3).....	154
44	Solvent diffusion rate of <i>in situ</i> forming microparticles prepared with different solvents (n=3).....	154
45	Maximum deformation force or hardness of <i>in situ</i> forming gels (n=6)	155
46	Ratio of remaining force/maximum deformation force or ratio of elasticity/plasticity of <i>in situ</i> forming gels (n=6).....	155
47	Maximum deformation force or hardness of <i>in situ</i> forming microparticles (n=6).....	155
48	Ratio of remaining force/maximum deformation force or ratio of elasticity/plasticity of <i>in situ</i> forming microparticles (n=6).....	155

## List of Figures

Figures		Page
1	Main compositions of shellac a) saleuritic acid b) butolic acid c) shellolic acid d) jalaric acid.....	11
2	Chemical structures of shellac: jalaric acid; R = CHO, R' = CH <sub>2</sub> OH, laccijalaric acid; R = CHO, R' = CH <sub>3</sub> .....	11
3	Chemical structure of dimethyl sulfoxide (DMSO), C <sub>2</sub> H <sub>6</sub> OS.....	12
4	Chemical structure of <i>N</i> -methyl-2-pyrrolidone (NMP), C <sub>4</sub> H <sub>9</sub> NO.....	12
5	Chemical structure of 2-pyrrolidone (PYR), C <sub>4</sub> H <sub>7</sub> NO.....	13
6	Chemical structure of doxycycline hyclate, (C <sub>22</sub> H <sub>24</sub> N <sub>2</sub> O <sub>8</sub> . HCl) 2. C <sub>2</sub> H <sub>6</sub> O. H <sub>2</sub> O.....	14
7	Chemical structure of olive oil, R <sub>1</sub> = oleic acid, R <sub>2</sub> = linoleic acid and R <sub>3</sub> = palmitic acid are alkyl group (20%) or alkenyl group (80%).....	15
8	Chemical structure of glyceryl monostearate (GMS), C <sub>21</sub> H <sub>42</sub> O <sub>4</sub> .....	15
9	(a) Schematic representation of a typical rheometer, with the sample loaded between two plates. (b) Schematic stress response to oscillatory strain deformation for an elastic solid, a viscous fluid and a viscoelastic material.....	18
10	Force-time curve to determine the mechanical and adhesive properties of the implants.....	20
11	Density of liquid compositions at 25°C (n=3), * p≤0.05.....	35
12	Surface tension of different solvents, olive oil and GMS-dispersed olive oil at 25°C (n=3), * p≤0.05.....	36
13	Interfacial tension of different solvents in olive oil at 25°C (n=3), * p≤0.05.....	36
14	Volume of solvent separation during 24 h at 25°C (n=3).....	37
15	Resonance effect of amides.....	38
16	pH of organic solvents, PBS 6.8, DI water and their solutions at 25°C (n=3).....	39
17	Solubility parameter of organic solvents, water and oil phase.....	40
18	Relative viscosities of diluted bleached shellac solution in different solvents (n=3).....	41
19	Droplet size of o/o emulsion with various concentrations of GMS at phase ratio 1:1 (n=150).....	43
20	Droplet size of o/o emulsion at various phase ratios (n=150).....	44
21	Droplet size of o/o emulsion with constant GMS concentration at various phase ratios (n=150).....	44
22	Appearance viscosity of solvents at 25°C (n=3), * p≤0.05.....	45
23	Appearance viscosity of bleached shellac solutions at 25°C (n=3), * p≤0.05.....	46
24	Appearance viscosity of ISMs at 25°C (n=3), * p≤0.05.....	47
25	Flow of bleached shellac solutions at 25°C (n=3).....	47
26	Flow of doxycycline hyclated-loaded bleached shellac solutions at 25°C (n=3).....	48

27	Flow of bleached shellac emulsions at 25°C (n=3).....	48
28	Strain dependence of G' for gels at $\omega = 1$ Hz under 25°C.....	50
29	Strain dependence of G' for emulsions at $\omega = 1$ Hz under 25°C.....	51
30	Frequency (0.1-10 Hz) dependence of G' and G'' for gels at 25°C.....	52
31	Frequency (0.1-10 Hz) dependence of G* and $\eta^*$ for gels at 25°C.....	52
32	Frequency (0.1-10 Hz) dependence of loss tangent (tan $\delta$ ) for gels at 25°C.....	53
33	Frequency (0.1-10 Hz) dependence of G' and G'' for emulsions at 25°C.....	54
34	Frequency (0.1-10 Hz) dependence of G* and $\eta^*$ for emulsions at 25°C.....	54
35	Frequency (0.1-10 Hz) dependence of loss tangent (tan $\delta$ ) for emulsions at 25°C.....	55
36	Temperature (20-45°C) dependence of G' and G'' for gels at frequency of 1 Hz.....	56
37	Temperature (20-45°C) dependence of G' and G'' for emulsions at frequency of 1 Hz.....	57
38	DSC curves of <i>in situ</i> forming gels and their compositions.....	60
39	DSC curves of <i>in situ</i> forming microparticles and their compositions.....	62
40	TG curves of <i>in situ</i> forming gels and their compositions.....	63
41	DTGA curves of <i>in situ</i> forming gels and their compositions.....	64
42	TG curves of <i>in situ</i> forming microparticles and their compositions....	65
43	DTGA curves of <i>in situ</i> forming microparticles and their compositions.....	66
44	Transformation of ISM with phase ratio of 1:1 (external phase: internal phase) comprising 5% GMS of external phase or 2.5% of whole system within 3 min.....	69
45	Transformation of systems with different ratios of external an internal phase: 5:5; 6:4; 7:3; 8:2 and 9:1 after contacting PBS pH 6.8 at 10 sec at magnitude of 20X.....	70
46	Transformation of systems using 2-pyrrolidone as solvent with different ratios of external and internal phase: a) 5:5; b) 4:6; c) 3:7; d) 2:8 and e) 1:9 after contacting PBS pH 6.8 at 10 sec at magnitude of 20X.....	71
47	Transformation of doxycycline hyclate-loaded systems with different ratios of external and internal phase: 5:5; 6:4; 7:3; 8:2 and 9:1 after contacting PBS pH 6.8 at 10 sec at magnitude of 20X.....	71
48	Release of DMSO, NMP and PYR from <i>in situ</i> forming gels in PBS pH 6.8 within 21 days (n=3).....	72
49	Initial solvent release of <i>in situ</i> forming gels in PBS pH 6.8 within 1 day (n=3).....	73
50	Release of DMSO, NMP and PYR from <i>in situ</i> forming microparticles in PBS pH 6.8 within 21 days (n=3).....	74
51	Initial release of DMSO, NMP and PYR from <i>in situ</i> forming microparticles in PBS pH 6.8 within 1 day (n=3).....	74
52	Drug release from <i>in situ</i> forming gels in PBS pH 6.8 within 21 days.....	76
53	Initial drug release of <i>in situ</i> forming gels in PBS pH 6.8 within 1 day.....	77

54	Drug release from <i>in situ</i> forming microparticles in PBS pH 6.8 within 21 days (n=3).....	78
55	Initial drug release from <i>in situ</i> forming microparticles in PBS pH 6.8 within 1 day (n=3).....	78
56	Identification of unknown peak by peak purity analysis mode of a release medium from DXP gel as specimen.....	79
57	Identification of unknown peak by peak purity analysis mode from diluted DXP gel in acetonitrile as reference peaks.....	80
58	Dynamic change in total mass of <i>in situ</i> forming gels (n=3).....	84
59	Dynamic change in mass of bleached shellac from <i>in situ</i> forming gels (n=3).....	85
60	Dynamic change in water content of <i>in situ</i> forming gels (n=3).....	85
61	Dynamic change in total mass of <i>in situ</i> forming microparticles (n=3)	86
62	Dynamic change in mass of bleached shellac from <i>in situ</i> forming microparticles (n=3).....	87
63	Dynamic change in water content of <i>in situ</i> forming microparticles (n=3).....	87
64	Water diffusion of <i>in situ</i> forming gels (n=3).....	89
65	Water diffusion of <i>in situ</i> forming microparticles (n=3).....	89
66	Water diffusion of <i>in situ</i> forming microparticles (n=3).....	93
67	Solvent diffusion distance of <i>in situ</i> forming gels prepared with different solvents (n=3).....	94
68	Solvent diffusion rate of <i>in situ</i> forming gels prepared with different solvents (n=3).....	94
69	Visual image of solvent diffusion from <i>in situ</i> forming microparticles prepared with different solvents.....	95
70	Solvent diffusion distance of <i>in situ</i> forming microparticles prepared with different solvents (n=3).....	96
71	Solvent diffusion rate of <i>in situ</i> forming microparticles prepared with different solvents (n=3).....	96
72	Photograph of <i>in situ</i> forming gels without drug loading in agarose pocket: a) DMSO gel, b) NMP gel, and c) PYR gel.....	101
73	Photograph of <i>in situ</i> forming gels with drug loading in agarose pocket: a) DXDM gel, b) DXN gel, and c) DXP gel.....	102
74	Maximum deformation force or hardness of <i>in situ</i> forming gels (n=6), * p≤0.05.....	102
75	Ratio of remaining force/maximum deformation force or ratio of elasticity/plasticity of <i>in situ</i> forming gels (n=6) * p≤0.05.....	102
76	Photograph of <i>in situ</i> forming microparticles without drug loading in artificial periodontal pocket: a) DMSO ism and b) PYR ism...	103
77	Photograph of drug-loaded <i>in situ</i> forming microparticles in artificial periodontal pocket: a) DXDM ism and b) DXP ism.....	103
78	Maximum deformation force or hardness of <i>in situ</i> forming microparticles (n=6), * p≤0.05.....	104
79	Ratio of remaining force/maximum deformation force or ratio of elasticity/plasticity of <i>in situ</i> forming microparticles (n=6), * p≤0.05.....	104

80	XRD spectra of the pure polymer and <i>in situ</i> forming gels after release test.....	106
81	XRD spectra of the pure polymer and <i>in situ</i> forming microparticles after release test.....	107
82	Scanning electron micrographs of <i>in situ</i> forming gel after release test at different times at magnitude 100X.....	109
83	Scanning electron micrographs of <i>in situ</i> forming gel after release test at different time at magnitude 500X.....	109
84	Scanning electron micrographs of ISM after release test at different time at magnitude 100X.....	110
85	Scanning electron micrographs of ISM after release test at different time at magnitude 500X.....	111
86	Calibration curve of DMSO in phosphate buffer pH 6.8 for the in vitro release study (UV-vis HPLC at 220 nm).....	137
87	Calibration curve of NMP in phosphate buffer pH 6.8 for the in vitro release study (UV-vis HPLC at 220 nm).....	137
88	Calibration curve of PYR in phosphate buffer pH 6.8 for the in vitro release study (UV-vis HPLC at 220 nm).....	138
89	Calibration curve of doxycycline hyclate in DMSO and phosphate buffer pH 6.8 for the in vitro release study (UV-vis HPLC at 273 nm).....	138
90	Calibration curve of doxycycline hyclate in NMP and phosphate buffer pH 6.8 for the in vitro release study (UV-vis HPLC at 273 nm).....	139
91	Calibration curve of doxycycline hyclate in PYR and phosphate buffer pH 6.8 for the in vitro release study (UV-vis HPLC at 273 nm).....	139

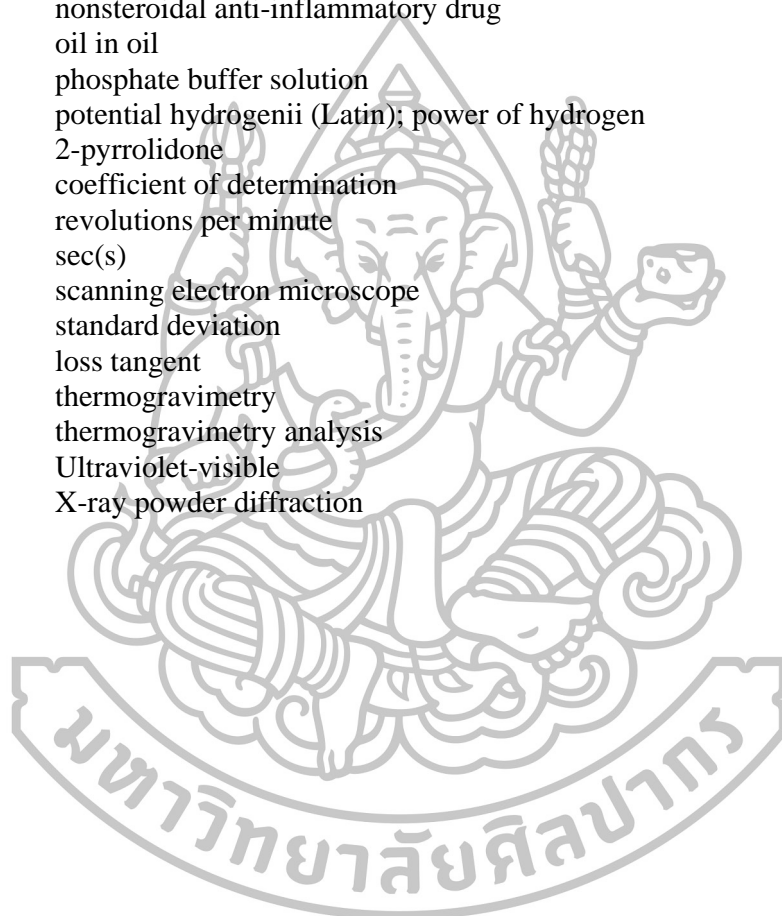


## List of Abbreviations

% w/w	percent weight by weight
%	percent
$\alpha$	alpha
$\beta$	beta
$\eta$	consistency index
$\omega$	frequency
$\delta$	solubility parameter
$\gamma$	strain
$\gamma_c$	critical strain
$\eta^*$	complex viscosity
®	trademark
° C	degree Celsius
±	plus per minus
µg	microgram(s)
µm	micrometer(s)
2θ	two theta
Abs	absorbance
AR grade	analytical reagent grade
BS	bleached shellac
cm	centimeter(s)
cm <sup>2</sup>	square centimeter
cps	centipoise
CO., LTD.	Company Limited
D/cm <sup>2</sup>	Dyne/square centimeter
DMSO	dimethyl sulfoxide
DSC	differential scanning calorimetry
e.g.	(Latin); for example
Eq.	equation
<i>et al.</i>	and others
etc.	et cetera (Latin); and other things/ and so forth
F <sub>max deformation</sub>	maximum deformation force
F <sub>remaining</sub>	remaining force
g	gram (s)
G'	elastic modulus, shear storage
G''	viscous modulus, shear loss
G*	complex modulus
GMS	glycerol monostearate
h	hour(s)
Hz	hertz
HPLC	High Performance Liquid Chromatography
ISM or ism	<i>in situ</i> forming microparticle
k	release rate
L	liter(s)
Log	logarithm
LVR	Linear viscoelastic region curves
mg	milligram(s)
min	minute(s)
mL	milliliter(s)

## List of Abbreviations

msc	model selection criterion
MW	molecular weight
N	newton
No.	number
n	solvent release exponent value
ng	nanogram(s)
nm	nanometer(s)
NMP	<i>N</i> -methyl-pyrrolidone
NSAID	nonsteroidal anti-inflammatory drug
o/o	oil in oil
PBS	phosphate buffer solution
pH	potential hydrogenii (Latin); power of hydrogen
PYR	2-pyrrolidone
$r^2$	coefficient of determination
rpm	revolutions per minute
s	sec(s)
SEM	scanning electron microscope
SD	standard deviation
$\tan \delta$	loss tangent
TG	thermogravimetry
TGA	thermogravimetry analysis
UV/vis	Ultraviolet-visible
XRD	X-ray powder diffraction





# CHAPTER 1

## INTRODUCTION

### 1.1 Statement and significance of the research problem

Periodontitis is a local inflammatory disease involving the destruction initially from gingiva to supportive periodontal tissues. Its clinical symptoms are bleeding, pus discharge, halitosis, tooth mobility and ultimately tooth loss (Divya and Nandakumar, 2006). This inflammatory process connects to the multiple pathogens and host immune response (Vyas *et al.*, 2005). A number of potential pathogenic bacteria are primarily Gram negative, facultative anaerobic species colonized in periodontal pocket, especially *Porphyromonas gingivalis* (Marcotte and Lavoie, 1998). At present, therapeutic approach for periodontitis is aimed to mechanically eliminate the bacteria including subgingival calculus and plaque from periodontal pockets: a procedure is called “scaling and root planning (SRP)” (Berezow and Darveau, 2011; Bonito *et al.*, 2005). However, the SRP is not able to eradicate all periodontal pathogens which can re-establish at least 2 months in poor oral hygiene (Chhokra *et al.*, 2012). Therefore the periodontitis healing further suggests the use of antimicrobial agents in combination with SRP (Berezow and Darveau, 2011) such as antibiotics (e.g. tetracycline (Friesen *et al.*, 2002), doxycycline (Tomasi and Jan, 2004), minocycline (Renvert *et al.*, 2006) and metronidazole (Jones *et al.*, 2002)) and antiseptics (e.g. chlorhexidine (Yoe *et al.*, 2004)). This type of drug treatment may gain access into deep lesion through systemic or local route of administration. As known, the serious limitations of systemic administration are potentially severe adverse effects, development of antibiotic resistance and patient compliance (Chhokra *et al.*, 2012). The local administration is designed to minimize these problems by directly delivering the agent into subgingival site (Schwach-Abdellaoui *et al.*, 2000). Recently, new approaches of local drug delivery system for treating periodontitis are fibers, film, injectable systems, gels, strips and compacts, vesicular systems, microparticle system, nanoparticle system, *in situ* forming systems etc. (Jain *et al.*, 2008).

*In situ* depot-forming systems are the transformation of low viscous solution in the body to a gel or solid depot with different strategies. *In situ* phase separation is one of various triggers (e.g. cross-linked systems and solidifying organogels) used to stimulate this transformation (Packhaeuser *et al.*, 2004). The phenomenon of phase separation undergoes the abrupt changes in solubility of polymer solution prior to solidifying into a solid form. Its formation is responded to different stimuli like pH change, temperature modulation and solvent exchange (Kempe and Mäder, 2012). The application of *in situ* forming systems provides the advantages over pre-shaped parenteral systems as followings; 1) easy administration through small needle sizes, 2) less painful, 3) less invasive, and 4) efficient spreading within the periodontal pocket (Hatefi and Armsden, 2002; Do *et al.*, 2014). This research investigated the *in situ* phase separations by solvent exchange.

*In situ* forming gel exhibits a sol-to-gel phase transition which polymer transforms from solution state into solid state or semisolid state with its convenient residence time at specific site (Foguery and Singh, 2009). This system can be easily applied and shaped within deep lesion, reduce frequency of administration, and provide good biodegradable ability (Liu *et al.*, 2010; Kapoor *et al.*, 2012). Unfortunately, the burst release is the major disadvantage of this *in situ* forming system (Kranz *et al.*, 2001), leading to potential local or systemic toxicities (Huang and Brazel, 2001). To overcome the burst, a novel approach has been developed by emulsifying the drug-loaded polymeric solution (inner phase) with external phase containing a stabilizer, and it then solidified upon exposure with aqueous conditions to form microparticles (Kranz *et al.*, 2001).

*In situ* forming microparticles (ISM) is an injectable emulsion. It comprises of an internal drug containing polymer phase which is dispersed into an external phase usually oil. The emulsion is achieved by pushing two syringes coupled with a connector for 50 mixing cycles (Voigt *et al.*, 2012). This research employed the *in situ* forming gel as an internal phase of ISM. After contacting this emulsion with body fluid, the droplets of internal phase solidified and spontaneously formed into a solid matrix. However, the main obstacle was the relatively low physical stability of ISM emulsion, especially coalescence of polymer solution droplets during solidification (Voigt, 2011; Voigt *et al.*, 2012).

Solvent exchange is the diffusion between solvent and water at target site. The organic solvent dissipates out of the *in situ* forming system and water ingresses, resulting in polymer precipitation into matrix formation (Graham *et al.*, 1999). This process can be described in term of diffusion pattern which is influenced by a number of factors such as polymer-solvent affinity and solvent miscibility including viscosity of solvent itself or formulation (Kranz and Bodmeier, 2008). This exchange of solvents significantly governs the release kinetics. Therefore, to comprehend the process of solvent exchange, it can lead to an efficient modification for optimal drug release.

Previously, the *in situ* forming formulations were prepared using bleached shellac as gelling agent for periodontal healing (Setthajindalert, 2013). It found that 1) an emulsion was not able to be prepared by internal phases dissolved in NMP, 2) types of organic solvent seriously affected on release patterns and degradation upon exposure to physiological buffer. The vital evidence was a soften matrix only formed from PYR whereas DMSO and NMP allowed stiff and friable matrices. These bizarre behaviors were possibly impacted from the chemical interaction and solvent exchange. It should further clarify the affinity between substances, the stepwise process of solvent exchange and its related parameters, and the behavior of solvent state in polymer. Hence this study expects to fulfill that crucial shortage information.

According to recent incomplete study (Setthajindalert, 2013), we continue to profoundly investigate the *in situ* forming gel and ISM comprising bleached shellac as a matrix former in the aspect of phase separation process by solvent exchange. First of all, it is necessary to introduce the formulation composition and preparation. Bleached shellac is a biocompatible polymer (Annina, 2010). It has been used as polymeric matrix for the antimicrobial agent-loaded *in situ* forming systems (Phaechamud *et al.*, 2016). This polymer was dissolved in dimethyl sulfoxide (DMSO), *N*-methyl-2-pyrrolidone (NMP) or 2-pyrrolidone (PYR). These solvents have low systemic toxicities and were approved to be

used as a constituent in medical devices (David, 1972; Jouyban *et al.*, 2010). Olive oil dispersed with GMS was employed as an external phase of emulsion. This natural oil has phenol compounds, especially oleocanthal which has a pharmacological effect similarly to NSAID (Yamada *et al.*, 2008). The emulsion was succeeded by pushing two syringes coupled with a connector for 50 mixing cycles. All systems were loaded with doxycycline hyclate as an antibiotic agent for periodontitis treatment. The formulations were initially prepared into solution and emulsion, and they then precipitated into matrix form upon contacting to aqueous fluids.

The main aim of this present research is to better understand the effect of types of solvent on stage of preparation and on physical phenomena throughout the phase separation. In preparation process, it was investigated for the mechanism of bleached shellac dissolving in solvents (pH measurement and solubility parameter) and emulsion stability (density, interfacial tension and phase separation rate of emulsion compositions). The physical characteristics entire the phase separation were examined for three phases related to the duration of aqueous buffer exposure as following:

- 1) Before (morphology of oil in oil (o/o) emulsion and its droplet size, viscosities, viscoelasticity and thermal analysis, the last three studies can directly criticize the solubility parameter which is important to predict release kinetics.)
- 2) During (transformation of sol to microparticles, solvent and drug releases, *in vitro* degradation, water diffusion rate and solvent diffusion.)
- 3) After (texture analysis, XRD pattern and SEM microphotograph.)

This strategy eventually explained the behavior of solvent state in polymer according to the major steps of phase separation by solvent exchange (water inflow, solvent and drug outflow, pore formation, and degradation.)

## 1.2 Objective of this research

- 1) To prepare and characterize the *in situ* forming gels and *in situ* forming microparticles using bleached shellac as a matrix former and loading doxycycline hyclate
- 2) To investigate the effect of types of organic solvent on pattern of solvent exchange
- 3) To investigate the effect of pattern of solvent exchange on the control of drug release.

## 1.3 The research hypothesis

- 1) Type of organic solvent influences on pattern of solvent exchange
- 2) Pattern of solvent exchange of doxycycline hyclate-loaded *in situ* forming gels and *in situ* forming microparticles has an influence on the preparation procedure (e.g. mechanism of bleached shellac dissolving in solvents, emulsion stability, etc.), physical characteristics of systems especially the control of drug release and behavior of solvent state in bleached shellac throughout this process.

## CHAPTER 2

### REVIEW OF RELATED LITERATURE

#### 2.1 Periodontitis

##### 2.1.1 Introduction to periodontitis

##### 2.1.2 Treatment

#### 2.2 *In situ* forming systems

#### 2.3 Solvent exchange-induced *in situ* forming gel

#### 2.4 *In situ* forming microparticle

#### 2.5 Formulation parameter

##### 2.5.1 Matrix former

###### 2.5.1.1 Bleached shellac

##### 2.5.2 Solvent

###### 2.5.2.1 Dimethyl sulfoxide (DMSO)

###### 2.5.2.2 *N*-methyl-2-pyrrolidone (NMP)

###### 2.5.2.3 2-pyrrolidone (PYR)

##### 2.5.3 Drug

###### 2.5.3.1 Doxycycline hyclate

##### 2.5.4 External phase

###### 2.6.4.1 Olive oil

###### 2.6.4.2 Glyceryl monostearate

#### 2.6 Evaluation

##### 2.6.1 Relative viscosity

##### 2.6.2 Viscoelastic behavior from rheology studies

##### 2.6.3 Mechanical analysis

## 2.1 Periodontitis

### 2.1.1 Introduction to periodontitis

Periodontitis is a gingival inflammation with progressing attachment loss of periodontal ligament, cementum and alveolar bone (Armitage, 1999). The mechanism underlying this destructive process involves the induction of bacterial plaque products and host immune responses (Silva-Boghossian *et al.*, 2013). Clinical features of periodontitis are plaque accumulation, gingival redness and bleeding, pus discharge, halitosis, pocket depths  $\geq 5$  mm (Divya and Nandakumar, 2006), pocket volume  $> 0.5$   $\mu\text{L}$  (Binder *et al.*, 1987), pH  $\sim 8$  (Eggert *et al.*, 1991), tooth mobility, functional impairment and ultimately tooth loss (Divya and Nandakumar, 2006). This infection affects individuals of all ages, but its prevalence, extent and severity increase in elderly individuals (Pihlstorm, 2001). Current etiology of periodontal disease concerns 3 groups of factors: a susceptible host, the presence of pathogenic species and the absence of beneficial bacterial or bacterial flora (Wolff *et al.*, 1994). The key etiological factor is generally oral biofilm consisted mainly of microbes and host proteins that adhere to teeth (Wolff *et al.*, 1994). Healthy gingival sulcus has an equal flora proportions of aerobic microorganisms, especially Gram positive cocci (i.e. *Streptococcus* spp, *Actinomyces* sp.), and facultative anaerobic organisms, spirochaetes including motile rods which mostly generate subgingival plaque. The severity of disease significantly increases with the proportions of strict anaerobic, Gram negative and motile organisms (Kesic *et al.*, 2008). The main pathogens of adult periodontitis are *Prophyromonas gingivalis* and *Aggregatibacter actinomycetemcomitans*. In addition, *Bacteroides forsythus*, *Prevotella intermedia*, *Peptostreptococcus micro*, *Fusobacterium nucleatum*, *Capnocytophaga species* and *Campylobacter rectus* have been strongly related to the progression of adult periodontal disease (Avila-Campos, 2003; Lovegrove, 2004).

*P. gingivalis* was one of periodontal pathogens in the antimicrobial test because it is the major pathogen among anaerobic Gram-negative bacteria involved in periodontitis (Valenze *et al.*, 2009). Antimicrobial activity of microparticles of poly (dl-lactic-co-glycolic acid) (PLGA) containing chlorhexidine/cyclodextrin complexation was performed with *P. gingivalis* (Yue *et al.*, 2004). *Streptococcus mutans* is associated with the onset of caries and high *S. mutans* levels appear directly co-associated with increased severity of periodontal disease at older ages in untreated patients (Contardo *et al.*, 2011). Antibacterial activity of poly(lactic-co-glycolic acid)-based *in situ* forming gel from *N*-methyl pyrrolidone-based liquid formulations was tested using streptococcus strains (Do *et al.*, 2014). However, the precise roles that such species play, singularly or in combinations, in the pathogenesis of periodontal breakdown remain to be determined. Unlike the majority of general infections, all the suspected periodontal pathogens are indigenous to the oral flora which *Candida albicans* courses of refractory periodontitis (Seymour and Measman, 1995b). *Staphylococcus aureus* could be isolated from the periodontal pockets of patients with aggressive periodontitis and *Escherichia coli* was considered as a microorganism usual in patients with periodontitis (Amel *et al.*, 2015).

### 2.1.2 Treatment

Treatment of periodontitis is aimed to eliminate or adequately suppress the infection in deep periodontal pocket (Pragatil *et al.*, 2009). Primary therapeutic approach includes patient education, training in personal oral hygiene, and counseling on control of risk factors e.g. smoking, medical status and stress. The usual clinical intervention is the mechanical removal of the microbial plaques and treatment of root surface irregularities called “root planning scaling (SRP)” (Sbordone *et al.*, 1990). In some cases, this procedure is incorporated into the surgical depth reduction of deeper pockets (Sbordone *et al.*, 1990). Poor oral hygiene induces reestablishment of microflora within two months of single SRP (Pihlstorm, 2001). This temporary effect points out an inability of this technique to eradicate all periodontal pathogens (Pihlstorm, 2001). Therefore microbial etiology of periodontitis further suggests the treatment with various antimicrobial agents which can access into deep periodontal pockets through systemic or local route of administration (Jain *et al.*, 2008). To prevent systemic side effect, local application containing antimicrobials have been introduced for specific site (Slots and Ting, 2000). The different drugs used for local delivery are antibiotics i.e. tetracycline, doxycycline, minocycline and metronidazole as well as antiseptic agent i.e. chlorhexidine (Schwach-Abdellaoui *et al.*, 2000). Recently, a variety of new controlled drug delivery approaches for periodontitis treatment include fibers, film, gels, strips, microparticles or nanoparticle system and *in situ* forming systems (Jain *et al.*, 2008).

### 2.2 *In situ* forming systems

*In situ* forming systems are injectable liquid that transformed at active site into a semisolid or solid depots (Packhaeuser *et al.*, 2004). These systems have been generally classified according to their mechanism of formation as followings; 1) *in situ* cross-linked polymer systems, 2) *in situ* solidifying organogels, and 3) *in situ* phase separation (Kempe and Mäder, 2012). The polymer networks of *in situ* cross-linked systems can be achieved by photo-initiated polymerization (Lee and Tae, 2007), physical cross-linking of specific monomers (Berger *et al.*, 2004) or chemical cross-linking of specific monomers (Mi *et al.*, 1999). *In situ* organogels or oleaginous gels are a three-dimensional networks of self-assembled gelator, especially amphiphilic lipids, swelled in water and formed various types of lyotropic liquid crystals (Nirmal *et al.*, 2010) by intermolecular physical interaction such as Van der Waals force and hydrogen bonding (Vintiloui and Leroux, 2008). The polymers of *in situ* phase separation systems undergo an abrupt decrease in their solubility in response to changes in their environmental temperature, pH or solvent exchange (Kempe and Mäder, 2012). These *in situ* forming systems serve various advantages over pre-shaped parenteral systems. For instances, they provide an easy administration through small needle sizes leading to less pain and invasion, and their features are able to efficiently spread within individual periodontal pockets (Hatefi and Armsden, 2002; Do *et al.*, 2014). This issue will exclusively focus on the *in situ* phase separations by solvent exchange.

### 2.3 Solvent exchange-induced *in situ* forming gel

Solvent exchange is the dynamic diffusion between solvent in polymer solution and water in surrounding environment at target site. It occurs as organic solvent diffuses out of the *in situ* forming depots while water inflows, causing the phase separation, a formation of polymer membrane at the interface and the complete matrix in finale (Graham *et al.*, 1999). This process is influenced directly by properties of organic solvent such as polymer-solvent affinity, solvent miscibility, viscosity and formulation (Kranz and Bodmeier, 2008). It also determines the separation characteristics, the depot morphology and the release kinetics (Graham *et al.*, 1999).

*In situ* forming gels are the viscous liquids that undergo sol-gel transition once administered *via* one or a combination of several strategies like temperature modulation, UV-irradiation, pH change, ionic strength and solvent exchange (Hatefi and Armsden, 2002). Among the different types, phase separation system by solvent exchange is more favorable because it allows a great commercial potential in terms of relatively lower production cost and simple manufacturing procedure (Hatefi and Armsden, 2002). The concept of solvent exchange-induced *in situ* forming gel involves the diffusion of solvent such as dimethyl sulfoxide (DMSO), *N*-methyl pyrrolidone (NMP) and 2-pyrrolidone (PYR) from polymer solution into aqueous conditions while water permeates into the depots, resulting in solidification of polymer matrix (Motto and Gailloud, 2000). Key parameters of *in situ* forming gel compositions to obtain an appropriate drug release are type of solvent, polymer ratio, polymer molecular weight and additives. This research aimed to better understand the influence of types of solvent on physical phenomena throughout the phase separation; therefore, this overview will emphasize on solvent types.

Solvents commonly used for dissolving polymer can be divided into two main categories; water miscible and partially water miscible solvents (Ahmed, 2015). Basic solvents for the forming *in situ* gels include dimethyl sulfoxide (DMSO), *N*-methyl-pyrrolidone (NMP), 2-pyrrolidone, propylene glycol (Dunn *et al.*, 1997), glycofurol (Eliaz and Kost, 2000) or low molecular weight PEG (Dittgen *et al.*, 1998). The ideal solvent for *in situ* systems needs to gain appropriate properties in term of water affinity, viscosity, ability to dissolve the polymer and its safety (Brodbeck *et al.*, 1999).

A solvent with low water affinity can extend the rate of phase separation, matrix formation and drug release (Graham *et al.*, 1999). Reducing the water affinity of solvent by water-immiscible or partially water miscible components such as benzyl benzoate, ethyl acetate, ethyl benzoate or triacetin (Graham *et al.*, 1999), is proposed to decrease the phase inversion rate and consequently provide the zero-order release pattern (Brodbeck *et al.*, 1999). The role of solvent properties on the dynamic of polymer precipitation and *in vitro* release of chicken egg white lysozyme protein had been explained that the release of protein from PLGA depots in NMP was initial burst while that in IFow water-affinity solvent (e.g. triacetin or ethyl benzoate) exhibited the lower initial burst because of slower phase separation process led to less porous, small pore size and less homogeneously dense (Brodbeck *et al.*, 1999). Another study on metoclopramide release prepared with PLGA in different solvent also confirmed this circumstance (Wang *et al.*, 2004). NMP provided the fastest release followed by triacetin and finally benzyl benzoate due to their water miscibility and limited water solubility (Wang *et al.*, 2004). To compare the release

behavior from both water miscible solvents (DMSO, NMP) and partially water miscible (tiracetin, ethyl acetate), the release of haloperidol in four different solvents was investigated (Ahmed *et al.*, 2012). DMSO led the higher initial drug release followed by NMP then ethyl acetate and finally tiracetin. It concluded that solvents type had a remarkable effect on haloperidol initial burst and slow phase inversion rate (Ahmed *et al.*, 2012).

The viscosity of solvent should be suitable to further facilitate an easy injection of formulations or good syringeability. Systems prepared with water-immiscible solvent exhibited a viscous feature leading to difficult injection which requires a warm-up step prior administration (Chen and Singh, 2005). This parameter also affects the diffusion of species in the matrix. A high viscosity will slow down the water influx and solvent-drug diffusion. Therefore it reduces the burst release as well as prolongs polymer degradation.

Compatibility between solvent and polymer should be concerned in term of good solvent and poor solvent. The chemical interactions in polymer solution mainly comprise with polymer-polymer interaction and polymer-solvent interaction. In good solvents, polymer-solvent interaction predominate polymer-polymer interaction, therefore lowering the viscosity. It presents the advantage of achievement the higher polymer and drug loading formulation which further reduces injection volume. In contrast, poor solvents possess more favored polymer-polymer interactions, leading to the aggregation of polymer chain and an increase of viscosity (Voigt *et al.*, 2012).

Organic solvents used for *in situ* forming system, should possess biocompatibility or low toxicity according to pharmaceutical acceptance. DMSO and NMP are rather safe because they have low systemic toxicities and also have been approved for employing in parenteral products by pharmaceutical precedence (Royals *et al.*, 1999). However, these organic solvents are freely miscible with water, resulting in a rapid burst as discussed above. The burst release of solvent may irritate tissue such as local inflammatory effect and myotoxicity (Matschke *et al.*, 2002; Srichan and Phaechamud, 2016; Phaechamud *et al.*, 2016, Phaechamud and Mahadlek, 2015).

Administration route for *in situ* forming gels are oral, ocular, rectal, vaginal, injectable, interperitoneal and periodontal pocket routes (Hatefi and Armsden, 2002; Kulkarni *et al.*, 2012). Recently, the treatment of periodontitis had been applied the *in situ* forming gels to release antibiotics at specific site. The *in situ* forming system using poly(lactide) (PLA) and poly(lactide-co-glycolide) (PLGA) as gelling agent extended the release of secnidazole and doxycycline hydrochloride by solvent exchange (Gad *et al.*, 2008). Gallen gum and sodium alginate formed *in situ* forming gels by ion-crosslinking mechanism. This system could prolong release and provide an easy administration at periodontal pocket (Kunche *et al.*, 2012). Poloxamer, a thermo-reversible polymer, was employed as gelling agent for forming *in situ* forming gel. This formulation was adjusted the adhesion property by hydroxypropylmethylcellulose (HPMC). It could sustain the release of articaine HCl for 7 hours and obtain the potential for pain relief in periodontitis (Kulkarni *et al.*, 2012). Another *in situ* forming system based on poloxamer, also added gellan gum and carbopol as gelling agent. Polymer solutions underwent sol-gel transformation due to temperature change. It was able to extend chlorhexidine HCl release for 6 hours (Garala *et al.*, 2013). Latest, the addition of plasticizer (acetyltributyl citrate



and dibutyl sebacate as well as of adhesive polymer (HPMC) significantly increased the stickiness of PLGA based *in situ* forming gels. The system obtained good plastic deformability and favorable doxycycline hyclate release pattern including good antimicrobial activity (Do *et al.*, 2014).

Atridox<sup>®</sup> is one of the *in situ* forming gels which becomes commercially available as a controlled local doxycycline treatment for periodontitis (Kempe and Mäder, 2012). It comprises of a two syringe mixing systems. After mixing syringe A (36.7% PLA in 63.3% NMP) and syringe B (doxycycline 50 mg), the final product is a yellow viscous solution. It is injected directly into periodontal pocket, and contacts with the gingival crevicular fluid. The NMP then diffuses into the environment and aqueous fluids penetrate into the formulation. The systems finally precipitated into matrix depot allowing the controlled release of drug about one week (Kempe and Mäder, 2012).

#### 2.4 *In situ* forming microparticle

*In situ* forming microparticle (ISM) systems consist of an internal phase (drug dissolved/dispersed in polymer solution) that is emulsified with an external phase (usually oil). Upon exposure this emulsion with aqueous fluids, the droplets of internal polymeric phase solidify and form microparticles spontaneously (Bodmeier, 1997; Kranz and Bodmeier, 1998). The conventional techniques for preparing microsphere are complicated and costly (Kranz *et al.*, 2008). Consequently, new simpler process is manipulated by two-syringe technique which loaded internal phase and external phase in each syringe. The syringes are coupled with a connector and pushed for 50 mixing cycles. Finally, ISM is ready for use after removing the connector (Luan and Bodmeier, 2006; Kranz and Bodmeier, 2007). The ISM exhibits many advantages over its corresponding *in situ* forming gel. For instances, it significantly reduced the initial burst release and viscosity owing to hydrophobicity and lubricating effect of an external oil phase respectively. Therefore, better syringability, less pain and myotoxicity have been accomplished (Kranz and Bodmeier, 1998; Kranz and Bodmeier, 2007). Additionally, the regular shape of formed ISMs after solidification can minimize morphological variations. Thus, they provide more consistency and reproducible release profile (Kranz and Bodmeier, 2007). However, the main drawback could be a lack of emulsion stability according to the coalescence of emulsion droplets during their solidification despite the use of surfactant. This lumps formation may interfere an injection through thin needles (Voigt *et al.*, 2012).

Recent studies in ISM have been modulated in different researches for achieving new injectable formulations. The comparison between *in situ* forming implant (ISI) and ISM, which emulsified ISI into peanut oil containing 2% w/w span as stabilizer, indicated that obtained ISM showed an easy injection with smaller need size. Therefore, it possibly allowed less painful in patients (Rungseevijitprapa and Bodmeier, 2009). The ISM based on PLGA prepared by emulsifying polymer solution in DMSO into different vegetable oils suspended by individual stabilizers. It was eventually concluded that glyceryl monostearate (GMS) at 5% w/w as emulsifier allowed the stable formulation for at least 12 h (Voigt *et al.*, 2012). The controlled ISM systems were prepared by emulsifying an internal phase or *in situ* forming gel based on PLGA into peanut oil exhibited the lower initial burst and

slower release of haloperidol which was further related to the pharmacokinetic data (Ahmed *et al.*, 2012). Both *in vitro* release profile of montelukast ISMs and their pharmacokinetic data were similar to previous research (Ahmed *et al.*, 2010).

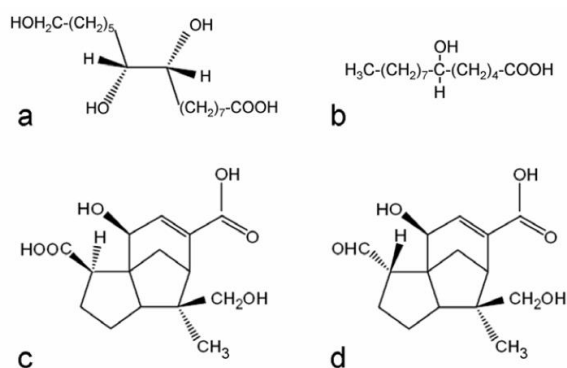
Ongoing ISM formulations are developed to deliver psychiatric and oncologic drugs. This technology aims for daily administration in chronic disease and long-lasting treatment. Risperidone-ISM<sup>®</sup>, has been studied in clinical trial at Phase I for schizophrenia disorder. Another clinical development introduces Letrozole-ISM<sup>®</sup> which is an aromatase inhibitor for treatment of dependent-hormone breast cancer (Rovi, 2011).

## 2.5 Formulation parameter

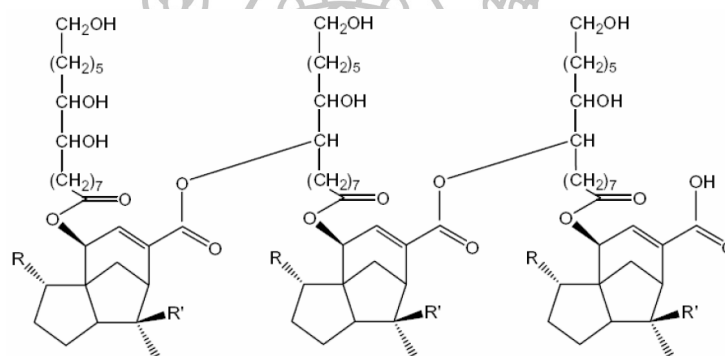
### 2.5.1 Matrix former

#### 2.5.1.1 Bleached shellac

Shellac is the natural product from resin lac which secreted by a parasitic insect, *Kerria Lacca* (Cardon, 2007). The chemical structure of this material comprises a complex mixture of esters and polyesters of polyhydroxy acids as shown in Fig 1 and 2. The total shellac composition is aleuritic acid, about 70 percent of homologous shellolic acid, and a small amount of free aliphatic acids (Carstensen, 2001). The acidic structure results in its solubility depended on pH therefore shellac is practically soluble in alkaline solution. Likewise, it can be dissolved in some organic solvents e.g. ethanol, methanol, and partially soluble in ether, ethyl acetate and chloroform (Cardon, 2007). Shellac is approved as GRAS by the FDA that it is non-toxic and physiologically harmless (Okamoto and Ibanez, 1986). Bleached shellac is prepared by treating the dissolved polymer with sodium hypochlorite (Roda *et al.*, 2007). According to its acidic character and approval, bleached shellac is mostly applied for enteric coating. Other pharmaceutical applications are controlled release, colon targeting, microencapsulation and matrix former in *in situ* forming systems (Roda *et al.*, 2007; Phaechamud *et al.*, 2016). Additionally, bleached shellac possesses low water vapor and oxygen permeability including high glossy feature so that it can be used as moisture barrier forming film (Moseson *et al.*, 2008). However, it possible undergoes aging by self-esterification which loses solubility, decreases acid value and enhances glass transition temperature. Hence the storage of bleached shellac should be in temperature below 27°C. It should be protected from light, and probably incorporated with proper antioxidant (Annina, 2010).



**Fig. 1** Main compositions of shellac a) saleuritic acid b) butolic acid c) shellolic acid d) jalaric acid (Farag and Leopold, 2010)

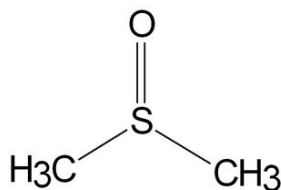


**Fig. 2** Chemical structures of shellac: jalaric acid;  $\text{R} = \text{CHO}$ ,  $\text{R}' = \text{CH}_2\text{OH}$ , laccijalaric acid;  $\text{R} = \text{CHO}$ ,  $\text{R}' = \text{CH}_3$  (Limmatvapirat *et al.*, 2007)

## 2.5.2 Solvent

### 2.5.2.1 Dimethyl sulfoxide (DMSO)

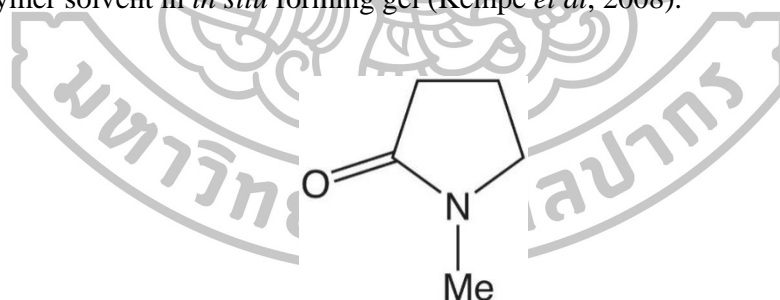
Dimethyl sulfoxide (DMSO),  $(\text{CH}_3)_2\text{SO}$  as shown in Fig. 3, is an organosulfer compound which is miscible to water and organic solvents. It has boiling point and melting point at  $189^\circ\text{C}$  and  $19^\circ\text{C}$ , respectively. At room temperature, DMSO generally presents a colorless liquid. In term of toxicity, it is safe for human ( $\text{LD}_{50}$  14,500 mg/kg in rat) (Brobyn, 2012). DMSO is therefore employed in medical use for reducing the topical pain, promoting the recovery of wounds, burns muscle and skeleton injuries, including intravenous administration for lowering abnormally high blood pressure in brain and for treatment of bladder infection (Geiss, 2001). Furthermore, DMSO plays an essential role in pharmaceutical field. Topical pharmaceutical formulations commonly establish DMSO as a penetration enhancer (Marren, 2011). It has been a polymer vehicle in *in situ* forming implant (Parent *et al.*, 2013) and ISM (Voigt *et al.*, 2012) as well.



**Fig. 3** Chemical structure of dimethyl sulfoxide (DMSO),  $C_2H_6SO$

### 2.5.2.2 *N*-methyl-2-pyrrolidone (NMP)

*N*-methyl-2-pyrrolidone (NMP), 1-methyl-2-pyrrolidone, or M-pyrrole is an organic compound with 5-membered lactam structure ( $C_5H_9NO$ ) as shown in Fig. 4. This chemical structure presents non-polar carbons or a large planar nonpolar region which possibly leads hydrophobic interactions, especially between NMP and some lipophilic drugs (Sanghvi, 2008). Additionally, a carbonyl functional group can bond with hydrogen atom from other molecules e.g. water, allowing it to perform as a co-solvent (Jouyban *et al.*, 2010; Lui and Venkatraman, 2012). Therefore NMP is not only miscible to some classical organic compounds such as ethyl acetate, chloroform, and benzene but also water. The melting point and boiling point of NMP are  $-24^{\circ}C$  and  $202-204^{\circ}C$ , respectively. Generally, its physical appearance is colorless to slightly yellow with a faint amine odor. Other properties of this organic vehicle include low volatility, low flammability and low toxicity ( $LD_{50}$  3,914 mg.kg in rat) (Jouyban *et al.*, 2010). NMP has been used in different fields, especially pharmaceuticals and medicines, due to its biodegradability. In pharmaceutical industry, it is widely used as solubilizing excipient (Stickley, 2004), penetration enhancer in transdermal products (Rachakonda *et al.*, 2008; Godavarthy *et al.*, 2009), a polymer solvent in *in situ* forming gel (Kempe *et al.*, 2008).

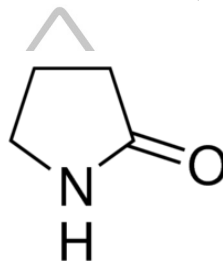


**Fig. 4** Chemical structure of *N*-methyl-2-pyrrolidone (NMP),  $C_5H_9NO$

### 2.5.2.3 2-pyrrolidone (PYR)

2-pyrrolidone (PYR),  $C_4H_7NO$ , is a chemical compound with a five-membered lactam as shown in Fig. 5 that presents a high-polar property, allowing it to be miscible with a wide variety of other solvents such as water, ethanol, diethyl ether, chloroform, benzene, ethyl acetate and carbon disulfide. Although it is an excellent solvent, the somewhat labile proton on the nitrogen limits its applications as an aprotic solvent (Budavari, 1996). The melting point and boiling point of this solvent is at  $25^{\circ}C$  and  $245^{\circ}C$ ,

respectively. Its apparent is a colorless to slightly yellow liquid with an unpleasant ammonia-like odor above (25°C) (Daubert and Danner, 1997). It has no teratogenic effect, no carcinogenicity, low toxicity (LD50 3288 mg/kg in rat), low acute toxicity in mammals with oral, and slight irritation at injection sites. Nevertheless, the derivatives of PYR has been reported that skin irritation is low (Sasaki *et al.*, 1990). The chemical and physical properties of PYR make it a unique solvent for certain applications and a useful chemical intermediate (Daubert and Danner, 1997). In pharmaceutical research, PYR is used as a plasticizer, solubilizing enhancer (Jain and Yalkowsky, 2007), penetration enhancer on transdermal drug delivery (Sasaki *et al.*, 1988), and polymer solvent in *in situ* forming gel system (Parent *et al.*, 2013) and ISM (Kranz *et al.*, 2001).



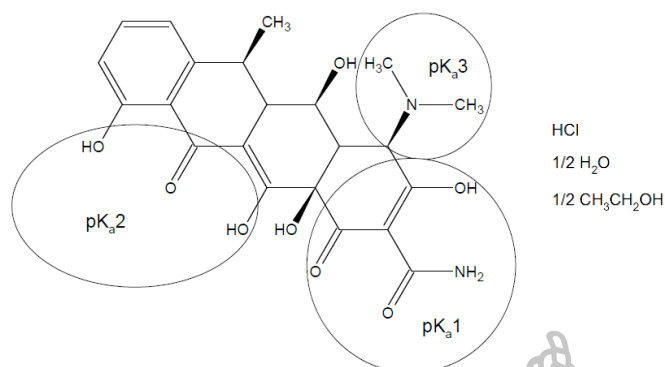
**Fig. 5** Chemical structure of 2-pyrrolidone (PYR), C<sub>4</sub>H<sub>7</sub>NO

## 2.5.3 Drug

### 2.5.3.1 Doxycycline hyclate

Doxycycline presents itself in three forms: hyclate, monohydrate and hydrochloride. From the doxycycline hyclate is possible to convert to other forms. The way hyclate dissolved in water and neutralized with sodium hydroxide becomes doxycycline monohydrate. This form with the addition of hydrochloric acid becomes doxycycline hydrochloride. The doxycycline hyclate (Fig. 6.) is the form hemihydrate and hemiethanolate (Naidong *et al.*, 1990). This drug presents the molecular formula (C<sub>22</sub>H<sub>24</sub>N<sub>2</sub>O<sub>8</sub>·HCl)<sub>2</sub>·C<sub>2</sub>H<sub>6</sub>O·H<sub>2</sub>O and molecular weight 1025.89 g.mol<sup>-1</sup> (Reynolds, 2007). The following pKa values for doxycycline hyclate as shown in Fig. 6: pKa<sub>1</sub> 3.02 ± 0.3; pKa<sub>2</sub> 7.97 ± 0.15; pKa<sub>3</sub> 9.15 ± 0.3 (Shariati *et al.*, 2009). The physical apparent of this antibiotic is hygroscopic yellow crystalline powder which should be stored in airtight containers and protected from light (Reynolds, 2007). Doxycycline is one of a broad-spectrum tetracycline antibiotics which inhibit bacterial protein synthesis through their link to the bacterial 30S ribosome, impeding access of aminoacyl-tRNA acceptor site in the mRNA-ribosome complex (Brunton *et al.*, 2006). However, it has been studied as an inhibitor of matrix metalloproteinases (intercellular substance), an action unrelated to its effects on bacterial protein synthesis (Skúlason *et al.*, 2003; Brunton *et al.*, 2006). The doxycycline hyclate is used to treat the infectious diseases e.g. respiratory tract infections, chronic prostatitis, sinusitis, syphilis, chlamydia, pelvic inflammatory disease, and also periodontal treatment (Brunton *et al.*, 2006; Ramesh *et al.*, 2010). The latter treatment has been reported that this antibiotic is active against infectious bacteria through bacteriostatic effect and also inhibits tissue collagenase activity at target site (Yu *et al.*, 1993; Seymour and Heasman, 1995a). The oral regimen for periodontitis is 250 mg doxycycline hyclate four time a day for up to 9 months, the dose of local treatment depended on the shape, size and number of pocket

(Polson *et al.*, 2008). Doxycycline has been used in pharmaceutical research such as *in situ* forming gel (Gad *et al.*, 2008), and in commercial product, Atridox<sup>®</sup> as well.

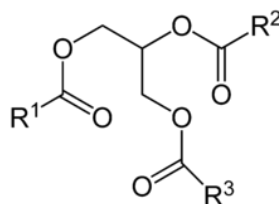


**Fig. 6** Chemical structure of doxycycline hyclate, (C<sub>22</sub>H<sub>24</sub>N<sub>2</sub>O<sub>8</sub> · HCl)<sub>2</sub> · C<sub>2</sub>H<sub>6</sub>O · H<sub>2</sub>O

## 2.5.4 External phase

### 2.5.4.1 Olive oil

Olive oil is a liquid fat established from the fruit of olive tree, *Olea europaea*, a primitive tree from Mediterranean region (Wahrburg *et al.*, 2002). It has been commonly used as the emollients, laxatives, nutritive, sedatives and tonics. In specific conditions this drug is traditionally treated the colic, alopecia, paralysis, rheumatic pain, hypertension and inflammatory (Gilani *et al.*, 2005; Visioli *et al.*, 2002). The components of olive oil are complex which the main chemical structure can be illustrated as in Fig. 7. The major categories of compositions which contribute to inhibit oxidative stress include oleic acid, phenolic compounds and squalene (Owen *et al.*, 2000). Many *in vivo* and *in vitro* studies have reported that phenolic compounds, mainly hydroxytyrosol, oleuropein and tyrosol, have significantly beneficial effects on inflammation, antioxidant status, and antimicrobial activity against bacteria, fungi and mycoplasma (Ciecerale *et al.*, 2012). Hydroxy tyrosol and oleuropein contain a catechol group which can exhibit an antioxidant by stabilizing free radicals through the formation of intramolecular hydrogen bonds (Visioli *et al.*, 2002). Additionally, a derivative of phenolic compound called oleocanthal is homologous with non-steroidal anti-inflammatory drug (NSAID) such as ibuprofen (Beauchamp *et al.*, 2005). It therefore shows a similar pharmacological activity prior to inhibit the same cyclooxygenase enzymes in the prostaglandin-biosynthesis pathway (Beauchamp *et al.*, 2005; Yamada *et al.*, 2008). In drug delivery systems, olive oil has been commonly used as oil base in emulsion for injection in neonates (Webb *et al.*, 2008), skin enhancer (Patel *et al.*, 2010) and lipid nanoemulsions (Nanjwade *et al.*, 2013).



**Fig. 7** Chemical structure of olive oil,  $R_1$  = oleic acid,  $R_2$  = linoleic acid and  $R_3$  = palmitic acid are alkyl group (20%) or alkenyl group (80%)

#### 2.5.4.2 Glyceryl monostearate

Glycerol monostearate (GMS) is an organic molecule (Fig. 8). The physical appearance of GMS includes colorless, odorless and sweet-tasting flaky powder. It has been used in food additive, cosmetics and controlled drug delivery system. GMS is lipophilic non-ionic surfactant with HLB 3.6-4.2 that can improve the physical stability and injectability of ISM based on PLGA to be stable for 12 h (Voigt *et al.*, 2012).



**Fig. 8** Chemical structure of glyceryl monostearate (GMS),  $C_{21}H_{42}O_4$

## 2.6 Evaluation

The concept of evaluation methods in this research had been introduced in chapter 4 before describing the result and discussion. However, some particular characterizations such as relative viscosity, viscoelasticity, and mechanical properties requires intensive basic knowledge in order to interpret the complicated data efficiently.

### 2.6.1 Relative viscosity

Relative viscosity ( $\eta_{rel}$ ) or also known as “solution solvent viscosity ratio” is ratio of the viscosities of the polymer solution and of the pure solvent at the same temperature. Relative viscosity ( $\eta_{rel}$ ) can be expressed in the following equation 1.

$$\eta_{rel} = \frac{\rho(Ct - \frac{E}{t^2})}{\rho_0(C_0t_0 - \frac{E_0}{t_0^2})} \quad [1]$$

Where:  $\rho$  = density,  $C$  = tube calibration constant (cSt/s),  $E$  = kinetic energy correction constant (cSt.s<sup>2</sup>), and  $t$  = flow time (sec).

In practical, viscosity of polymer solution with known concentration will be measured compared with viscosity of pure solvent. The value of both viscosities is determined by measuring flow time using viscometer e.g. Oswald viscometer or Ubbelohde viscometer. Therefore relative viscosity ( $\eta_{rel}$ ) can be calculated from equation 2.

$$\eta_{rel} = \frac{\eta_{solution}}{\eta_{solvent}} = \frac{t}{t_0} \quad [2]$$

Where:  $t_0$  = flow time of pure solvent,  $t$  = flow time of polymer solution (McNaught and Wilkinson, 1997). This parameter was employed to clarify the role of solvents on drug release form *in situ* forming systems (Kranz and Bodmeier, 2008).

Additionally, the relative viscosity ( $\eta_{rel}$ ) can be applied to calculate other parameters, which are for polymer quality control, such as logarithmic viscosity number, specific viscosity, reduced viscosity, intrinsic viscosity, K-value and molar mass (g/mol); the mass of a given substance divided by its amount of substance (Honek *et al.*, 2005). The intrinsic viscosity, practically calculated from the value of relative viscosity, was used to predict the release profile from matrix tablets tailored with individual types of polymer (Körner *et al.*, 2009) and also the pattern of protein release from matrices casted from polymer solution with different solvents (Madsen *et al.*, 2015)

### 2.6.2 Viscoelastic behavior from rheology studies

Viscoelasticity is established of two words: viscosity and elasticity. Viscosity is a fluid property and is a measure of resistance to flow. Elasticity is a solid material property. Therefore, a viscoelastic material possesses both fluid and solid properties. The behavior of material with viscoelasticity depends on time, so called “time-dependent material” (Özkaya *et al.*, 2012).

Almost biological materials including polymer plastics exhibit gradual deformation and recovery when they are subjected to loading and unloading at high temperature. Their response depends on the magnitude and rate of the stress which is applied to or removed from the material prior to deformation (Özkaya *et al.*, 2012). Hence, the stress-strain relationship for a viscoelastic material is a function of the time or the rate at which the stresses and strains are employed in the material. Viscoelastic body can store some of the energy which supplied to deform the shape (strain energy), and release the remainder as heat. This situation presents the hysteresis loop which is an area enclosed by the loading and unloading paths, in stress-strain diagram. It represents the energy dissipated as heat during the deformation and recovery phases, and it also increases the temperature of the material. Additionally, the hysteresis loop points out that viscoelastic materials can remember the history of deformations when they undergo and react by time (Özkaya *et al.*, 2012). In other words, they will return to its original shape or an elastic response after removal the load, and that response may take time which describes a viscous component (Vincent, 2012).

The performance of viscoelastic materials can be investigated by two major categories of experiment: transient and dynamic. Transient experiments involve the creep experiment and the stress-relaxation experiment, which belong to the deformation of material by simple elongation and by time, respectively. On the other hand, dynamic experiment is an oscillatory response that either harmonic stress or strain (usually strain) is varied with time sinusoidally, and the response is monitored at a range of different frequencies of deformation. Mathematics for the creep and stress-relaxation models rely on



linearity of response which considerably appropriates for strains at less than 0.01. However, all biological materials normally respond in nonlinear type and function at strains more than 0.5. The attainable model of viscoelasticity at large strains therefore remains the oscillatory approach (Vincent, 2012).

The basic concept of an oscillatory test is an induction of sinusoidal shear deformation in the samples in order to measure the stress response as a resultant. The oscillation frequency ( $\omega$ ) of the shear deformation determines the time scale probed. In a typical experiment, the specimen is loaded between two plates as shown in Fig 9 a. The top plate stands stationary whereas a motor rotates the bottom plate, thereby setting a time dependent strain ( $\gamma$ ) on the sample. Meanwhile, the time dependent stress ( $\sigma$ ) is quantified by measuring the torque that the sample places on the top plate. This time dependent stress ( $\sigma$ ) response at a single frequency suddenly presents major difference between materials e.g. elastic solid, viscous fluid and viscoelastic material as shown in Fig 9 b. All types of materials possess the same strain input ( $\gamma$ ) as in equation 3. (Macosko, 1994; Larson, 1999)

$$\gamma = \gamma_0 \sin(\omega.t) \quad [3]$$

If the material in a sinusoidal oscillatory test is ideally elastic solid, stress ( $\sigma$ ) response would be in phase:

$$\sigma = \sigma_0 \sin(\omega.t) \quad [4]$$

For an ideally viscous fluid (Newtonian), the stress ( $\sigma$ ) response lags  $\pi/2$  radians behind the strain ( $\gamma$ ) input and they are out of phase:

$$\sigma = \sigma_0 \sin(\omega.t - \frac{\pi}{2}) \quad [5]$$

Viscoelastic materials behave somewhere in between these cases that contain both in-phase and out-of-phase and their response is described by:

$$\sigma = \sigma_0 \sin(\omega.t - \delta) \quad [6]$$

The viscoelastic behavior of the system at  $\omega$  is characterized by the storage modulus ( $G'$ ) and the loss modulus ( $G''$ ) which respectively characterize the solid-like and fluid-like, respectively contributions to the measured stress response.

$$\sigma = \sigma_0 \cos\delta \sin(\omega.t) + \sigma_0 \sin\delta \cos(\omega.t) \quad [7]$$

$$\sigma = G' \gamma_0 \sin(\omega.t) + G'' \gamma_0 \cos(\omega.t) \quad [8]$$

Where  $\sigma_0 \cos\delta$  is the first magnitude in phase with strain or  $G'$

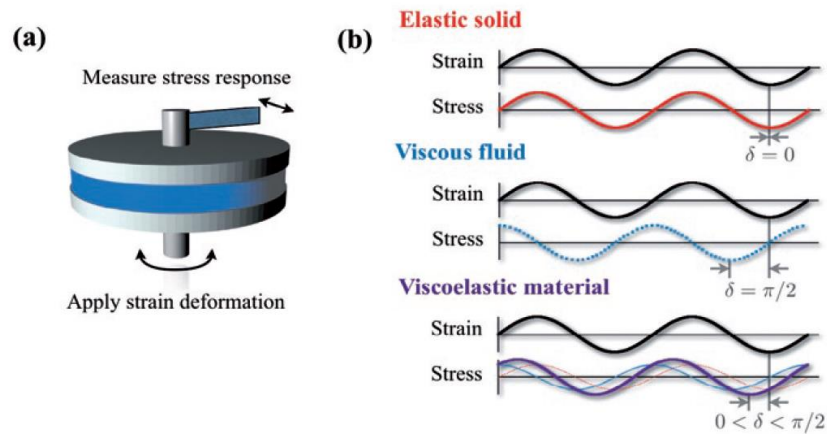
$\sigma_0 \sin\delta$  is the second magnitude which is  $90^\circ$  out of phase with strain or  $G''$

Also, the loss modulus ( $G''$ ) can also be defined in terms of loss tangent ( $\tan\delta$ )

$$\tan\delta = \frac{G''}{G'} \quad [9]$$

However, the summation of shear modulus can be express in a complex shear modulus ( $G^*$ ) (Osswald and Menges, 2003; Ward and Sweeney, 2004; Meyers and Chawla, 2009).

$$G^* = G' + G'' \quad [10]$$



**Fig. 9** (a) Schematic representation of a typical rheometer, with the sample loaded between two plates. (b) Schematic stress response to oscillatory strain deformation for an elastic solid, a viscous fluid and a viscoelastic material (Wyss *et al.*, 2007)

The principle of viscoelastic materials has been applied in biomaterial and pharmaceutical sciences. For instances, the hydrophilic polyvinyl alcohol (PVA)-based hydrogel (so called “PB hydrogel”) was modified by adding cellulose nanoparticles (CNPs) (e.g. cellulose crystals, cellulose nanofibers), or borax. The study underlying characterized the dynamic rheological behavior of the obtained hydrogels and explored the plausible mechanism for the multi-complexation between compositions in order to understand the relationship between 3D network structure and hydrogel properties. Borax functioned as a reversible intermediate between PVA and CNPs. The incorporation of well-dispersed CNPs to PB systems significantly enhanced the viscoelasticity and stiffness of hydrogels including self-recovery behavior. This novel biomaterial further applied for artificial muscles, bio-actuators, soft machines, tissue scaffolds and drug delivery devices (Han, *et al.*, 2014). In thermo-sensitive drug delivery system, the poloxamer *in situ* forming hydrogel was optimized mechanical properties and mucoadhesive force by incorporating the hyaluronic acid (HA). The viscoelastic analysis revealed that the addition of HA delayed the gelation temperature without interfering the self-assemble process of poloxamer and HA also increased the strength of gel structure by interacting with micelles through hydrogen bonds. Consequently, the platform was able to prolong and control drug release for more than 6 h (Mayol *et al.*, 2008).

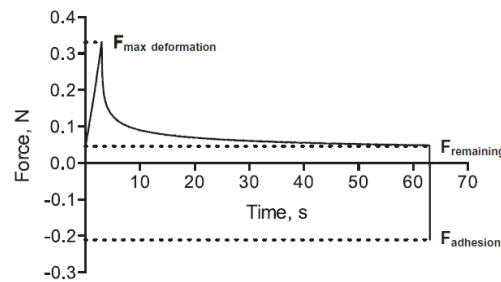
### 2.6.3 Mechanical analysis

Material properties are inferred from the resulting mechanical response upon the applying stress or strain. Mechanical tests generally involves the deformation or breakage of regimens (Ashby and Jones, 1996). When a force is accounted on a solid material, it may result in the strength, tension, hardness, translation, rotation, or deformation which constitutes both change in shape, *distortion*, and change in size/volume, *dilatation* (William and Callister, 2004). The results of those tests are applied for two elementary purposes: 1) engineering design for new materials, and 2) quality control to verify the manufacturing process or to confirm the product specifications (Ashby and Jones, 1996).

Material deformation can be temporary or permanent. The temporary deformation disappears after removal of the applied forces i.e. the deformation is recoverable, that inferred to elastic deformation. Whereas permanent deformation is irreversible i.e. stays even after removal of the applied forces, that defined as plastic deformation. When a material is subjected to applied forces, the material initially performs elastic deformation followed by plastic deformation (William and Callister, 2004).

The ability of material to oppose the applied force without any deformation is expressed in two ways, i.e. strength and hardness. Strength is defined in many ways as per the design requirements, while the hardness may be defined as resistance of a material to penetration. Methods to evaluate the hardness can be divided into three primary categories: 1) Scratch Tests, 2) Rebound Tests, and 3) Indentation Tests (Ashby and Jones, 1996). The popular method for characterizing the mechanical properties of composite materials such as hydrogel, matrix and etc. belongs to indentation tests (Aherane *et al.*, 2008).

Indentation tests practically generate a permanent compact in the surface of material. The force and size of the impression relates to a quantity which probably refers to hardness (Ashby and Jones, 1996). This technique operates by inserting a probe (cone or cylinder) into a regimen at a single point with a predetermined displacement depth or alternatively depth of penetration of a probe under a constant load for a giving time, and measuring the response force. As the probe penetrates the sample, the material in its path is fractured and dissipated apart. The progress of the probe is retarded to an extent depending on the hardness of the material in its path, the adhesion of the material to its surface (which depends on the depth of penetration into material and the thickness of the needles, or angle of the cone, used). The monitoring data are recorded in term of force-displacement or force-time curve as illustrated in Fig. 10. (Aherane *et al.*, 2008; Do *et al.*, 2014). The profile obtains individual parameters e.g.  $F_{\text{max deformation}}$ ,  $F_{\text{remaining}}$  and  $F_{\text{adhesion}}$ . The maximum deformation force is the force measured at maximum probe penetration into the regimen. After that, the probe is held for 60 s and the remaining force is recorded. In this case, the adhesion force is the force with setup during the upward movement of the probe, indicating the invert direction of force which is labelled in negative value. The elasticity/plasticity of sample is detected by ratio of  $F_{\text{max deformation}}/F_{\text{remaining}}$ . High values represent high elasticity which low values imply high plasticity (Do *et al.*, 2014).



**Fig. 10** Force-time curve to determine the mechanical and adhesive properties of the implants (Do *et al.*, 2014)

The penetration test usually applied in food research as well as pharmaceutical research. For instances, the soft cheeses (e.g. Camembert, Coulommier, Munster) were penetrated by a cylindrical probe (5mm diameter at a speed of 10 mm/min to a depth of 10 mm). It found that the force at 10 mm penetration gave a high correlation with sensory firmness ( $r = 0.94$ ,  $n = 19$ ). The technique is, therefore, appropriated as rapid method for texture analysis in soft cheese (Hennequin and Hardy, 1993). In novel *in situ* forming implants, the formulation based poly (lactic-co-glycolic acid) (PLGA) was modified its limited adhesion to the surrounding tissue due to the accidental expulsion of implants from periodontal pockets. The mechanical analysis presented that the addition of different types and amounts of plasticizer (acetyltributyl citrate and dibutyl sebacate) including of adhesive polymers (hydroxypropyl methylcellulose, HPMC) significantly increased the stickiness of system and provided good plastic deformability. Overall, these depots were much more adhesive than prior systems, provided suitable plasticity and desired drug release patterns (Do *et al.*, 2014).



## CHAPTER 3

### MATERIALS AND METHODS

#### 3.1 Materials

#### 3.2 Equipment

#### 3.3 Methods

##### 3.3.1 Preparation of the injectable *in situ* forming systems from bleached shellac

###### 3.3.1.1 Preparation of the *in situ* forming gel systems from bleached shellac dissolved in various solvents

###### 3.3.1.2 Preparation of the *in situ* forming microparticle systems from bleached shellac dissolved in various solvents

##### 3.3.2 Evaluation of formula composition

###### 3.3.2.1 Density study

###### 3.3.3.2 Surface and interfacial tension study

###### 3.3.3.3 Rate of macroscopic phase separation of emulsion composition

###### 3.3.3.4 pH study

###### 3.3.3.5 The relative viscosity study

##### 3.3.3 Evaluation of *in situ* forming gel properties

###### 3.3.3.1 Evaluation of *in situ* forming gel systems before exposure to solvent exchange

###### 3.3.3.1.1 Appearance viscosity and rheological behavior studies

###### 3.3.3.1.2 Viscoelastic behavior studies

###### 3.3.3.1.3 Thermal property studies

###### 3.3.3.2 Evaluation of *in situ* forming gel systems during exposure to solvent exchange

###### 3.3.3.2.1 *In vitro* drug and solvent release studies

###### 3.3.3.2.2 Analysis of drug and solvent release data

###### 3.3.3.2.3 *In vitro* degradability study

###### 3.3.3.2.4 Rate of water diffusion into *in situ* forming systems study

#### 3.3.3.2.5 Solvent diffusion study

### 3.3.3.3 Evaluation of *in situ* forming gel systems after exposure to solvent exchange

#### 3.3.3.3.1 Mechanical property studies

#### 3.3.3.3.2 Powder X-ray diffraction study

#### 3.3.3.3.3 Determination of surface morphology

### 3.3.4 Evaluation of *in situ* forming microparticle properties

#### 3.3.4.1 Evaluation of *in situ* forming microparticle systems before exposure to solvent exchange

##### 3.3.4.1.1 Morphology studies of o/o emulsion

##### 3.3.4.1.2 Appearance viscosity and rheological behavior studies

##### 3.3.4.1.3 Viscoelastic behavior studies

##### 3.3.4.1.4 Thermal property studies

#### 3.3.4.2 Evaluation of *in situ* forming microparticle systems during exposure to solvent exchange

##### 3.3.4.2.1 Transformation of sol into microparticle study

##### 3.3.4.2.2 *In vitro* drug and solvent release studies

##### 3.3.4.2.3 Analysis of drug and solvent release data

##### 3.3.4.2.4 *In vitro* degradability study

##### 3.3.4.2.5 Rate of water diffusion into *in situ* forming systems study

##### 3.3.4.2.6 Solvent diffusion study

#### 3.3.4.3 Evaluation of *in situ* forming microparticle systems after exposure to solvent exchange

##### 3.3.4.3.1 Mechanical property studies

##### 3.3.4.3.2 Powder X-ray diffraction study

##### 3.3.4.3.3 Determination of Surface morphology

### 3.3.5 Statistical analysis

### 3.1 Materials

1. 2-Pyrrolidone (lot no. BCBG8182V, Fluka, Germany)
2. Agarose (Lot H7014714, Vivantis, Malaysia)
3. Amaranth
4. Bleached shellac (BS) (Ake shellac Co., Ltd., Lumpang, Thailand)

Acid value 70-95 mg

Loss on drying less than or equal 3.5%

Color index 2

5. Dialysis tube (Spectra / Por<sup>®</sup> membrane MWCO: 6,000-8,000, lot no. 32644, Spectrum Laboratories, Inc., Fluka, Swizerland)
6. Dimethyl sulfoxide (lot no. 1367140, Fluka, Switzerland)
7. Doxycycline hyclate (DX) (Batch No. 1303082, Huashu pharmaceutical corporation, Shijiazhuang, China)
8. Ethanol, Absolute (Lot no. G17W62, J.T. Baker, USA)
9. Glyceryl monostearate (PC Drug Co., Bangkok, Thailand)
10. Hexane, Grade AR (Lot no. 135157-1216, QReC, New Zealand)
11. *N*-mthyl-2-pyrrolidone (NMP) (lot no. A0251390, Fluka, New Jersey, USA)
12. Olive oil (Lot no. L4418R, Bertolli, Italy)
13. Potassium dihydrogen orthophosphate (lot no. E23W60, Ajax Finechem, Australia)
14. Sodium hydroxide (lot no. AF310204, Ajax Finechem, Australia)

### 3.2 Equipment

1. Analytical balance (Sartorisu model BP2100S and Sartorius model CP224S, Germany)
2. Attachable digital C-mount camera (Moticam2, Motic®, Chaina)
3. Brookfield viscometer DV-III ULTRA (Brookfield Engineering Laboratories. Inc., USA)
4. Differential scanning calorimetry (DSC) (Pyris Sapphire DSC, Standard 115V, Perkin Elmer instruments, Japan)
5. Digital camera (LG 4XHD, Korea)
6. Filter set & membrane filter 0.45  $\mu$ m
7. Freezer -20°C (Sanden, Intercool, Thailand)
8. Freeze dryer (Triad<sup>™</sup> Labconco, Missouri, USA)
9. Glass bottle pycnometer 10 mL
10. Goniometer (FTA 1000, First Ten Angstroms, USA)
11. Heating incubator (biocotek, Zhejiang, China)
12. High performance liquid chromatography (HPLC) (Agilent 1100 series, Agilent Technologies, USA)

13. HPLC column (Packing: ReproSil-Pur Basic C18, 5  $\mu$ m, 150x4.6 mm, Dr Maisch, Germany)
14. HPLC guard (EasyGuard Kit, C18, Dikma, USA)
15. Homogenizer (Ultra-Turrax T10 basic, IKA, Germany)
16. Hot air oven (Heraeus UT6760, Kendro laboratory; Germany)
17. Inverted microscope (Nikon DXM 1200, Japan)
18. Image frame work software (Nikon DXM 1200, Japan)
19. Laminar air flow hood (wiwatsan lab, Nonthaburi; Thailand)
20. Magnetic stirrer (Becthai Bangkok Equipment and chemical. Ltd, Bangkok, Thailand)
21. Magnetic stirrer (M6, Ingenieurbüro Cat M. Zipperer GmbH, Germany)
22. Micropipette 1mL, 5mL, 10mL
23. pH meter (Ultra Basic UB-10, Denver Instrument, Bohemia, New York)
24. Scanning electron microscope (Maxim 200 Camscan, Cambridge, England)
25. Shaking incubator Model SI4 (Shel Lab, Cornelius, USA)
26. Shaking incubator (HandyLAB®, NB205, N-Biotek. Inc., Korea)
27. Sonication bath (Transsonic T890/H, Elma, Australia)
28. Stereo zoom microscope (SMZ-171 Series, Motic, China)
29. Syringe connector (Qosina, USA)
30. Texture analyzer (TA.XT plus, Charpa Techcenter, Godalming, Stable micro Systems Ltd., UK)
31. Thermogravimetric analyzer (TGA) (Pyris/TGA, PerkinElmer, USA)
32. Ubbelohde calibrated viscometer (size 0C, CAT 9721-R53, CANNON®, USA)
33. Viscoelastic rheometer (Kinexus rheometer, model KNX 2100, Marvern, UK)
34. Water bath (Buchi Heating Bath B-490, New Hampshire, USA)
35. X-ray powder diffractometer (Miniflex II, Rigaku Corp. Tokyo, Japan)



### 3.3 Methods

The abbreviations of *in situ* forming systems have been defined in Table 1.

**Table 1** Definition of abbreviation in formulation

Abbreviation	Definition
ISG, gel	<i>In situ</i> forming gel
ISM, ism	<i>In situ</i> microparticle
DX	Doxycycline hyclate
DMSO, DM	Dimethyl sulfoxide
NMP, N	<i>N</i> -methyl-2-pyrrolidone
PYR, P	2-Pyrrolidone

#### 3.3.1 Preparation of the injectable *in situ* forming systems from bleached shellac

##### 3.3.1.1 Preparation of the *in situ* forming gel systems from bleached shellac dissolved in various solvents

The 30% w/w bleached shellac was dissolved in various solvents (DMSO, NMP or PYR) under intermittent stirring for 3 days to obtain the homogenous mixture. The 10% w/w doxycycline hyclate was dissolved in solvent before incorporated with bleached shellac. The final formulations of *in situ* forming gel are shown in Table 2.

**Table 2** Composition formula of *in situ* forming gel

Formula	Amount (%w/w)				
	Bleached shellac	Doxycycline hyclate	DMSO	NMP	PYR
DMSO gel	30	-	qs to 100	-	-
NMP gel	30	-	-	qs to 100	-
PYR gel	30	-	-	-	qs to 100
DXDM gel	30	10	qs to 100	-	-
DXN gel	30	10	-	qs to 100	-
DXP gel	30	10	-	-	qs to 100

### 3.3.1.2 Preparation of the *in situ* forming microparticle systems from bleached shellac with various solvents

Internal phase was prepared from *in situ* forming gel in 3.3.1.1. Individually, the external phase, GMS (5% w/w of external phase) was dispersed in olive oil at 80°C under continuous mixing until obtaining a clear solution. Then it was suspended to convert into the milky dispersion under ambient condition. ISM emulsion was manipulated in 2 syringes coupled with a connector. This comprised with constant volume ratios of external and internal phases at 1:1. The emulsification was achieved by back-and-forth movement of the syringe plungers for 50 mixing cycles for 1-2 min in 3 mL single-use syringe as previously described (Kranz and Bodmeier, 2008; Rungseevijitprapa and Bodmeier, 2009).

**Table 3** Composition formula of *in situ* forming microparticle

Formula	Amount (% w/w)						Olive oil	GMS
	Internal phase			External phase				
	Bleached shellac	Doxycycline hycalte	Solvent	DMSO	NMP	PYR		
DMSO ism	15	-	qs to 100	-	-	-	47.5	2.5
PYR ism	15	-	-	-	-	qs to 100	47.5	2.5
DXDM ism	15	5	qs to 100	-	-	-	47.5	2.5
DXP ism	15	5	-	-	-	qs to 100	47.5	2.5

### 3.3.2 Evaluations of formulation

#### 3.3.2.1 Density study

Density of liquid compositions were investigated by pycnometer. The accurate weight of samples in precise 10 mL pycnometer was determined under ambient temperature. All tests were performed in triplicate and calculated the density from equation 11.

$$\rho = \frac{m}{v} \quad [11]$$

#### 3.3.2.2 Surface and interfacial tension study

An automatic system of maximum liquid drop volume is a widely used method to measure the surface tension and interfacial tension of liquid compositions (Hartland *et al.*, 1974). Surface and interfacial tension were determined with pendant drop method using goniometer. The residual amount of liquid on the tip (diameter 0.9140 mm) was determined

in the air and quartz cell comprising olive oil to measure the surface tension and interfacial tension, respectively. The distilled water was used as a control for both couple studies. Total measurements were recorded in triplicate under room temperature.

### 3.3.2.3 Rate of macroscopic phase separation of emulsion composition

Solvent and olive oil were the emulsion compositions in the internal phase and external phase, respectively. The principle of emulsion is to assembly an incompatible couple parts with an emulsifier. This experiment aimed to measure the separation rate of compositions from these incompatible parts. The preliminary study of interaction between dyes and emulsion compositions i.e. olive oil or organic solvents demonstrated that amaranth was able to be dissolved in solvent only, and it provided more stable color than other dyes as well (data were not shown) therefore it was selected as a coloring maker for monitoring the separation rate of solvent from olive oil. To certainly analyze, all samples were suspended with 1 mg amaranth and loaded in 10 mL syringe. Each syringe was setup vertically in ambient condition. In process of separation, olive oil had arisen upward where the colored solvent moved downward. The rate of solvent separation from olive oil was correlated as following equation 12 at pre-determined time.

$$\text{Rate of solvent separation from the olive oil} = \frac{\text{Distance of solvent front diffusion (mm)}}{\text{time (min)}} \quad [12]$$

### 3.3.2.4 pH study

The pH value of pure solvents from *in situ* forming systems and doxycycline hyclate (5% and 10% w/w) dissolved in each solvent were measured using a pH meter in triplicate. All samples were compared with distilled water, phosphate buffer pH 6.8 and doxycycline hyclate dissolved in these two media.

### 3.3.2.5 Relative viscosity study

The viscosities of diluted polymer in each solvent were measured by using Ubbelohde calibrated viscosimeter (Size 0 C, Cannon®, USA) operating instructions for a given capillary at room temperature. Bleached shellac was dissolved in DMSO, NMP or PYR in the concentration range of 0.625-1.000 g/100 mL and sonicated the solutions for 1 day before test. The relative viscosity was calculated by equation 13

$$\eta_{rel} = \frac{\eta}{\eta_0} = \frac{t_{corrected}}{t_0 \text{ corrected}} \quad [13]$$

Where  $\eta$  and  $\eta_0$  are the viscosities of the polymer solutions and the solvents,  $t$  and  $t_0$  are the corrected flow times of the polymer solutions and solvents. It should start timing after sample flows down into capillary as the meniscus pass the upper mark and stop when the meniscus passes the lower mark. Generally, it recommends 3 timing which the difference should not be more than 0.2-0.4 sec (Kranz and Bodmeier, 2008; Körner *et al.*, 2009; Madsen *et al.*, 2015).

### 3.3.3 Evaluations of *in situ* forming gel properties

#### 3.3.3.1 Evaluations of *in situ* forming gel systems before exposure to solvent exchange

##### 3.3.3.1.1 Appearance viscosity and rheological behavior studies

The appearance viscosity and rheology of the prepared formula (ISG) was investigated using Brookfield DV-III Ultra programmable rheometer with spindles (CP-40 and CP-52) (n=3). Viscosity parameters were collected at different shear rate with 15 seconds equilibration time at every shear rate under room temperature. It had been reported that the flow property correlated with the viscosity. The viscosity about  $1 \times 10^4$  m Pas was adequate for a proper flow property (Sato *et al.*, 2012).

The flow parameters were characterized using the exponential formula (Martin, 1993):

$$F^N = \eta G \quad [14]$$

$$\text{Log } G = N \text{Log } F - \text{Log } \eta \quad [15]$$

Where F is shear stress, G is shear rate which a progressive shearing deformation is applied to some materials, N is an exponential constant and  $\eta$  is a viscosity coefficient (Martin, 1993).

##### 3.3.3.1.2 Viscoelastic behavior studies

The viscoelastic properties of *in situ* forming gels were assessed using a small-amplitude oscillatory shear experiment. The dynamic rheological behaviors, including dynamic strain sweep, dynamic frequency sweep and dynamic temperature sweep were investigated with Kinexus rheometer using plate-and-plate geometry (CP1/50 diameter 50 mm). For each measurement, to minimize shearing during sample loading, approximately 0.56 mL of each sample was carefully loaded onto the plate using a tablespoon and repeated three times.

###### Dynamic strain sweep

Dynamic strain sweep was first performed from 0.01 to 100% at  $\omega = 1.0$  Hz before the dynamic viscoelastic measurements. The storage modulus was recorded to define the linear viscoelastic region (LVR) in which the storage modulus is independent to the strain amplitude. Select a strain ( $\gamma$ ) in the serial oscillation tests which the dynamic oscillatory deformation of each sample was within the LVR.

###### Dynamic frequency sweep

The viscoelastic parameters (log mode), including shear storage modulus or elastic modulus ( $G'$ , “solid like”) and loss modulus or viscous modulus ( $G''$ , “liquid like”) as functions of angular frequency ( $\omega$ ) were measured over the range 0.1-10 rad/s at selected strain ( $\gamma$ ) of sample series under 25°C. The complex modulus ( $G^*$ ), complex viscosity ( $\eta^*$ ) and loss tangent ( $\tan \delta$ ) were calculated by equations 16-18, respectively (Han *et al.*, 2014).

$$G^* = \sqrt{G'^2 + G''^2} \quad [16]$$

$$\eta^* = \frac{G''}{\omega} \quad [17]$$

$$\tan \delta = \frac{G''}{G'} \quad [18]$$

#### Dynamic temperature sweep

The gelification temperature of the polymeric systems was investigated by monitoring the variation of the elastic and viscous moduli with the temperature in the range from 20-45°C, at a fixed frequency of 1 Hz, heating rate 50°C/min and selected strain ( $\gamma$ ) of sample series (Li *et al.*, 2001).

#### 3.3.3.1.3 Thermal property studies

Thermal properties of *in situ* forming gels with different solvents were determined by using the thermal gravimetric analysis (TGA) and differential scanning calorimetry (DSC). Both measurements were tested using in TGA (Pyris TGA, PerkinElmer, USA) and, DSC (Pyris Sapphire DSC, Standard 115V, Perkin Elmer instruments, Japan) respectively. TGA curve may provide the useful information regarding the thermal stability and composition of the sample under investigation (Patil *et al.*, 2012). TGA experiments were conducted in the temperature range from ambient temperature to 400°C. The constant heating rate was 5°C/min. The activation energies of crystallization and phase transformation of the samples were also measured by DSC experiments. For solid samples, the temperature range was ambient temperature to 300°C except bleached shellac was evaluated in the temperature range from ambient temperature to 100°C and -100°C to 300°C. For liquid samples, the temperature range was 100°C to 100°C. All DSC tests were studied at heating rates of 10°C/min which commonly used in thermal analysis by researchers (Lecomte and Liggat, 2008).

#### 3.3.3.2 Evaluation of *in situ* forming gel systems during exposure to solvent exchange

##### 3.3.3.2.1 *In vitro* drug and solvent release studies

One gram of the respective formulation was injected into dialysis tube (MW cut off 5000-8000) using a standard syringe and sealed with dialysis clip at the end of tube. Dialysis tube with sample was carefully added into bottle of 100 mL phosphate buffer pH 6.8 (simulated environment of gingival crevicular fluid) (Esposito *et al.* 1996) to initiate the solvent exchange and *in situ* forming formation. The bottles were vertically shaken at 37°C at 50 rpm. At pre-determined time points, the bulk fluid was completely withdrawn and replaced with a 10 mL fresh medium. The amount of drug and solvent in the samples was determined HPLC-spectrophotometrically at room temperature ( $\lambda = 273$  nm for doxycycline hyclate,  $\lambda = 220$  nm for solvents; Agilent 1100 series, Agilent Technologies, USA). All tests were performed in triplicate and the results were shown as mean values  $\pm$  standard deviation. A 20  $\mu$ L volume was injected onto a Dr. Maisch® C18, 5  $\mu$ m column using as the mobile phase which was acetonitrile/phosphate buffer mixture (15:85) at a flow rate of 0.8 mL/min for solvents and an acetonitrile/phosphate buffer mixture (40:60) at a flow rate of 1.5 mL/min for doxycycline hyclate. Solutions of DMSO, NMP or PYR

and doxycycline hyclate in phosphate buffer pH 6.8 of known concentrations were used to generate the calibration curves.

### 3.3.3.2.2 Analysis of drug and solvent release data

The data of *in vitro* drug and solvent release were analyzed by a nonlinear computer program, Scientist<sup>®</sup> for Windows, version 2.1 (MicroMath Scientific Software, SaltLake City, UT, USA). Different mathematical release equations are the essential tool for fitting the cumulative percentage of drug release profiles in range of 10% to 80%. Considerable models of mathematic equation for this experiment are power law, zero order, first order, and Higuchi's. The coefficient of determination ( $r^2$ ) and model selection criteria (msc) were parameters for indicating the degree of curve fitting (Micromath Scientist Handbook, 1995; Mahadlek, 2012).

### 3.3.3.2.3 *In vitro* degradability study

One gram *in situ* forming gels were filled in dialysis tube ( $M_{mix}$ ) containing 30% w/w of bleached shellac ( $M_o$ ) and were treated as described in Section 3.3.2.1. Along 45 days, *in situ* forming gels were withdrawn at pre-determined time intervals, washed with distilled water, weighed in the wet state ( $M_{wet}$ ), vacuum-dried to constant weight ( $M_{dry}$ ) and stored at  $-20^\circ\text{C}$  for further analysis. The study was conducted by triplicate.

The total *Mass Loss*, Bleached shellac (BS) *Mass Loss* and *Water Content* of the *in situ* forming gels were calculated using the following equation 19-21, respectively.

$$\% \text{ Total MassLoss} = \frac{M_{total} - M_{dry}}{M_{total}} \quad [19]$$

$$\% \text{ BS MassLoss} = \frac{M_o - M_{net\ dry}}{M_o} \quad [20]$$

$$\% \text{ WaterContent} = \frac{M_{wet} - M_{dry}}{M_{dry}} \quad [21]$$

Where  $M_{net\ dry}$  is the weight of dry sample without residual solvent and doxycycline hyclate (Boimvaser *et al.*, 2012).

### 3.3.3.2.4 Rate of water diffusion into *in situ* forming systems study

Water diffusion plays a crucial role for solvent exchange which is one another key mechanism of this research. The observation of water diffusion into gels was studied by filling each sample into transparent tube (diameter 6 mm) immersed in test tube containing with phosphate buffer solution pH 6.8 (15 mL). When water diffused into the gels, the apparent system was changed from transparent to opaque. The distance of water front diffusion (opaque front) was recorded at various time within 5 days. The rate of water diffusion into gels was correlated as diffusion distance and time as the following equation 22 (Mahadlek, 2012):

$$\text{Rate of water diffusion into the gels} = \frac{\text{Distance of water front diffusion (mm)}}{\text{time (min)}} \quad [22]$$

### 3.3.3.2.4 Solvent diffusion study

For checking the characteristic of solvent diffusion, experimental was setup to simulate an artificial periodontal pocket from agarose and was analyzed under stereo microscope (Motic SMZ-171 Series). Briefly, agarose was dissolved in boiling water (0.6% w/v), and the solutions were poured into petri dishes (diameter 4.5 cm). The gel formed upon cooling down to room temperature. At the center of the gels, cylindrical holes (diameter 6 mm) were made and filled with 150  $\mu$ L liquid formulation using a standard syringe (Do *et al*, 2014). To simply analyze, all samples were dyed with amaranth (0.1g/10mL). During solvent exchange, the change was captured with stereo microscope every 5 min within 30 min. Solvent fronts were measured for 5 zones in triplicate. The rate of solvent diffusion into agarose gels was correlated as following equation 23.

$$\text{Rate of solvent diffusion into the gels} = \frac{\text{Distance of solvent front diffusion (mm)}}{\text{time (min)}} \quad [23]$$

### 3.3.3.3 Evaluation of *in situ* forming gel systems after exposure to solvent exchange

#### 3.3.3.3.1 Mechanical property studies

The mechanical properties of the investigated *in situ* forming gels were determined with a texture analyzer (TA.XT plus, Charpa Techcenter, Godalming, Stable micro Systems Ltd., UK) using agarose gel with cylindrical hole as an artificial periodontal pocket. The preparation of agarose gel has been described previously in section 3.3.3.2.4. Upon solvent exchange exactly completed in 1 week, the *in situ* gel formed. At the end of gel transformation, a cylindrical probe (diameter 3 mm) was driven downwards at a speed of 0.5 mm/s. Once in contact with *in situ* forming gel, the applied force and displacement of the probe were recorded as a function of time. The position was held for 60 sec since penetration depth was 1.5 mm. Subsequently, the probe was driven upwards at a speed of 10 mm/s.

The force measured at maximum probe penetration into *in situ* forming gel is called the maximum deformation force ( $F_{max\ deformation}$ ). The remaining force ( $F_{remaining}$ ) is a force measured after 60s holding time. The ratio " $F_{remaining}/F_{max\ deformation}$ " is used as a measure for the elasticity/plasticity of *in situ* forming gel. High values indicate high elasticity, low values indicate high plasticity. Each experiment was repeated for 6 times and results are presented as mean values  $\pm$  standard deviation (Do *et al*, 2014).

#### 3.3.3.3.2 Powder X-ray diffraction study

The crystallinity of all solid compositions was determined using a powder X-ray diffractometer (Miniflex II, Rigaku Corp. Tokyo, Japan) with Ni-filtered Cu radiation generated in a sealed tube operated at 30 kV and 15 mA. The XRD patterns were measured at  $2\theta$  from 4-60 degree and scanning rate of 2 degree/sec at room temperature.

#### 3.3.3.3.3 Determination of surface morphology

The dried *in situ* gels were coated under an argon atmosphere with gold-palladium and then observed with a scanning electron microscope (Maxim 200 Camscan,

Cambridge, England) in order to examine the surface morphology after incubation in phosphate buffer pH 6.8 at 1, 7, and 45 days.

### **3.3.4 Evaluation of *in situ* forming microparticle properties**

#### **3.3.4.1 Evaluation of *in situ* forming microparticle systems before exposure to solvent exchange**

##### **3.3.4.1.1 Morphology studies of o/o emulsion**

The morphology of the ISM systems was determined by using an inverted microscope (Nikon DXM 1200, Japan). This experiment shown the effect of stabilizer concentration and volume phase ratio on emulsion droplet size. GMS, the stabilizer in external phase for oil in oil emulsion, was varied its amount from 0%, 1.25%, 2.5%, 3.75% and 5% w/w of external phase. ISM emulsion was manipulated with various volume ratios of external and internal phases. Two different series were prepared (ordinary series with 5% GMS of external phase or 2.5% of whole system: 1:9, 2:8, 3:7, 4:6, 5:5, 6:4, 7:3, 8:2 and 9:1 and series of fixed stabilizer as 2.5% w/w of system: 4.75:5, 5.75:4, 6.75:3, 7.75:2 and 8.75:1). The characteristic of ISM emulsion was studied by dropping samples onto slide and visually recorded the results every 10 seconds for 3 minutes. The average droplet size was analyzed by image frame work software (n=150; 3 regimens, 50 droplets per regimen) (Voigt *et al*, 2012).

##### **3.3.4.1.2 The other evaluations**

The evaluations of prepared oil in oil emulsion were performed with the methods as discussed in 3.3.3.1.1-3.3.3.1.3.

#### **3.3.4.2 Evaluation of *in situ* forming microparticle systems during exposure to solvent exchange**

##### **3.3.4.2.1 Transformation of emulsion into microparticle study**

The transformation was observed under the same condition as described in section 3.3.4.1.1 where phosphate buffer pH 6.8 approximately 60  $\mu$ L was dropped to sample with the same amount on the glass slide and recorded every 10 sec for 3 min.

##### **3.3.4.2.2 The other evaluations**

The evaluations of *in situ* forming microparticles were performed with the methods as discussed in 3.3.3.2.1-3.3.3.2.5.

#### **3.3.4.3 Evaluation of *in situ* forming microparticle systems after exposure to solvent exchange**

All evaluations of *in situ* forming microparticles were performed with the methods as discussed in 3.3.4.3.1-3.3.3.2.3.



### 3.3.5 Statistical analysis

Analysis of variance (ANOVA) and student *t*-test were used for statistical comparison. Samples were considered significantly different when  $p < 0.05$ .



## CHAPTER 4

### RESULTS AND DISCUSSION

#### Part 1

#### **4.1 Appearance of liquid formulations**

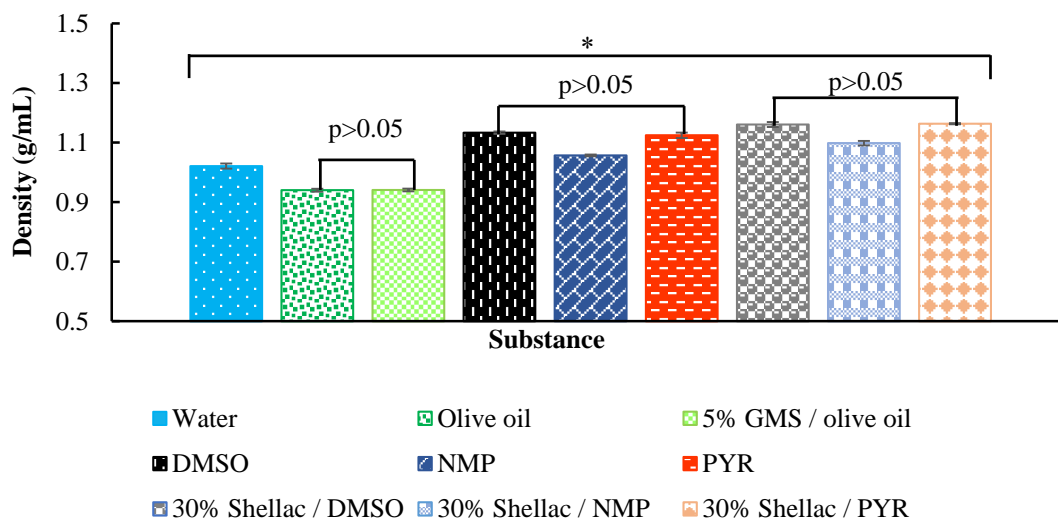
The internal phase was a brownish fluid due to natural color of bleached shellac while the external phase was a turbid dispersion under ambient temperature. The obtained prepared o/o emulsion appeared as a turbid yellowish homogeneous system.

#### **4.2 Evaluation of formulation composition**

##### **4.2.1 Density**

The density of substance has a substantial influence on a stability of emulsion. It is a major factor for instability processes of emulsion i.e. creaming, coalescence or flocculation which an emulsion separates into bulk internal and external phases. Those processes are well demonstrated by taking an emulsion of limited stability. Initially, for the internal phase with a density less than the external phase, a “rising” of the cream is observed. Then, as larger droplets rise and concentrate, they begin to appear at the top. Finally, the drops coalesce to form a separate layer of oil on top. Thus the difference of density between both phases should be minimized to inhibit a separation process (Becher, 1983).

The density of liquid compositions at room temperature is shown in Fig. 11. The control group in this study was distilled water which the apparent density was about 1.02 g/cm<sup>3</sup>. The oil samples had significantly lower density ( $p < 0.05$ ) (approximately 0.94 g/cm<sup>3</sup>) while the shellac solutions showed a higher unique density depending on type of solvents. Comparison among three solvents, DMSO and its bleached shellac solution had the highest density around 1.13-1.16 g/cm<sup>3</sup>. Similarly, density of PYR and its system was slightly lower. NMP systems showed the least significant density ( $p < 0.05$ ) around 1.05-1.10 g/cm<sup>3</sup>. According to these data, it might predict that emulsion from shellac solution in NMP should be more stable than other systems.



**Fig. 11** Density of liquid compositions at 25°C (n=3), \*  $p \leq 0.05$

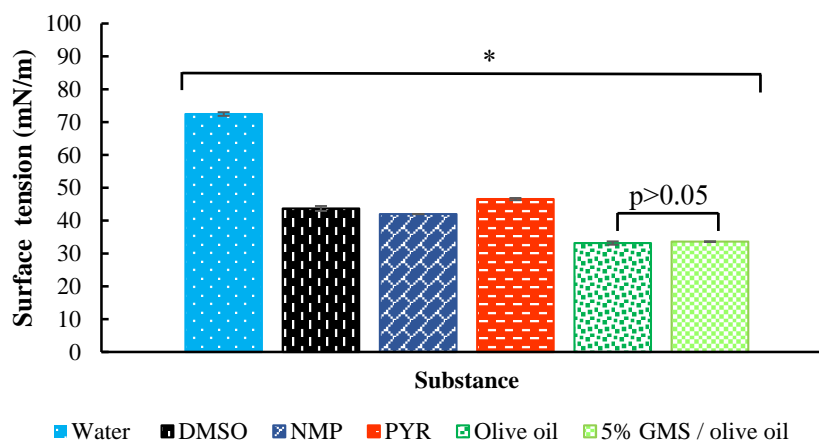
#### 4.2.2 Surface and interfacial tensions study

The determination of liquid/liquid interfacial tensions between internal phase and external phase is useful for understanding the stability of emulsions. Interfacial tension is a force required to change the shape of two liquids. The increased surface contact during emulsification increases the internal energy of the system and leads to an inherently unstable situation that attempts to rectify itself by coalescence of the two phases. Decreasing the interfacial tension between the two phases decreases the free energy and increases the inherent (thermodynamic) stability of the emulsion (Harkins *et al.*, 1915).

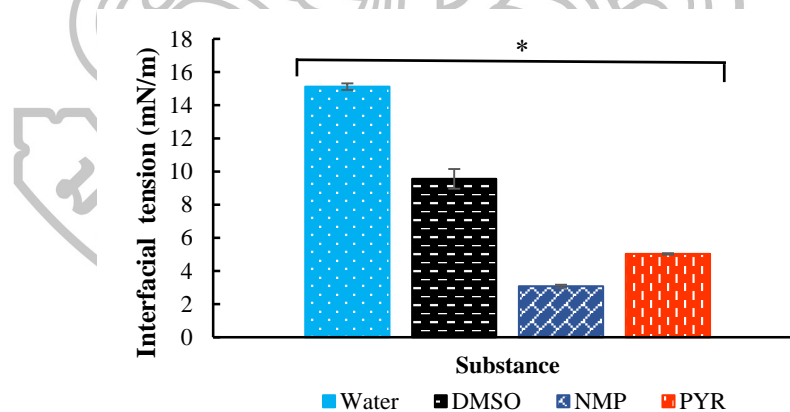
The relationship of liquid/liquid interfacial tension to emulsion stability was explored using a pendant drop method in this research. Data of surface tension (air/liquid interfacial tension) and density were determined initially to apply for determining the interfacial tension. The air/liquid surface tensions of some liquids compared with DI water (deionized water) at room temperature (25°C) are given in Fig. 12. The surface tension of deionized (DI) water was 72.8 m N/m which was significantly different ( $p < 0.05$ ) from that of used solvents (42.0-46.6 m N/m (PYR > DMSO > NMP)) whereas that of olive oil and GMS dispersed in olive oil was 33.1-33.6 m N/m, respectively.

The liquid/liquid interfacial tensions between solvents and olive oil along with data of DI water are compiled in Fig. 13. GMS dispersed in olive oil interfered the functioning of digital photography capture due to its turbidity thus there was no result between it and solvents. The interfacial tension of DI water and olive oil was 15.1 m N/m. For pure solvents, it was interesting to note that the interfacial tension of solvents between 42 and 47 significantly decreased ( $p < 0.05$ ) by increasing its density i.e. NMP 3.1 m N/m, PYR 5.0 m N/m and DMSO 9.6 m N/m, respectively. This can be explained by the density profile at the interface (Pichot, 2010). While the two pure immiscible liquids (olive oil and solvent) were mixed, a free energy increased in system. Combination system attempted to minimize its free energy. The density profile in the interface was obviously driven by the minimization of the free energy into the interface (Miller *et al.*, 2008). Materials in the interface would have the densities of intermediate values between the density of olive oil

and that of solvent. At the interface, each material can only interact with material of the same density. Usually, the density varies sharply in the interface. Interactions between materials having the same density are more probable at broad interface than at sharp interface. The sharper interface is, the greater density difference is (Cahn and Hilliard, 1958). Therefore, a system with small density gradient could proficiently minimize the free energy after dropping solvent into oil. NMP had the minimum interfacial tension hence it might be anticipated that emulsion from shellac solution in NMP should be more stable than other systems.



**Fig. 12** Surface tension of different solvents, olive oil and GMS-dispersed olive oil at 25°C (n=3), \*  $p \leq 0.05$



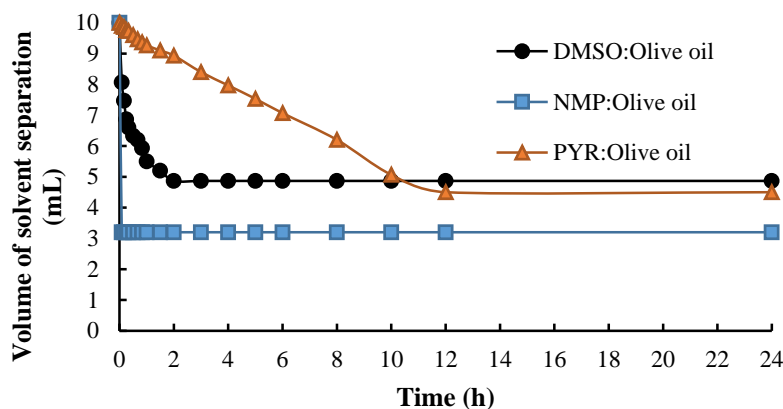
**Fig. 13** Interfacial tension of different solvents in olive oil at 25°C (n=3), \*  $p \leq 0.05$

#### 4.2.3 Rate of macroscopic phase separation of emulsion composition

The aim of this experiment is to compare the rate of macroscopic phase separation of the internal phase from the external phase (ratio of 1:1). The major compositions of each phase were solvent and olive oil, respectively. According to principle of emulsion, they should be completely incompatible when they were without stabilizer.

When the agitation was stopped and, these two phases separated under gravity, solvent would obviously fall down straight to the bottom (Walstra, 1993). This study could estimate the phase separation with correlation between volume of solvent separation and time. The final volume of DMSO and PYR front was approximately 5 mL while the final volume of NMP front was lower (Fig. 14). It might express in term of lipophilicity (log P) of each solvent i.e. DMSO (-1.35), NMP (-0.46) and PYR (-0.71) (Sangster, 1997). NMP has the minimum log P thus it was possibly partial compatible with olive oil. The rate of phase separation, was as following: NMP > DMSO >>> PYR. NMP completed its separation within less than 1 h. Therefore NMP had the highest rate which was explained from its partial miscibility with olive oil. When the partial miscibility between oil and NMP reached to equilibrium, the excess NMP molecules assembled back and rapidly fell downward to the bottom under gravity. Nevertheless, DMSO and PYR demonstrated the slower rate of phase separation which probably caused by appearance viscosity which would be further studied.

Although the results of density and interfacial tension implied that bleached shellac emulsion prepared with NMP should have the highest stability, the preparation of this emulsion practically failed by rapid phase separation before 30 min (critical time upon administration of dosage form) which had been report recently (Setthajindalert, 2012). To consider the volume of solvent separation, NMP was partial compatible with olive oil as seen from Fig. 14. When the internal and external phases are partially miscible, emulsion droplets may enlarge until eventual phase separation by Ostwald ripening. This process is irreversible and does not require any contact between droplets that differs from coalescence. Ostwald ripening is an important mechanism of instability in sub-micrometer emulsions (Aulton and Taylor, 2013). However, it can be avoided by the addition of a small amount of the immiscible second oil to the main partially miscible oil for decreasing molecular diffusion of this major component (Aulton and Taylor, 2013). Therefore the bleached shellac emulsion prepared from NMP was practically instable because its partial miscibility with oil resulting in growth to larger droplets at the expense of smaller ones or Ostwald ripening effect. Thus this research excluded NMP from ISM evaluation instead of adding the immiscible second oil because this might disturb the authentic behaviors of solvent and subsequently provoke a complicated interpretation.

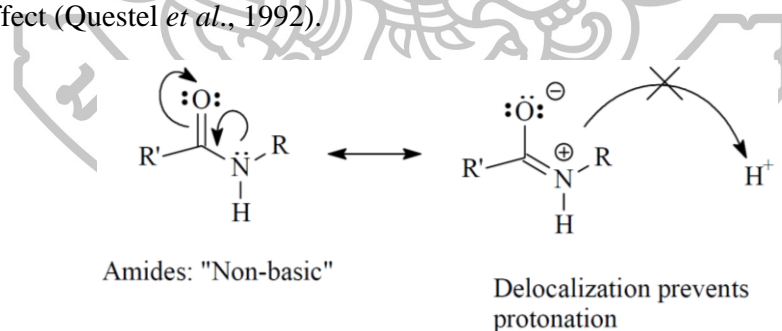


**Fig. 14** Volume of solvent separation during 24 h at 25°C (n=3)

#### 4.2.4 pH

pH study essentially measures the electro-chemical potential of hydrogen ions or the potential of hydrogen from a known liquid. It is used to specify the acidity or alkalinity of a solution (Lim, 2006). This research worked on *in situ* forming systems comprising shellac as matrix polymer for locally delivering doxycycline hyclate to periodontal pocket. Shellac, a biodegradable polyester type of resin, is soluble in alkaline solutions due to acidic character and also soluble in various organic solvents but insoluble in water. This finding has confirmed that hydroxyl, and carbonyl groups are present in shellac (Gardner *et al.*, 1929). Recently, the pH solubility profile demonstrated that shellac was completely dissolved at pH more than 7.0 (Limmatvapirat *et al.*, 2004). Polyester chain of shellac was prone to be hydrolyzed in alkaline environment. To measure pH of liquid compositions, it is a useful evidence to comprehend the phenomena in further studies such as dissolution, degradation and etc.

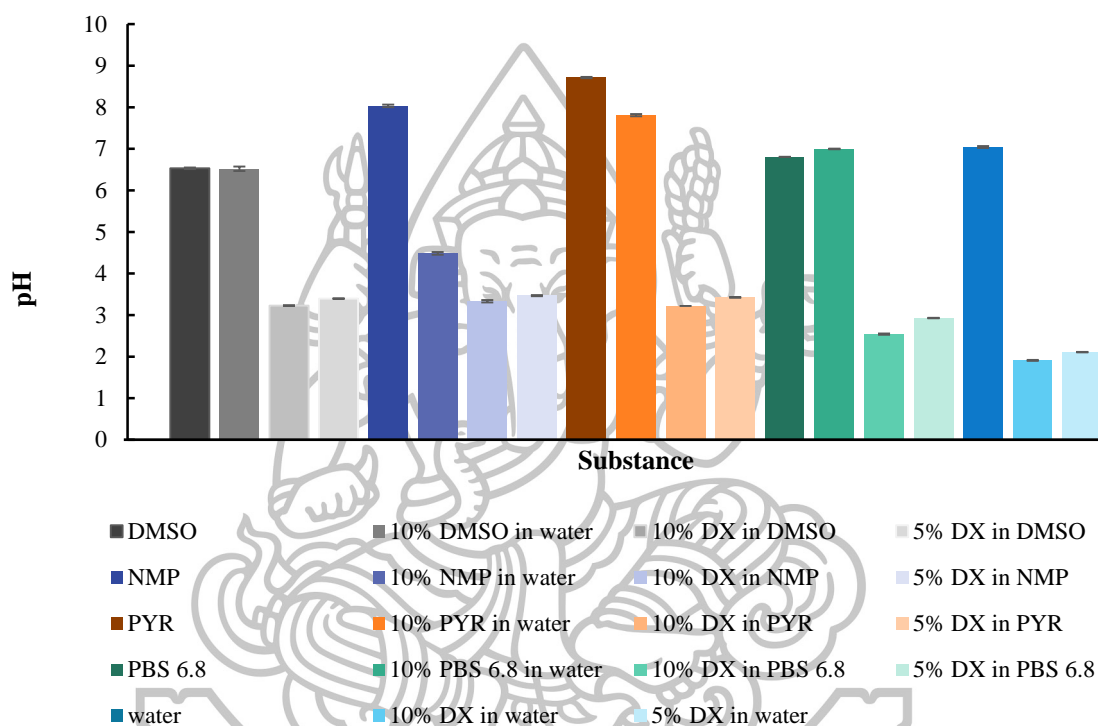
This work designed a pattern of pH measurement for 5 groups as shown in Fig. 16. A major aim was to definitely estimate a pH gradient of pure solvents, diluted solvents and their 5%, 10% w/v doxycycline hyclate solutions. These solvent collections were compared to two controls, deionized water and phosphate buffer pH 6.8. The pH value of DMSO, NMP, PYR, PBS 6.8 and DI water were 6.53, 8.03, 8.72, 6.81 and 7.04, respectively. PYR was a maximum alkaline liquid hence it showed an ability to dissolve shellac. Upon adding deionized water, 10% w/v DMSO showed the constant pH value while this value was decreased in diluted NMP and PYR. The change of pH value in 10% w/v NMP was from 8.03 to 4.48 and in 10% w/v PYR was from 8.72 to 7.81. In general, amides with coplanar structure are not basic because the entire electrons of nitrogen atom undergo the resonance effect thus there is no free electron to act as H-bond acceptors for water molecules (Fig. 15) (Deruiter, 2005). In case of NMP and PYR, their carbonyl group and lone pair electrons of nitrogen atom are not coplanar that do not cause the resonance effect. Therefore water molecules can protonate hydrogen atom to those electrons, resulting in an increase of acidity (Deruiter, 2005). NMP was less acidic than PYR owing to steric hindrance effect (Questel *et al.*, 1992).



**Fig. 15** Resonance effect of amides (Deruiter, 2005)

Each 5% w/v and 10% w/v doxycycline hyclate solution had successively higher acidity than pure and diluted solvents i.e. in DMSO (pH 3.23-3.40), NMP (pH 3.33-3.47), PYR (pH 3.22-3.43), PBS 6.8 (pH 2.54-2.93) and DI water (pH 1.91-2.11). The doxycycline hyclate solutions exhibited similar acidity among three organic solvents. Whereas they had less acidity than that in PBS 6.8 and DI water due to organic solvents themselves had higher pH and doxycycline hyclate partial ionized in them. Doxycycline hyclate is an un-ionized form of weak base which formed salt with hydrochloride, a strong acid including hemihydrate and hemiethanolate. The molecule of hydrochloride and ethanolate can protonate the hydrogen ions in solvent which increases the acidity (Pandit,

2007). To consider the preparation of *in situ* forming systems, doxycycline hyclate firstly dissolved in each organic solvent until homogeneous solution was obtained then shellac was added into the system. It might expect that shellac dissolved in that solution via strongly hydrogen bonding (Barton, 1990; McGowan-Jackson, 1992) between its carboxyl, hydroxyl and carbonyl groups and sulfoxide group (DMSO) or amine group (NMP, PYR) more than pH dependent solubility. Furthermore, the weak base groups of doxycycline might interact with weak acidic groups of shellac which affected the physical properties such as viscosity of *in situ* forming systems. Recently, these organic solvents had been used in fabrication of bleached shellac gels (Mahadlek, 2012; Phaechamud, 2016).



**Fig. 16** pH of organic solvents, PBS 6.8, DI water and their solutions at 25°C (n=3)

#### 4.2.5 Solubility parameter

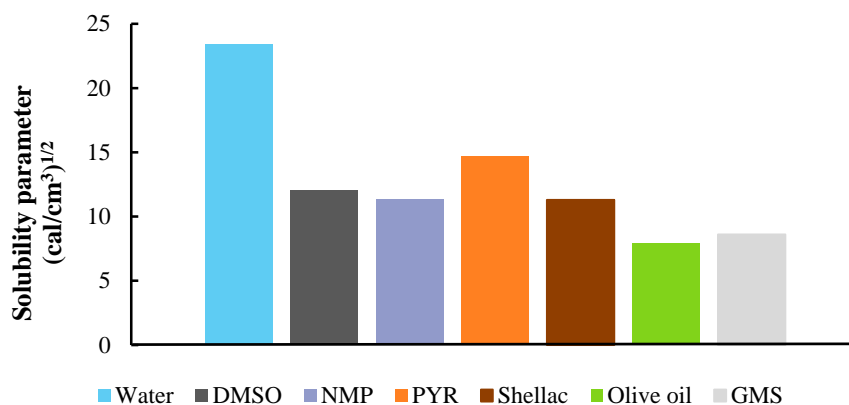
Hildebrand or one-component solubility parameter ( $\delta$ ) is a numerical value that indicates the relative solvency behavior of a specific solvent. This parameter can divide into three partial solubility parameters that are influenced from different forces such as dispersion force, permanent dipole, and hydrogen bonding. In case of miscibility between polymer and non-aqueous solvent, the solubility parameter should be consider as the total van der Waals force or dipole interaction which reflects in the simplest solubility value (Burke, 1984). However, polymer/aqueous solvent affinity can be discussed in term of hydrogen bonding. The van de Waals force is the sum of the attractive or repulsive forces between molecules due to induced electrical interactions (Oss *et al.*, 1980). The accurate predictions of solubility behavior depend on determining the degree of intermolecular attractions between molecules and in discriminating between different types of polarities

as well (Burke, 1984). Consequently, the solubility parameter is a useful tool for the prediction of the solubility of shellac in different organic solvents.

According to literature review (Hansen, 1967; Vaughan, 1985; Mishra, 1987; Jan and Bart, 2006), the solubility parameter of compositions was compared with water (Table 4, Fig. 17). All compositions were from both parts of *in situ* systems. There were shellac and organic solvents from the gel system or the internal phase whereas olive oil and GMS represented as components from the external phase. One component solubility parameter of shellac was equal to NMP (11.30) while this value of DMSO (12.00) and PYR (14.70) was higher than that of shellac. These three organic solvents could potentially dissolve shellac, especially NMP because the degree of intermolecular attractions and type of polarities between shellac and these solvents was apparently favorable. The molecular interaction in these solutions was not only by strongly hydrogen bond, but also by van der Waals forces among reasonable alkyl groups in both shellac and solvent. If degree and type of these molecular parameters did not harmonize, shellac did not dissolve in that solvent (Burke, 1984). In the cases of olive oil (7.87) and GMS (8.61) they had much lower solubility parameter than water (23.40) thus they were immiscible with water.

**Table 4** Solubility parameter of organic solvents, water and oil phase

Sample	Solubility parameter	Reference
Water	23.40	Vaughan, 1985
DMSO	12.00	Hansen, 1967
NMP	11.30	Hansen, 1967
PYR	14.70	Hansen, 1967
Shellac	11.30	Mahendra, 1987
Olive oil	7.87	Vaughan, 1985
GMS	8.61	Jan and Bart, 2006



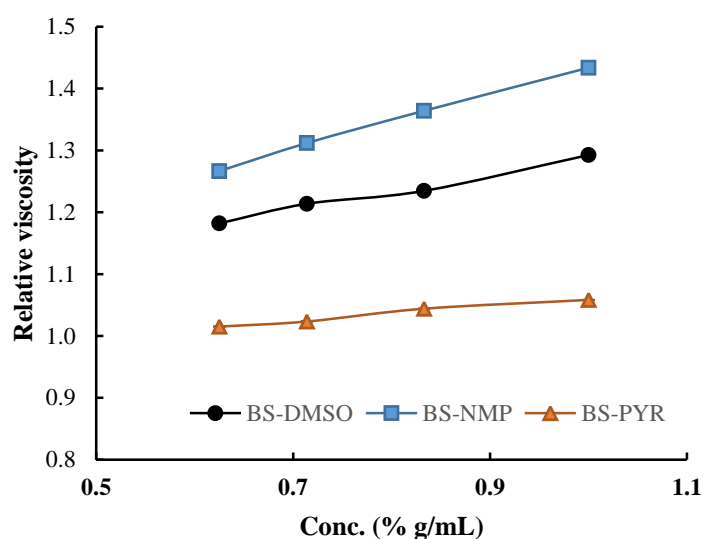
**Fig. 17** Solubility parameter of organic solvents, water and oil phase



#### 4.2.6 Relative viscosity study

Relative viscosity is self-explanatory, defined as the ratio of the solution viscosity ( $\eta$ ) to that of the solvent ( $\eta_s$ ) (Kurata *et al.*, 1989). This parameter carries out the interaction between polymer and solvent at dilute concentration of polymer. Polymer molecules present the different chain configuration owing to the affinity with the solvent. In diluted polymer solutions, the polymer/solvent interaction is highly outstanding therefore viscosity increases with increasing solvent power or good solvent. In contrast to higher polymer concentration, the viscosity of poor solvents is higher than of good solvents (Kaufman and Falcetta, 1977). For viscosity determination of low polymer concentration, this interaction could be examined using a capillary viscometer.

The relative viscosity of diluted samples in each solvent is presented in Fig. 18. The viscosity of bleached shellac in NMP was higher compared to that in DMSO and PYR, respectively. This evidence corresponded to solubility parameter from literature as previously described (Burke, 1984). Therefore NMP was a good solvent and it had the strongest interaction with bleached shellac. In the case of high polymer concentration, the apparent viscosity measurement should be performed to assure the solvent/bleached shellac interaction and forward to discuss on a solvent-exchange.



**Fig. 18** Relative viscosities of diluted bleached shellac solution in different solvents (n=3)

#### Summary

Because of minimum values for density and interfacial tension of NMP and close to those values of olive oil, the emulsion prepared with them should theoretically have the highest physical stability. However, its preparation practically failed by rapid phase separation before 30 min due to partial miscibility of NMP with olive oil resulting in Ostwald ripening effect. Therefore, this research excluded NMP from ISM evaluation whereas DMSO and PYR were employed for further investigation.

The pH measurement revealed that doxycycline hyclate solutions in organic and aqueous solvents were more acidic than pure solvents owing to protonation of acid salts (i.e. hydrochloride, hemihydrate and hemimethanolate) from drug. According to the acid character of shellac, it is reasonably soluble in alkaline solutions. In this research, bleached shellac therefore dissolved in organic solvents *via* strongly hydrogen bonding rather than pH dependent solubility. Furthermore, the molecular interaction in these solutions was also driven by van der Waal forces among alkyl groups in both shellac and solvent as literally mentioned in solubility parameter review. The values of solubility parameter of NMP and shellac were identical hence NMP was the fittest solvent for dissolving. The relative viscosity study also confirmed that NMP was a good solvent and it powerfully interacted with bleached shellac.



## Part 2

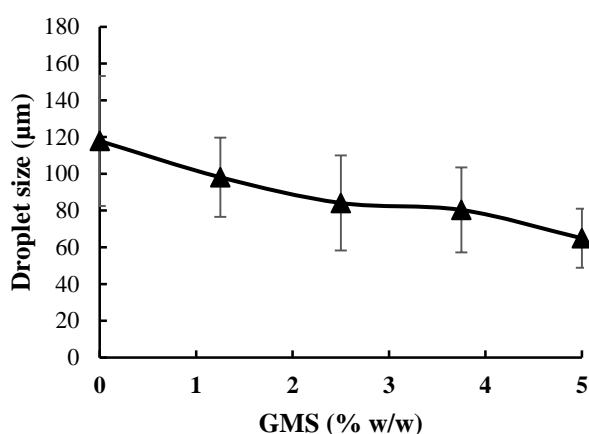
### 4.3 Evaluation of *in situ* forming system properties

#### 4.3.1 Evaluation of *in situ* forming systems before exposure to solvent exchange

##### 4.3.1.1 Morphology studies of o/o emulsion

##### Effect of stabilizer concentration on droplet size

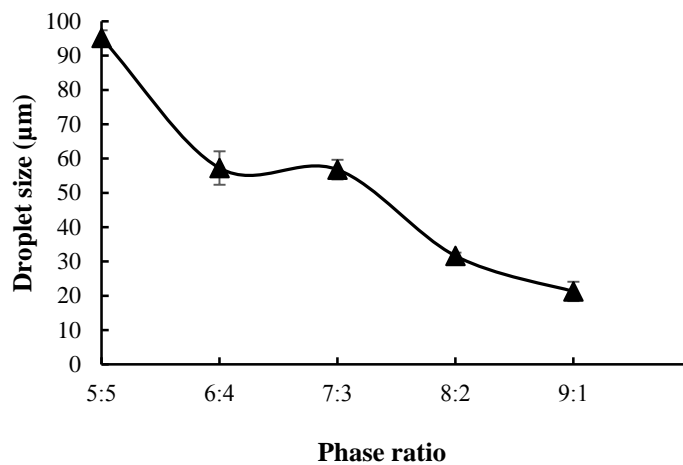
The average droplet size of emulsion with phase ratio of 1:1 internal phase: external phase was significantly decreased ( $p < 0.05$ ) from approximate 118  $\mu\text{m}$  to 65  $\mu\text{m}$  when the amount of GMS in the external phase was increased from 0 to 5% (Fig. 19). This circumstance clarified that GMS was able to gel the vegetable oils by forming its network (Chen and Terentjev, 2009; Daniel and Marangoni, 2012) remaining intact upon emulsification in non-aqueous ISM emulsion containing 5% GMS, and it also decreased a droplet coalescence of emulsions (Chen and Terentjev, 2009; Hodge and Rousseau, 2005).



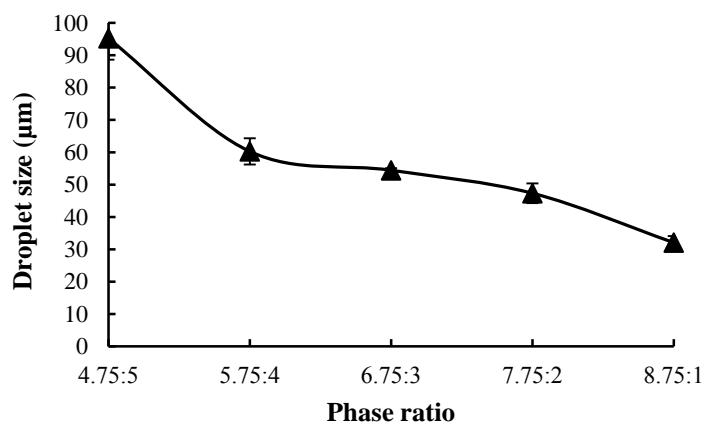
**Fig. 19** Droplet size of o/o emulsion with various concentrations of GMS at phase ratio 1:1 (n=150)

##### Effect of phase ratio on droplet size

When the amount of the external phase was increased from 1:1 to 9:1 (Fig. 20) and 4.75:5 to 8.75:1 (Fig. 21), the emulsion droplet size of 2-pyrrolidone systems with and without the constant concentration of stabilizer tended to be significantly decreased ( $p < 0.05$ ) from approximately 95  $\mu\text{m}$  to 30  $\mu\text{m}$  as shown in Figs. 20 and 21. For the environment of higher quantity of the internal phase, the particles were easier to merge together resulting in the coalescence (Tcholakova *et al.*, 2002). At phase ratio of 7:3 (external phase: internal phase) for both cases, ISM emulsion size was approximately 55  $\mu\text{m}$  (Fig. 20). Thus, the phase ratio dominantly affected the size of o/o emulsion.



**Fig. 20** Droplet size of o/o emulsion at various phase ratios (n=150)



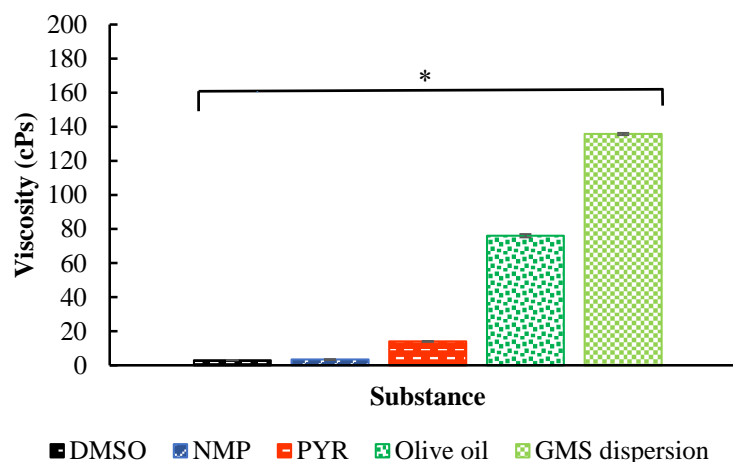
**Fig. 21** Droplet size of o/o emulsion with constant GMS concentration at various phase ratios (n=150)

#### 4.3.1.2 Appearance viscosity and rheological behavior studies

Viscosity is an internal property of a fluid that offers the resistance to flow affecting the abundant properties of *in situ* forming systems, especially the character of solvent exchange and diffusion rate. The major compositions of these systems were shellac, solvent and olive oil with stabilizer. Primarily, the viscosity of pure liquid substances was determined for basically clarifying overall systems. The viscosity of solvents was significantly different ( $p < 0.05$ ) as shown in Fig. 22. The viscosity of PYR was highest ( $14.03 \pm 0.13$  cps) while NMP and DMSO exhibited a lower viscosity ( $3.44 \pm 0.11$  and

$3.02 \pm 0.08$  cps, respectively) or  $\text{PYR} \gg \text{NMP} > \text{DMSO}$ . This measurement supported the phase separation rate of emulsion composition. PYR was the most viscous solvent thus it chiefly resisted the separation flow from olive oil (Sjoblom, 2005). Whereas DMSO and NMP were more fluid-like hence they offered the minute resistance to flow (Sjoblom, 2005).

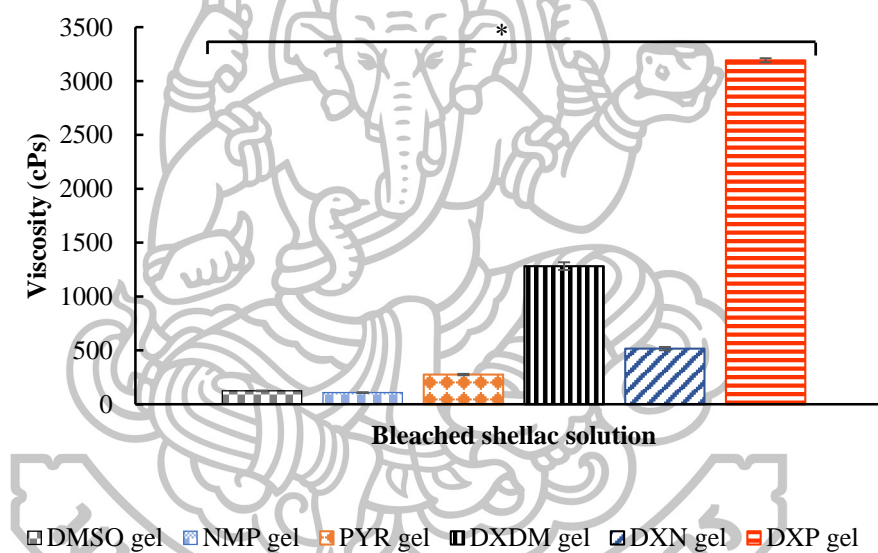
The appearance viscosity of olive oil with GMS ( $135.75 \pm 0.61$  cPs) was significantly higher than pure olive oil ( $76.05 \pm 0.95$  cPs) ( $p < 0.05$ ) as presented in Fig. 22 owing to the formation of GMS gel network in olive oil. GMS is a mixture of monoacylglyceride (MAG) and some di- or triacylglycerols. It enables an effective emulsifier in food and pharmaceutical products (Widlak, 1999). This research employed GMS in olive oil as a continuous phase for *in situ* forming microparticle system. The anhydrous  $\beta$  crystalline dispersion of GMS structured olive oil to form an organogel (or oleogel as an edible organogel) (Daniel and Marangoni, 2012). The morphology of these crystals in olive oil was needle-like with 5 to 15  $\mu\text{m}$  in length (Kesselman and Shimoni, 2007; Da Pieve *et al.*, 2010). The function of GMS as an organogelator in this case was thickening ability to control the oil migration upon mixing with the internal phase (Daniel and Marangoni, 2012). Some researchers had recently discovered that emulsions stabilized with GMS showed no signs of phase separation over more than 1 h independent of whether medium chain triglycerides (MCT) or sesame oil was used as continuous phase because it formed a fine matrix of amorphous-like and rod-like GMS crystals embedded in the oily continuous phase (Voigt, 2011). After emulsification, a bi-refrangent layer instead of the rod-like crystals was located at the interface between the oil phase and the PLGA solution droplets (Voigt, 2011).



**Fig. 22** Appearance viscosity of solvents at 25°C (n=3), \*  $p < 0.05$

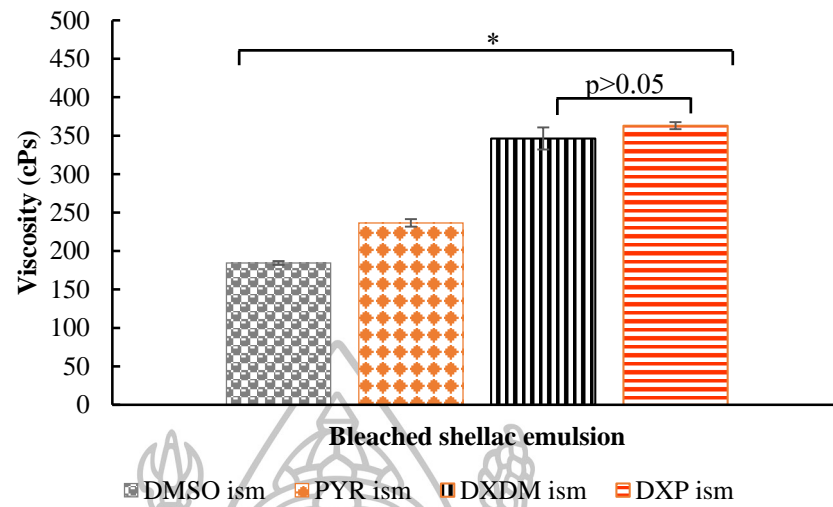
The *in situ* forming gels with or without doxycycline hyclate exhibited a significantly different viscosity values ( $p < 0.05$ ). Both gel systems had the same trend of this character as following;  $\text{PYR gel} \gg \gg \text{DMSO gel} > \text{NMP gel}$  and  $\text{DXP gel} \gg \gg \text{DXDM gel} \gg \text{DXN gel}$  (Fig. 23). This phenomenon contrasted to the relative viscosity of low polymer concentration as described in previous study. It was possibly caused by viscosity of solvent itself and solvent affinity to the polymer. PYR gel demonstrated the highest viscosity as a result of its poor solvent for this resin thus polymer-polymer interactions are

avored, leading to the formation of aggregates and an increased viscosity of polymer solution. In the case of good solvent, polymer-solvent interactions predominate over polymer-polymer ones (Camargo *et al.*, 2013), therefore lowering the viscosity was evident in NMP systems. In accordance with solubility parameter in previous study, it literately presented that NMP had its value as equal to shellac. This equivalence indicates a reasonable affinity for each other (Hansen, 2009). The doxycycline hyclate-loaded liquids exhibited a higher viscosity because the amount of drug replaced some of solvent in system (Johns, 2007; Setthajindalert, 2013). On the other hand, there might be the interaction between hydroxyl or carboxyl groups in shellac and amine groups of weak basic drug which probably reinforced the polymer aggregation and finally enhanced the viscosity of gels. The viscosity of systems was increased when drug was incorporated as some research reported the drug-polymer interaction increased a viscosity of the gel system (Mayol *et al.*, 2008; Phaechamud and Mahadlek, 2015).



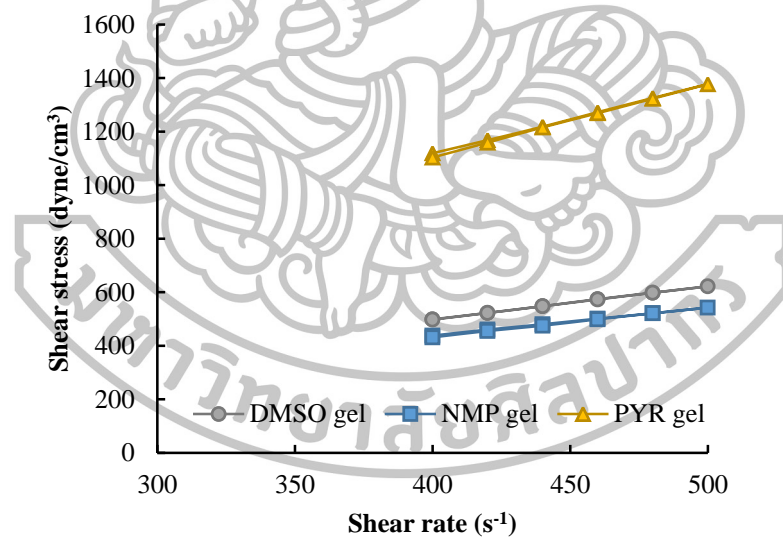
**Fig. 23** Appearance viscosity of bleached shellac solutions at 25°C (n=3), \*  $p \leq 0.05$

The appearance viscosity of ISM systems without doxycycline hyclate were significantly different ( $p < 0.05$ ). PYR ism was more viscous than DMSO ism as shown in Fig. 24 due to apparent higher viscosity of solvent itself and affinity for each other as mentioned previously. For doxycycline hyclate-loaded ISM systems with, they exhibited a noticeable higher viscosity as described in previous explanation. By comparison, ISM exhibited particularly a lower viscosity than *in situ* forming gel because the viscosity was predominant from the oil presented in the external phase (Rungseevijitprapa and Bodmeier, 2009). Furthermore, oil not only exhibited the lubricant effect enhance an ease of administration, but also acted as a barrier which retarded the solvent diffusion and drug release (Rungseevijitprapa and Bodmeier, 2009).

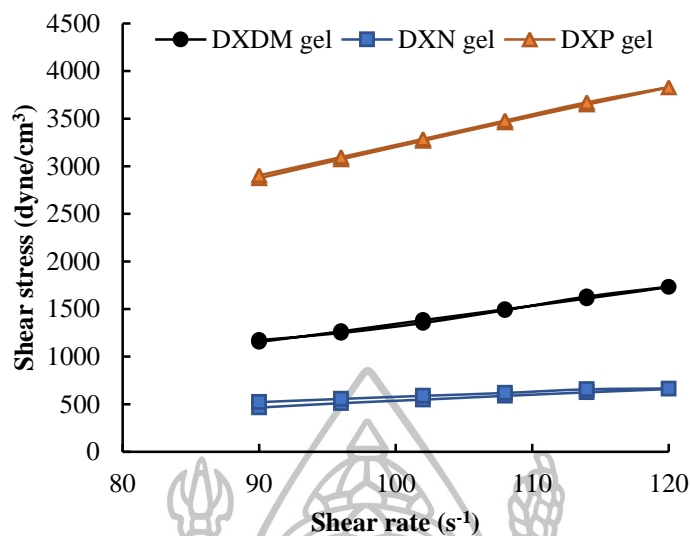


**Fig. 24** Appearance viscosity of ISMs at 25°C (n=3), \*  $p \leq 0.05$

The rheological behaviors of free drug or drug-loaded *in situ* forming gel systems showed the overlapped up curve and down curve (Figs. 25 and 26). The shear stress value of both systems was as followed: PYR  $\gg$  DMSO  $>$  NMP at the same shear rate.

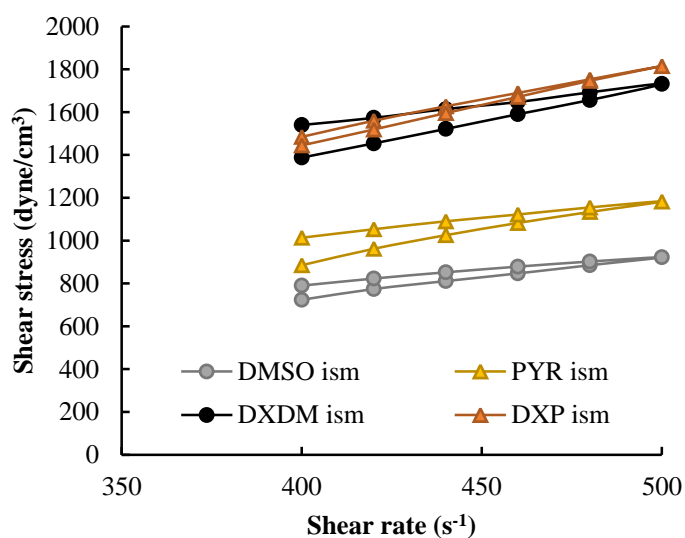


**Fig. 25** Flow of bleached shellac solutions at 25°C (n=3)



**Fig. 26** Flow of doxycycline hyclate-loaded bleached shellac solutions at 25°C (n=3)

The free drug or drug-loaded ISM systems showed a thixotropic behavior as depicted in Fig. 27. Because the aggregation of microparticles in olive oil induced viscous texture at rest condition, this microstructure was then disrupted toward fluid under agitation, and returned to a viscous state after taking a relaxing time (Souza, 2009). The shear stress value of both systems was as followed: PYR ism > DMSO ism which correlated with shear stress value of *in situ* gel systems.



**Fig. 27** Flow of bleached shellac emulsions at 25°C (n=3)

The flow index of all formula without doxycycline hyclate was approximately close to 1 indicating the Newtonian flow (Table 5) because the appearance viscosity was constant with an increase of shear rate (Bjorn *et al.*, 2012). *In situ* forming gel formula containing doxycycline hyclate showed significantly the different flow indices ( $p < 0.05$ ) as presented in Table 5. The flow index of DXP gel was close to 1 while DXDM gel and DXN gel was lower than 1. Therefore, the flow behavior of this system was Newtonian and



Pseudoplastic, respectively which was suitable for injectable gel because it did not provide the higher resistance during syringe administration (Bjorn *et al.*, 2012). For both systems with and without doxycycline, the consistency index of gels fabricated by PYR was significantly different and higher than gels prepared using DMSO and NMP as solvent ( $p < 0.05$ ).

**Table 5** Flow index and consistency index of prepared solutions at 25°C (n=3), \*  $p \leq 0.05$

Sample	Flow index (N)		Consistency index ( $\eta$ )	
	mean	$\pm$ SD	mean	$\pm$ SD
DMSO gel	1.00	$\pm$ 0.02	1.22	$\pm$ 0.17*
NMP gel	1.00	$\pm$ 0.02	1.09	$\pm$ 0.13*
PYR gel	1.03	$\pm$ 0.02	3.56	$\pm$ 0.66*
DXDM gel	0.72	$\pm$ 0.09*	1.99	$\pm$ 1.23*
DXN gel	0.82	$\pm$ 0.04*	1.76	$\pm$ 0.36*
DXP gel	1.00	$\pm$ 0.02*	32.57	$\pm$ 5.69*

ISM system without doxycycline hyclate loading had a significantly different flow index ( $p < 0.05$ ). The flow index of DMSO ism was close to 1 while PYR ism was lower than 1. Consequently, the flow type of this system was Newtonian and Pseudoplastic, respectively. Nevertheless, the flow index of all doxycycline hyclate-loaded ISM formula in Table 6 was approximately close to 1 indicating the flow type as Newtonian. Both systems with and without doxycycline displayed a consistency index of PYR ism significantly different and higher than DMSO ism ( $p < 0.05$ ).

**Table 6** Flow index and consistency index of ISMs at 25°C (n=3), \*  $p \leq 0.05$

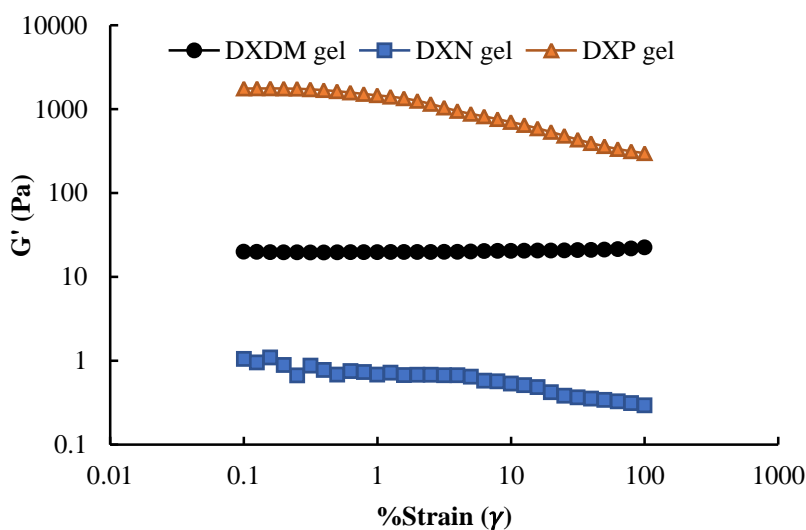
Sample	Flow index (N)		Consistency index ( $\eta$ )	
	mean	$\pm$ SD	mean	$\pm$ SD
DMSO ism	0.96	$\pm$ 0.04*	0.51	$\pm$ 0.14*
PYR ism	0.78	$\pm$ 0.04*	3.44	$\pm$ 0.43*
DXDM ism	0.98	$\pm$ 0.15*	4.09	$\pm$ 0.12*
DXP ism	0.99	$\pm$ 0.23*	14.21	$\pm$ 0.31*

#### 4.3.1.3 Viscoelastic behavior studies

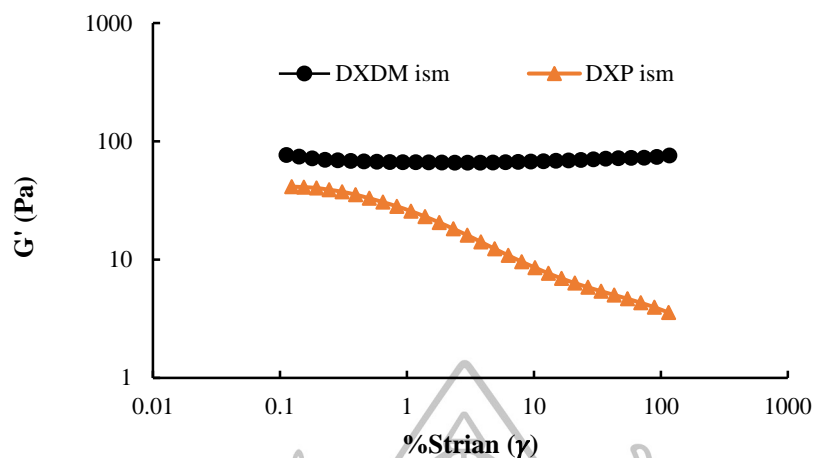
Viscoelasticity exhibits both viscous and elastic characteristics of materials when undergoing deformation. Viscoelastic response is often used as a probe in polymer science, since it is sensitive to the material's chemistry and microstructure (Aklonis *et al.*, 1972). The gel formation closely related to the disappearance fluidity in colloidal system which frequently occurs in a polymer solution (Almdal *et al.*, 1993). To clarify three dimensional networks coming from cross-links between chains, research works of gel usually accompany the change in viscoelastic properties. Experimental studies on the viscous and elastic properties of emulsions are commonly referred to dispersions of the internal phase in external phase (Sherman, 1983; Pal, 1997). Viscosity data do not inform about the elasticity of such emulsions and gels. This research work reports firstly the viscoelastic

behavior of gels and emulsions from *in situ* forming systems using the steady shear and sinusoidal oscillatory tests.

Linear viscoelastic region (LVR) curves in Figs. 28 and 29 show the  $G'$  as a function of strain ( $\gamma$ ) for each sample based on the results from the dynamic strain sweep tests which demonstrated a typical elastic response of gels and emulsions, respectively (Gao *et al.*, 2008). Within LVR, the  $G'$  values of these samples were basically independent of the applied strain ( $\gamma$ ), behaving like a viscoelastic solid. The points at which  $G'$  values derived by more than 5% from the plateau zone indicated a departure from linear viscoelastic behavior and hence were defined as the critical strains ( $\gamma_c$ ) for each sample (Gao *et al.*, 2008). The  $G'$  values then gradually decreased above the  $\gamma_c$ , presenting a transition of the samples from the quasi-solid state to a quasi-liquid state. A strain ( $\gamma$ ) of 1% for gel and 0.1% for emulsion and a frequency ( $\omega$ ) of 1 Hz was selected for further oscillatory measurements (except for frequency sweeps which were carried out at frequency ( $\omega$ ) varying from 0.1 to 10 Hz). In general, the LVR is shortest when the sample is in its most solid form. DXP gel presented a higher  $G'_{\max}$ , a shorter LVR and consequently a lower  $\gamma_c$  than DXDM gel and DXN gel. This circumstance revealed that DXP gel was the strongest gel. However, in the case of ISM, the strain limit was strongly affected by olive oil in external phase. DXDM ism inversely showed slightly higher  $G'_{\max}$ .



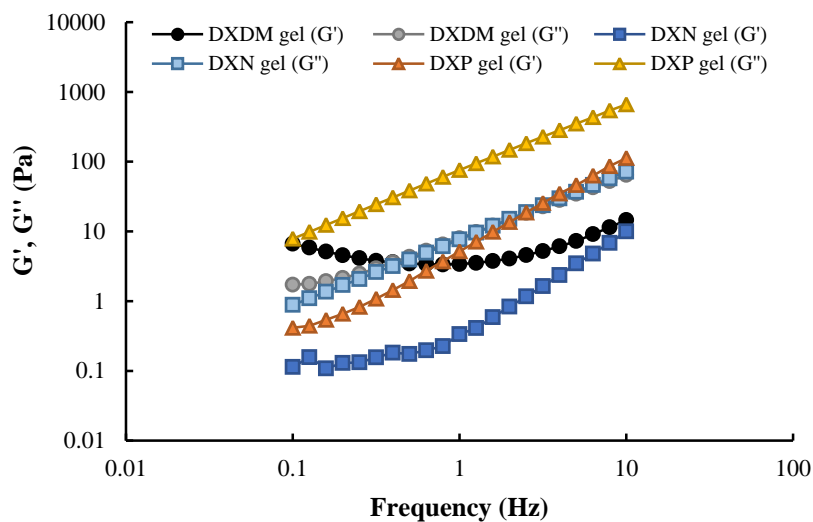
**Fig. 28** Strain dependence of  $G'$  for gels at  $\omega = 1$  Hz under 25°C



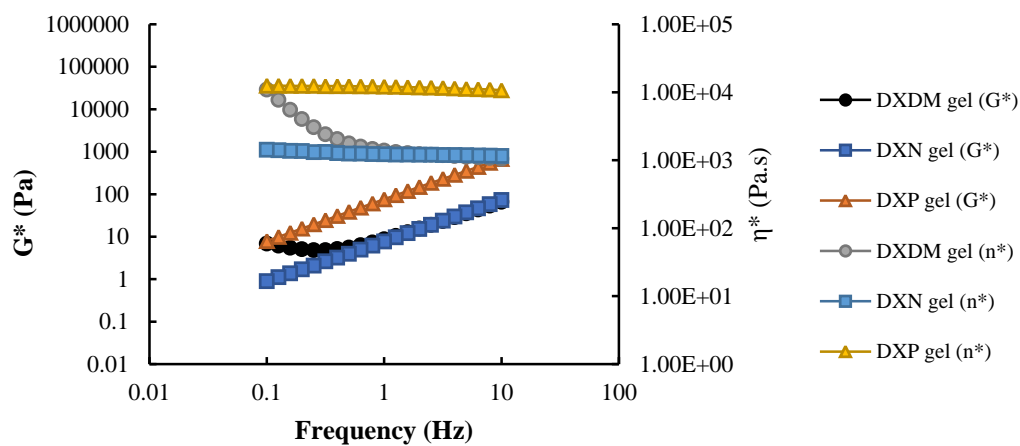
**Fig. 29** Strain dependence of  $G'$  for emulsions at  $\omega = 1$  Hz under  $25^\circ\text{C}$

To study the effect of solvents on rheological behavior of shellac gels and emulsions, the value of  $G'$ ,  $G''$ ,  $G^*$ ,  $\eta^*$  and loss tangent ( $\tan \delta$ ) respectively were plotted against frequency for systems prepared using DMSO, NMP or PYR as solvent. The  $G'$  (elasticity) and  $G''$  (viscosity) as a function of  $\omega$  for gels within linear deformation range are illustrated in Fig. 30. DXN gel and DXP gel exhibited typically as a viscous fluid because  $G''$  was always higher than  $G'$  ( $\tan \delta > 1.0$ ) as shown in Fig. 30 in all the frequency range. DXDM gel obviously distinguished from others at low frequencies where  $G' > G''$  ( $\tan \delta < 1.0$ ) as presented in Fig. 30, which indicated that the elastic character became dominant or a typical solid-like character. Simultaneously, at crossover point where  $G' = G''$ , introducing the entanglement of polymer chains and the formation of an elastic gel network (Wang and Chen, 2011). After this crossover point, DXDM gel behaved a viscous fluid as same as others. The plots of complex modulus ( $G^*$ ) and complex viscosity ( $\eta^*$ ) as a function of  $\omega$  in Fig. 31 provided the order of  $G^*$  and  $\eta^*$  as following: DXP gel  $>$  DXDM gel  $>$  DXN gel. It confirmed that DXP gel showed the strongest texture among test samples. The  $\tan \delta$  value of only DXDM gel was lower than 1 at initial stage, exhibiting its high elasticity at this period (Fig. 32). On the other hand, DXN gel and DXP gel possessed an inconstant  $\tan \delta$  in equivalent and higher than 1 throughout the whole  $\omega$  range (Fig. 32). It is well known that  $\tan \delta$  represents the ratio of a dissipated energy to a stored energy during the stress deformation (Yang *et al.*, 2012). The  $\tan \delta$  values of DXDM gel were lower than 1 at first low frequencies because the polymer chains containing physical entanglements were disentangled and then reconstituted during dynamic strains. The dynamic entanglement-disentanglement equilibrium process provided the network with the energy release capacity (Yang *et al.*, 2012). Its elastomeric nature was probably due to the entanglements between DMSO and shellac via hydrogen bonds at low frequencies. To compare the bonding of each solvent, sulfoxide group (DMSO) has potential hydrogen bond acceptor than carbonyl group of NMP and PYR due to its stronger electronegativity (Brown *et al.*, 2008). After increase of frequencies, the system gained an excess energy then destroyed those entanglements. Consequently, DXDM gel behaved like quasi-liquid at higher frequencies. In addition, the results of  $G^*$ ,  $\eta^*$  and  $\tan \delta$  signified apparently that DXP gel and DXN gel was unsteady viscous-like character. Especially, PYR provided the

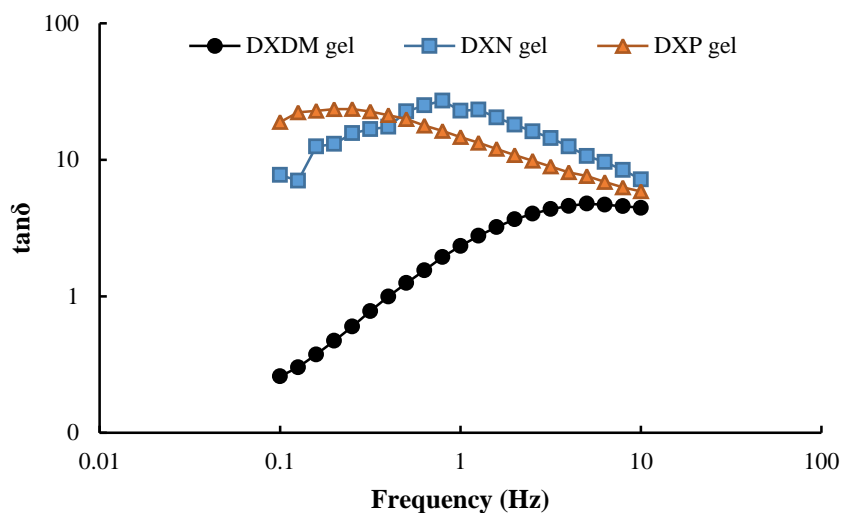
strongest gel (by the dominance of polymer-polymer interaction as described in appearance viscosity study) whereas DXDM gel showed a higher elasticity at low frequency.



**Fig. 30** Frequency (0.1-10 Hz) dependence of  $G'$  and  $G''$  for gels at 25°C

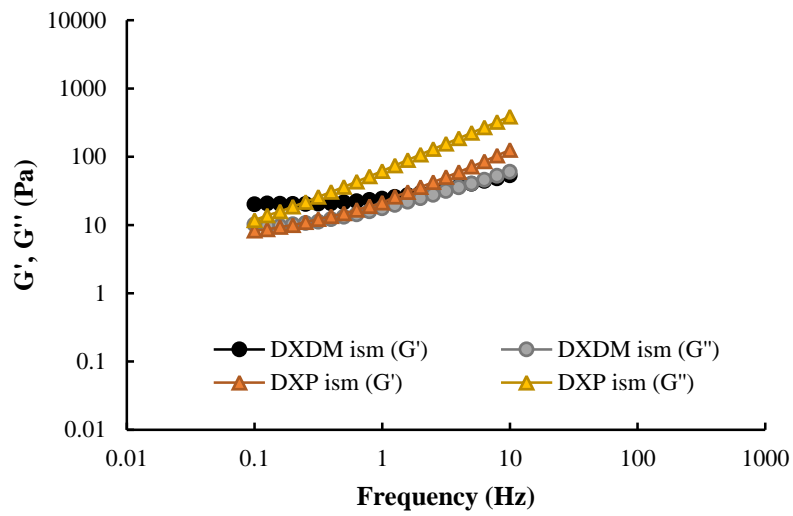


**Fig. 31** Frequency (0.1-10 Hz) dependence of  $G^*$  and  $\eta^*$  for gels at 25°C

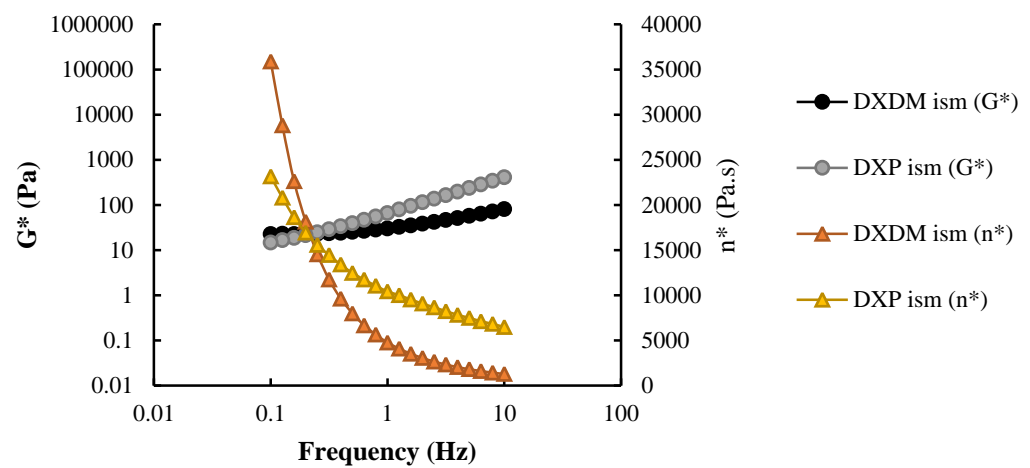


**Fig. 32** Frequency (0.1-10 Hz) dependence of loss tangent ( $\tan \delta$ ) for gels at 25°C

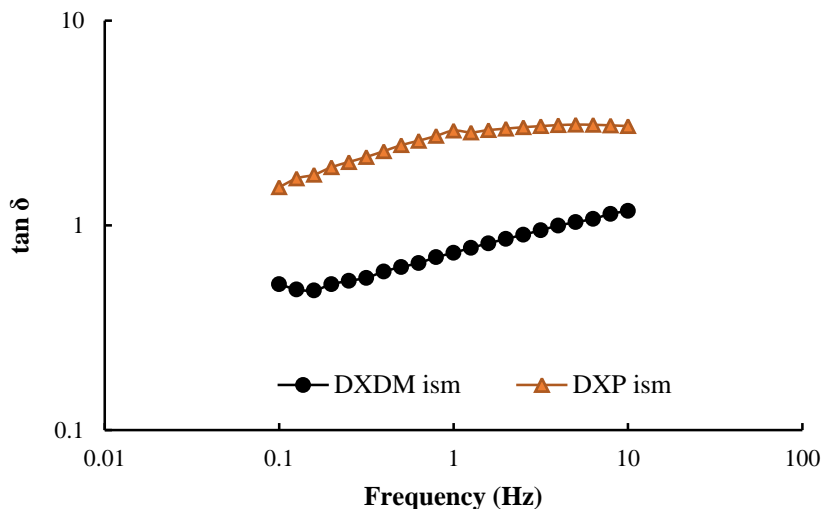
The  $G'$  (elasticity) and  $G''$  (viscosity) as a function of  $\omega$  for emulsions within linear deformation range are illustrated in Fig. 33. The rheological behavior of DXP ism and DXDM ism was similar to that of gels which quasi-liquid behavior was dominant. It has been noted that DXDM ism exhibited a crossover range where  $G' = G''$  all over higher frequencies which was discussed previously. The plots of complex modulus ( $G^*$ ) and complex viscosity ( $\eta^*$ ) as a function of  $\omega$  in Fig. 34 attributed the order of  $G^*$  and  $\eta^*$  as following: DXDM ism  $>$  DXP ism. This behavior was different from gels because DXDM ism was stronger due to robust interaction between sulfoxide group of DMSO and hydroxyl group from GMS compared to carbonyl group of PYR (Petrucci *et al.*, 2007). The  $\tan \delta$  values of these emulsions in Fig. 35 showed a similar trend with that of gels. Surprisingly, there was the trend of all plots which the values of  $G'$ ,  $G''$ ,  $G^*$ ,  $\eta^*$  and  $\tan \delta$  were lower and more invariable than those of gels. Olive oil and GMS (stabilizer) in the external phase influenced notably on this behavior owing to hindrance and lubricant effect.



**Fig. 33** Frequency (0.1-10 Hz) dependence of  $G'$  and  $G''$  for emulsions at 25°C



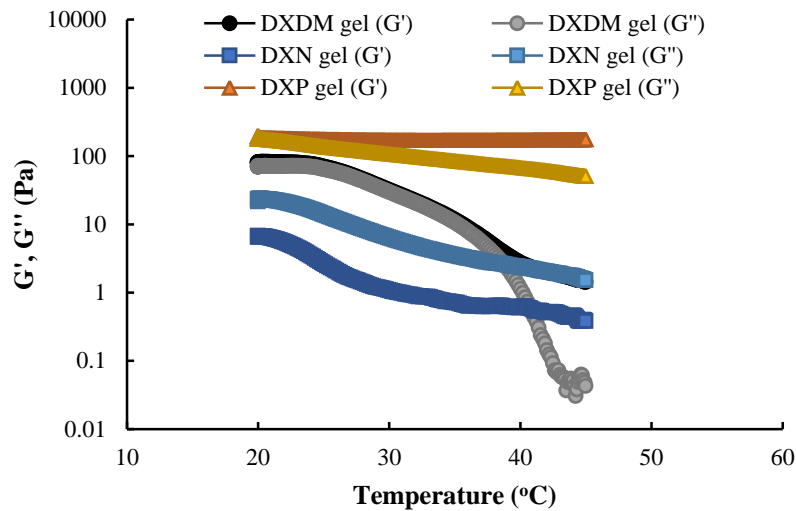
**Fig. 34** Frequency (0.1-10 Hz) dependence of  $G^*$  and  $\eta^*$  for emulsions at 25°C



**Fig. 35** Frequency (0.1-10 Hz) dependence of loss tangent ( $\tan \delta$ ) for emulsions at 25°C

Temperature sweep study is an essential oscillation measurement to understand the behavior of gels and emulsions at different energy states. Generally, to monitor the variation of the elastic and viscous moduli with the range of temperatures at constant frequency is for investigating the gelation process or gelification temperature at which  $G'$  and  $G''$  curves intersect each other (Hagerstorm *et al.*, 2000). Shellac is a non-thermosensitive gelling material therefore the gel point is not necessarily equal to the calculated value at  $G' = G''$  (Winter, 1987; Núñez *et al.*, 2005). Another criterion is that gelation occurs when viscosity increases exponentially to infinity (Laza *et al.*, 1998). For this study, the gels and emulsions were therefore evaluated via the cooling-heating process to comprehend profoundly the relation between temperature and viscoelastic behavior of bleached shellac.

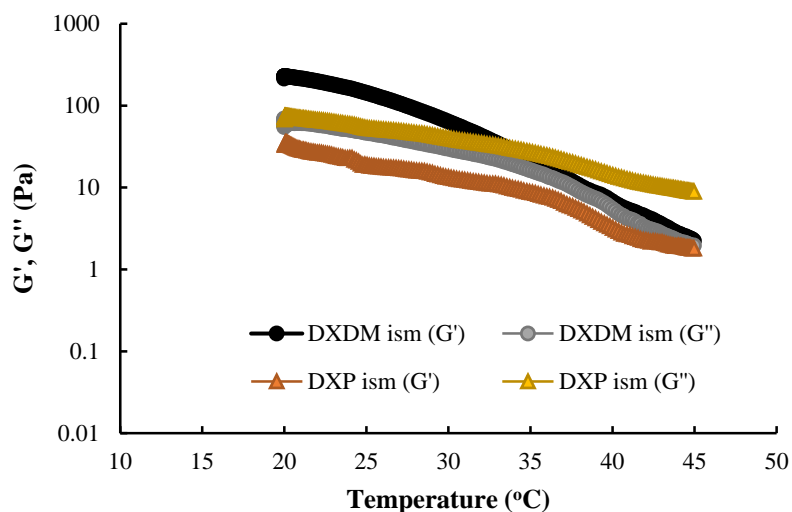
The elastic and viscous moduli of gels as a function of temperature, at a frequency value of 1 Hz, are shown in Fig. 36. With elevating temperature a negligible increase of the  $G'$  was observed in DXP gel due to an increase in stiffness of gels (Hameed *et al.*, 2007). In case of DXDM gel and DXN gel,  $G'$  decreased which attributed to the increase in the molecular mobility of the polymer chains owing to elevating energy from higher temperature (Paiva and Frollini, 2006). During the whole circle, DXN gel exhibited  $G''$  value higher than  $G'$  value, implying a viscous response of material. Inversely, DXDM gel and DXP gel appeared the two stages of viscoelastic behavior. At the start of curing both  $G'$  and  $G''$  decreased as the cross-linking reaction progresses to a crossover point; here the systems presented both elastic and viscous behavior with storing a similar amount of the dissipated energy. At higher temperature greater than 25°C and 40°C, the  $G'$  was higher than  $G''$ , indicating an elastic shellac network.



**Fig. 36** Temperature (20-45°C) dependence of  $G'$  and  $G''$  for gels at frequency of 1 Hz

The elastic and viscous moduli of emulsions as a function of temperature, at a frequency value of 1 Hz, are shown in Fig. 37. The rheological behavior of DXDM ism and DXP ism was slightly different from gels. When an elevating temperature was conducted a decrease of the  $G'$  was observed in all formulations as discussed previously. Throughout the entire process, DXP ism had  $G''$  higher than  $G'$ , indicating a typical liquid-like character. Whereas DXDM ism exhibited the two stages of viscoelastic behavior. At the start of curing  $G'$  was higher than  $G''$ , indicating an elastic shellac network at lower temperature (37-38°C). Later,  $G'$  and  $G''$  decreased as the cross-linking reaction progressed to a crossover point; here the systems presented both elastic and viscous behavior. Notably, the trend of all emulsion plots appeared a similar trend with near values of  $G'$ ,  $G''$  while these values of gel were as following: DXP gel > DXDM gel > DXN gel. The hindrance and lubricant effect of the olive oil and GMS (stabilizer) in external phase crucially influenced for this occurrence.





**Fig. 37** Temperature (20-45°C) dependence of  $G'$  and  $G''$  for emulsions at frequency of 1 Hz

This research works demonstrated that solvents played an important functional role on the 3D-network formation within the bleached shellac gels or emulsions, leading to a significant enhancement in strength and viscoelasticity of these formulations. The differences in the enhancement effect originated in solvent nature used for gels or ISMs preparations. For this reason, the crosslinking (entanglement) capacity of solvent should be rational in the order of  $\text{PYR} > \text{DMSO} > \text{NMP}$ , which was in agreement with the results of oscillation test as a function of frequency and of temperature. Thus gel, tailored with PYR, showed the maximum mechanical strength and crosslinking density. In regard to ISM systems that order of crosslinking capacity was changed to  $\text{DMSO} > \text{PYR}$  because not only bleached shellac but also GMS (in external phase) was able to interact with solvent.

#### 4.3.1.4 Thermal property studies

Thermal analysis studies are techniques in which a physical property of a substance is measured as a function of temperature while the substance is subjected to a controlled temperature program. The various modes of individual thermo-analytical techniques are commonly used which are distinguished from one another by the property to be measured. Thermogravimetry (TG) and differential scanning calorimetry (DSC) are the principal thermal analysis methods of this research (Hemming and Sarge, 1998).

##### Differential scanning calorimetry (DSC)

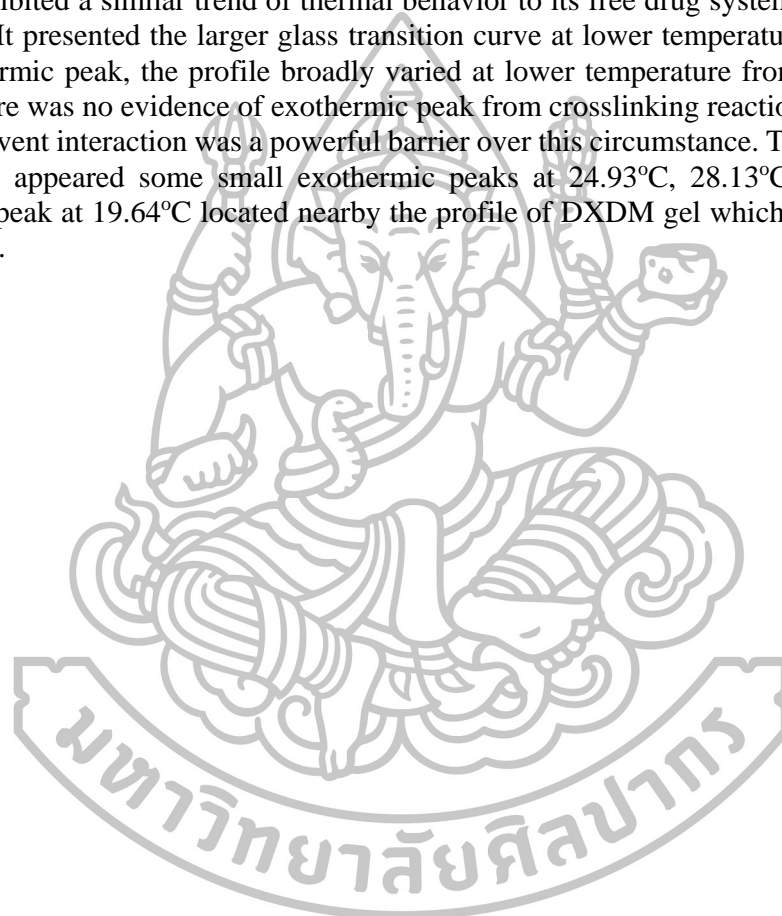
DSC is a technique which measures the difference between heat flow rates into a sample and a reference material. It provides information about thermal changes or enthalpy (Ahmad and Huglin, 1994). This technique is extensively used for examining the solvent state in polymer. Some solvents may encourage the crystallization by enhancing the mobility of the molecules in the amorphous phase. However, solvents may also induce a crystallization in semi-crystalline polymers that have a tendency to undergo a secondary crystallization. The thermograms of polymer-solvent system attain the solvent/polymer melting point and energy, the freezing point of solvent in different states, the heat of

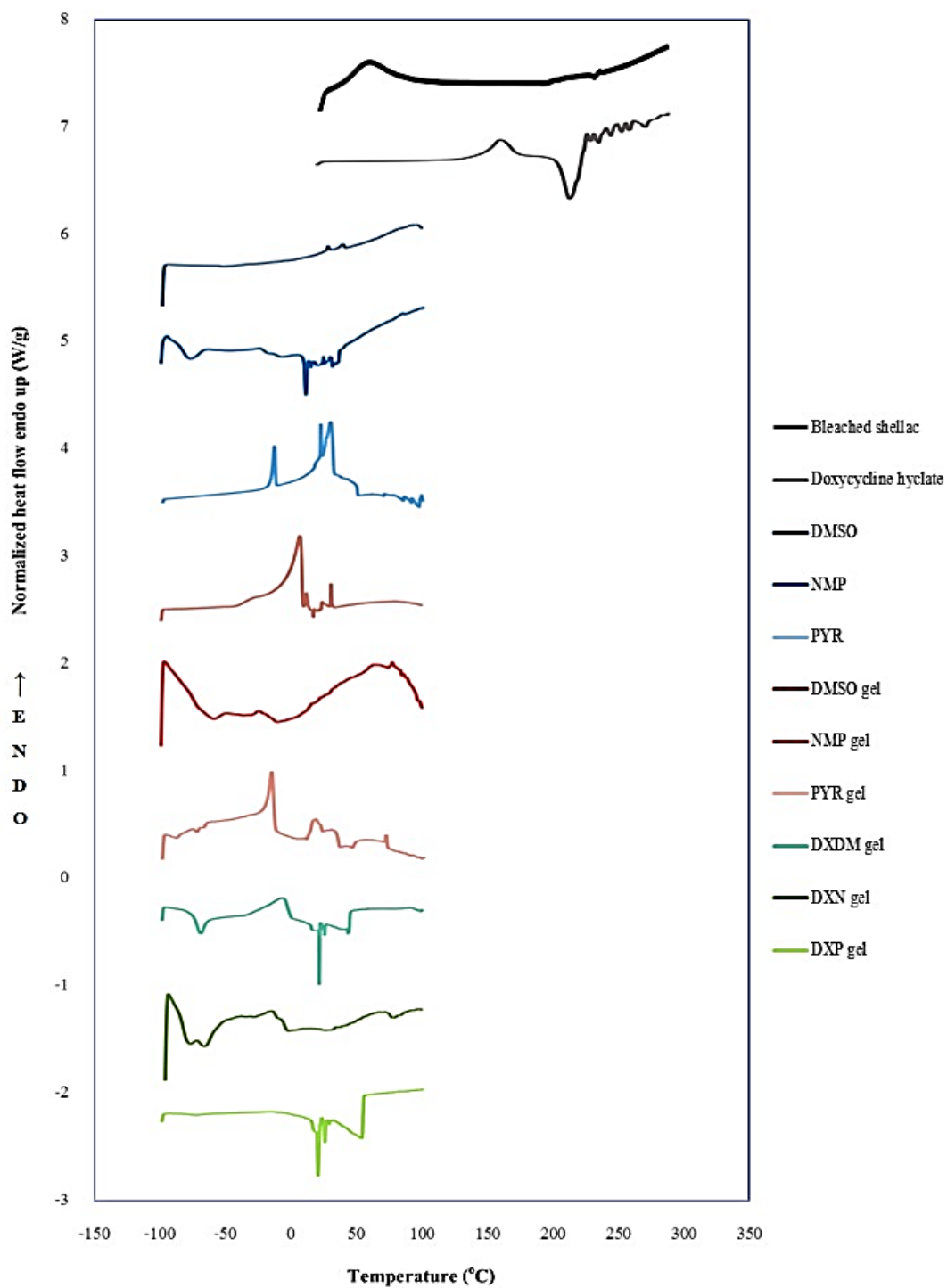
solvent/polymer melting or crystallization (Scheirs, 2000). The effect of solvents on the *in situ* forming systems was investigated to understand the behavior of solvent state in bleached shellac. The discussion of *in situ* forming gel will be driven in the priority as following; the DSC thermograms for pure substances (i.e. bleached shellac, doxycycline hyclate, DMSO, NMP and PYR) and bleached shellac systems with and without drug loading (i.e. DMSO gel, NMP gel, PYR gel, DXDM gel, DXN gel and DXP gel) are shown in Fig. 38.

Firstly, a set of pure substances was discussed for their thermal characteristics with DSC. Bleached shellac showed only prominent endothermic peak due to its melting at 59.83°C which is consistent with that reported previously (Limmatvapirat *et al.*, 2008). Doxycycline hyclate showed an endothermic peak due to the melting of the drug at 168.5°C, followed by a large exothermic thermal degradation peaks at around 222.83°C. DMSO presented two quite small endothermic peaks at 32.8°C and 37.9°C. For NMP there was the glass transition and crystallization events at -76.71°C and 10.27°C, respectively. PYR obviously exhibited the endothermic phase transitions from solid to liquid at -14.18°C and the double endothermic peaks at 21.27°C and 28.96°C.

Secondly, the systems without drug loading were characterized. The bleached shellac saturated in DMSO exhibited the explicitly sharp endothermic peak at 6.91°C and the series of small endothermic peaks at 11.72°C, 17.86°C, 24.36°C and 30.48°C. The endothermic peaks typically associated with gel melting was expected to occur but in certain cases were not observed during gel heating (Marangoni and Garti, 2011). DMSO has rather good affinity for bleached shellac according to small difference between values of solvent solubility parameter. The endothermic peak might correspond to a formation of new hydrogen bonds between sulfoxide group from DMSO and hydrogen atom from bleached shellac (Alavi, 2003). The solution of bleached shellac in NMP revealed a larger glass transition curve at lower temperature (-96.88°C) and a broad endothermic peak from -10.56°C to 99.53°C. The border and shift glass transition indicated that some of amorphous regions could not participate in the cooperative rearrangement. Generally, the molecular mobility in amorphous regions is influenced by the presence of crystallites. In the case of bleached shellac in NMP, an amorphous region of polymer was interfered by crystallites from solvent from test condition during cooling step. This rigid amorphous phase located at the surface of the chain-folded crystals. Besides, the DSC curve would just show a broad endothermic peak owing to the size distribution of crystallites or the evaporation of the solvent (Riesen and Schawe, 2000). Furthermore, the value of solubility parameter of NMP and bleached shellac is equal indicating the best good solvent-solute condition and the strongest affinity for polymer. The robust interactions between solvents and polymer promoted the NMP molecules bound to bleach shellac chain and disrupted the inter-chain bond, thereafter the crystallinity of solvent disappeared (Yang *et al.*, 2000). It should be noted that NMP did not provide a new endothermic peak possibly caused by weaker hydrogen bond between solvent and polymer as previously described in section 4.3.1.4 (viscoelastic behavior studies). The bleached shellac dissolved in PYR presented the sharp endothermic peaks at -16.22°C and small-broad double endothermic peaks at 17.75°C and 30.49°C. The DSC profile of this system was similar to pure PYR with peak shifting to lower temperatures. Among three solvents, PYR is a poor solvent due to the largest differences between values of solubility parameter of itself and polymer. It exhibited as weak interaction with bleached shellac and inability to disrupt the inter-segment bonds in the amorphous forms of polymer chain resulted in an increase of solvent in free volume of system. Some free PYR molecules were detectable as an independent phase in DSC (Yang *et al.*, 2000).

Lastly, the consideration for DSC analysis of the systems with drug loading was carried on. DXDM gel showed an endothermic peak at  $-7.72^{\circ}\text{C}$ , small exothermic peaks at  $-69.96^{\circ}\text{C}$ ,  $24.93^{\circ}\text{C}$  and sharp exothermic peak at  $20.79^{\circ}\text{C}$ . The DSC studies showed endothermic peak where a formation of new hydrogen bonds between solvent and polymer took place as previously described. In a general exothermic process, it involved a change in the material such as crystallization, some cross-linking processes, oxidation reactions, and some decomposition reactions (Dean, 1995). For drug analysis, DSC is a tool for studying curing processes leading to the cross-linking (Skoog *et al.*, 1998). Hence, the exothermic peaks signified for pointing toward the possibility of crosslinking reactions between polymer and drug molecules. The solution of bleached shellac with drug loading in NMP exhibited a similar trend of thermal behavior to its free drug system as discussed previously. It presented the larger glass transition curve at lower temperature ( $-96.84^{\circ}\text{C}$ ). For endothermic peak, the profile broadly varied at lower temperature from  $-69.05^{\circ}\text{C}$  to  $5.45^{\circ}\text{C}$ . There was no evidence of exothermic peak from crosslinking reaction because the polymer-solvent interaction was a powerful barrier over this circumstance. The DSC curve of DXP gel appeared some small exothermic peaks at  $24.93^{\circ}\text{C}$ ,  $28.13^{\circ}\text{C}$  and a sharp exothermic peak at  $19.64^{\circ}\text{C}$  located nearby the profile of DXDM gel which related to the crosslinking.



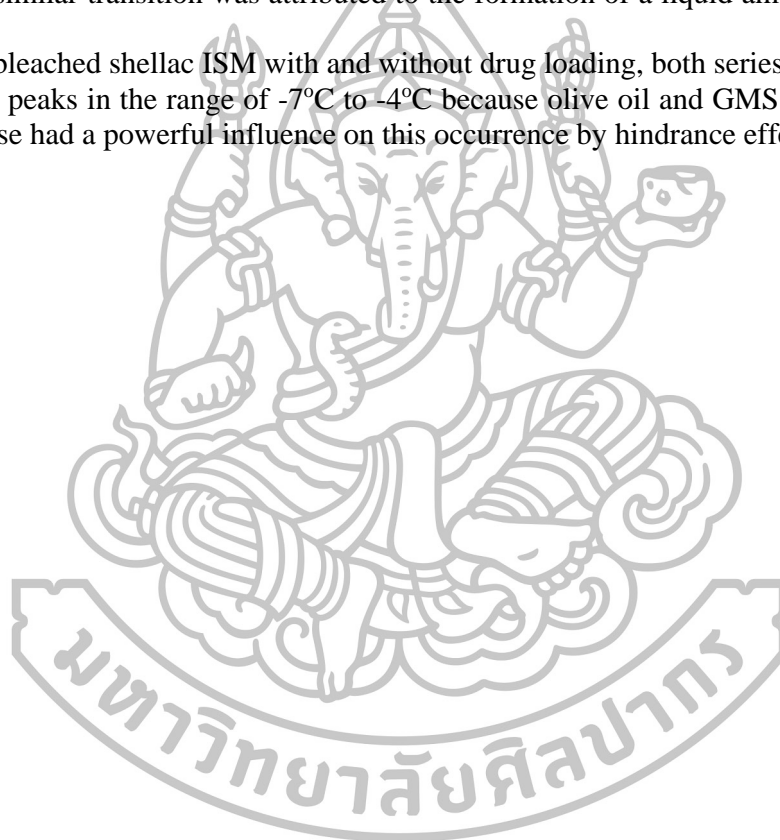


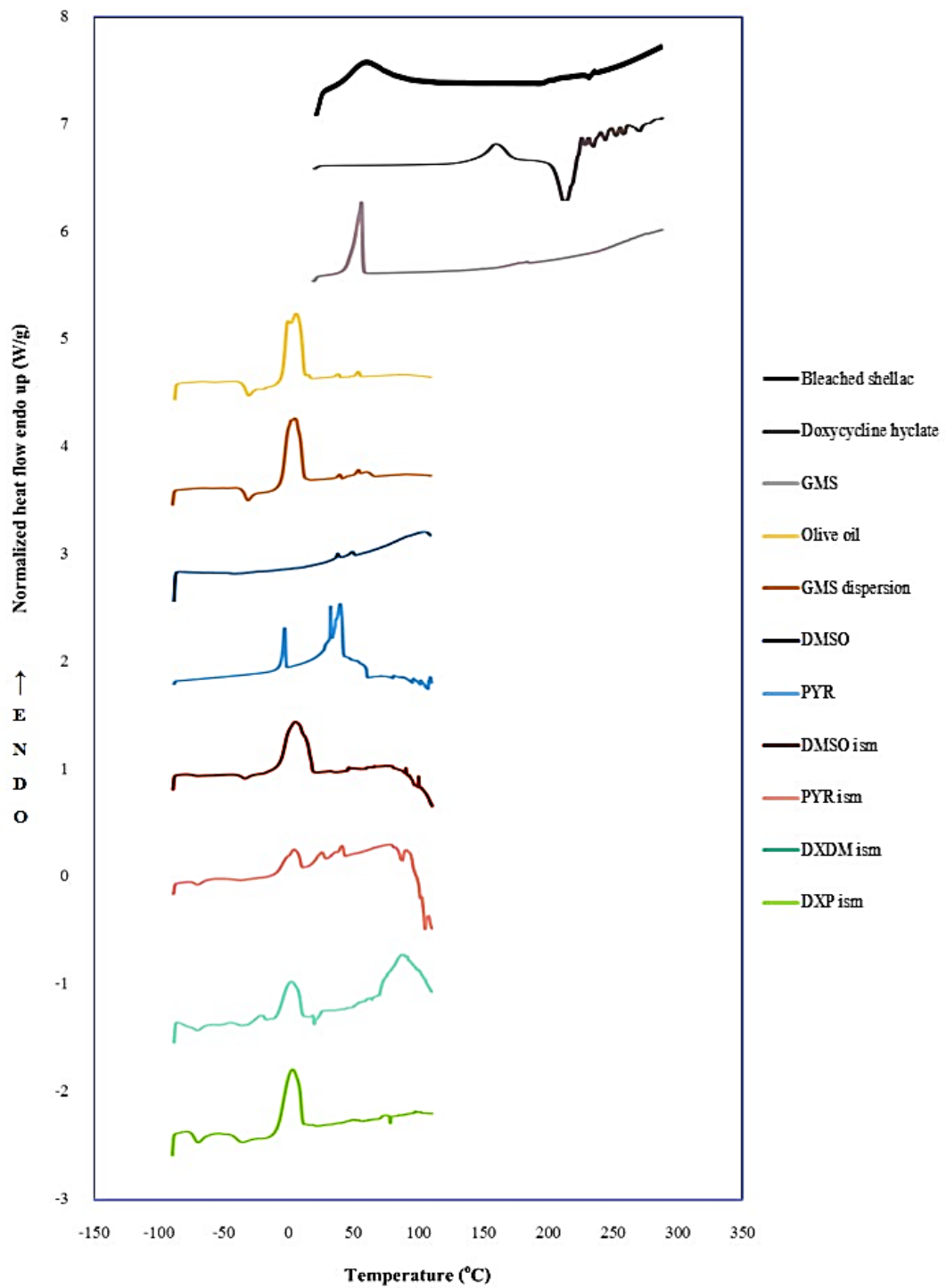
**Fig. 38** DSC curves of *in situ* forming gels and their compositions

DSC thermograms of ISM were described with priority as following; the DSC thermograms for pure substances (i.e. bleached shellac, doxycycline hyclate, GMS, olive oil, GMS dispersion, DMSO and PYR) and bleached shellac systems with and without drug loading (i.e. DMSO ism, PYR ism, DXDM ism and DXP ism) are shown in Fig. 39. Some of them was described previously especially for some pure substance.

GMS exhibited an endothermic melting peak with onset at 63.17°C due to the melting of the  $\beta$ -form (Hagemann, 1988). Olive oil was detected for their sharp double endothermic peaks at -11.18°C, -4.54°C and some small melting peaks at 5.07°C, 28.47°C, 43.79°C. The presence of multiple peaks in DSC profiles of vegetable oils can be attributed to the complex feature of triacylglycerol (TAG) distribution in lipids (Tan and Che, 2002). GMS dispersion showed the thermogram similar to that of pure olive oil. There were the double endothermic peaks at -7.52°C, -4.71°C and some small melting peaks at 27.93°C, 44.47°C. A similar transition was attributed to the formation of a liquid amorphous GMS phase.

For bleached shellac ISM with and without drug loading, both series presented the endothermic peaks in the range of -7°C to -4°C because olive oil and GMS (stabilizer) in external phase had a powerful influence on this occurrence by hindrance effect.



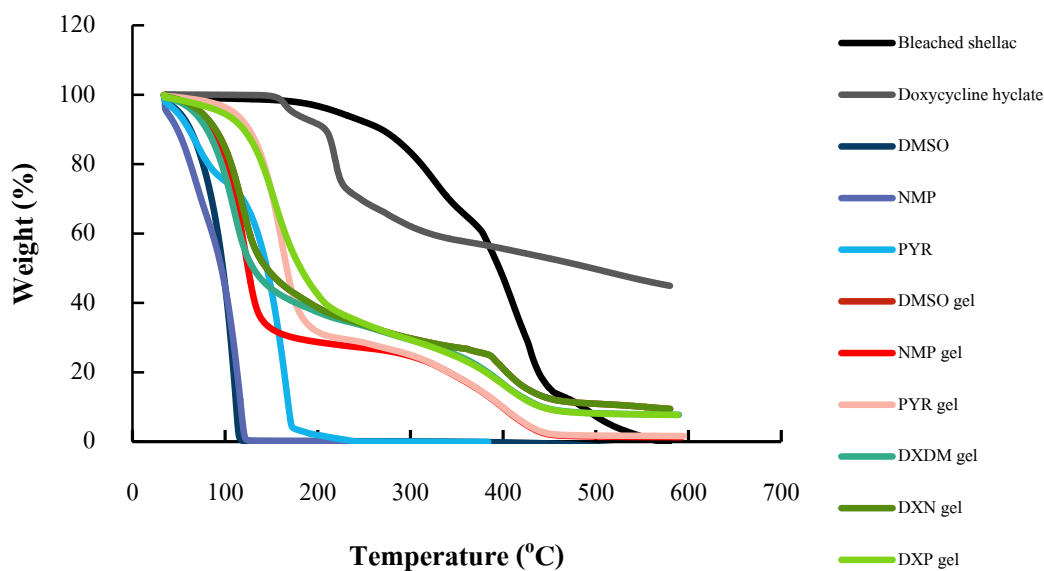


**Fig. 39** DSC curves of *in situ* forming microparticles and their compositions

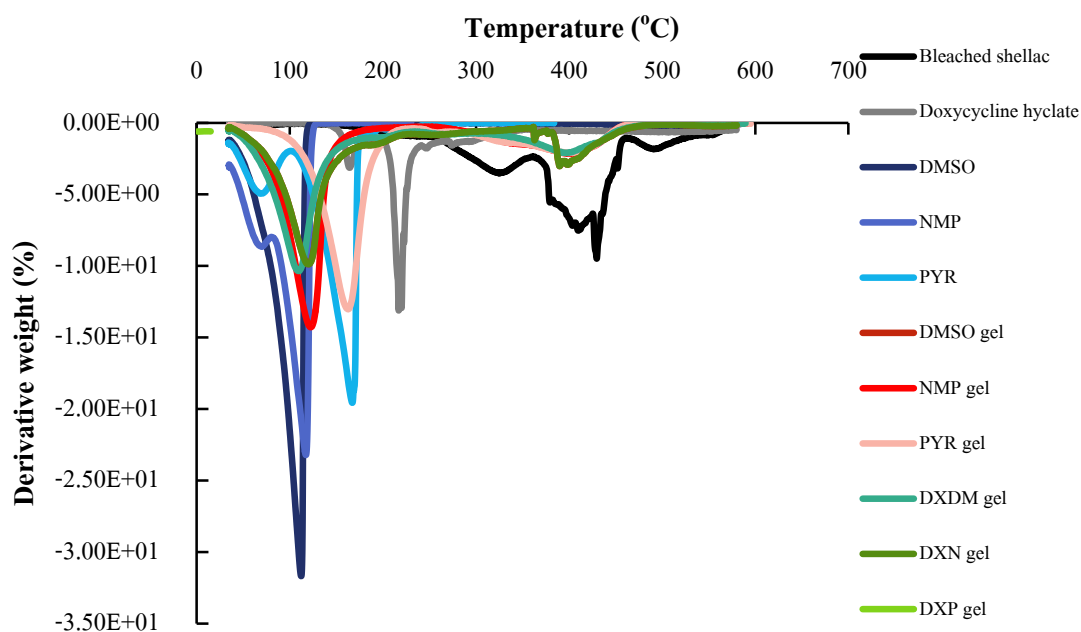
### Thermogravimetry (TG)

Thermogravimetry (TG) is an essential lab tool to characterize the changes in mass or weight at different temperatures. The measured weight loss curve provides the certain information such as the changes in sample composition, thermal stability, decomposition, loss of moisture or dissociation of the crystals. A derivative weight loss curve can point where weight loss is most noticeable (Hemminger and Sarge, 1998).

TGA and differential DTGA results for *in situ* forming gels and their compositions are depicted in Figs. 40 and 41. The TGA values indicated that the samples prepared with DMSO or NMP showed the higher degradation temperature rate compared to the samples prepared with PYR, possibly associated with the difference in intermolecular strength forces and viscosity. The systems with drug loading revealed the slower degradation temperatures rate, pointing to a replacement with doxycycline hyclate required the greater degradation energy. For all *in situ* forming gels, the TG and DTGA curves at initial step showed that the rate of weight loss increased quickly at low temperatures approximately 100-200°C (Table) due to solvent evaporation by around 70 % of weight loss. Subsequently, the rate of weight loss decreased slowly at moderate temperatures about 200-450°C (Table) because of the decomposition of bleached shellac (approximately 20-30 % of weight loss). The final stage, the samples without drug loading completely degraded at higher 450°C while the *in situ* forming gels with drug loading still remained a residual of doxycycline hyclate around 10% of weight loss. The partial weight losses of each sample correspond to the quantity of compositions in *in situ* forming formulations. It could primarily reflect the weight change of substance in formulation with heat.



**Fig. 40** TG curves of *in situ* forming gels and their compositions



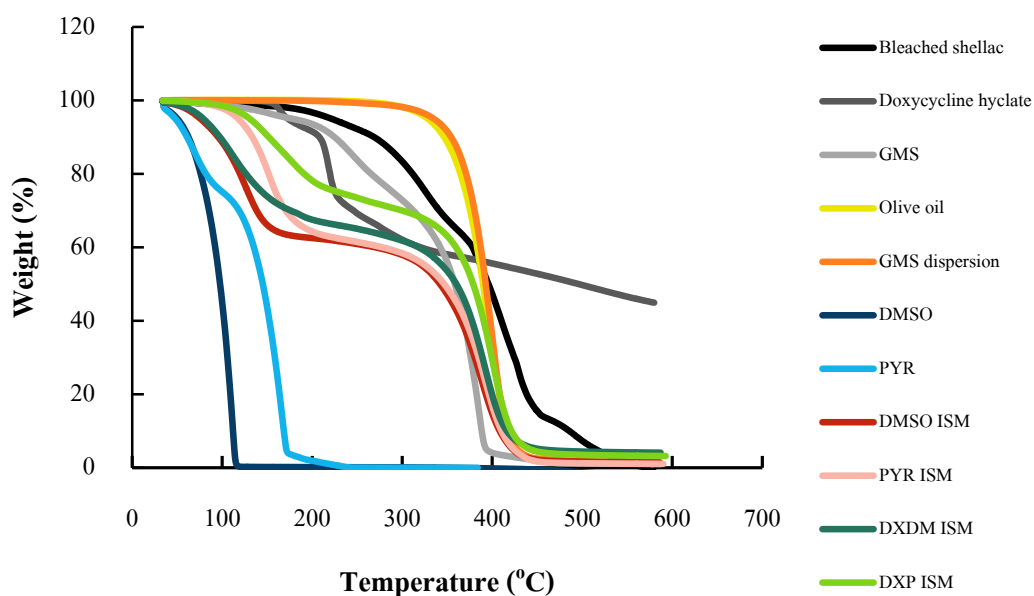
**Fig. 41** DTGA curves of *in situ* forming gels and their compositions

**Table** DTGA peaks of *in situ* forming gels and their compositions

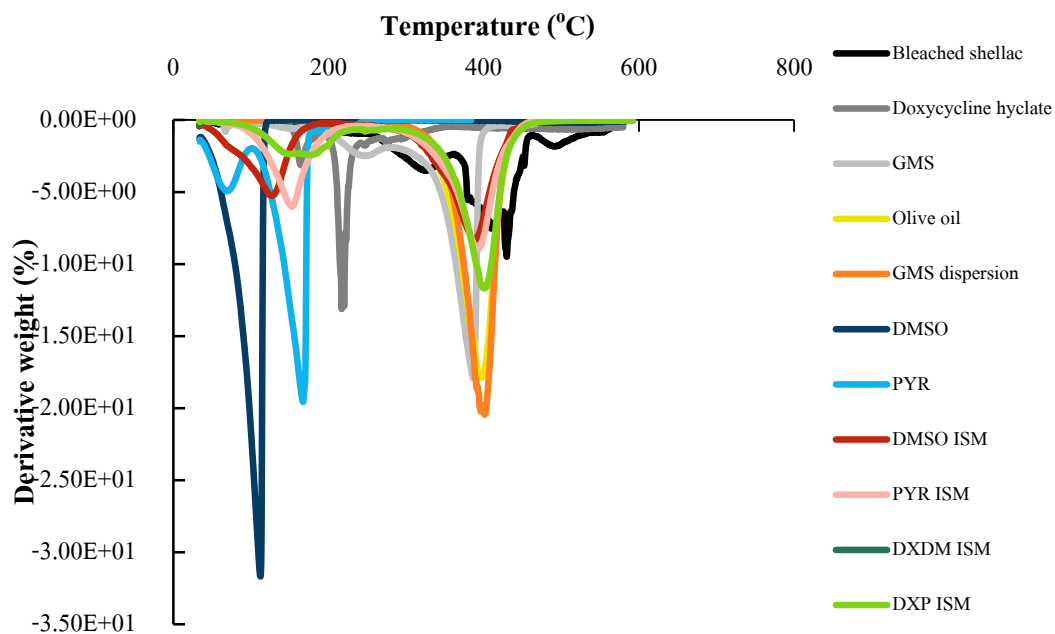
Substance	Temperature (°C)	Derivative weight (%)
Bleached shellac	429.64	-9.492
Doxycycline hyclate	216.96	-13.115
DMSO	112.21	-31.677
NMP	117.25	-23.214
PYR	167.23	-19.564
DMSO gel	119.17	-9.878
	397.76	-2.916
NMP gel	122.18	-14.286
	402.53	-2.153
PYR gel	162.6	-13.026
	399.29	-2.108
DXDM gel	109.67	-10.351
	397.74	-2.102
DXN gel	119.17	-9.878
	397.59	-2.916
DXP gel	154.34	-7.864
	398.79	-1.959



The weight loss profiles and differential weight loss profiles of the ISM samples and their compositions were obtained from TGA as reported in Figs. 42 and 43. The ISM systems presented a similar trend of thermal decomposition. There was a higher decrease rate of thermal degradation from sample prepared with DMSO compared to that prepared with PYR. The systems with drug loading appeared a slower decrease rate of thermal degradation. These phenomena had been discussed in previous section. The values of the partial weight losses and their characteristic temperatures determined from TG profiles and the minimum of the two peaks (Table) observed on the derived TG curves of the ISM samples. The first decomposition observed in the temperature range of 100 to 200°C with a higher increase rate of weight loss, mainly involved the solvent evaporation (30-35% of weight loss due to a presence of olive oil). The second stage was from 250°C to 450°C with a slow decrease rate of weight loss which might correspond to the structural decompositions of GMS dispersion and bleached shellac, respectively (nearly 65% of weight loss). The last step, the samples without drug loading totally decomposed at temperature higher than 450°C while the ISM with drug loading still remained a residual of doxycycline hyclate by mostly 5% of weight loss. This was interesting to clarify a relationship between each partial weight loss of samples and amount of substances in formulation which basically assures that in process of manufacture did not damage the compositions of ISM system.



**Fig. 42** TG curves of *in situ* forming microparticles and their compositions



**Fig. 43** DTGA curves of *in situ* forming microparticles and their compositions

**Table** DTGA peaks of *in situ* forming microparticles and their compositions

Substance	Temperature (°C)	Derivative weight (%)
Bleached shellac	429.64	-9.492
Doxycycline hyclate	216.96	-13.115
GMS	386.03	-17.923
Olive oil	327.38	-17.888
GMS dispersion	400.94	-20.448
DMSO	112.21	-31.677
PYR	167.23	-19.564
DMSO ism	129.11	-5.204
	388.36	-8.346
PYR ism	153.24	-6.02
	393.06	-8.97
DXDM ism	148.89	-2.36
	391.82	-9.691
DXP ism	151.92	-2.52
	399.58	-11.683

## Summary

In accordance with morphology studies of o/o emulsion, the stabilizer concentration and phase ratio were definitely influenced on droplet size. An increase of GMS concentration significantly reduced the average droplet size of emulsion because it formed the gel network with olive oil towards to decrease a coalescence. The 5% w/w GMS effectively stabilized emulsion with the droplet size approximately 65  $\mu\text{m}$  so that it was selected for further study. In the case of phase ratio, the external phase ratio directly affected the emulsion size and formation. Only higher quantity of this phase could form into the complete emulsion droplets. Particle size of emulsion droplets for both systems with and without constant concentration of GMS tended to be decreased approximately 95  $\mu\text{m}$  to 30  $\mu\text{m}$  since there was an adequate formation area of microparticle which could prevent the particle accumulation or coalescence.

The appearance viscosities of solvents and other compositions were in the rank of order as following: PYR >> NMP > DMSO and GMS dispersion (or olive oil with GMS) > olive oil. This dispersion was more viscous than pure oil owing to the formation of gel network between needle-like crystals of GMS and oil molecules. These crystals could stabilize the emulsion by locating at the interface between the oil phase and the internal phase. The *in situ* forming gels exhibited the trend of viscosities as following: PYR gel >>> DMSO gel > NMP gel and DXP gel >>> DXDM gel >> DXN gel. PYR formulations were the most viscous whereas those prepared with NMP were contrary. PYR could interact with bleached shellac less than NMP. They were defined as poor solvent and good solvent, respectively. The appearance viscosity result was opposite to the relative viscosity study owing to different theoretical aspects of polymeric interaction with solvents as previous mentioned. The doxycycline-loaded systems presented a higher viscosity which probably caused by a replacement of drug in solvent or a functional group interaction between drug and bleached shellac. In the case of ISM systems, the trend of viscosity was similar with gels but their viscosity was lower because it was predominant from the oil presented in the external phase. The flow behavior of all formulations was Newtonian or Pseudoplastic which was proper for injectable dosage forms due to its low resistance during syringe administration.

The role of solvent on the 3D-network formation and viscoelastic behavior within bleached shellac gels and emulsion was clarified by steady shear and sinusoidal oscillatory tests. It indicated that the crosslinking (entanglement) capacity of solvent was rational in the order of PYR > DMSO > NMP. Therefore PYR was able to enhance the maximum mechanical strength and crosslinking density while NMP was vice versa. The rheological behavior of gels in PYR and NMP were typical liquid-like in all frequency and temperature range but the systems prepared with DMSO differently presented both solid and liquid-like characters from low to high frequencies. This solid-like nature was probably due to the entanglements between DMSO and shellac via hydrogen bonds at low frequencies. Sulfoxide group (DMSO) has greater potential hydrogen bond acceptor compared to carbonyl group of NMP and PYR because of its stronger electronegativity. For crosslinking capacity of ISM systems, it exhibited the inverse order as following: DMSO > PYR because GMS could interact with each solvent by different bond as well. However, ISMs had similar rheology behavior to the gels.

Thermal changes or enthalpy information from DSC technique showed the behavior of solvent state in polymer. Each solvent possessed a heterogeneous interaction with bleached shellac. DMSO was able to form some new hydrogen bonds between its sulfoxide group and hydrogen atom from bleached shellac while NMP did not provide this weak bond as criticized in viscoelastic study. The crystallinity was found in NMP, and the surface of these chain-folded crystals interfered an amorphous region of polymer during cooling cycle temporarily. The disappearance of crystallinity was caused by the robust interactions between solvents and polymer. These interactions promoted the NMP molecules bonded to bleached shellac and eventually disrupted the inter-chain bond. PYR is poor solvent compared to previous ones. It formed the weak bond with bleached shellac molecule and inability to disrupt the inter-segment bonds in the amorphous forms of polymer chain resulted in an increase of free solvent in system. Additionally, the behavior of solvent state in drug-loaded gels showed a similar trend to free drug systems, and it also exhibited the crosslinking reaction between doxycycline hyclate molecules and polymer, especially in DXDM ism. For bleached shellac ISMs, their thermograms were covered by hindrance effect from olive oil and GMS (stabilizer) in external phases.

The weight loss at different temperatures provided the changes in sample composition. DMSO or NMP in the *in situ* forming systems exhibited the higher thermal degradation rate than PYR, probably related with the differences in intermolecular strength forces and viscosity. A replacement some of them with doxycycline hyclate in the formula actually required a greater degradation energy so that it quite decreased the thermal degradation rate. At the end of thermal measurement, all systems remained a residual of drug. The partial weight losses of each sample correspond to the quantity of compositions in *in situ* forming formulations. It basically assures that in process of manufacture did not damage the compositions.



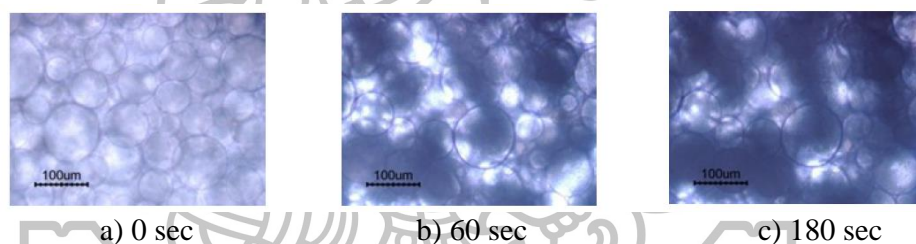
### Part 3

#### 4.3.2 Evaluation of *in situ* forming gel systems during exposure to solvent exchange

##### 4.3.2.1 Transformation of sol into microparticle study

###### Effect of stabilizer concentration on ISM formation

According to the previous study for the effect of stabilizer concentration on droplet size, the concentration of GMS was varied from 0 to 5% of external phase. The system comprising 5% w/w GMS showed the smallest droplet size of emulsion therefore this concentration was selected for further study. ISM systems transformed from the emulsion to microparticle owing to phase separation triggered by solvent exchange. This study explored the solidifying droplets of the internal phase from emulsion upon contact with environmental fluids under inverted microscope. Dynamic ISM formation study revealed that only 5% GMS of external phase or 2.5% GMS of whole system could induce the system transforming to the microparticles after exposure to phosphate buffer pH 6.8 within 3 min as shown in Fig. 44. Therefore GMS was able to gel the vegetable oils by forming its network remaining intact upon emulsification in non-aqueous ISM emulsion containing 5% GMS and also decreasing droplet coalescence of emulsions (Chen and Terentjev, 2009; Hodge and Rousseau, 2005). Consequently, 5% GMS of external phase was employed as emulsion stabilizer for further investigation.



**Fig. 44** Transformation of ISM with phase ratio of 1:1 (external phase: internal phase) comprising 5% GMS of external phase or 2.5% of whole system within 3 min

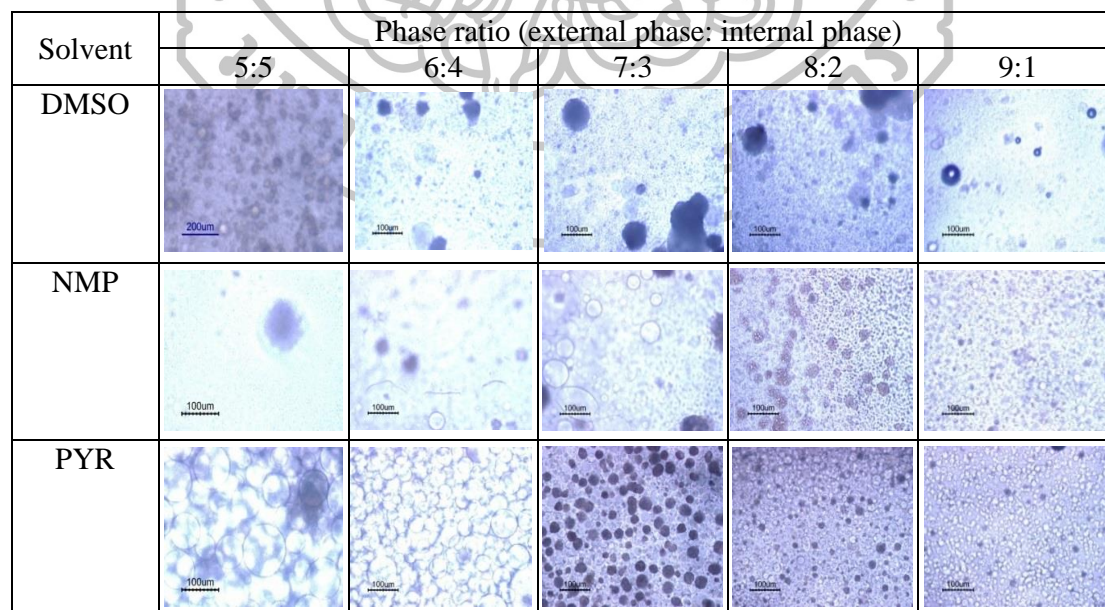
###### Effect of phase ratio and type of solvent on ISM forming

The phase ratios as 5:5, 6:4, 7:3, 8:2 and 9:1 (in term of external phase: internal phase) was tested for ISM development. Three solvents were used for dissolving bleached shellac and used as the internal phase while 5% GMS of the external phase or 2.5% GMS of whole system was dispersed in olive oil as the external phase. From dynamic transformation study under an inverted microscope revealed that all ISM systems with different solvents transformed into microparticle suddenly after contacting with PBS. The PYR was the most appropriate solvent for producing massive microparticles with regular shape especially at the phase ratio of 7:3 as depicted in Fig 45. Contact between ISM and an aqueous medium triggered a phase separation of bleached shellac by solvent exchange in the polymeric emulsions, which finally resulted in polymer precipitation into microparticles. Key parameters of the phase inversion dynamics of ISM are the influx of aqueous medium (i.e. water) as well as the outflow of polymer solvent (Parent *et al.*, 2013). The flows are possible depending on a role of miscibility between solvent and water, basically indicated by solubility parameter ( $\delta$ ). Materials with similar values of  $\delta$  are likely

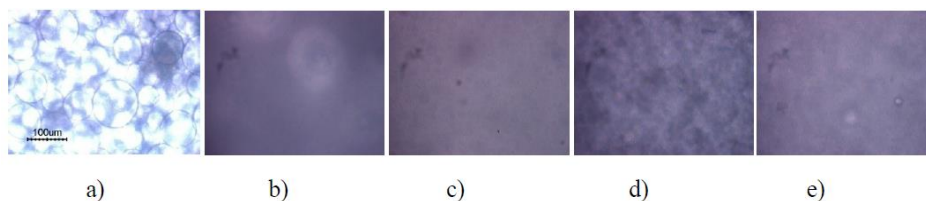
to be miscible. The  $\delta$  value of DMSO, NMP, PYR, water, and bleached shellac were literally 12.0, 11.3, 14.7, 23.4 and 11.3, respectively (Barton, 1975). PYR is most likely to be miscible with water whereas it is the worst solvent for this polymer. Therefore, PYR tended to outflow from the *in situ* system. In the case of water-miscible solvents, an injection of the polymeric solution into water leads to a fast diffusion of the solvent towards the aqueous medium. This triggers the formation of solidified polymer layer at the top of the depot (Young and Chen, 1995). Considering to this research work, the solubility of bleached shellac in PYR was rather low while the solvent had a larger affinity to water, resulted in an increase rate of polymer precipitation and a rapid formation of numerous microparticles.

Besides, the phase ratios were also designed by reducing the external phase to internal phase as 5:5, 4:6, 3:7, 2:8 and 1:9 in the suitable solvent system. When the ratio of external phase was less than the internal phase, the system did not form into the microparticles in PBS as shown in Fig. 46. Furthermore, in the case of drug-loaded system, only that of DMSO series (Fig. 47) exhibited the larger amount and size of microparticles compared to PYR and NMP series (Fig. 47) which might be due to crosslinking reactions between polymer and drug molecules as previously described in thermal analysis.

The above studies varied the phase ratio by increasing the external phase which caused the rising of amount of stabilizer as well. Therefore, the additional investigation was conducted by fixing GMS concentration at 2.5% w/w of the whole systems and selecting the most suitable system to be a representative. The similar outcome was attained as the previous studies (data not shown). This phenomenon could be explained that in the environment of higher quantity of internal phase, particles could be easier to merge together promoting the coalescence. Therefore, the decreasing internal phase: external phase ratio improved the stability of ISM emulsion against the droplet coalescence (Tcholakova *et al.*, 2002). Thus the varying phase ratios dominantly affected this transformation.



**Fig. 45** Transformation of systems with different ratios of external an internal phase: 5:5; 6:4; 7:3; 8:2 and 9:1 after contacting PBS pH 6.8 at 10 sec at magnitude of 20X



**Fig 46.** Transformation of systems using 2-pyrrolidone as solvent with different ratios of external and internal phase: a) 5:5; b) 4:6; c) 3:7; d) 2:8 and e) 1:9 after contacting PBS pH 6.8 at 10 sec at magnitude of 20X

Solvent	Phase ratio (external phase: internal phase)				
	5:5	6:4	7:3	8:2	9:1
DMSO					
NMP					
PYR					

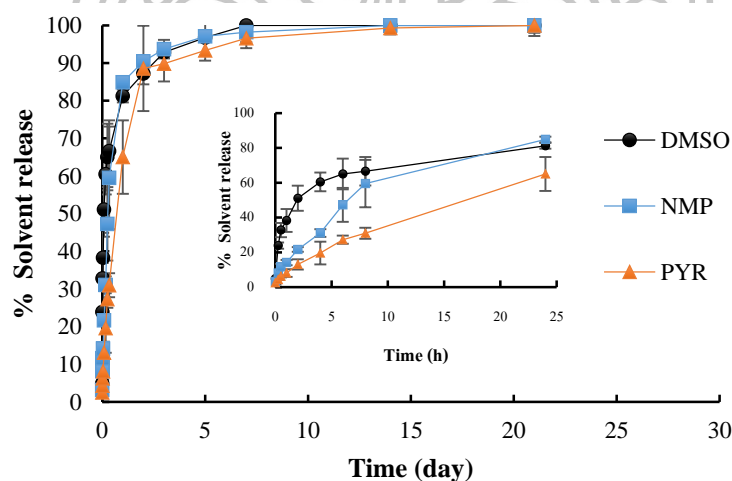
**Fig. 47** Transformation of doxycycline hyclate-loaded systems with different ratios of external and internal phase: 5:5; 6:4; 7:3; 8:2 and 9:1 after contacting PBS pH 6.8 at 10 sec at magnitude of 20X

#### 4.3.2.2 *In vitro* solvent and drug release studies

Solvent-exchanged *in situ* forming system is based on phase separation of polymer by solvent movement which the organic solvent (dissolving the polymer) flows out from the system and the water inflows via diffusion inducing polymer precipitation (Graham *et al.*, 1999). This process relates in sol-to-gel transformation causing polymer precipitation or solidification and forming into polymer matrix to control the drug release (Nirmal *et al.*, 2010; Parent *et al.*, 2013). Four major diffusional motions have to be considered for the formation of *in situ* forming gels or ISM: solvent diffusion out, non-solvent diffusion in, drug out and probably fractions of polymer out (Kranz and Bodmeier, 2008). In this section, this research finely examined two important factors i.e. solvent diffusion out and drug diffusion out using HPLC assay. For non-solvent diffusion in and fractions of polymer diffusion out would be considered in further studies.

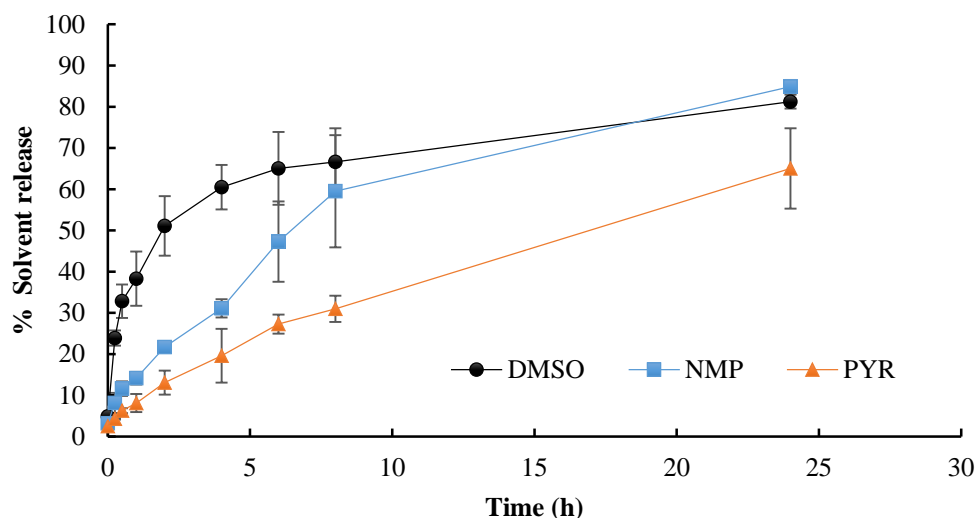
### *In vitro* solvent release study

The solvent release from the polymer solutions upon contact with aqueous medium was investigated as depicted in Figs. 48 and 49. DMSO, NMP and PYR released from *in situ* forming gel at first 8 hours of 67%, 60% and 31%, respectively. All *in situ* forming gels completed their solvent release at least 7 days. The solvent release rate initially decreased in the rank order as DMSO > NMP > PYR, which is identical to another earlier research (Kranz & Bodmeier, 2008). To further explain the *in vitro* solvent release rates, the interaction between polymer and shellac was an essential role to consider. The smaller differences in the solubility parameter of the polymer and of the solvent point out the higher polymer/solvent interaction or solvating power. Generally, a solvent with higher solvating power provides the slower rate of precipitation and the apparent non-solvent (i.e. water) required for polymer precipitation (Kranz and Bodmeier, 2008). A slower polymer precipitation leads to a less porous matrix surface, thus decreasing the solvent and drug release (Graham *et al.*, 1999). According to this principle and previous discussions (i.e. review literature of solubility parameter and relative viscosity study), NMP was a better solvent for bleached shellac than DMSO and PYR. Therefore bleached shellac in NMP remained in liquid state for a long time. It might explain a slower NMP release from *in situ* gel compared to that prepared with DMSO. Nevertheless, it cannot explain the slowest PYR release from this system. To consider the viscosity of concentrated shellac solution in PYR and of solvent itself, which mentioned in apparent viscosity study, could appropriately explain the slower solvent liberation rate from DXP gel. Typically, an increasing viscosity of solvent including polymer solution retards the solvent and drug diffusion rates (Kranz and Bodmeier, 2008).



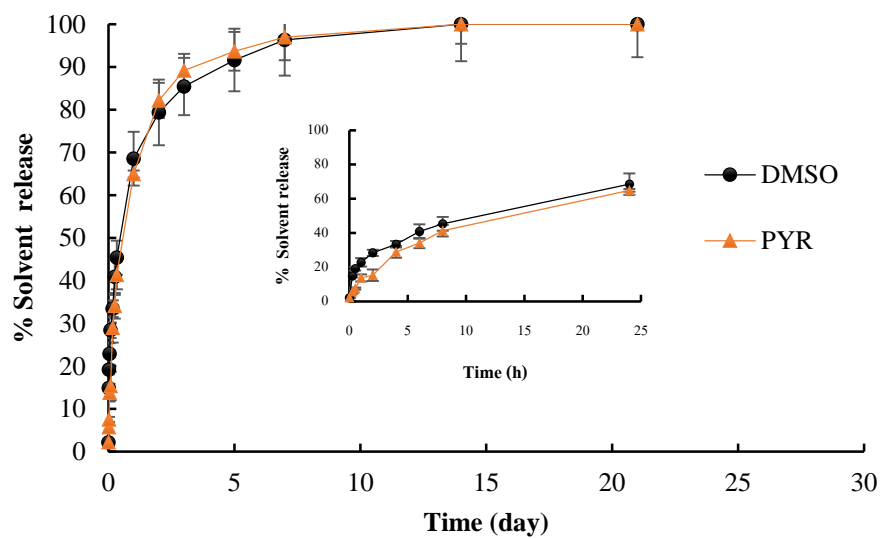
**Fig. 48** Release of DMSO, NMP and PYR from *in situ* forming gels in PBS pH 6.8 within 21 days (n=3)



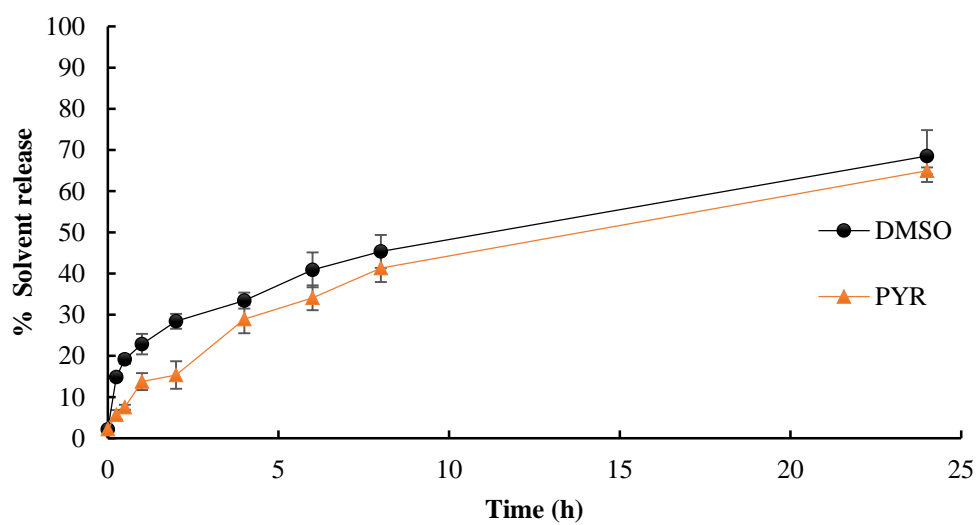


**Fig. 49** Initial solvent release of *in situ* forming gels in PBS pH 6.8 within 1 day (n=3)

Regarding contact the polymer emulsion of selected ISM to aqueous environment, the solvent release was evaluated as illustrated in Figs. 50 and 51. The 45% DMSO and 41% PYR released into the buffer medium at 8 h. Both ISMs accomplished their solvent release at least 14 days which were apparently slower than that from *in situ* forming gel systems. The solvent release rate of DMSO was higher than that of PYR which showed a similar trend to that of *in situ* forming gels. Therefore, it can explain this circumstance as mentioned in previous part. In addition, the polymer/solvent interaction distinctly influenced the relative viscosity and transformation studies. It revealed that bleached shellac emulsion tailored with PYR was able to undergo polymer precipitation rapidly and form into the numerous microparticles because PYR appeared the greater affinity to water than bleached shellac. However, the viscosity of solvent itself and of polymer emulsion was dominant over this occurrence which resulted in a decrease of diffusion. By comparison with *in situ* forming gels, the ISM showed the lower initial burst and slower release of solvent because oil in the external phase acted as a barrier for the solvent diffusion (Ahmed *et al.*, 2014).



**Fig. 50** Release of DMSO, NMP and PYR from *in situ* forming microparticles in PBS pH 6.8 within 21 days (n=3)



**Fig. 51** Initial release of DMSO, NMP and PYR from *in situ* forming microparticles in PBS pH 6.8 within 1 day (n=3)

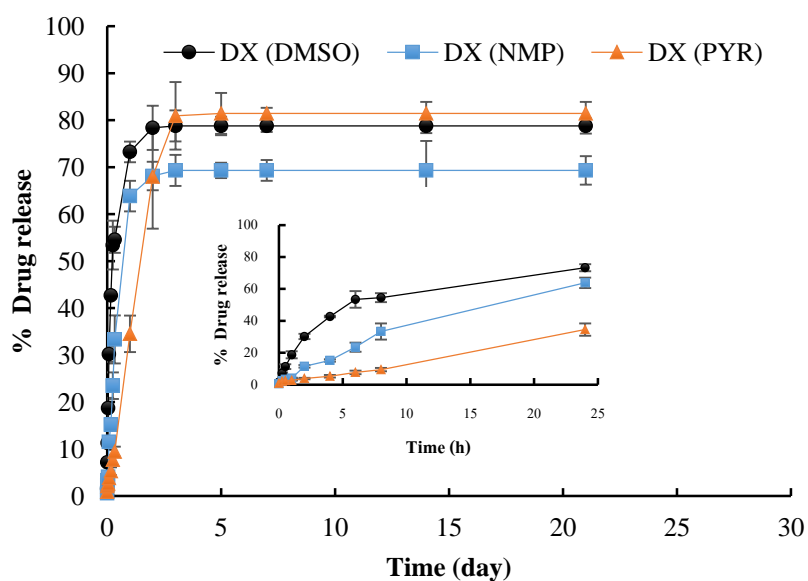
### ***In vitro* drug release study**

During the solvent exchange process after administration of *in situ* forming systems into aqueous environment, drug release is essentially occurring with solvent outflow through the polymer or water filled channels (Fredenberg *et al.*, 2011). This study investigated *in vitro* drug release from the prepared systems as a function of type of solvent. The drug release profiles as shown in Figs. 52 and 53 revealed that the extent of doxycycline hyclate released from DMSO, NMP and PYR was 55%, 33% and 9%, respectively at first 8 h. The *in situ* forming gels exhibited a trend of drug release pattern, similar to solvent release, in the rank order as following: DMSO > NMP > PYR. It previously comprehended that the viscosity of concentrated bleached shellac in PYR and of solvent itself were more influential on polymer solidification toward the solvent release than the interaction between solvent and shellac therefore this character also influenced as the slower drug diffusion rate from DXP gel. Practically, the water miscibility and viscosity of the polymer solvent play a critical role for drug release because they impact on the aqueous medium governing drug diffusion (Parent *et al.*, 2013).

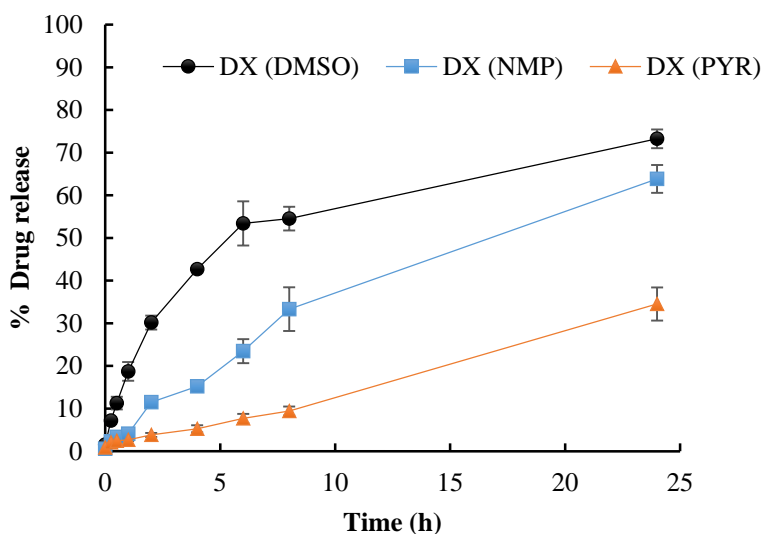
Three systems incompletely finished drug release within 3 days (Fig. 52) with final amount for DMSO (79%), NMP (69%) and PYR (81%), contrasted to ISM (Fig. 54) which drug completely liberated. The amount of drug release from *in situ* forming gels had a priority in the following order of PYR > DMSO >> NMP. The main factors affecting an incomplete drug release are drug-drug interactions (Fredenberg *et al.*, 2011), matrix polymer-drug interactions (Wischke and Schwendeman, 2008), physical structure of matrix such as particle size, surface area (Nazzal *et al.*, 2002; Sander and Holm, 2009) and pore space topologies (Saltzman, 2001), and robust environmental conditions such as flow rate, buffer concentration, temperature and the presence of enzymes or release residual (Li *et al.*, 1996).

It surprisingly found an incomplete drug release of *in situ* gels in contrast to ISM. Although ISM did deal with a barrier from external oil phase, it was able to achieve a complete drug leached out pattern. Therefore, the drug-drug interaction or polymer-drug interaction may not have an influence on the incomplete profile of *in situ* gels. In addition to release conditions, both *in situ* forming systems were incubated under uniform environment, and pH value of aqueous medium was approximately 6.8 which could practically higher dissolve doxycycline hyclate than polymer solvents (Stippler, 2004). The latter consideration was a change of pH value after long incubation in PBS buffer. An earlier solvent release study showed that the initial solvent release from *in situ* gels was notably faster compared to that of ISM, resulted in larger diffusion of drug. These release products did not vanish easily from the release medium, which caused a decrease in pH as previously discussed in pH study. However, the solubility of doxycycline hyclate in slightly acidic buffers (pH 6.8) and strong acidic buffer (pH 1.2) was reported as about 28 mg/mL and 40 mg/mL, respectively (Stippler, 2004) while the total drug concentration in 100 mL aqueous medium which released from overall *in situ* forming system (1g) was merely 1 mg/mL. Thus drug precipitation should not be evident in medium after long incubation in aqueous medium. These release condition and pH value of environmental medium were not able to affect the incompleteness of release.

Some studies verified that a decrease of particle size practically enlarged the surface area to volume ratio to the effective drug release (Hile *et al.*, 2000; Khadka *et al.*, 2014). At equivalent weight, ISM had the lower volume and higher surface area of matrix particles compared to *in situ* forming gel. It rationally anticipated a uniform distribution of drug throughout the matrices from ISM rather than gel. This apparent larger surface area was available for solvation towards drug diffusion from matrix particles (Witt, 2001). In the case of *in situ* forming gel, drug might densely aggregate and be trapped in matrix core upon phase inversion. Therefore it probably resulted in the incomplete drug release. Furthermore, type of solvent affected the final amount of drug release from gels for DMSO (79%), NMP (69%) and PYR (81%). It was interesting that PYR had the slowest solvent release rate, reversely demonstrated the largest release extent at the end. This occurrence possibly related with microstructural alignment of pores in matrices after long immersion in aqueous environment (Saltzman, 2001). It might hypothesize that a large amount of viscous PYR accumulated in porous matrix and it had the strongest water affinity to probably enhance an osmotic force to attract more water inflow, leading in higher hydrolysis at ester bond of bleached shellac. The ester hydrolysis was able to fracture the porous matrix structure, and finally extrude the trapped drug molecules inside of core. By comparison for DMSO and PYR, it can be explained by viscosity of solvent itself as earlier criticized. However, this presumption could be verified in further studies such as degradation, SEM and etc.

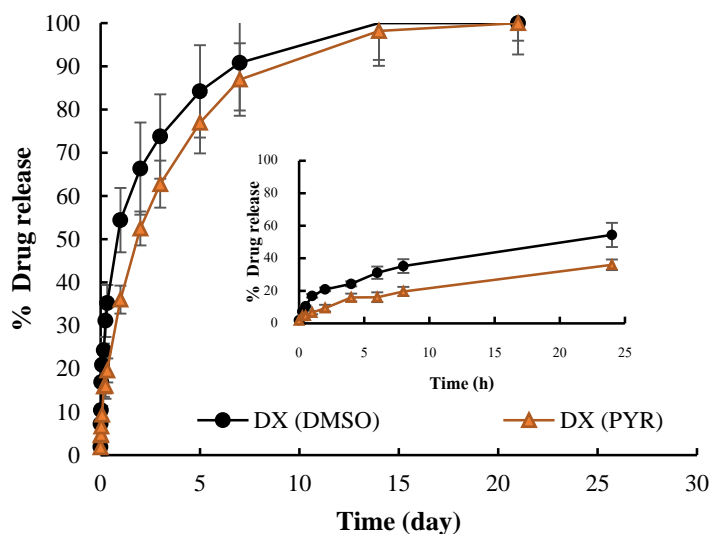


**Fig. 52** Drug release from *in situ* forming gels in PBS pH 6.8 within 21 days (n=3)

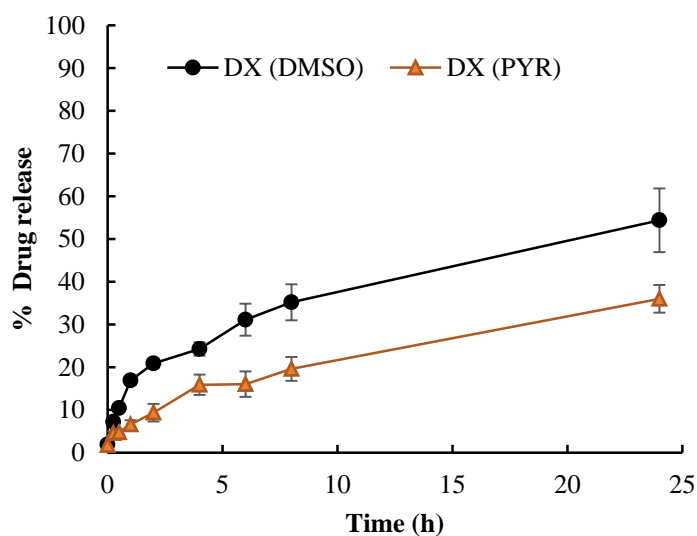


**Fig. 53** Initial drug release of *in situ* forming gels in PBS pH 6.8 within 1 day (n=3)

Upon ISM contacted to aqueous environment, the drug release was measured as illustrated in Figs. 54 and 55. The extent of drug release from DXDM ism and DXP ism was 35% and 20%, respectively at first 8 h. Both ISMs completed their drug release near to 100% at 21 days. The drug release rate of DMSO ism was higher than that of PYR ism, corresponding to that from *in situ* forming gels. The polymer/solvent interaction and viscosity of solvent itself were the important influence on the release rate as previously discussed. The overall results confirmed that ISM system significantly reduced a burst effect because of the retardation for both of solvent and drug diffusions owing to the hydrophobicity of an external oil phase (Ahmed *et al.*, 2014). The larger surface area to volume ratio of ISM compared to gel, prevented the drug accumulation in the matrix core and finally provided the complete drug release as previous mentioned. It was the essential evidence to approve that doxycycline hyclate in polymer solution or internal phase did not decompose throughout preparation as the evidence from TG result and no drug accumulation in residual matrix. Therefore the developed ISM systems were able to modulate a drug release effectively.



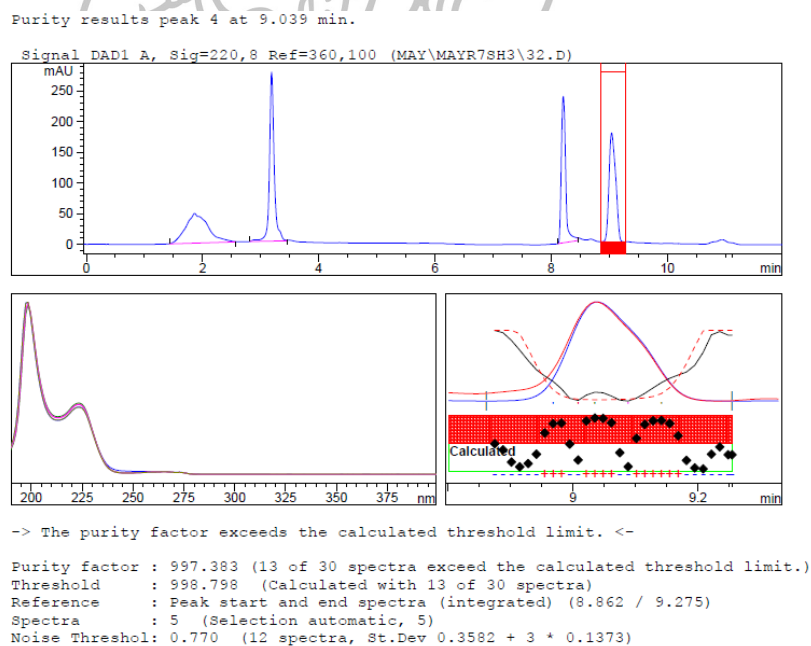
**Fig. 54** Drug release from *in situ* forming microparticles in PBS pH 6.8 within 21 days (n=3)



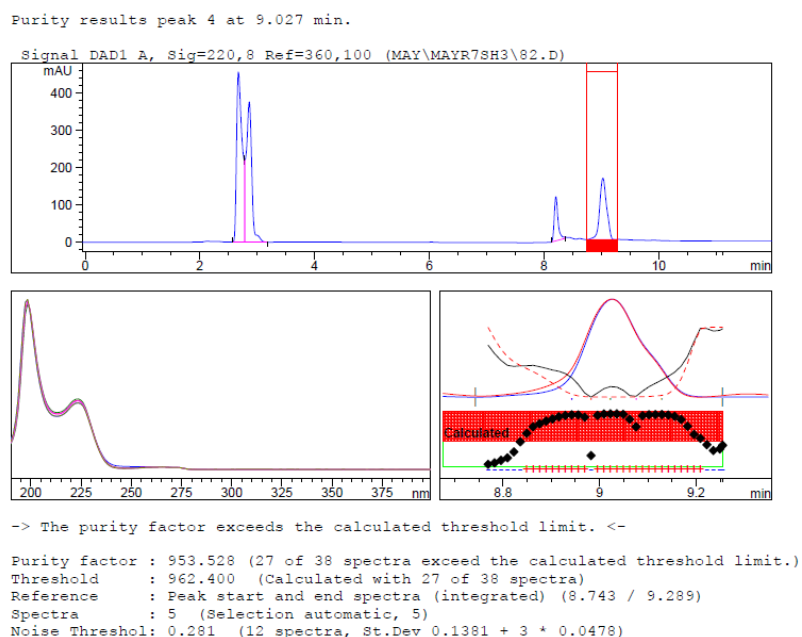
**Fig. 55** Initial drug release from *in situ* forming microparticles in PBS pH 6.8 within 1 day (n=3)

Surprisingly, the quantitative HPLC assay revealed the presence of unknown peak at the latest retention time from all *in situ* forming systems. It was primarily hypothesized that this unknown peak might be a compound from some chemicals from bleached shellac and it should be identified by peak purity analysis mode. The identification was conducted on scanning a wavelength range for UV absorption of bleached shellac (maximum peak at 223 nm, Farag and Leopold, 2009) from 200 to 400 nm. The release specimen from DXP gel was sampled to identify its constituent. The HPLC peaks of this sample (Fig. 56) were compared to the reference peaks (Fig. 57) which acquired from a well diluted DXP gel in

acetonitrile. In the case of other formulations, they provided the mutual pattern hence these data were not shown. The retention time of unknown peak was optional on the top of peak purity analysis sheets and obtained the same value at approximately 9.0 min. On the left side below the chromatogram was an overlay of the different peak spectra which clearly showed their degree of similarity and therefore also the purity of the chromatographic peak investigated. Both samples appeared the perfect overlap signals with similar purity factor near to 1,000 indicated high degree of similarity, and including its UV maximum absorbance at 225 nm which was also related to other report (Farag and Leopold, 2009). On the right side below the chromatogram, they were the similarity-threshold curves and the purity ratio which effectively determined the peak purity with high sensitivity. However, this study focused to identify the unknown peak therefore it was not necessary to consider the purity of substance as presented in a frame on the right side. According to retention time, purify factor, and UV maximum absorption peak between sample and control were identical, it could be concluded that unknown peak is a residual unit from bleached shellac. Furthermore, the possible chemical structure of a compound would rather be a ring form related to shelloic acid and its isomer due to a retention time of unknown was near of doxycycline hyclate which had four hydrocarbon rings as well. Therefore the bleached shellac matrices from *in situ* forming systems were able to be degraded upon contact with in PBS buffer pH 6.8.



**Fig. 56** Identification of unknown peak by peak purity analysis mode of a release medium from DXP gel as specimen



**Fig. 57** Identification of unknown peak by peak purity analysis mode from diluted DXP gel in acetonitrile as reference peaks

#### 4.3.2.3 Analysis of solvent and drug release data

The mathematical modeling is a quantitative analysis to comprehend all phenomena affecting drug release kinetics and this has a very significant value in the formulation optimization. This research aimed to elucidate the effect of solvent type on physical properties of polymer matrix formation of *in situ* forming gel and ISM. Solvent exchange process is a major mechanism to solidify the polymer solution into the matrix form and initiate the drug release. Therefore it is interesting and necessary to study the release mechanism of solvent and drug from the *in situ* forming systems by describing the pattern of drug release mathematically. In order to fit the release data to mathematical models, this study applied four drug release kinetic models (first order, Higuchi's, zero order and power law) and calculated the value of coefficient of determination ( $r^2$ ) and model selection criteria (msc) to indicate the degree of goodness-of-fit. The release rate (k) and release exponent values (n) from power law model were also determined.

##### Analysis solvent release data

Solvent release data of all *in situ* forming systems were fitted to mathematical models (first order, Higuchi's, zero order and power law) which the estimated  $r^2$  and msc are shown in Table 7. The high value of these parameters indicated a superiority of the release profile fitting to mathematical model. Solvent release profile of DMSO and NMP formed *in situ* gel systems fitted well with a power law model and had an intimate relationship with a Higuchi's kinetic model. This solvent release behavior related to the dissolution from polymer matrix of water soluble drug as reported previously (Shoaib *et al.*, 2006). Another *in situ* forming system fabricated with PYR obviously fitted with a first



order model. This *in vitro* drug release behavior has been reported in pharmaceutical dosage form containing water-soluble drug in porous matrices (Silvina *et al.*, 2002; Phaechamud and Mahadlek, 2015). The solvent release exponent value (n) from curve fitting with a power law equation of DMSO and NMP formulations was close to 0.45 indicating that the solvent released by a Fickian diffusion mechanism (Table 8). This mechanism was strongly controlled by liquid diffusion rate rather than relaxation rate of the polymeric chains (Perioli *et al.*, 2004). In general, a release mechanism of matrix system is probably a Fickian diffusion driven, which is associated with concentration gradient, diffusion distance and the degree of swelling (Siepmann and Siepmann, 2008). In the case of PYR formulation, the solvent release exponent value (n) was  $0.45 < n < 0.89$  which was influenced by an anomalous (non-Fickian) transport. It indicated that the drug release was dominated by both mechanism of diffusion and polymeric chain relaxation (Pahwa *et al.*, 2011). The solvent release rate (k) of these systems were significantly different ( $p < 0.05$ ) and priority in order of DMSO > NMP > PYR which corresponded to previous release study.

**Table 9** Comparison of degree of goodness-of-fit from curve fitting of solvent release from *in situ* forming gel systems

Formula (solvent)	First order		Higuchi's		Zero order		Power law	
	r <sup>2</sup>	msc	r <sup>2</sup>	msc	r <sup>2</sup>	msc	r <sup>2</sup>	msc
DXDM gel	0.9584	0.45	0.9752	1.97	0.9541	0.35	0.9985	3.51
DXN gel	0.9836	2.35	0.9912	2.63	0.9680	1.34	0.9929	2.51
DXP gel	0.9997	6.29	0.9982	4.49	0.9873	2.51	0.9986	4.36

**Table 10** Estimate parameter from curve fitting of solvent release from *in situ* forming gel systems

Formula (solvent)	k ± S.D.	n ± S.D.	Release mechanism
DXDM gel	0.1932 ± 0.0192	0.20 ± 0.02	Fickian diffusion
DXN gel	0.0368 ± 0.0182	0.44 ± 0.07	Fickian diffusion
DXP gel	0.0130 ± 0.0047	0.53 ± 0.05	Anomalous transport

In the case of ISM, both systems fitted well with a power law model and had a close relationship with a Higuchi's kinetic which indicated the characteristic of dissolution of water soluble drug from polymer matrix (Table 9) (Shoaib *et al.*, 2006). The solvent release exponent value (n) from curve fitting with power law of both formulations were close to 0.45 indicating of solvent release by a Fickian diffusion mechanism (Table 10) as previously mentioned. The solvent release rate (k) of DMSO was significantly higher than that of PYR as mentioned in earlier part.

**Table 11** Comparison of degree of goodness-of-fit from curve fitting of solvent release from ISM

Formula (solvent)	First order		Higuchi's		Zero order		Power law	
	r <sup>2</sup>	msc	r <sup>2</sup>	msc	r <sup>2</sup>	msc	r <sup>2</sup>	msc
DXDM ism	0.9903	2.45	<u>0.9918</u>	2.62	0.9771	1.59	<u>0.9986</u>	4.11
DXP ism	0.9807	1.80	<u>0.9907</u>	2.54	0.9750	1.55	<u>0.9953</u>	2.93

**Table 12** Estimate parameter from curve fitting of solvent release from ISM

Formula (solvent)	k ± S.D.	n ± S.D.	Release mechanism
DXDM ism	0.0575 ± 0.0100	0.33 ± 0.02	Fickian diffusion
DXP ism	0.0291 ± 0.0087	0.41 ± 0.08	Fickian diffusion

### Analysis drug release data

Drug release data of prepared *in situ* forming gels fitted well with a power law model (Table 11) and obeyed Fickian diffusion mechanism. These formulations had the significantly different ( $p < 0.05$ ) drug release rate (k) with priority in order of DXDM gel > DXN gel > DXP gel. The entire behaviors of drug release corresponded to the solvent release behavior except PYR formulation which presented an anomalous (non-Fickian) mechanism instead (Table 12). In this PYR case, chemical potential gradient of doxycycline hyclate itself might play a stronger role on molecular drug diffusion through the porous matrix than solvent driven, it therefore performed with a Fickian diffusion transport (Singhvi and Singh, 2011).

**Table 13** Comparison of degree of goodness-of-fit from curve fitting of drug release from *in situ* forming gel systems

Formula (DX)	First order		Higuchi's		Zero order		Power law	
	r <sup>2</sup>	msc	r <sup>2</sup>	msc	r <sup>2</sup>	msc	r <sup>2</sup>	msc
DXDM gel	0.9166	0.17	<u>0.9366</u>	1.20	0.8949	0.84	<u>0.9968</u>	2.90
DXN gel	0.9481	0.64	<u>0.9684</u>	1.14	0.9192	0.66	<u>0.9888</u>	1.85
DXP gel	0.9523	0.98	<u>0.9709</u>	1.18	0.8817	0.15	<u>0.9863</u>	1.54

**Table 14** Estimate parameter from curve fitting of drug release from *in situ* forming gel systems

Formula (DX)	k ± S.D.	n ± S.D.	Release mechanism
DXDM gel	0.1359 ± 0.0242	0.23 ± 0.03	Fickian diffusion
DXN gel	0.0785 ± 0.0402	0.27 ± 0.07	Fickian diffusion
DXP gel	0.0361 ± 0.0124	0.36 ± 0.14	Fickian diffusion

Drug release from ISM formula in Table 13 was best explained by a power law model but they had a close relationship with a Higuchi's kinetic. Their drug release

mechanism was driven by a Fickian diffusion and DXDM ism attained a drug release rate (k) significantly higher ( $p < 0.05$ ) than that of DXP ism as shown in Table 14. Release behaviors of drug related to a solvent release. Both solvent and drug release kinetics of all ISM formulations were best described by a power law model based on the highest linearity, and they were close to a Higuchi model. Their mechanism of release from ISM was a Fickian diffusion controlled.

**Table 15** Comparison of degree of goodness-of-fit from curve fitting of drug release from ISMs

Formula (DX)	First order		Higuchi's		Zero order		Power law	
	r <sup>2</sup>	msc	r <sup>2</sup>	msc	r <sup>2</sup>	msc	r <sup>2</sup>	msc
DXDM ism	0.9428	0.63	0.9910	2.48	0.8044	0.93	0.9988	4.25
DXP ism	0.9919	2.22	0.9982	3.73	0.9884	1.86	0.9998	5.38

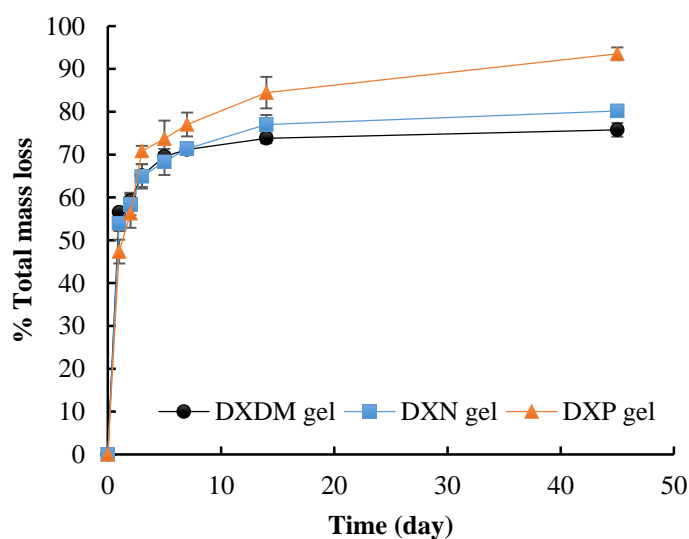
**Table 16** Estimate parameter from curve fitting of drug release from ISMs

Formula (DX)	k ± S.D.	n ± S.D.	Release mechanism
DXDM ism	0.0553 ± 0.0099	0.31 ± 0.02	Fickian diffusion
DXP ism	0.0224 ± 0.0039	0.40 ± 0.02	Fickian diffusion

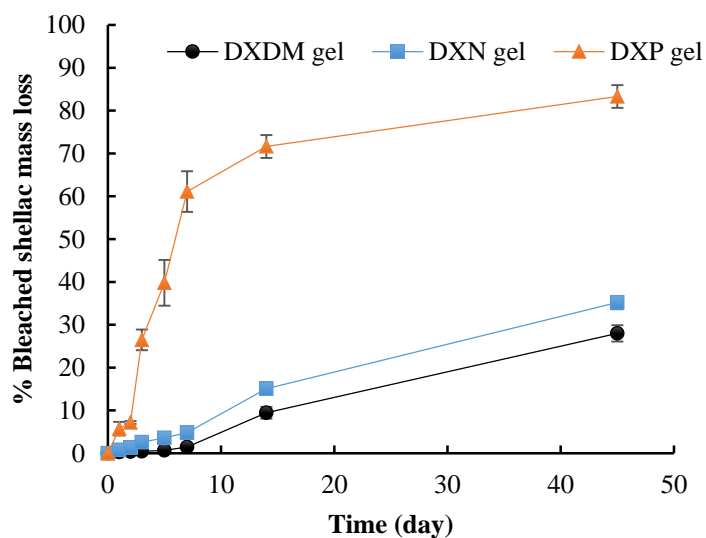
#### 4.3.2.4 *In vitro* degradability study

Polymer degradation is a breakdown of macromolecule under the influence of one or more environmental factors such as heat, moisture, oxygen, light or radiation, chemicals (i.e. acids, alkalis and some salts), mechanical stresses and biological agencies. Usually, several types of degradation processes take place simultaneously in a polymer depending on its chemical and physical characteristics (Ravve, 2012). The characteristics of the biodegradable polymer strongly impact the degradation (Parent *et al.*, 2013). Bleached shellac structure contains polyesters which are probably auto-catalyzed the ester bond via alkaline hydrolysis (Limmatvapirat *et al.*, 2008). Hydrolytic degradation is a fast process that its rate depends on characteristics of polymer (i.e. molecular weight, type of chemical bond, degree of crystallinity and co-monomer composition) and environmental conditions (i.e. drug type, additive substances, pH, and water uptake) (Boimvaser *et al.*, 2012; Thakur *et al.*, 2014). The prepared *in situ* forming formulations initiate the drug release by solvent exchange process between water influx and solvent efflux. This study formulated these systems by dissolving bleached shellac in different solvents. Thus, the hydrolytic degradation might attack the polyester of bleached shellac and degradation rate should be controlled by heterogeneous environmental conditions of system such as solvent component and also pH. To profoundly understand the effect of solvent type from *in situ* forming formulations on polymer degradation, the dynamic changes in mass of prepared system were monitored gravimetrically and calculated the mass loss of bleached shellac with some quantitative data from solvent/drug release studies. The water content was gravimetrically measured because it is the main trigger force of matrix degradation. All these changes might reflect the solvent exchange kinetics.

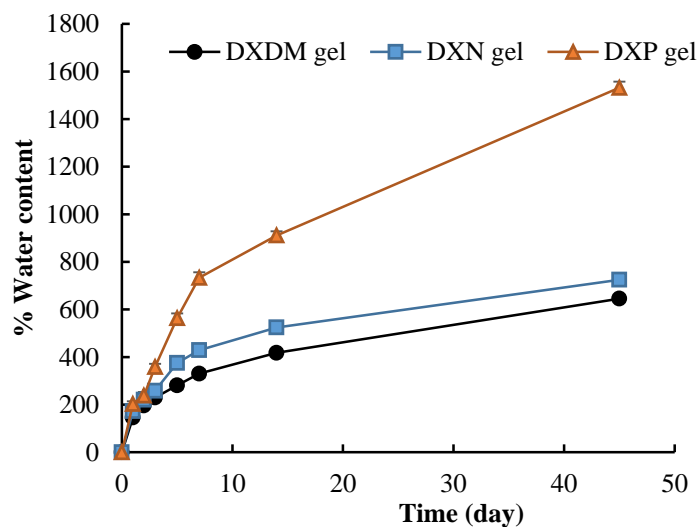
The % total mass loss and % bleached shellac mass loss of *in situ* forming gels are presented in Figs. 58 and 59. After exposure with aqueous medium, the initial rate of total mass loss of the systems was similar to that of solvent release as following; DMSO > NMP > PYR due to a higher amount of solvent outflow while water inflow leading to a larger mass release of solvent (Chu *et al.*, 2013). When the solvent and drug were at steady state, the total mass loss was as following: PYR > NMP > DMSO, probably related to polymer degradation. This could be described by polymer weight loss as shown in Fig. 59. The mass loss of bleached shellac generally increased during the observation period, signifying the polyester degradation under aqueous environment. The maximum mass loss of bleached shellac from different systems was approximately 83%, 35% and 28% (of systems using PYR, NMP and DMSO as solvent, respectively). Bleached shellac in PYR exhibited the highest hydrolytic degradation compared to that in NMP and DMSO, respectively. Water uptake should be the critical factor for promoting this phenomenon. The water content in the systems (Fig. 60) rationally indicated that PYR provoked the highest water uptake. Previous studies indicated that the use of PYR as solvent for bleached shellac induced the slowest rate of drug release due to a viscous character of PYR therefore the largest residual of this solvent should be evident in polymer matrix. The osmotic pressure of the residual solvent can force the water molecules in the medium to penetrate through the dense matrix (Chu *et al.*, 2013; Phaechamud *et al.*, 2016) and solvent with strong water miscibility will reinforce this driving force from constrained solvent in the depots. Earlier, the solubility parameter literally reported that PYR exhibits high water miscibility. Therefore PYR not only possessed as a large residual but also had a powerful water affinity that was able to promote an osmotic force to drive more water influx, resulting in more rapid polymer degradation. In case of DMSO and NMP, the circumstance was in vice versa. During degradation, however, physical changes could take place such as softening, pore creation/closure due to the decrease in polymer mass and it would be verified by further studies i.e. text analysis, SEM or else. Thus it was eventually concluded that bleached shellac matrix could undergo a hydrolytic degradation in aqueous environment and types of solvent noticeably affected the degradation rate.



**Fig. 58** Dynamic change in total mass of *in situ* forming gels (n=3)



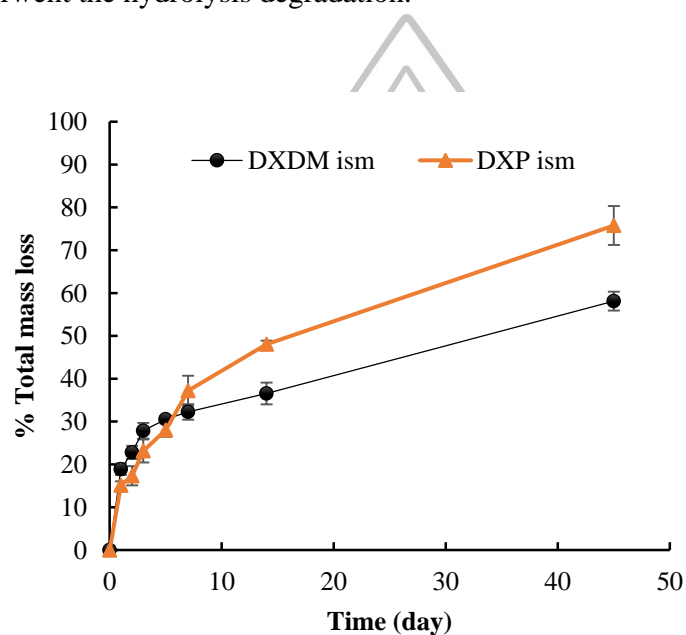
**Fig. 59** Dynamic change in mass of bleached shellac from *in situ* forming gels (n=3)



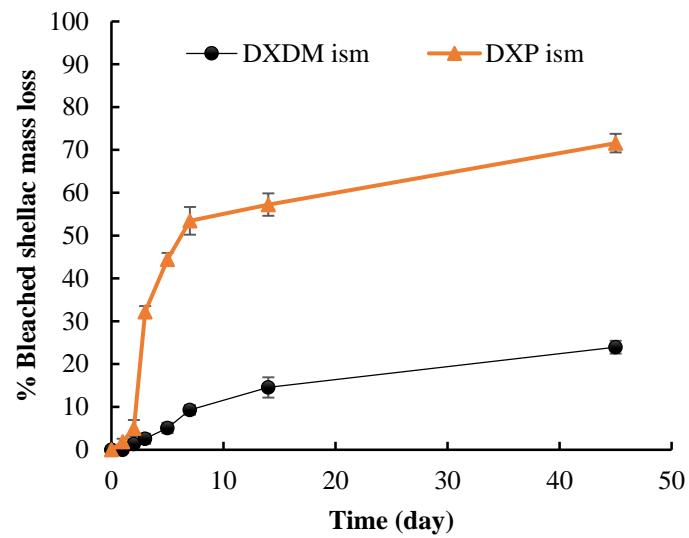
**Fig. 60** Dynamic change in water content of *in situ* forming gels (n=3)

ISM systems demonstrated a pattern of % total mass loss, % bleached shellac mass loss and % water content in Figs. 61-63, which the results were similar to those of *in situ* gels. However, the value of each parameter was apparently lower because the external oil phase minimized the substrate diffusion. Because this continuous phase acted as a diffusion barrier (Kranz and Bodmeier, 2008; Frelichowska *et al.*, 2009) not only for the solvent-drug release but also water uptake after residual solvent in matrix induced the osmotic pressure. The final mass loss of bleached shellac from each solvent of ISM was 72% for PYR and 24% for DMSO as depicted in Fig. 62. Therefore bleached shellac fabricated into

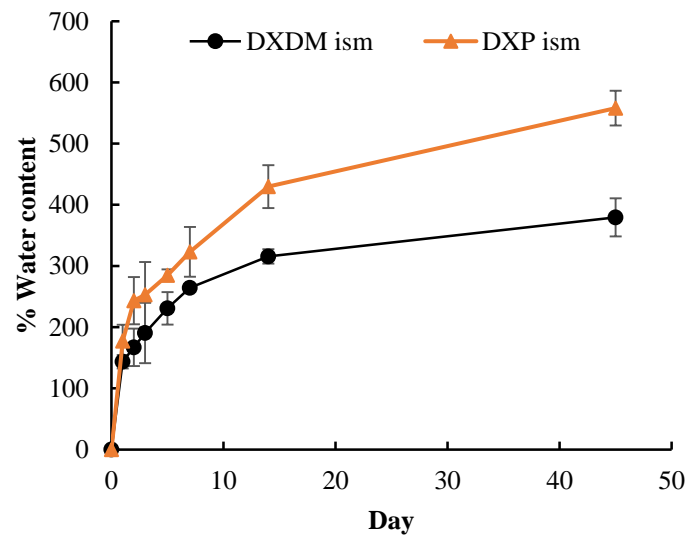
*in situ* forming systems could degrade through hydrolysis degradation mechanism under aqueous environment. The complete dissolution of shellac was literally recorded at pH > 7.0, and it partially dissolved at pH 7.0 and lower (Limmatvapirat *et al.*, 2004; Limmatvapirat *et al.*, 2008; Farag and Leopold, 2009). Previous pH study revealed that pH value of doxycycline hyclate solutions in each solvent was familiar (pH ~ 3.3 to 3.4). This range was not appropriated to degrade bleached shellac. However, the *in situ* forming systems, which possessed a large residual solvent inside of matrices upon solvent exchange, were able to promote an osmotic force leading more water influx. It could subsequently neutralize the pH of doxycycline hyclate solutions nearly to pH 7.0, and bleached shellac finally underwent the hydrolysis degradation.



**Fig. 61** Dynamic change in total mass of *in situ* forming microparticles (n=3)



**Fig. 62** Dynamic change in mass of bleached shellac from *in situ* forming microparticles (n=3)



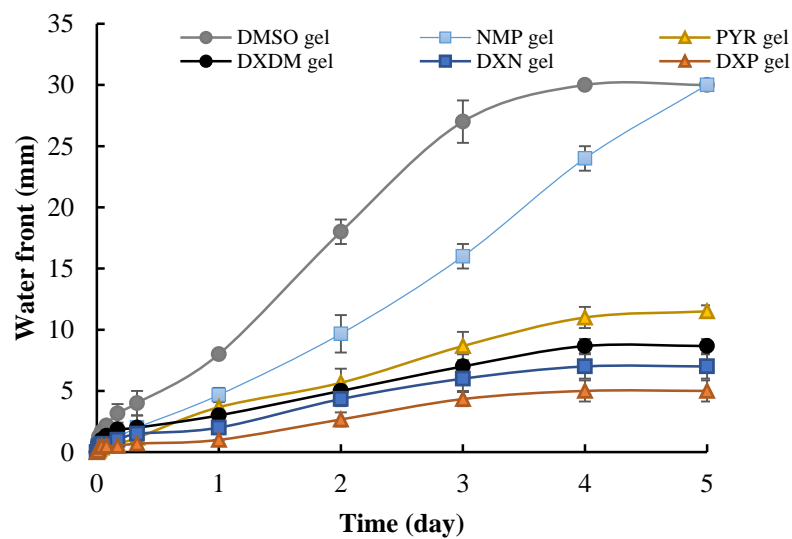
**Fig. 63** Dynamic change in water content of *in situ* forming microparticles (n=3)

#### 4.3.2.5 Rate of water diffusion into *in situ* forming systems study

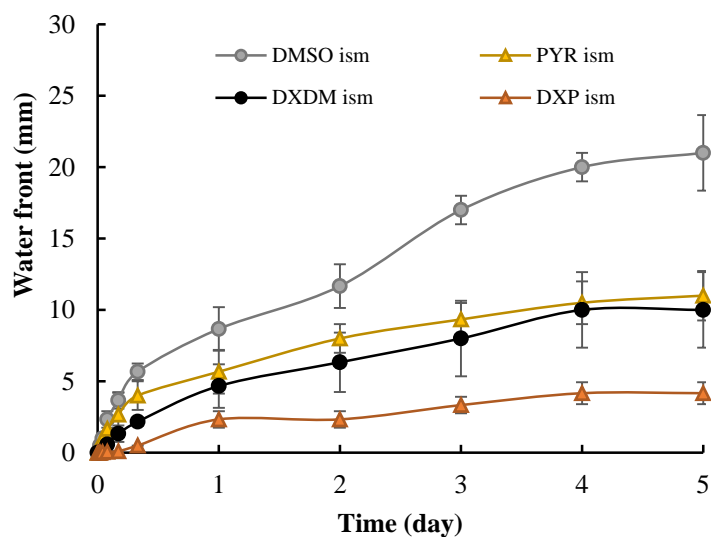
In order to understand the solvent exchange of such *in situ* forming systems, the fundamental knowledge of water diffusion in such systems is necessarily required. Dynamic flow of water evaluated by NMR technique could provide the self-diffusion coefficient (D) of water in gel (Hurley *et al.*, 2003; Davies *et al.*, 2010). Another simple technique for monitoring the water diffusion behavior was conducted in transparent tube immersed in phosphate buffer solution. When water diffused into test system, the transparent liquid was transformed into opaque matrix to check the movement of water or water front (Mahadlek, 2012). This simple strategy was employed in this investigation to study the water influx in term of water diffusion rate calculated from opaque distance as a function of time.

The *in situ* forming gels provided a pattern of water diffusion as illustrated in Fig. 64. The water diffusion rate of formulation without drug loading was definitely higher than that with drug loading owing to the increase of apparent viscosity after adding doxycycline hyclate in systems retarding water diffusion. The water influx rate of system dissolved in DMSO was higher than that dissolved in NMP and PYR, respectively or  $DMSO > NMP > PYR$ . In addition to the water influx, a front of surface gels then precipitated into opaque and harder matrix by distance provoked in a decrease of water diffusion rate afterwards. The profit of this character was easy and convenient to describe the rate of solvent and drug release (Wang *et al.*, 2012, Phaechamud and Mahadlek, 2015; Phaechamud *et al.*, 2016). A trend of water diffusion corresponded to solvent and drug release studies which had been previously discussed. The pattern of water inflow and solvent outflow was similar which controlled by precipitated layer of bleached shellac matrix. On the other hand, this experiment resulted in contrast to water content data. The appropriate explanation might involve with direction of water flux. Water accumulation generally referred to the trapped water molecules inside of system. It was gravimetrically measured by dialysis method which water flowed in. If the residual solvent (i.e. PYR) was strongly miscible with water, it would attract the water molecules and to be finally trapped in polymer matrix. Whereas the rate of water diffusion was operated and determined by a transparent tube technique, a fixed shape, that water penetrated each layer in only one vertical direction therefore water molecules would rather pass through a surface than be trapped in the bleached shellac matrix. If the solvent (i.e. DMSO) easily flowed out, it would fluently exchange with the water molecules toward to system likewise. Therefore the outcome of this technique logically distinguished from the dialysis method and more directly reflected to water influx as a function of time than the other one. The water diffusion profiles of the ISM in Fig. 65 revealed the similar pattern to that of *in situ* forming gels. The water influx rate of formulation using DMSO as solvent was apparently higher than that using PYR. However, all outcomes were totally less than of gels due to the powerful hindrance effect of the external oil phase and the drug-polymer interaction.





**Fig. 64** Water diffusion of *in situ* forming gels (n=3)



**Fig. 65** Water diffusion of *in situ* forming microparticles (n=3)

#### 4.3.2.6 Solvent diffusion study

Practically the solvent diffusion is one of driving forces of solvent exchange process which it chiefly causes a controlled drug release (Parent *et al.*, 2013). Diffusion behavior of solutes in polymer solutions and gels has been studied for decades by the use of various techniques such as gravimetric method, membrane permeation, fluorescence, radioactive labeling, dynamic light scattering and NMR (Masaro and Zhu, 1999). According to our research experiments, the solvent release with quantitative analysis was previously performed. However, the character of solvent outflow could be completely evident if it was fulfilled with qualitative data. This study aimed to clarify the transport phenomena by a simple image analysis technique (Samprovalaki *et al.*, 2012). This study visualized the polymer precipitation line, the migration of dyed (amaranth, a marker colorant) solvent into agar gel under stereomicroscope, and calculated the solvent front as a function of time. Amaranth could solubilize in used solvent (DMSO, PYR and NMP) but not in oil therefore the diffusion of this dye indicated these solvent front into the agar gel (0.6% w/v agarose using PBS pH 6.8 as solvent).

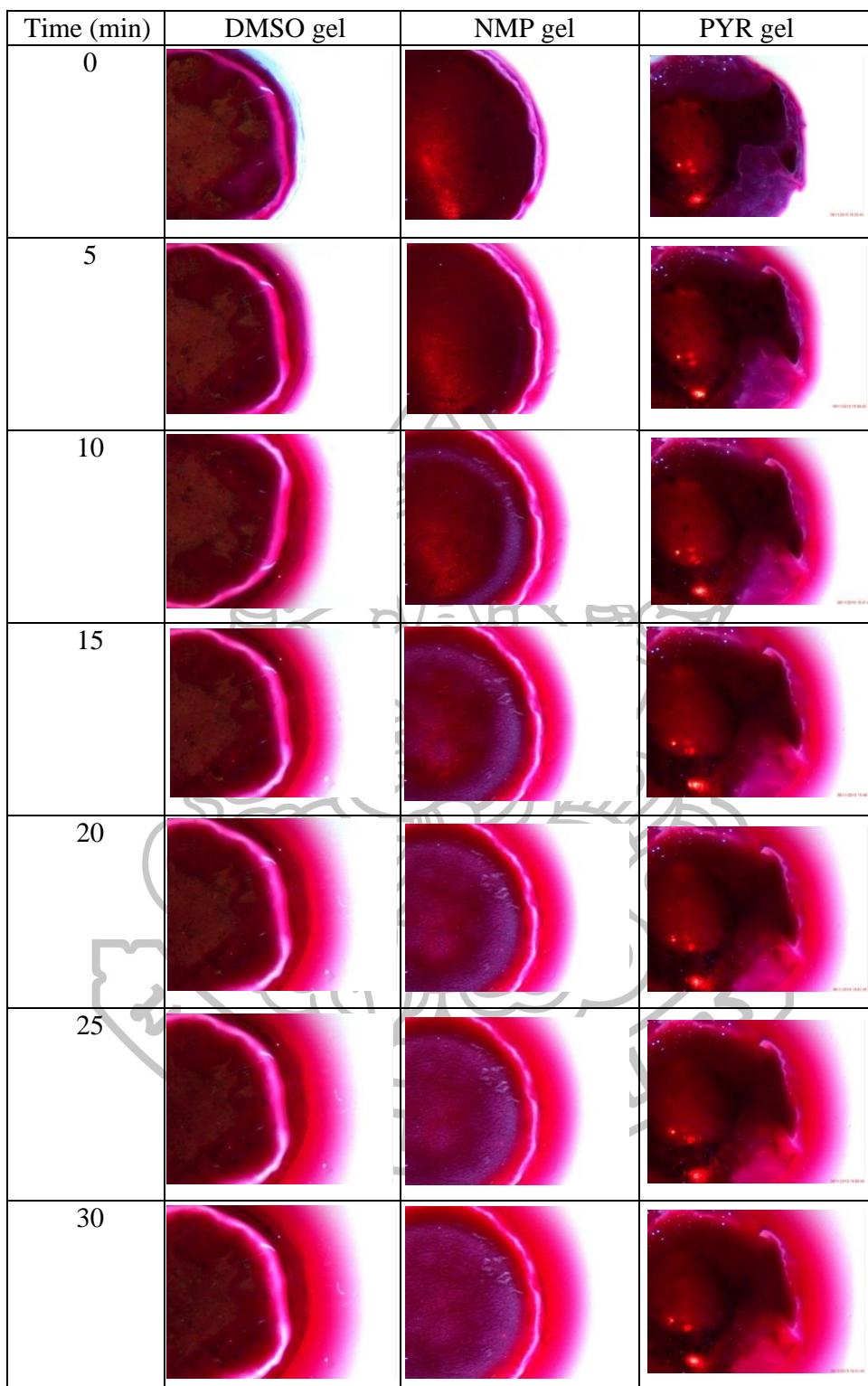
For the visual images of solvent diffusion into *in situ* forming gels (Fig. 66), a white ring represented a phase inversion zone which precipitated from outer area to inner area. The enlargement of this band was increased by time. The opaque ring immediately appeared after sample contacting to agarose gel whereas coloring front became visible at 5 min later. Thus the solvent exchange process was probably driven initially by water influx and onward by solvent efflux. A ring diameter apparently increased as following DMSO gel > NMP gel > PYR gel. It reflected the rate of precipitation that of DMSO gel was fastest precipitated as presented in another previous research work (Sithajindalert, 2013; Mahadlek, 2012). However, an opaque band of PYR gel was slightly noticeable due to high viscosity of solvent itself. This evidence was an important drawback for phase inversion procedure as earlier criticized in solvent and drug release studies.

The solvent front and solvent diffusion rate of *in situ* forming gels were calculated as a function of time as illustrated in Figs. 67 and 68. Net flux movement of solvent progressed along the agar gel. Both parameters presented a different trend from solvent release data. The rank of solvent front and solvent diffusion rate was DMSO >> PYR ≥ NMP. The diffusion rates of solvents unsteadily decreased by time. According to another research work (Kranz and Bodmeier, 2008) and this solvent release study, NMP practically released faster than PYR. In addition, these solvent diffusion data contrasted to the pattern of opaque band in optical image that the phase inversion zone of DMSO formulation was larger than those of NMP and PYR formulations, respectively. A size of ring reflected the polymer precipitation rate which related to the previous results from solvent release study. This uncommon phenomenon might implicate with the interaction between amaranth and solvents. For this image analysis technique of transport phenomena, the dye diffusion into gels occurred by simple diffusional model which related to Fickian theory (Kemp and Fryer, 2007; Samprovalaki *et al.*, 2012). Diffusion refers to the net random movement of particles, taking place from a region of high concentration to one of lower concentration (Agutter *et al.*, 2000). Fick's law of diffusion is useful in the studies of the solid, where concentrations vary with site and time (Cussler, 1984). A system is govern by Fick's first law only when the concentration gradient is steady or diffusive flux is independent of

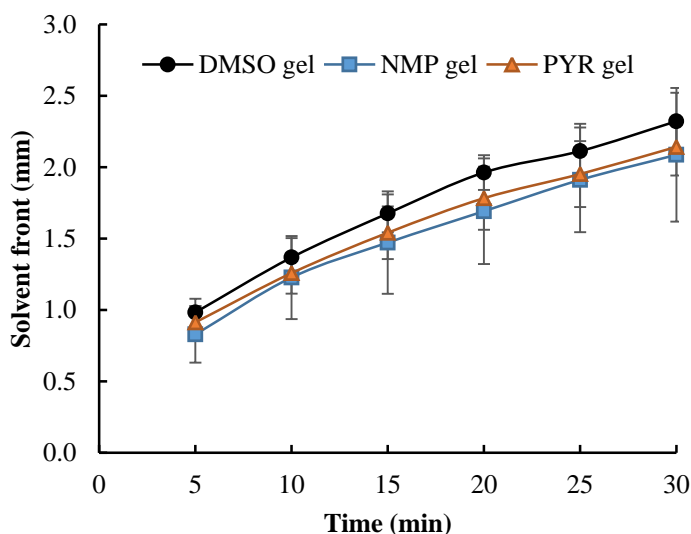
concentration whereas Fick's second law (often called non-Fickian behavior) applies to non-steady state diffusion which describes the change in concentration gradient with time (Crank, 1975). For this experimental section, the measurement of solutes concentration with time to solvent front with time was conducted to define as the rate of diffusion. There are many actual physical situations which occur simultaneously with diffusion such as swelling, change of state, formation of elastic stresses, loss of extracted material, etc. These processes may be correctly explained by Fick's second law (Wypych, 2004). In the case of solute diffusion through gels where a type of partitioning can happen, gel properties can be sensitive to the concentration of the diffusing species. If this concentration gradient is larger on one side, the diffusivity on this side must be smaller to maintain the steady flux. This physical occurrence could be owing to a change in pore size in gel which in turn changes the effective diffusivity and gives non-Fickian diffusion (Crank, 1975). In regard to the dye diffusion model, the diffusing species were colorant (amaranth) and solvent molecules. Both solutes outflowed from formulation into hydrogel. DMSO and NMP systems exhibited a diffusion behavior of solvent corresponded to solvent release because they were less viscous than PYR, leading to together diffused with amaranth molecules. Furthermore the concentration of polymer solvents were definitely higher, they then controlled the rate of diffusion instead of dye. PYR was a highly viscous solvent, resulting in slow diffusion hence amaranth molecules were able to self-diffuse. It could confirm from unclearly precipitation band. The rank of solvent front and solvent diffusion rate was  $\text{DMSO} \gg \text{PYR} > \text{NMP}$ , and the result of DMSO and NMP data reflected to diffusion of colorant and solvent. Therefore the rate of pure amaranth diffusion was lower than that of DMSO but higher than that of NMP and this circumstance would rather fit for low viscous polymer solvent. However, the pattern of diffusion was not steady with time or obtained a non-Fickian behavior. This contrasted to mathematical analysis of solvent release data which mainly presented a Fickian diffusion. To understand the different environmental condition between measurement and solvent release study, the basic understanding of agar gel structure was necessarily required. The structure of agar gel, a type of hydrogels, is heterogeneous, which composed of molecular random and immobile polymer chains (Amsden, 1998 a, b). The network of these chains was described as a mesh, with the spaces filled with water. The virtual openings are constant in size and location. A great deal of inter-polymer interaction induces the capillary force responded for solvent retention. Solutes are able to transport within agar at water-filled regions and their size should be smaller than the spaces between polymer chains (Muhr and Blanshard, 1982). To compare the diffusion features between gel model and buffer solution condition, it should be noticed that 1) the polymer reduces its available volume or area to the total one (referred to the exclusion effect) and 2) the impermeable segments of polymer molecules increase the path length for a diffusing solute (referred to the obstruction effect). Besides the presence of impenetrable polymer chains causes an increase in the path length for diffusive transport or the obstruction effect which is sometimes represented by the tortuosity factor in porous materials. These two major reasons causes the effective diffusivity in a gel is lower than the corresponding diffusivity in aqueous medium (Westrin, 1991). Therefore the pattern of diffusion in agar model was a non Fickian behavior due to the influence of gel structure rather than that of the formulation system, and to determine the type of diffusive transport should be examined with direct quantitative analysis such as solvent release study. Furthermore, the interaction between amaranth and agarose gel might concern to this

uncommon diffusion behavior. Consideration to charge of functional groups, agarose chain contains uncharged methyl groups (Alistair *et al.*, 2006) while amaranth is an anionic dye (Stone and Lorenze, 1984) hence the charge-charge interaction should practically disappear. It assured that gel structure is a primary reason for non Fickian behavior of solutes diffusion. Eventually, this model might be appropriated for basically monitoring the phase inversion character.

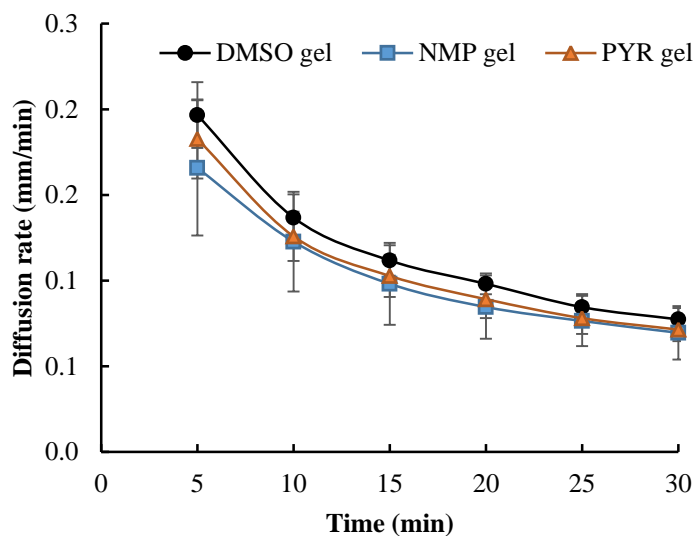




**Fig. 66** Visual image of solvent diffusion from *in situ* forming gels prepared with different solvents



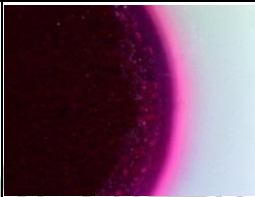

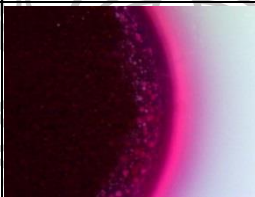
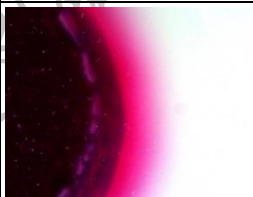
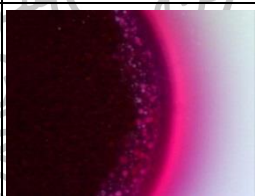



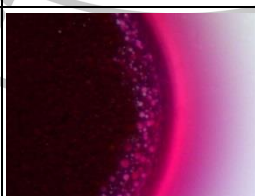

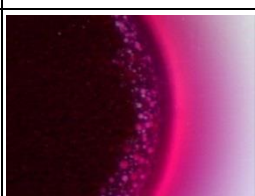

**Fig. 67** Solvent diffusion distance of *in situ* forming gels prepared with different solvents (n=3)



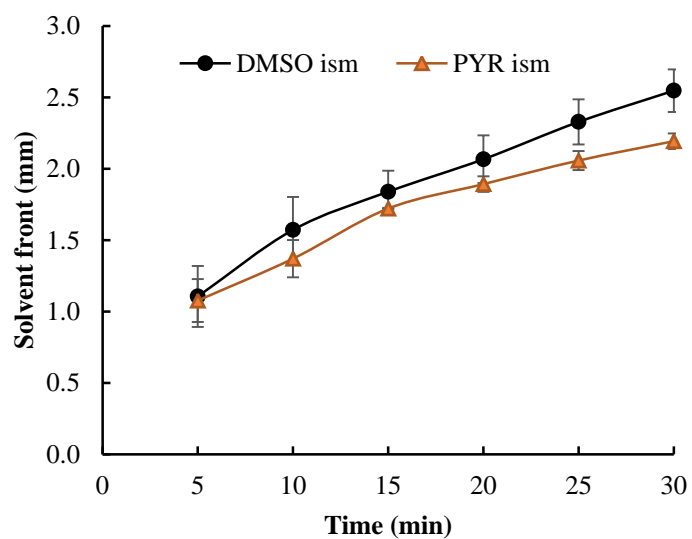
**Fig. 68** Solvent diffusion rate of *in situ* forming gels prepared with different solvents (n=3)

The visual images of solvent diffusion from ISM every 5 min are shown in Fig. 69. The precipitation zone initiated from outer region to inner region. There were a number of white particles within phase inversion band. These particles certainly precipitated from droplets of the internal phase of emulsion. Their opaque trace and size of precipitation region became evident with time. DMSO system formed a thin membrane with higher porous matrix structure and more regular shape compared to PYR system as demonstrated in another previous research work (Sittthajindalert, 2013) because DMSO was less viscous and promoted a rapid phase inversion (Packhaeuser *et al.*, 2004).

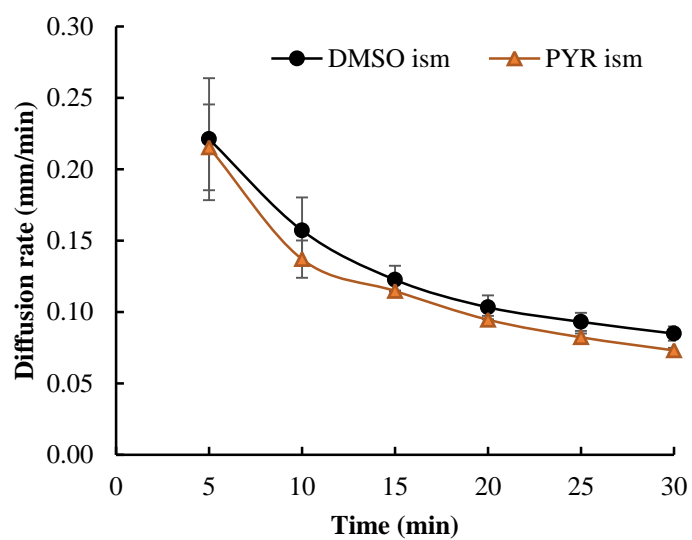
The solvent front and solvent diffusion rate of ISM were calculated as a function of time as depicted in Figs. 70 and 71. The solvent efflux forwarded along the hydrogel. Both parameters (ring size and solvent front) and the rate of diffusion demonstrated a similar trend with that of *in situ* forming gels. In brief, all diffusive data of DMSO system valued higher than that of PYR system. This physical occurrence was influenced by viscosity of polymer solvent, interaction between two diffusive species and gel structure as recently discussed above.

Time (min)	DMSO ism	PYR ism
5		
10		
15		
20		
25		
30		

**Fig. 69** Visual image of solvent diffusion from *in situ* forming microparticles prepared with different solvents



**Fig. 70** Solvent diffusion distance of *in situ* forming microparticles prepared with different solvents (n=3)



**Fig. 71** Solvent diffusion rate of *in situ* forming microparticles prepared with different solvents (n=3)



## Summary

The effect of stabilizer concentration and phase ratio on transformation of emulsion to microparticles were focused in this part. The 5% GMS of external phase was enough for the o/o emulsion to transform to microparticle after exposure to aqueous medium within 3 min by solvent exchange, and GMS then formed its network to gel the olive oil. The increasing external phase: internal phase ratio improved the stability of the o/o emulsions against the droplet coalescence. However, if the ratio of the external phase was less than the internal phase, the system could not form the microparticles. PYR was the most appropriate solvent for producing massive microparticles with regular shape especially at the phase ratio of 7:3. The solubility of bleached shellac in PYR was low while PYR had a largest affinity to water, resulted in a high rate of polymer precipitation and a rapid formation of numerous microparticles. In the case of drug-loaded system, only DMSO series exhibited the largest amount and size of microparticles which possibly caused by crosslinking reactions between polymer and drug molecules as previously described in thermal analysis.

All *in situ* forming gels completed their solvent release at least 7 days with rate in the rank order; DMSO > NMP > PYR. The trend of solvent release from ISMs was similar to gels but the final release extended to 14 days. The higher viscosity of PYR and its polymer solution retarding the drug release were the reasons behind this circumstance. DMSO and its formulation were slightly viscous than NMP series but the solvent release rate of DMSO ones was faster owing to less interaction between solvent and shellac. The oil in external phase of ISM was a barrier for solvent diffusion which resulted in the lower initial burst and slower release of solvent compared to gels. A trend of drug release pattern of all *in situ* forming systems associated with the solvent release profiles. However, three gels incompletely finished drug release within 3 days whereas ISMs completed their drug release near to 100% at 21 days. The incomplete diffusion of *in situ* forming gel possibly explained by dense drug accumulation and drug trapping in matrix core. ISMs possessed the larger surface area to volume ratio thus it could prevent those problems. It approved that doxycycline hyclate in polymer solution or internal phase did not decompose throughout preparation as the evidence from TG result. The incomplete drug release from dissolution profiles of gels showed the largest drug release extent at the end from system tailored with PYR. PYR could enhance an osmotic force to attract more water inflow due to its high water miscibility, and its high viscosity which left a large residual in porous matrix. Water molecules fractured the porous matrix and finally released the trapped drug out of core. By comparison for DMSO and NMP, it can be explained by viscosity of solvent itself and molecular interaction. Furthermore, HPLC assay revealed the presence of unknown peak near drug peak from all *in situ* forming systems. This was technically proved that it was a residual unit from bleached shellac related to shelloic acid which presents in a pentacyclic structure nearly to hexacyclic ring in doxycycline hyclate structure. Solvent release profiles of *in situ* gels dissolved in DMSO or NMP including ISMs, and also drug release profiles of all drug-loaded systems fitted well with a power law model. They had intimate relationship with a Higuchi's kinetic model. The mechanism of these systems were Fickian diffusion. Only solvent release of PYR formed *in situ* gel obviously fitted with a first order model and presented an anomalous mechanism instead. However, the drug release pattern of gel in PYR was different from its solvent profile because chemical

potential gradient of doxycycline hyclate itself might play a stronger role on molecular drug diffusion through the porous matrix than solvent driven, it therefore performed a Fickian diffusion transport. All formulations demonstrated the release rate (k) and release exponent values (n) corresponded to release and apparent viscosity studies.

Degradation studies revealed that the initial rate of total mass loss of the *in situ* gel systems was influenced by solvent outflow. Its priority order was DMSO > NMP > PYR, practically related with solvent release. When the solvent and drug diffusion were at steady state, the total mass loss converted to PYR > NMP > DMSO that represented polymer degradation and it generally increased by time. This latter was similar to water content pattern. ISM systems obtained a similar pattern of these parameters with lower value as well because of barrier effect from oil. PYR formulations gained a high amount of water, leading to polymeric degradation because this solvent enhance the osmotic pressure by its high viscosity and water miscibility. Additionally, the buffer molecules also subsequently neutralized the pH of doxycycline hyclate solutions nearly to pH 7.0; therefore, bleached shellac finally underwent the hydrolysis degradation. In case of DMSO and NMP, it could explain in vice versa. Along this decrease in polymer mass, there were some physical changes such as softening, pore creation/closure which would be verified by further studies i.e. texture analysis, SEM or else.

The water diffusion rate was monitored using a transparent tube technique. Formulations without drug loading demonstrated the higher value of this parameter than drug-loaded systems due to a rise of apparent viscosity after adding drug. The water influx rate of all systems was in solvent rank order as following: DMSO > NMP > PYR. ISMs outcomes were totally less than of gels due to the powerful hindrance effect of the external oil phase and the drug-polymer interaction. However, that result of water influx rate was in contrast to water content data which probably involved with direction of water. This technique detected the opaque front of systems filled in fixed-shape tube that water penetrated each layer in only one planar vertical direction. For this reason, the water molecules would rather pass through a surface than be trapped in and then induced the polymeric matrix formation. If the solvent (i.e. DMSO) was less viscous, it would easily flowed and exchange with the water molecules.

The solvent diffusion study visualized under a stereomicroscope the character of solvent flow with amaranth in agar gel. After contacting sample with buffer, the opaque ring from phase inversion immediately appeared, and coloring front became visible at 5 min later. Thus the solvent exchange was probably driven initially by water influx and onward by solvent efflux. ISM presented a number of white particles, which certainly precipitated from emulsion droplets, were within that phase inversion band as well. A ring diameter of all *in situ* systems apparently increased in solvent with order as following DMSO > NMP > PYR. A size of ring reflected the polymer precipitation rate and related with the solvent release and other studies. The rank of solvent front and solvent diffusion rate was DMSO >> PYR > NMP, and these rates unsteadily decreased by time. This uncommon phenomenon was about the interaction between amaranth and solvents. PYR was a highly viscous solvent so that it could diffuse slowly thus the dye molecules diffused by itself. Whereas, DMSO and NMP were less viscous hence they together diffused with dye molecules. This technique would rather appropriate for low viscous polymer solvent.

However, the pattern of diffusion was a non-Fickian behavior which contrasted to mathematical analysis in release studies. It was more influenced by agar gel structure than system formation. Consequently, this model might be appropriated for basically monitoring the phase inversion character.



## Part 4

### 4.3.3 Evaluation of *in situ* forming gel systems after exposure to solvent exchange

#### 4.3.3.1 Mechanical property studies

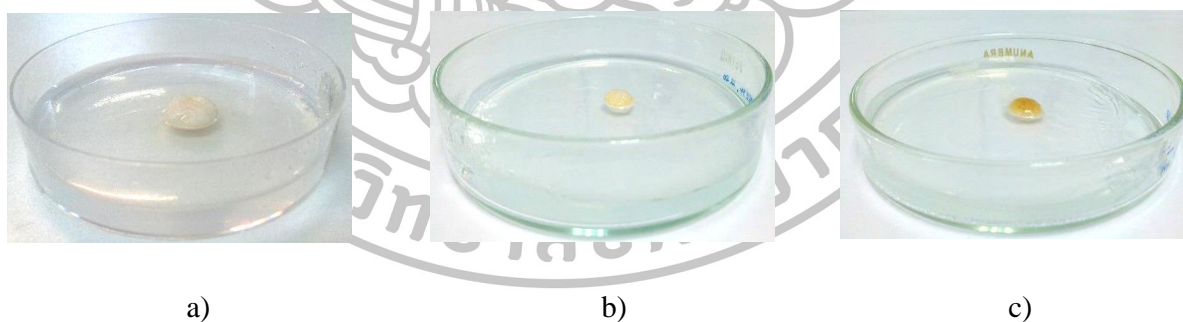
The mechanical properties of material naturally relates with physical forces. It is a result of the inherent mechanical characteristic of each substance such as strength, ductility and fatigue under different conditions (Soboyejo, 2005). With regard to the dental application of these *in situ* forming systems, they aimed for treatment of periodontitis. Understanding the mechanical strength of porous matrices, after solidification from solvent exchange using different types of solvent, could verify the deformability of specimen and its capacity to reside in the artificial periodontal pocket. This deformability also essentially relates to the performances of solvent/drug release, degradation and porosity under SEM. For this study, the important mechanical properties, which could basically indicate the deformability, were hardness and ratio of elasticity/plasticity. Therefore, this study determined these basic parameters in this part.

The physical appearance of the *in situ* forming gels after loading into the agarose gel for a week as shown in Figs. 72 and 73 indicated that all polymer matrices had rough surface bulge in rank of solvent orders as following: DMSO > NMP > PYR, which corresponded to the rate of solvent diffusion in previous studies. In case of drug-loaded systems, the colorless translucent hydrogel turned into brownish feather due to the outflow of drug. The bulky precipitant of DXDM gel and DXN gel was quite white and brown, respectively, resulted from different rate of drug release. However, there was no evident for matrix of DXP gel. Drug could literally have an intimate effect on the degradation of polymer matrices, which in turn affected drug release rate (Thakur *et al.*, 2014). The presence of hydrophilic doxycycline hyclate might contain the water molecules or possess H-bond donating functional groups which could interact catalytically with polymer chains and therefore increased the exposition of ester bonds to water molecules, resulting in more rapid polymer degradation (Liu *et al.*, 2010). Not only drug but types of solvent were also the crucial factors for this phenomenon. As previous mentioned, PYR released from the gradually transforming drug-loaded liquid into matrix-like system with slowest rate owing to its viscous feature. This remaining solvent highly accumulated the water molecules as described in water content studies. Therefore drug and PYR reinforced to completely accelerate the polymer degradation.

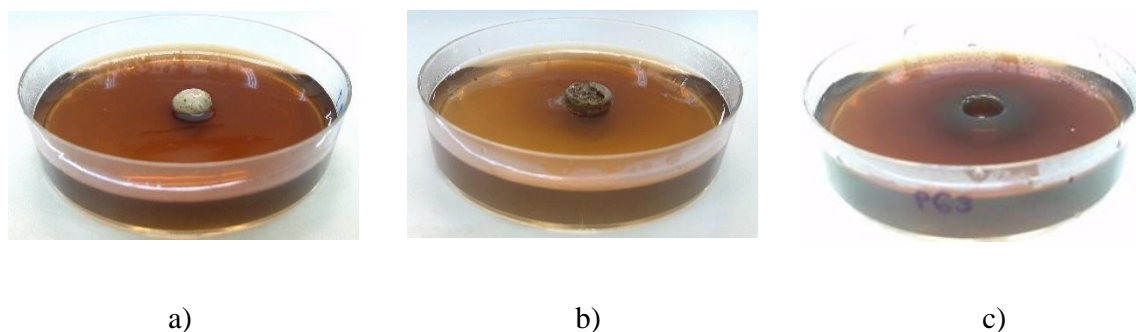
The mechanical properties were examined quantitatively using a texture analysis. Fig. 74 shows the maximum deformation force (hardness) for the matrices under compression (Lai *et al.*, 2003). Its peak force occurred during the first compression as mentioned previously (Soboyejo, 2005). The hardness of all free drug systems were significantly different ( $p < 0.05$ ). These differences in the mechanical properties probably resulted from the differences in solubility parameters and viscosities of solvents, which affected the interaction between the polymer chain and solvent molecule, causing difference in the porosity of matrices as previously discussed (Kranz and Bodmeier, 2008; Tetteh *et al.*, 2014). The PYR (4.93 N) matrix showed superior mechanical hardness strength than those of NMP (3.09 N) and DMSO (2.63 N) matrices, respectively because it provided a slow phase separation, leading to lower porosity. (Kranz and Bodmeier, 2008; He *et al.*, 2014). In the case of a fast phase separation where large pores were evident, it

was exclusively responsible for crack initiation after compression (Yi *et al.*, 2003). The drug-loaded matrices were clearly considerably more resistant to compression than the systems without drug loading except DXP gel because the replacement of drug particles in spaces of matrix might obstruct the solvent diffusion, resulted in few porous layers. Additionally, the hardness of DXDM (4.01 N) matrix was not significantly different from that of DXN (3.96 N) matrix ( $p>0.05$ ).

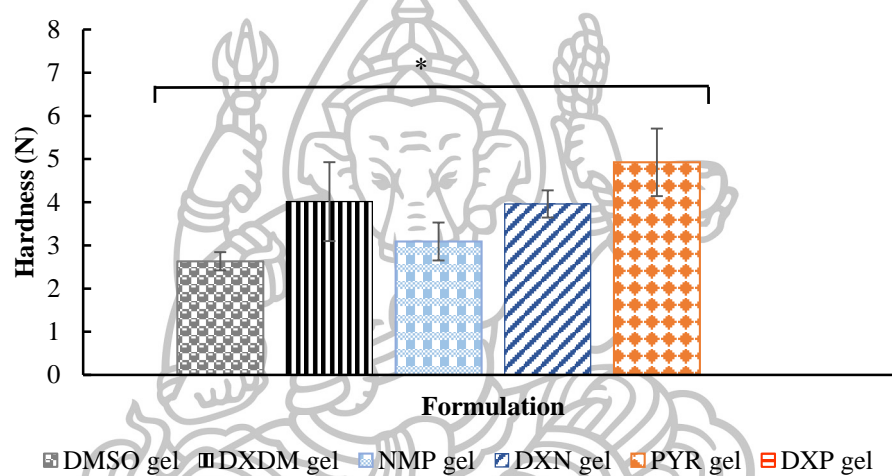
All the investigated *in situ* forming gels exhibited the  $F_{\text{remaining}}/F_{\text{max deformation}}$  ratios as seen in Fig. 75. This ratio referred to elasticity/plasticity which was expected to play a major role for residence time in the patients' periodontal pocket (Do *et al.*, 2014). Based on results of all free drug systems, the  $F_{\text{remaining}}/F_{\text{max deformation}}$  ratios of DMSO and NMP matrices were not significantly different ( $p>0.05$ ) but significantly different from that of PYR matrix ( $p<0.05$ ). A ratio value of PYR matrix (0.68) was more nearly to 1 and higher than those of other two free-drug formulations, indicated that the system was close to elastic which could not change its inner structure during the holding time in a permanent manner and fully recovers, whereas a low value of DMSO matrix (0.03) and NMP matrix (0.04) indicated that the specimen was likely to be able to adapt its geometry to dynamic changes in the periodontal pocket's size and shape with time or plastic behavior (Do *et al.*, 2014). Microstructural variables such as particle materials, density of porosity, amount of solid phase bonding and, pore characters have an important influence on elastic properties (Zhang *et al.*, 2003). Regions of high porosity generally reduce the elasticity (Carr *et al.*, 2015); therefore, the systems with fast solidification such as DMSO and NMP gels, resulted in high porosity. The drug-loaded formulations provided the higher value of elasticity/plasticity except DXP gel, demonstrated that they deformed elastically. The elastic deformation of DXDM gel (0.53) was significantly higher than that of DXN gel (0.32), possibly caused by the difference of interaction between solvent and drug molecules ( $p<0.05$ ).



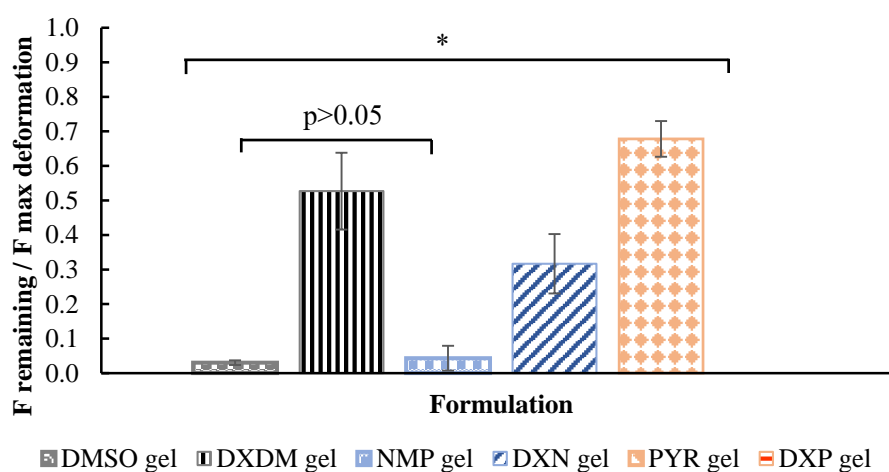
**Fig. 72** Photograph of *in situ* forming gels without drug loading in agarose pocket: a) DMSO gel, b) NMP gel, and c) PYR gel



**Fig. 73** Photograph of *in situ* forming gels with drug loading in agarose pocket: a) DXDM gel, b) DXN gel, and c) DXP gel



**Fig. 74** Maximum deformation force or hardness of *in situ* forming gels (n=6), \*  $p \leq 0.05$

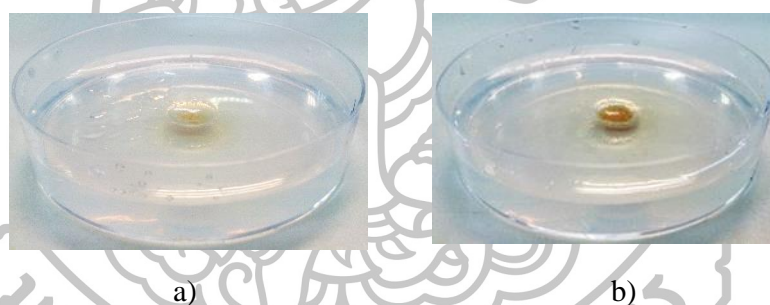


**Fig. 75** Ratio of remaining force/maximum deformation force or ratio of elasticity/plasticity of *in situ* forming gels (n=6) \*  $p \leq 0.05$

Upon loading specimen into agarose pocket for 7 days, the physical appearance of all ISM matrices as shown in Figs. 76 and 77 was less convex surface compared to those of the *in situ* forming gel ones because an external oil phase acted as a barrier for water penetration. DMSO apparently affected to the size of bulk than PYR owing to its high rate of solvent diffusion as previously described. Doxycycline hyclate efflux was detected by changing color of translucent agar form colorless to brownish. The bulky matrix of DXDM ism was brown whereas there was no evident matrix of DXP ism. This phenomenon can be similarly explained for its polymeric degradation as *in situ* forming gels.

ISM systems had similar trend of hardness to *in situ* forming gel systems as illustrated in Fig. 78. The hardness of PYR ism matrix (1.73 N) was significantly higher than that of DMSO ism matrix (0.22 N) ( $p < 0.05$ ). The precipitant from DXP ism could not be found as before. However, the hardness between DMSO ism (0.22 N) and DXDM ism (0.22 N) matrices was not statistically significant, that was probably influenced by an external oil phase ( $p > 0.05$ ).

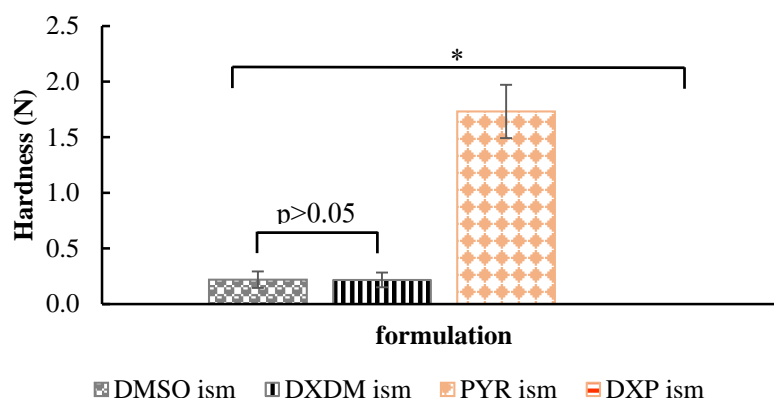
Fig. 79 shows the elasticity/plasticity ratios of the respective ISM systems. PYR ism matrix (0.82) exhibited significantly a higher elastic deformation than DMSO ism matrix (0.17) ( $p < 0.05$ ). Doxycycline hyclate was independent on the deformation of systems fabricated with DMSO but it strongly influenced to the matrix formed by PYR exchange, which finally vanished in 7 days. This circumstance was able to be discussed as in earlier part.



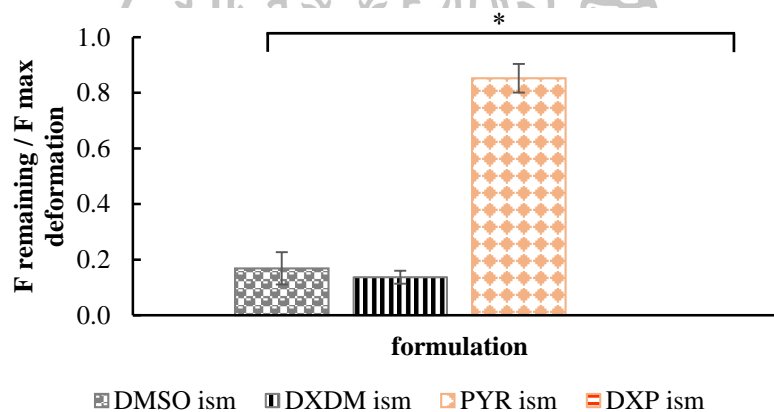
**Fig. 76** Photograph of *in situ* forming microparticles without drug loading in artificial periodontal pocket: a) DMSO ism and b) PYR ism



**Fig. 77** Photograph of drug-loaded *in situ* forming microparticles in artificial periodontal pocket: a) DXDM ism and b) DXP ism



**Fig. 78** Maximum deformation force or hardness of *in situ* forming microparticles (n=6), \*  $p \leq 0.05$



**Fig. 79** Ratio of remaining force/maximum deformation force or ratio of elasticity/plasticity of *in situ* forming microparticles (n=6), \*  $p \leq 0.05$

#### 4.3.3.2 X-ray powder diffraction study

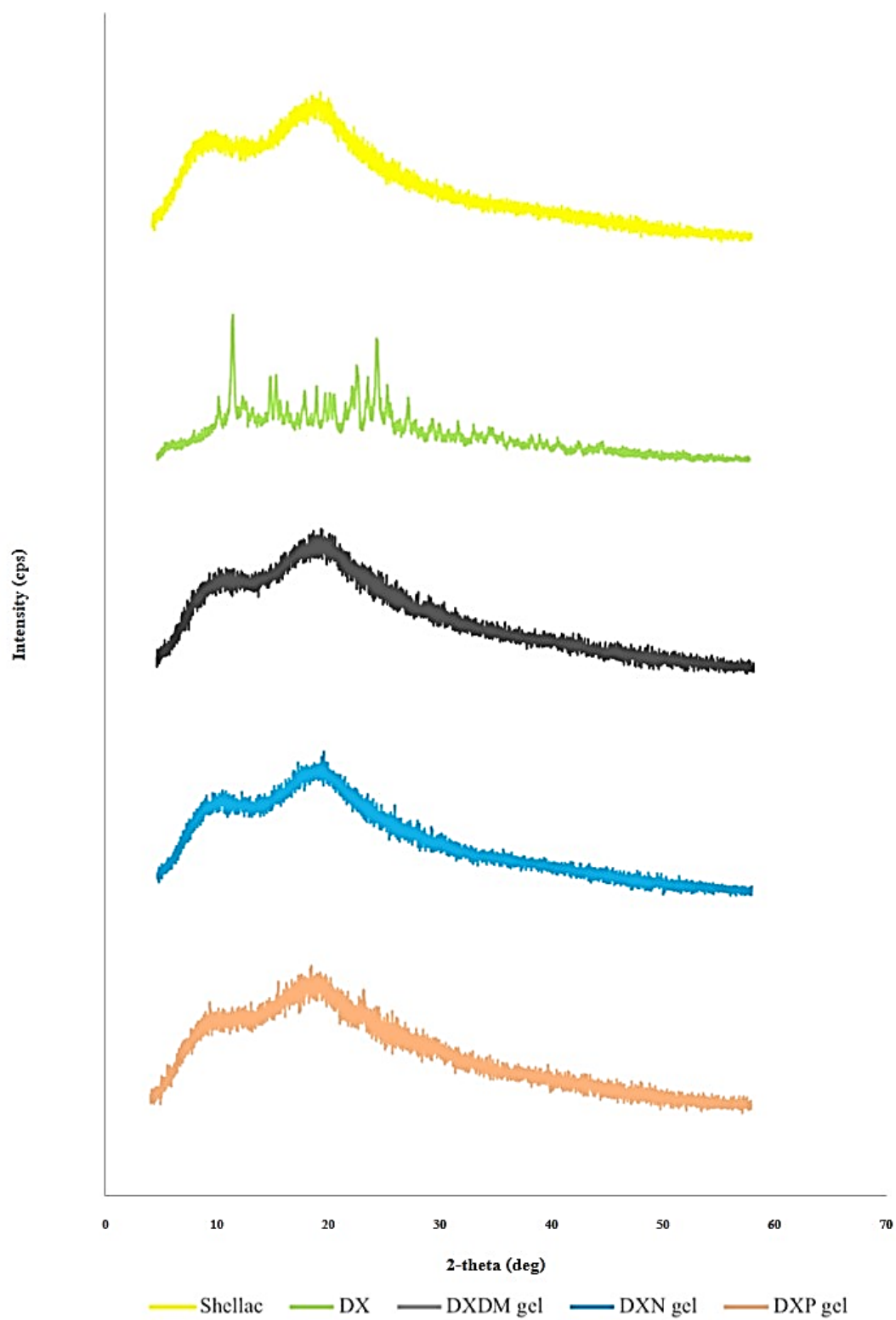
X-ray powder diffraction (XRD) is an analytical technique basically used for fingerprint characterization of crystalline materials and the determination of their crystalline structure (Ortiz-Cruz *et al.*, 2012). This study purposed to evaluate the effect of solvents on the crystalline structure of bleached shellac after the achievement of solvent and drug release. Prior to analyzing with X-ray diffractometer, the samples were dehydrated by freeze drying technique prior to grinding into powder with mortar and pestle.

The XRD pattern of the dried *in situ* forming gels and microparticles and their formulation compositions such as pure bleached shellac, doxycycline hyclate, and GMS are depicted in Figs. 80 and 81. XRD spectra of the pure polymer and the specimens were practically identical. Comparing this XRD pattern of bleached shellac with other literatures (Kojima *et al.*, 2000; Wang *et al.*, 2015), it showed that bleached shellac existed in an amorphous state over the  $2\theta$  range 15-20. The crystalline peaks of other pure substances

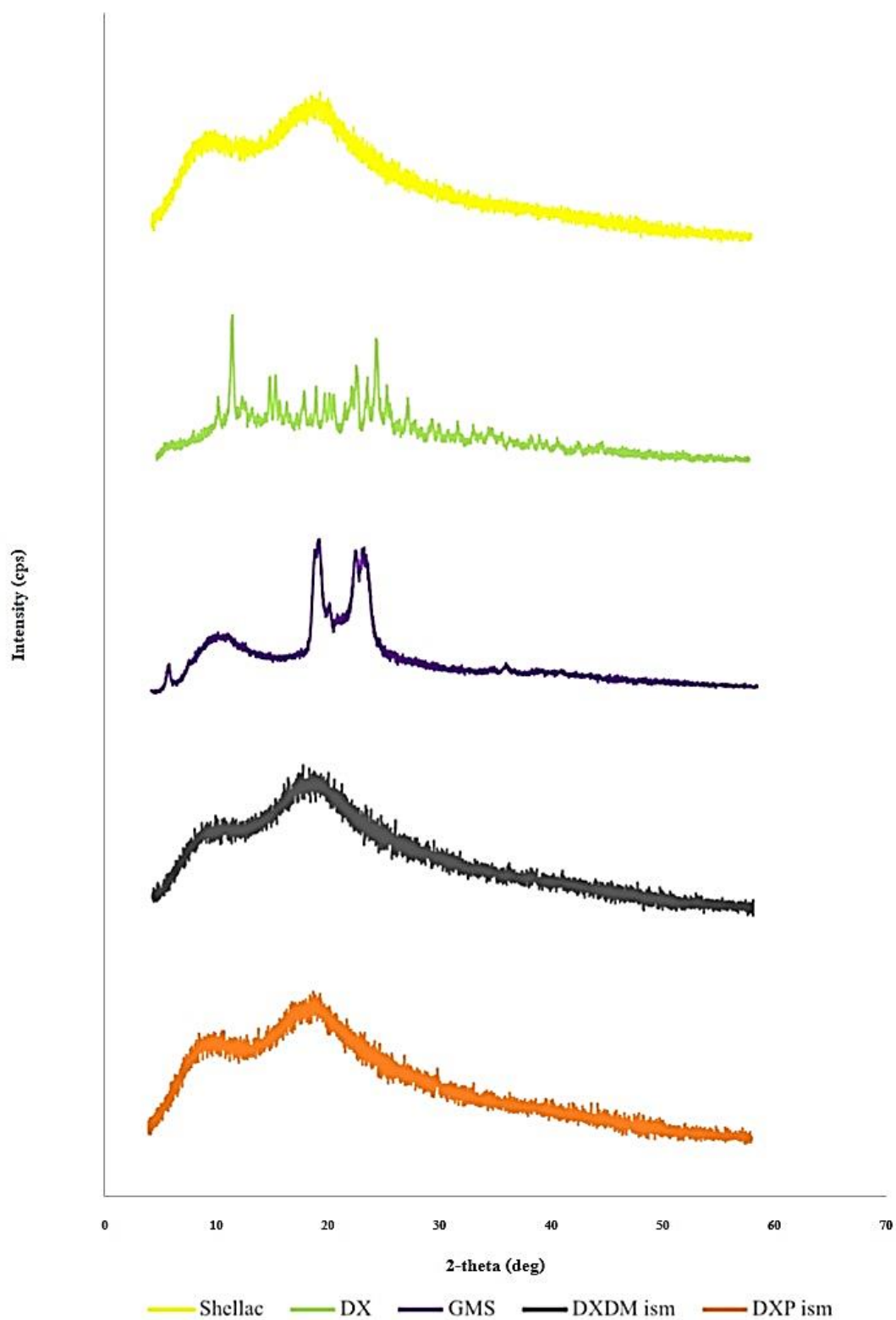


were not found in samples after release test. Therefore, all solvents had no influence on the structure of remained bleached shellac after solvent exchange (Buoltz and Feigenson, 1999; Ishii *et al.*, 2007) or release test.





**Fig. 80** XRD spectra of the pure polymer and *in situ* forming gels after release test

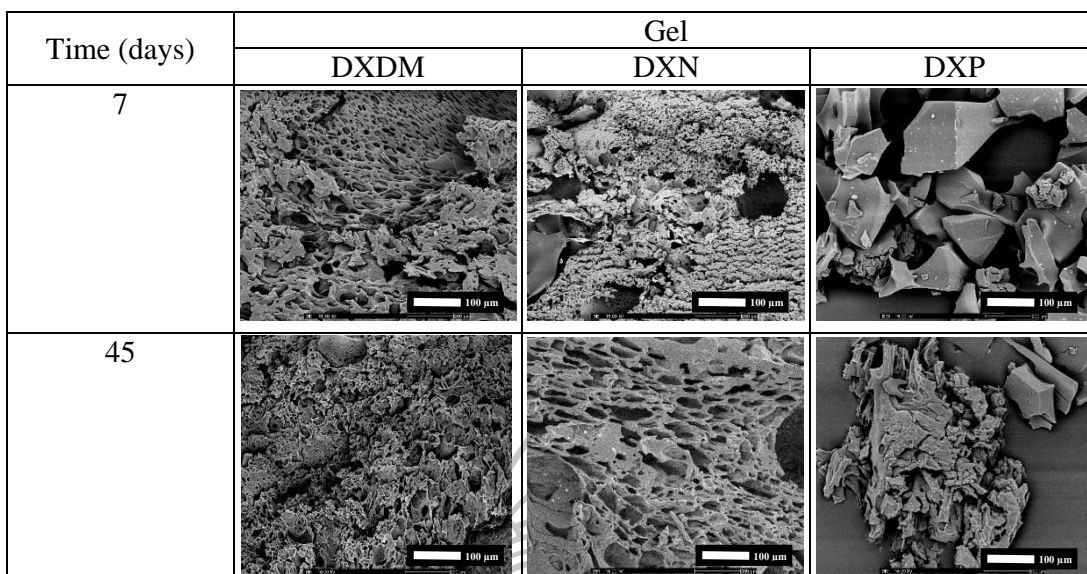


**Fig. 81** XRD spectra of the pure polymer and *in situ* forming microparticles after release test

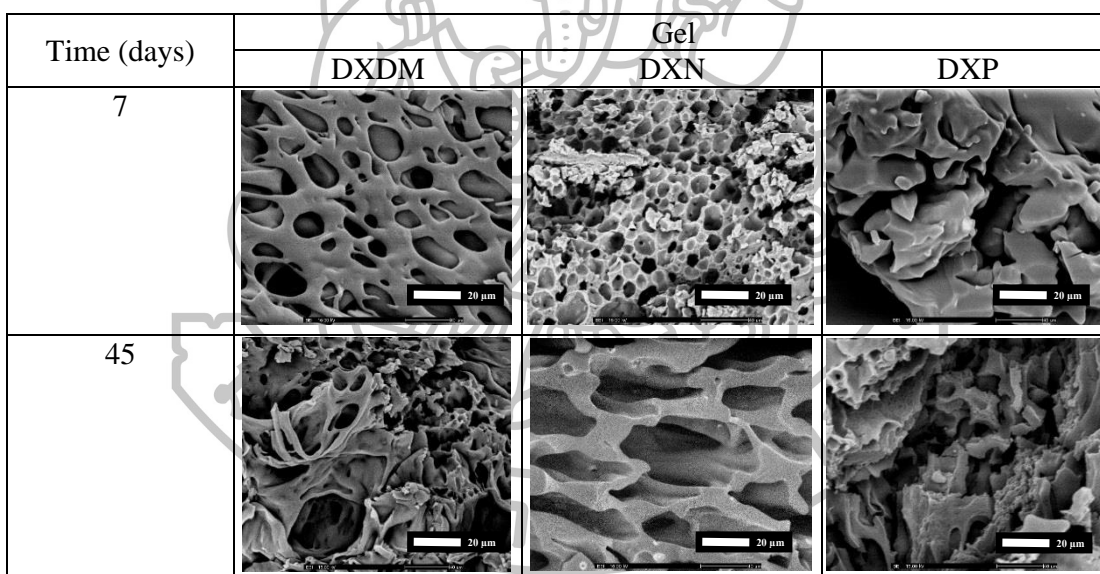
#### 4.3.3.3 Determination of surface topography

Scanning electron microscopy (SEM) is one of direct methods for characterizing the micro-structure of substance (Mfanacho *et al.*, 2010). The formation of *in situ* forming systems was described under solvent exchange process. Contact of these systems into an aqueous medium initiated a diffusion of solvent towards the water. Following the penetration of water, the polymer progressively solidified triggering to phase separation and porous matrix (Parent *et al.*, 2013). SEM was performed in order to relate the porosity character of the precipitated gels or microparticles, to drug release including other physical properties (Kranz and Bodmeier, 2008).

To investigate the effect of the solvent release rates on the surface morphology of matrices, scanning electron micrographs from *in situ* forming gels were prepared as a function of the type of solvent during release time interval at magnitude of 100X and 500X, respectively as illustrated in Figs. 82 and 83. The SEM microphotographs of precipitated gels revealed that the highly unidirectional pore architecture or sponge-like structure was found in matrices of DXDM and DXN gels at first 7 days whereas that of DXP gels allowed an introduction of diminutive pores which prolonged solvent and drug release as previous criticized. The size and density of pores increased by time in the rank of formulation order as following DXDM gel > DXN gel >> DXP gel. This evidence was attributed to the fastest diffusion rate of DMSO out of the systems owing to its low viscosity, as mentioned in solvent release study and also reported previously (Kranz and Bodmeier, 2008). This behavior then led to the rapid phase separation and polymer precipitation therefore in the same time periods DMSO contributed the highest porosity. NMP exhibited a lower efflux rate than DMSO because of the stronger polymer/solvent interaction. Although PYR is a poor solvent and expected to be shorter in the liquid state compared to a solution of bleached shellac in DMSO or NMP, its viscous character conducted for the slowest efflux and polymer precipitation rate and thereafter less porous matrix surface (Kranz and Bodmeier, 2008). The level of porosity of each matrix reflected the mechanical strength that a structure with higher porosity collapsed easily whereas a dense matrix was considerably more resistant to compression as previous described in mechanical properties part (Yi *et al.*, 2003; He *et al.*, 2014). Furthermore the alignment of DXP matrix explicitly disconnected at the end of time interval as the results in degradation and mechanical properties. According to viscous character and good water miscibility of PYR, these reasons probably ascribed for the prolongation of PYR remaining in the system and accumulated some water molecules leading to a rapid hydrolysis at ester bond of polymer chain.



**Fig. 82** Scanning electron micrographs of *in situ* forming gel after release test at different times at magnitude of X100

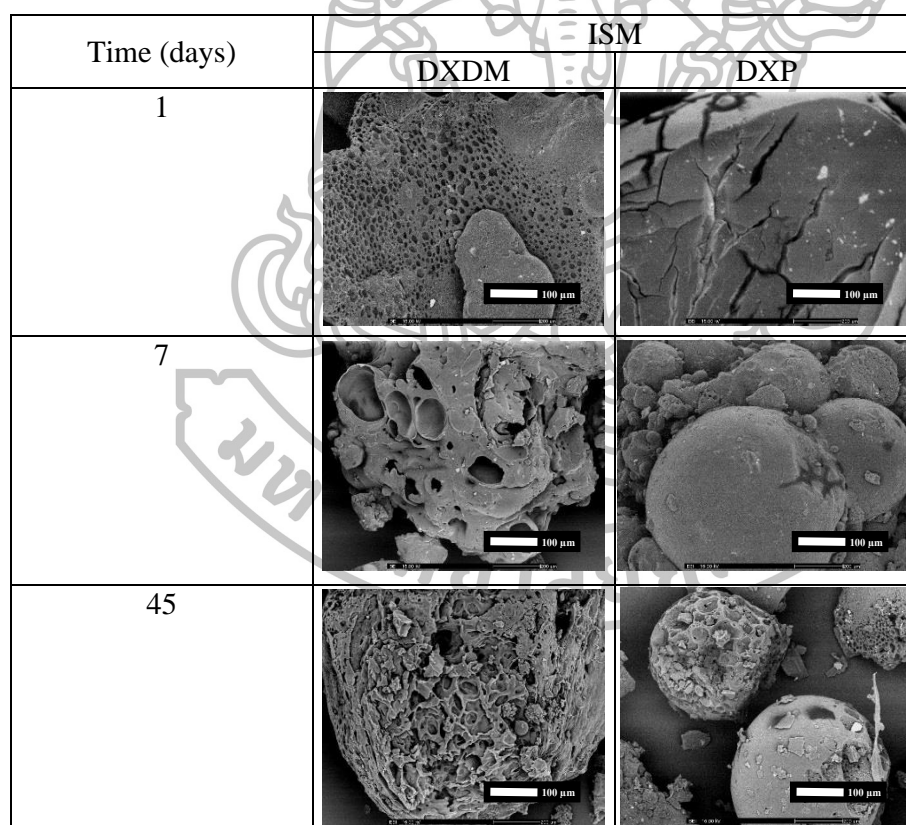


**Fig. 83** Scanning electron micrographs of *in situ* forming gel after release test at different time at magnitude of X500

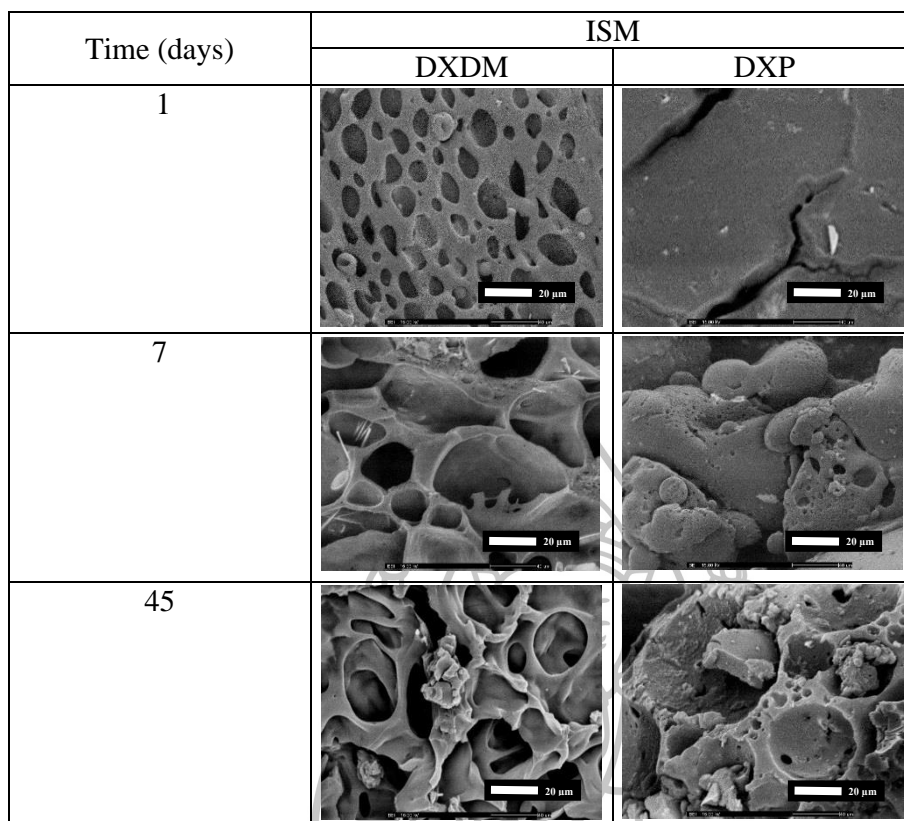
The morphology of ISM after release test at different time periods was studied using SEM at magnitude of 100X and 500X. Figs. 84 and 85 showed the matrix particles of DXDM ism with complex pore orientations. DXP ism initiated some fractures on first day, and they altered to the pore alignments at 7 and 45 days later. An increase of pore size and porosity was governed by time in the similar rank of formulation order to *in situ* forming gel as following DXDM ism  $\gg$  DXP ism. However, ISM matrices provided less pore density than *in situ* forming gel because the external oil phase acted as a barrier for the solvent diffusion (Kranz and Bodmeier, 2008). It was reciprocal to another study that ISM containing polylactic-co-glycolic acid (PLGA) in water-miscible solvent such as

DMSO and NMP, exhibited a lower initial burst and had a less porous surface owing to a retardation of drug diffusion rate from barrier effect of external oil phase (Ahmed *et al.*, 2014). As expected, the pore architecture of DXP matrix particle partially dissipated at the end. These phenomena could be clearly explained as discussed in *in situ* forming gel part.

The optimum *in situ* forming systems should be manipulated with PYR. Although PYR is not a good solvent for bleached shellac, its viscous feature conveys an appropriated extended drug release profiles and higher rate of polymer degradation which are the essential requirement of injectable local drug delivery systems used in dentistry (Kaplish *et al.*, 2013). However, the liquid formed from PYR, especially gel, deformed elastically or the texture was not able to change its geometry to dynamic changes in the periodontal pocket's size and shape with time. This drawback perhaps modified by the addition of plasticizer such as PEG 400. It could not only plasticize but also increased the stability of shellac. According to its large molecule, PEG 400 promised to hinder the interaction between carboxyl groups and hydroxyl groups within inner bleached shellac structure in order to block aging polymerization (Luangtana-anan *et al.*, 2007).



**Fig. 84** Scanning electron micrographs of ISM after release test at different time at magnitude of X100



**Fig. 85** Scanning electron micrographs of ISM after release test at different time at magnitude of X500

### Summary

The physical texture of gel matrices was higher rough and bulge than that of ISM owing to oil barrier of the latter. The order of mechanical hardness of transformed system prepared with different solvents was presented as  $\text{PYR} > \text{NMP} > \text{DMSO}$ , influenced by phase separation rate and porosity. A fast phase separation where large pores were evident, it was exclusively responsible for crack initiation after compression. However, regions of high porosity generally decreased the elasticity thus the matrices obtained from formula prepared with NMP and DMSO were more likely plastic or able to adapt its geometry to dynamic changes while matrix obtained from formula prepared with PYR was elastic. The drug-loaded matrices was more resistant to compression except DXP gel and DXP ism because the replacement of drug particles in spaces of matrix might obstruct the solvent diffusion, resulted in few porous layers and deformed elastically. Nevertheless, ISM matrices with drug loading was still governed by the oil in external phase. Its consequence was reasonably plastic instead. The XRD pattern of the dried *in situ* forming systems and their formulation compositions showed that solvent had no effect on the structure of remained bleached shellac after solvent exchange or release test. The SEM microphotographs of both precipitated gels and ISMs revealed sponge-like structure of formula prepared with DMSO and NMP whereas that prepared with PYR only initiated diminutive pores which retarded the solvent and drug release. The size and density of pores

increased by time in the rank of solvent order related with diffusion rate as following DMSO > NMP > PYR. However, ISM matrices had less pore density than that from *in situ* forming gel because the solvent diffusion out was lower owing to the barrier effect of the external oil. The level of porosity of each matrix reflected the mechanical strength that a higher porous structure collapsed easily but a dense matrix considerably resisted to a compression. The alignment of matrices of systems prepared from PYR explicitly dissipated at the end of time interval from the hydrolysis at ester bond of bleached shellac which was accelerated by PYR-induced water accumulation. The most appropriated solvent for preparing the *in situ* forming systems was PYR definitely because the formulations formed from PYR demonstrated a proper retarded drug release profiles and preferable self-degradation in physiological condition.





## CHAPTER 5

### CONCLUSION

The *in situ* forming gels and ISMs using bleached shellac as matrix former were prepared into solution and emulsion forms respectively using different solvents. Although bleached shellac possesses the acid character, it dissolved in organic solvent such as DMSO, NMP or PYR *via* strongly hydrogen bonding and van der Waals forces among alkyl groups rather than pH dependent solubility. The solubility parameter, apparent viscosity and relative viscosity values confirmed that NMP was a good solvent for dissolving bleached shellac. In addition, the density and interfacial tension measurements theoretically pointed out its proper suitability as another phase of emulsion for emulsifying with olive oil comprising GMS as an emulsifier. However, NMP was partially miscible with this oil; thus, practically generated a rapid phase separation by Ostwald ripening effect. Therefore only bleached shellac solutions using DMSO and PYR as the solvents were able to fabricate into an emulsion with olive oil using GMS as an emulsifier. GMS emulsified these systems by forming the gel network with olive oil thereafter decreasing a coalescence effect. The 5% w/w of GMS was an appropriated concentration to succeed the smallest oil droplet approximately 65  $\mu\text{m}$ . There should be an adequate formation area to prevent the particle accumulation; hence only higher amount of this phase could form the complete emulsion droplets with a decrease of size from approximately 95  $\mu\text{m}$  to 30  $\mu\text{m}$ . The prepared ISMs are suitable for local injection because of their Newtonian or Pseudoplastic flow. NMP or PYR could make systems become liquid-like but DMSO showed both liquid and solid-like due to its stronger bonding with shellac. After exposure to buffer pH 6.8 simulated to gingival crevicular fluid, the internal phase gradually transformed to free drug or drug-loaded bleached shellac solid matrices. Finally, the process of preparation did not damage the compositions basically assured by TGA.

The solubility parameter is an important tool for prediction of solvent and drug release from polymer matrices by the polymer-solvent interaction. This calculated value could be indirectly criticized in terms of viscosities, viscoelasticity and thermal analysis. The miscibility of each solvent to bleached shellac could be in rank of the solvent order as following: NMP > DMSO > PYR. NMP was described as the best “good solvent” because it has high affinity to bleached shellac contrasting to PYR. Similarly, this solubility parameter rank is proportional to the relative viscosity of dilute polymer solution and vice versa in the case of apparent viscosity. Owing to drug replacement, the doxycycline hyclate-loaded systems become more viscous might be owing to crosslinking of drug with polymer. However, PYR itself was more viscous than DMSO and NMP, respectively. In a good solvent, polymer-solvent interactions are favored resulting in polymer extension and stretching, while polymer-polymer interactions are promoted in a poor solvent causing polymer coiling up. These arrangements of polymer chains correlated to viscoelastic behavior that stronger crosslink capacity were from solution made in poor solvent rather than good one. The higher intermolecular strength of polymer could delay the thermal

degradation rate as well. In emulsion, the intermolecular force not only related with solvent but also stabilizer therefore the stronger bonding between solvent and GMS triggered superior entanglement as system prepared in DMSO. DSC profiles also supported all these behaviors of solvent state in polymer but ISM was covered by hindrance effect of oil phase.

The main approach for triggering the *in situ* gel and microparticle formations of bleached shellac is solvent exchange. The solvent remarkably played a crucial role on release kinetics, matrix morphology and polymer degradation. To simply understand the behavior of solvent, it should be described according to the crucial steps of mechanism.

**1) Water inflow;** upon loading sample into aqueous environment, the water molecules flowed into polymeric system with different rate in rank of the solvent order as following: DMSO > NMP > PYR which further explained in the next phase. This water permeation provoked a decrease in the solubility of bleached shellac, and it then precipitated from phase separation because it is insoluble in aqueous environment. The *in situ* systems turned to solid matrix depended on dosage form. For an emulsion, the dispersed internal phase droplets transformed into the opaque particles dispersed in oil. The size of precipitation zone was proportional to rate of water inflow. However, this zone of transformation of ISMs was totally less than gels due to hindrance effect of oil.

**2) Solvent and drug outflow;** the solvent molecules initially diffused out when water influx was driven in a few minutes later. They also transported the drug molecules with similar release pattern. The diffusion rate of all species was presented in term of solvent applied in formulation as DMSO > NMP > PYR. Their kinetic model and mechanism related to Higuchi's model and Fickian diffusion, respectively, except gel in PYR. The release of solvent from PYR system rather obeyed with a First order model and an anomalous mechanism. PYR formula had the slowest release rate of solvent and drug because solvent itself and its systems were higher viscous. Whereas, all diffusion profiles from DMSO and NMP systems were governed by solubility parameter. DMSO interacted minimally with bleached shellac therefore resulting in the fastest release. As known that oil is an important barrier in ISM, it rationally retarded all diffusions yet it succeeded the complete release contrasted to gels. However, *in situ* forming gel using PYR as a solvent showed the largest extent of drug release at the end caused by osmotic force-induced water influx.

**3) Pore formation;** as the exchange between water and solvent molecules progressed, pores were supplied with these fluxes. The size and density of pores were increased by time similarly to the release rate of solvent and drug. DMSO and NMP systems exhibited the highly sponge-like structure whereas PYR matrices only initiated the diminutive pores and it eventually dissipated due to hydrolysis at ester bond which was accelerated by PYR-induced water accumulation. Additionally, ISMs consisted of oil as a barrier so that their matrices had a less pore density than gels. Subsequently, the level of porosity reflected the mechanical strength and elasticity/plasticity behavior. A higher porous structure collapsed easily and it was more likely plastic but a dense one considerably resisted to a compression and deformed elastically which considered as inferior and probably modified by the addition of some plasticizers such as PEG 400.

**4) Degradation;** when all *in situ* forming systems achieved the complete solidification, the degradation of bleached shellac in aqueous condition actually started. The initial rate of total mass loss of all systems was influenced by solvent outflow. At steady state, the total mass loss converted to  $PYR \gg NMP > DMSO$  which was similar to a water content pattern. PYR could gain the high amount of water and pH of doxycycline hyclate solution in matrix was maintained by buffer pH nearly to 7, resulting in the large hydrolysis at polyesters. The oil barrier still obstructed the degradation in ISMs.

From powder X-ray diffraction pattern, the solvent had no effect on the structure of remained bleached shellac after solvent exchange. PYR was the most appropriated solvent for preparing the *in situ* forming systems because its formulations demonstrated the proper sustained drug release profiles and preferable self-degradation in physiological condition.



## Bibliography

- Agutter, P.S., Malone, P.C., Wheatley, D.N. (2000). Diffusion theory in biology: a relic of mechanistic materialism. **Journal of the History of Biology**. 33: 71-111.
- Aherane, M., Yang, Y., Liu, K. (2008). **Mechanical characterisation of hydrogels for tissue engineering applications, in: Topics in tissue engineering**. Vol 4, Eds. Ashammakhi, N., Reis, R., Chiellini, F. (e-book)
- Ahmad, M., Huglin, M. (1994). DSC studies on states of water in crosslinked poly (methyl methacrylate-co-N-vinyl-2-pyrrolidone) hydrogels. **Polymer International**. 33 (3): 273-277.
- Ahmed, T. (2015). Approaches to develop PLGA based *in situ* gelling system with low initial burst. **Pakistan Journal of Pharmaceutical Sciences**. 28 (2): 657-665.
- Ahmed, T.A., Ibrahim, H.M., Ibrahim, F., Samy, A.M. Kaseem, A., Nutan, M.T., Hussain, M.D. (2012). Development of biodegradable *in situ* implant and microparticle injectable formulations for sustained delivery of haloperidol. **Journal of Pharmaceutical Sciences**. 101 (10): 3753-3762.
- Ahmed, T.A., Ibrahim, H.M., Ibrahim, F., Samy, A.M. Kaseem, A., Nutan, M.T., Hussain, M.D. (2014). Biodegradable injectable *in situ* implants and microparticles for sustained release of montelukast: *in vitro* release, pharmacokinetics, and stability. **American Association of Pharmaceutical Scientists**. 15 (3): 772-780.
- Ahmed, T.A., Ibrahim, H.M., Ibrahim, F., Samy, A.M., Kaseem, A., Nutan, M.T., Hussain, M.D. (2011). Development of injectable *in situ* implant and microparticle formulations for controlled delivery of montelukast, **AAPS Journal**. 12 (78): S2.
- Aklonis, J.J., MacKnight, W.J., Shen, M. (1972). **Introduction to Polymer Viscoelasticity**. Wiley-Interscience, New York.
- Alavi, S. (2003). Starch research over the years. **Food Research International**. 36: 307–308
- Alistair, M.S., Phillips, G.O., ed. (2006). **Food polysaccharides and their applications**. CRC Press. 226.
- Almdal, K., Dyre, J., Hvidt, S., Kramer, O. (1993). Towards a phenomenological definition of the term 'gel'. **Polymer Gels and Networks**. 1: 5-17.
- Amel, Y., Bouziane, D., Leila, M., Ahmed, B. (2015). Microbiological study of periodontitis in the west of Algeria. **West Indian Medical Journal**. 5: 7-12.
- Amsden, B. (1998a). Diffusion in hydrogels: mechanisms and models. **Macromolecules**. 31: 8382–8395.
- Amsden, B. (1998b). Solute diffusion in hydrogels. An examination of the retardation effect. **Polymer Gels and Networks**. 6: 13–43.

- Annina, M. (2010). Characterization of different shellac types and development of shellac coated dosage forms. **Hamburg**. 8-19.
- Armitage, G.C. (1999). Development of a classification system for periodontal diseases and conditions. **Annals of Periodontology**. 4: 1-6.
- Ashby, M.F., Jones, D. R. H. (1996). **Engineering Materials 1, an introduction to Their Properties and Applications**. Second edition, Butterworth-Heinemann, Woburn, UK.
- Aulton, M.E., Taylor, K. (2013). **Aulton's Pharmaceuticals: The Design and Manufacture of Medicines**. Elsevier Health Sciences. 459-461.
- Avila-Campos, M.J. (2003). PCR detection of four periodontopathogens from subgingival clinical samples. **Brazilian Journal of Microbiology**. 34 (1): 81-84.
- Barton, A.F.M. (1975). **Solubility parameters**. Chemical Reviews. 75: 731-753.
- Barton, A.F.M. (1990). **Handbook of Polymer-Liquid Interaction Parameters and Solubility Parameters: Shellac**. CRC Press. 650.
- Beauchamp, G.K., Keast, R.S., Morel, D., Lin, J., Pika, J., Han, Q., Lee, C.H., Smith, A.B., Breslin, P.A. (2005). Phytochemistry: Ibuprofen like activity in extravirgin olive oil. **Nature**. 437: 45-46.
- Becher P. (Ed). (1983). **Encyclopedia of Emulsion Technology, Volume 1: Basic Theory**. Marcel Dekker, New York
- Berezow, A.B., Darveau, R.P. (2011). Microbial shift and periodontitis. **Periodontol**. 2000 (55): 36-47.
- Berger, J., Reist, M., Mayer, J.M. Felt, O., Peppas, N.A., Gurny, R. (2004). Structure and interactions in covalently and ionically crosslinked chitosan hydrogels for biomedical applications. **European Journal of Pharmaceutics and Biopharmaceutics**. 54: 19-34.
- Bettelheim, F., Brown, W., Campbell, M., Farrell, S., Torres, O. (2012). **Introduction to general, organic and biochemistry: amines**. Henry VII, England. Cengage Learning. 446-463.
- Binder, T.A., Goodson, J.M., Socransky, S.S. (1987). Gingival fluid levels of acid and alkaline phosphatase. **Journal of Periodontal Research**. 22: 14-9
- Bjorn, A., Monja, P., Karlsson, A., Ejlertsson, J., Svensson, B. (2012). Rheological characterization. **Biogas**. 1: 63-76.
- Bodmeier, R. (1997). **Verfahren zur in-situ Herstellung von Partikeln**. Offenlegungsschrift, DE 197 24 784.
- Boimvaser, S., Cabrera, M.I., Grau, R. (2012). Degradation of porous implants formed *in situ*. **Procedia Materials Science**. 1: 454-460.

- Bonito, A.J., Lux, L., Lohr, K.N. (2005). Impact of local adjuncts to scaling and root planning in periodontal disease therapy: a systemic review. **Journal Periodontol.** 76: 1227-1236.
- Brobyn, R. (2012). The human toxicology of dimethyl sulfoxide. **Bain Clinical Medicine Insights.** 10: 497-506.
- Brodbeck, K.J., DesNoyer, J.R., McHugh, A.J. (1999). Phase inversion dynamics of PLGA solutions related to drug delivery part ii the role of solution thermodynamics and bath-side mass transfer. **Journal of Controlled Release.** 62: 333-344.
- Brown, et al. (2008). **Chemistry: The Central Science.** 11th ed. Upper Saddle River, New Jersey. Pearson/Prentice Hall.
- Brunton, L.L., Lazo, J.S., Parker, K.L. (2006). Goodman & Gilman: **As bases farmacológicas da terapêutica.** 11st ed. McGraw Hill Interamericana do Brasil: Rio de Janeiro.
- Buboltz, J.T., Feigenson, G.W. (1999). A novel strategy for the preparation of liposomes: rapid solvent exchange. **Biochimica et Biophysica Acta.** 1417 (2): 232-45.
- Budavari, S. (ed.). (1996). **The Merck Index - an encyclopedia of chemicals, drugs, and biologicals.** Whitehouse Station, NJ: Merck and Co., Inc. 1378.
- Burke, J. (1984). **Physico-chemical.** The Oakland Museum of California August 1984 Appeared in the AIC Book and Paper Group Annual, Volume 3 C223 Craig Jensen, Editor, pg. 13-58.
- Cahn, J.W. and Hilliard, J.E. (1958). Free energy of a nonuniform system. I. interfacial free energy. **The Journal of Chemical Physics.** 28: 258 - 267.
- Camargo, J.A., Sapin, A., Nouvel, C., Daloz, D., Leonard, M., Bonneaux, F., Six, J.L., Maincent, P. (2013). Injectable PLA-based *in situ* forming implants for controlled release of ivermectin a BCS Class II drug: solvent selection based on physico-chemical characterization. **Drug Development and Industrial Pharmacy.** 39: 146-155.
- Cardon, D. (2007). **Natural Dyes: Sources, Tradition, Technology and Science.** Archetype Publications Ltd., London. 656.
- Carr, J., Milhet, X., Gadaud, P., Boyer, S.A.E., Thompson, G.E., Lee, P. (2015). Quantitative characterization of porosity and determination of elastic modulus for sintered micro-silver joints. **Journal of Materials Processing Technology.** 225: 19-23.
- Carstensen, J.T. (2001). **Advanced Pharmaceutical Solids.** Marcel Dekker, New York.
- Chen, C. H., Terentjev, E. M. (2009). Aging and metastability of monoglycerides in hydrophobic solutions. **Langmuir.** 25 (12): 6717-6724.

- Chen, S., Singh, J. (2005). Controlled delivery of testosterone from smart polymer solution based systems: *in vitro* evaluation. **International Journal of Pharmaceutics**. 295: 183-190.
- Chhokra, M., Dodwad, V., Vaish, S., Mahajan, A. (2012). Magic bullet to treat periodontitis: a targeted approach. **Journal of Pharmaceutical and Biomedical Sciences**. 20 (19): 1-5.
- Chu, D., Curdy, C., Riebesehl, B., Beck-Broichsitter, M., Kissel, T. (2013). *In situ* forming parenteral depot systems based on poly (ethylene carbonate): Effect of polymer molecular weight on model protein release. **European Journal of Pharmaceutics and Biopharmaceutics**. 85: 1245-1249.
- Cicerale, S., Lucas, L.J., Keast, R.S. (2012). Antimicrobial, antioxidant and antiinflammatory phenolic activities in extra virgin olive oil. *Current Opinion in Plant Biology*. **Biotechnology Journal**. 23: 129–135
- Contardo, M.S., Díaz, N., Lobos, O., Padilla, C., Giacaman, R.A. (2011). Oral colonization by *Streptococcus mutans* and its association with the severity of periodontal disease in adults. **Revista clínica de periodoncia, implantología y rehabilitación oral**. 4: 9-12.
- Crank, J. (1975). *The Mathematics of Diffusion*. Oxford University Press. New York.
- Cussler, E.L. (1984). **Diffusion, Mass Transfer in Fluid Systems**. Cambridge University Press. New York.
- Da Pieve, S., Calligaris, S., Co, E., Nicoli, M.C., Marangoni, A.G. (2010). Shear nanostructuring of monoglyceride organogels. **Food Biophysics**. 5: 211–217.
- Daniel, E., Marangoni, A.G. (2012). Organogels: An Alternative Edible Oil-Structuring Method. **Journal of the American Oil Chemists' Society**. 89: 749–780.
- Daubert, T.E., Danner, R.P. (1997). **Physical and thermodynamic properties of pure chemicals: data compilation**. Design institute for physical property data, American institute of chemical engineers. Hemisphere Pub. Corp., New York, NY. 5.
- David, N.A. (1972). The pharmacology of dimethyl sulfoxide. **Annual Review of Pharmacology and Toxicology**. 12: 222-235.
- Davies, E., Huang, Y., Harper, J.B., Hook, J.M., Thomas, D.S., Burgar I.M., Lillford P.L. (2010). Dynamics of water in agar gels studied using low and high resolution <sup>1</sup>H NMR spectroscopy. **International Journal of Food Science & Technology**. 45: 2502–2507.
- Dean, J.A. (1995). **The Analytical Chemistry Handbook**. New York: McGraw Hill, Inc. 15.1–15.5.
- Deruiter, J. (2005). **Amides and related functional groups**. Principles of Drug Action 1.

- Dittgen, M., Fricke, S., Gerecke, H., Moller, I.P. Volkel, C. (1998). **Injection implant**. PCT/DE1997/002903[WA/1998/030245]. Germany.
- Divya, P.V., Nandakumar, K. (2006). Local drug delivery poriocol in periodontics. **Trends in Biomaterials & Artificial Organs**. 19 (2): 74-80.
- Do, M.P., Neut, C., Delcourt, E., Certo, T.S., Siepmann, J., Siepmann, F. (2014). In situ forming implants for periodontitis treatment with improved adhesive properties. **European Journal of Pharmaceutics and Biopharmaceutics**. 88: 342-50.
- Dunn, R.L., Tipton, A.J., Southard, G.L., Rogers, J.A. (1997). **Biodegradable polymer composition**. US patent [5599552].
- Eggert, F.M., Drewell, L., Bigelow, J.A., Speck, J.E., Goldner, M. (1991). The pH of gingivalcrevices and periodontal pockets in children, teenagers and adults. **Archives of Oral Biology**. 36: 233-8.
- Eliaz, R., Kost, J. (2000). Characterization of a polymer PLGA-injectable implant delivery system for the controoled release of proteins. **Journal of Biomedical Materials Research**. 50: 388-396.
- Esoposito, E., Carotta, V., Scabbia, A., Trombelli, L., Antona, P.D. (1996). Comparative analysis of tetracycline-containing dental gels: poloxamer and monoglyceride-based formulations. **International Journal of Pharmaceutics**. 37 (2): 101-109.
- Farag, Y., Leopold, C.S. (2009). Physicochemical properties of various shellac types. **Dissolution Technologies**. 33-39.
- Fogueri, L.R., Singh, S. (2009). Smart polymers for controlled delivery of proteins and peptides: a review of patents. **Recent Patents on Drug Delivery and Formulation**. 3: 40-48.
- Fredenberg, S. Wahigren, M., Reslow, M., Axelsson, A. (2011). The mechanisms of drug release in poly (lactic-co-glycolic acid)-based drug delivery systems-a review. **International Journal of Pharmaceutics**. 415: 34-55.
- Frelichowska, J., Bolzinger, M.A., Valour, J.P., Mouaziz, H., Pelletier, J., Chevalier, Y. (2009). Pickering w/o emulsions: drug release and topical delivery. **International Journal of Pharmaceutics**. 23 (368) (1-2): 7-15.
- Friesen, L.R., Williams, K.B., Kraus, L.S., Killow, W.J. (2002). Controoled local delivery of tetracycline with polymer strips in the treatment of periodontitis. **Journal Periodontol**. 73: 13-19.
- Gad, H., Mohamed, A., Nabarawi, E., Hady, S. (2008). Formulatoin and evaluation of PLA and PLGA in situ implant containing secnidazole and/or doxycycline for treatment of periodontitis. **AAPS PharmSciTech**. 9 (3): 878-884.
- Gao, S.J., Guo, J. M., Nishinari, K. (2008). Thermoreversible konjac glucomannan gel crossinked by borax. **Carbohydrate Polymers**. 72 (2): 315-325.



- Garala, K., Joshi, P., Shah, M., Ramkishan, A., Patel, J. Formulation and evaluation of periodontal in situ gel. **International Journal of Pharmaceutical Investigation**. 3 (1): 29-41.
- Gardner, W. H. & Whitmore, W. F. (1929). Action of Organic Solvents. **Journal of Industrial & Engineering Chemistry**. 21: 226.
- Geiss, J. (2001). **The century of space science**. Kluwer Academic. P. 20.
- Gilani, A.H., Khan, A.U., Shah, A.J., et al. (2005). Blood pressure lowering effect of olive is mediated through calcium channel blockade. **International Journal of Food Sciences and Nutrition**. 56: 613-620.
- Godavarthy, S.S., Yerramasetty, K.M., Neely, B.J., Madihally, S.V. et al. (2009). Design of improved permeation enhancers for transdermal drug delivery. **Journal of Pharmaceutical Sciences**. 98: 4085-4099.
- Graham, P.D.D., Brodbeck, K.J.J., McHugh, A.J.J. (1999). Phase inversion dynamics of PLGA solutions related to drug delivery. **Journal of Controlled Release**. 58: 233-245.
- Hagemann, J.W. (1988). **Thermal behaviour and polymorphism of acylglycerides**. In: Garti N, Sato K, editors. Crystallization and polymorphism of fats and fatty acids. New York: Marcel Dekker. pp 9-95.
- Hagerstorm, H., Paulsson, M., Edsman, K. (2000). Evaluation of mucoadhesion for two polyelectrolyte gels in simulated physiological conditions using a rheological method. **European Journal of Pharmaceutics and Biopharmaceutics**. 3: 301-309.
- Hameed, N., Sreekumar, P. A., Francis, B., Yang, W., Thomas, S. (2007). Composites Part A. **Applied Science and Manufacturing**. 38: 2422.
- Han, J., Lei, T., Wu, Q. (2014). High-water-content mouldable polyvinyl alcohol-borax hydrogels reinforced by well-dispersed cellulose nanoparticles: dynamic rheological properties and hydro gel formation mechanism. **Journal of Carbohydrate Chemistry**. 102: 306-316.
- Han, J., Lei, T., Wu, Q. (2014). High-water-content mouldable polyvinyl alcohol-borax hydrogels reinforced by well-dispersed cellulose nanoparticles: dynamic rheological properties and hydrogel formation mechanism. **Carbohydrate Polymers**. 102:306-316.
- Hansen, C.M. (1967). The three dimensional solubility parameter-key to paint component affinities: II and III. **Journal of Paint Technology**. 39: 505-514.
- Hansen, C.M. (2009). **Hansen solubility parameters: A User's Handbook**. Second Edition: Solubility parameters an introduction. CRC Press. 1-25.
- Harkins, W. D. and Humphery, E. C. (1915). **The surface-tension at the interface between two liquids**. Proceedings of the National Academy of Sciences of the United States of America National Academy of Sciences (US). 1 (12): 585-590.

- Hartland, S., Srinivasan, P. S. (1974). The basis of theoretical correction factor for use with the drop weight method of surface tension measurement. **Journal of Colloid and Interface Science**. 49: 318.
- Hatefi, A., Amsden, B. (2002) Biodegradable injectable *in situ* forming drug delivery systems. **Journal of Controlled Release**. 80: 9–28.
- He, X., Kawazoe, N., Chen, G. (2014). Preparation of cylinder-shaped porous sponges of poly (l-lactic acid), poly (dl-lactic-co-glycolic acid), and poly(-caprolactone). **BioMed Research International**. 2014: 1-8.
- Hemminger, W., Sarge, S.W. (1998). **Handbook of thermal analysis and calorimetry**, Vol. 1, M. E. Brown (Ed.), Chap. 1, Elsevier, Amsterdam.
- Hennequin D., Hardy J. (1993). Évaluation instrumentale et sensorielle de fromages à pâte molle. **International Dairy Journal**. 3: 635-647.
- Hile, D.D., Amirpour, M.L., Akgerman, A., Pishko, M.V. (2000). Active growth factor delivery from poly (D, L-lactide-co-glycolide) foams prepared in supercritical CO<sub>2</sub>. **Journal of Controlled Release**. 66: 177–185.
- Hodge, S. M., Rousseau, D. (2005). Continuous-phase fat crystals strongly influence water-in-oil emulsion stability. **J. Am. Journal of the American Oil Chemists' Society**. 82 (3): 159-164.
- Honek, T., Hausnerova, B., Saha, P. (2005). Relative viscosity models and their application to capillary flow data of highly filled hard-metal carbide powder compounds. **Polymer Composites**. 26 (1): 29–36.
- Huang, X., Brazel, C.S. (2001). On the importance and mechanisms of burst release in matrix-controlled drug delivery systems. **Journal of Controlled Release**. 73: 121-136.
- Hurley, C., De Deene, Y., Meder, R., Pope, J.M., Baldock, C. (2003). The effect of water molecular self-diffusion on quantitative high-resolution MRI polymer gel dosimetry. **Physics in Medicine and Biology**. 48 (18): 3043-3058.
- Ishii, D., Kanazawa, Y., Tatsumi, D., Matsumoto, T. (2007) Effect of Solvent Exchange on the Pore Structure and Dissolution Behavior of Cellulose. **Journal of Applied Polymer Science**. 103: 3976-84.
- Jain, N., Gaurav, K., Javed, S., Iqbal, Z., Talegaokar, S. Ahmad, F.J., Khar, R.K. (2008). Recent approaches for the treatment of periodontitis. **Drug Discovery Today**. 1 (21-22): 932-943.
- Jain, P., Yalkowsky, S. (2007). Solubilization of poorly soluble compounds using 2-pyrrolidone. **International Journal of Pharmaceutics**. 342 (1-2): 1-5.
- Jan C., J. Bart. (2006). **Polymer additive analytics: industrial practice and case studies**. Firenze University Press, Italy.

- Johns D. (2007). Pharmaceutical applications of polymers for drug delivery: application of polymer for drug delivery system. **Smithers Rapra Press**. 16-40.
- Jones, S.D., Woolfson, D.A., Brown, F.A., Michael, J., Neill, O. (2002). Mucoadhesive, syringeable drug delivery systems for controlled application of metronidazole to periodontal pocket. *In vitro* release kinetics, syringeability, mechanical and mucoadhesive properties. **Journal of Control Release**. 49 (1): 71-79.
- Jouyban, A., Fakhree, M.A., Shayanfar, A. (2010). Review of pharmaceutical applications of N-methyl-2-pyrrolidone. **Journal of Pharmaceutical Sciences**. 13 (4): 524-535.
- Kaplish, V., Walia, M.K., Kumar H.S.L. (2013). Local drug delivery systems in the treatment of periodontitis: a review. **Pharmacophore**. 4 (2): 39-49.
- Kapoor, D.N., Katare, O.P., Dhawan, S., 2012. *In situ* forming implant for controlled delivery of an anti-HIV fusion inhibitor. **International Journal of Pharmaceutics**. 426: 132–143.
- Kaufman, H.S., Falcetta, J.J. (1977). **Introduction to polymer science and technology**. In: SPE Textbook. John Wiley & Sons: New York, USA. pp. 1-268.
- Kemp, M.R., Fryer, P.J. (2007). Enhancement of diffusion through foods using alternating electric fields. **Innovative Food Science and Emerging Technologies**. 8 (1): 143–153.
- Kempe, S., Mäder, K. (2012). *In situ* forming implants - an attractive formulation principle for parenteral depot formulations. **Journal of Controlled Release**. 161 (2): 668-79.
- Kempe, S., Metz, H., Mader, K. (2008). Do *in situ* forming PLG/NMP implants behave similar *in vitro* and *in vivo*: a non-invasive and quantitative EPR investigation on the mechanism of the implant formation process. **Journal of Controlled Release**. 130: 220-225.
- Kesic, L., Milasin, J., Igetic, M., Obradovic, R. (2008). Microbial etiology of periodontal disease – mini review. **Medicine and Biology**. 15: 1-6.
- Kesselman, E., Shimoni, E. (2007). Imaging of oil/monoglyceride networks by polarizing near-field scanning optical microscopy. **Food Biophysics**. 2: 117–123.
- Khadka, P., Ro, J., Kim, H., Kim, I., Kim, J.T., Kim, H., Cho, J.M., Yun, G., Lee, J. (2014). Pharmaceutical particle technologies: An approach to improve drug solubility, dissolution and bioavailability. **Asian Journal of Pharmaceutical Sciences**. 9: 304-316.
- Kojima, M., Ogawa, K., Kohayakawa, K. (2000). Effect of shellac on some physicochemical properties of cornstarch extrudates. **Journal of Applied Polymer Science**. 47: 16-17.
- Körner, A., Piculell, L., Iselau, F., Wittgren, B., Larsson, A. (2009). Influence of different polymer types on the overall release mechanism in hydrophilic matrix tablets. **Molecules**. 14: 2699-2716.

- Kranz, H., Brazeau, G.A., Napaporn, J., Martin, R.L., Millard, W., Bodmeier, R. (2001). Myotoxicity studies of injectable biodegradable *in-situ* forming drug delivery systems. **International Journal of Pharmaceutics**. 212 (1):11-18.
- Kranz, H., Bodeier, B. (2008). Structure formation and characterization of injectable drug loaded biodegradable device: *in situ* implants versus *in situ* microparticles. **European Journal of Pharmaceutical Sciences**. 34: 164-172.
- Kranz, H., Bodmeier, R. (1998). A biodegradable *in situ* forming system for controlled drug release. **Journal of Pharmaceutical Sciences**. 1 (suppl): 414.
- Kranz, H., Bodmeier, R. (2007). A novel *in situ* forming drug delivery system for controlled parenteral drug delivery. **International Journal of Pharmaceutics**. 332: 107-114.
- Kranz, H., Bodmeier, R. (2008). Structure formation and characterization of injectable drug loaded biodegradable devices: *In situ* implants versus *in situ* microparticles. **European Journal of Pharmaceutical Sciences**. 34: 164-172.
- Kranz, H., Brazeau, G.A., Napaporn, J., Martin, R.L., Millard, W., Bodeier, R. (2001). Myotoxicity studies of injectable biodegradable *in situ* forming drug delivery systems. **International Journal of Pharmaceutics**. 212: 11-18.
- Kranz, H., Yilmaz, E., Brazeau, G.A., Bodmeier, R. (2008). *In vitro* and *in vivo* drug release from a novel *in situ* forming drug delivery system. **Pharmaceutical Research**. 25 (6):1347-1354.
- Kulkarni, A.P., Khan, S.K.A., Dehghan, M.H. (2012). Evaluation of poloxamer-based *in situ* gelling of articain as drug delivery system for anesthetizing periodontal pockets-an *in vitro* study. **Journal of Dental Research**. 3 (4): 201-208.
- Kunche, H.B., Ahmed, M.G., Rompicharla, N.C. (2012). Development and evaluation of *in situ* gels of moxifloxacin for the treatment of periodontitis. **Indonesian Journal of Pharmacy**. 23 (3): 141-146.
- Kurata M., Tsunashima Y. (1989). **Viscosity-molecular weight relationships and unperturbed dimensions of linear chain molecules**. In Polymer Handbook, 3 Eds; Bandrup t J. Immergut E.H., Etd. John Wiley & Sons: New York, USA. pp. 1-59.
- Lai, H.L., Abu'Khalil, A., Craig, D.Q. (2003). The preparation and characterisation of drug-loaded alginate and chitosan sponges. **International Journal of Pharmaceutics**. 251 (1-2):175-81.
- Larson R.G. (1999). **The structure and rheology of complex fluids**. Oxford University Press, New York.
- Laza, J.M., Julian, C.A., Larrauri, E., Rodriguez, M., Leon, L.M. (1998). Thermal scanning rheometer analysis of curing kinetic of an epoxy resin: 2. an amine as curing agent. **Polymer**. 40: 35-45.

- Lecompte, H.A., Liggat, J.J. (2008). Commercial fire-retarded PET formulations—relationship between thermal degradation behaviour and fire-retardant action. **Polymer Degradation and Stability**. 93: 498–506.
- Lee, S.Y., Tae, G. (2007). Formulation and in vitro characterization of an in situ geable photo-polymerizable pluronic hydrogel suitable for injection. **Journal of Controlled Release**. 119: 313-319.
- Li S., Girod-Holland S., Vert M. (1996). Hydrolytic degradation of poly (DL-lactic acid) in the presence of caffeine base. **Journal of Controlled Release**. 40: 41.
- Li, L., Thangamathesvaran, P. M., Yue, C.Y., Tam, K.C., Hu, X., & Lam, Y.C. (2001). Gel network structure of methylcellulose in water. **Langmuir**. 17 (26): 8062-8068.
- Lim, Kieran F. (2006). Negative pH does exist. **Journal of chemical education**. 83 (10): 1465.
- Limmatvapirat, S., Limmatvapirat, C., Luangtana-Anan, M., Nunthanid, J., Oguchi, T., Tozuka, Y., Yamamoto, K., Puttipipatkachorn, S. (2004). Modification of physicochemical and mechanical properties of shellac by partial hydrolysis. **International Journal of Pharmaceutics**. 278 (1): 41-9.
- Limmatvapirat, S., Limmatvapirat, C., Puttipipatkachorn, S., Nuntanid, J., Luangtana-Anan, M. (2007). Enhanced enteric properties and stability of shellac films through composite salts formation. **European Journal of Pharmaceutics and Biopharmaceutics**. 67: 690-698.
- Limmatvapirat, S., Panchapornpon, D., Limmatvapirat, C., Nunthanid, J., Luangtana-Anan, M., Puttipipatkachorn, S. (2008). Formation of shellac succinate having improved enteric film properties through dry media reaction. **European Journal of Pharmaceutics and Biopharmaceutics**. 70: 335-344.
- Liu, H. Venkatraman, S.S. (2012). Cosolvent effects on the drug release and depot swelling in injectable *in situ* depot-forming systems. **Journal of Pharmaceutical Sciences**. 101 (5): 1783–1793.
- Liu, Q., Zhang, H., Zhou, G., Xie, S., Zou, H., Yu, Y., Li, G., Sun, D., Zhang, G., Lu, Y., Zhong, Y. (2010). In vitro and in vivo study of thymosin alpha1 biodegradable *in situ* forming poly (lactide-co-glycolide) implants. **International Journal of Pharmaceutics**. 397 (1-2): 122-9.
- Lovegrove, J.M. (2004). Dental plaque revisited: bacteria associated with periodontal disease. **Journal of the New Zealand Society of Periodontology**. 87: 7-21.
- Luan, X., Bodmeier, R. (2006). *In situ* forming microparticle system for controlled delivery of leuprolide acetate: influence of the formulation and processing parameters. **European Journal of Pharmaceutical Sciences**. 27: 143-149.
- Luangtana-anan, M., Limmatvapirat, S., Nuntanid, J., Wanawongthai, C. (2007). Effect of salts and plasticizers on stability of shellac film. **Journal of Agricultural and Food Chemistry**. 55: 687-692.

- Parent, M., Nouvel, C., Koerber, M., Sapin, A., Maincent, P., Boudier, A. (2013). PLGA *in situ* implants formed by phase inversion: critical physicochemical parameters to modulate drug release. **Journal of Controlled Release**. 172: 292-304.
- Macosko, W. (1994). **Rheology: Principles, Measurements and Applications**. Wiley-VCH, New York.
- Madsen, C.G., Skov, A., Baldursdottir, S., Rades, T., Jorgensen, L., Medlicott, N.J. (2015). Simple measurements for prediction of drug release from polymer matrices - solubility parameters and intrinsic viscosity. **European Journal of Pharmaceutics and Biopharmaceutics**. 92: 1-7.
- Mahadlek, J. (2012). **Preparation of in situ forming gel system for delivery of antimicrobial agents for periodontitis treatment**. Thesis for the degree of doctor of philosophy program in pharmaceutical technology graduate school. Nakhon Pathom: Silpakorn University.
- Mahendra, K.M. (1987). Solution properties of shellac, 4. Solubility parameter of shellac. **Angewandte Makromolekulare Chemie**. 147 (1): 5
- Marangoni, A.G., Garti, N. (2011). **Edible oleogels: structure and health implications**. Academic Press and AOCS Press. pp. 305.
- Marcotte, H., Lavoie, M.C. (1998). Oral microbial ecology and the role of salivary immunoglobulin A. **Microbiology and Molecular Biology Reviews**. 62: 71-109.
- Marren, K. (2011). Dimethyl sulfoxide: an effective penetration enhancer for topical administration of NSAIDs. **The Physician and Sports medicine**. 39 (3): 75-82.
- Martin, A. (1993). **Physical pharmacy**. Philadelphia, PA: Lea and Febiger: 393-476.
- Masaro, L., Zhu, X.X. (1999). Physical models of diffusion for polymer solutions, gels and solids. **Progress in Polymer Science**. 24: 731-775.
- Matschke, C., Isele, U., Van Hoogenest, P., Fahr, A. (2002) Sustained-release injectables formed *in situ* and their potential use for veterinary products. **Journal of Controlled Release**. 85: 1-15.
- Mayol, L., Quaglia, F., Borzacchiello, A., Ambrosio, L., La Rotonda, M.I. (2008). A novel poloxamers/hyaluronic acid *in situ* forming hydrogel for drug delivery: rheological, mucoadhesive and *in vitro* release properties. **European Journal of Pharmaceutics and Biopharmaceutics**. 70 (1): 199-206.
- McGowan-Jackson, H. (1992). **Shellac conservation**. Bulletin. 18 (1-2): 29-44.
- McNaught, A.D., Wilkinson, A. (1997). **Compendium of Chemical Terminology**, 2nd ed. Gold Book. Blackwell Scientific Publications. Oxford.
- Meyer, M., Chawla, K. (2009). **Mechanical Behaviour of Materials**. 2nd Ed, Cambridge University Press.
- Mfanacho, S. M., Hemang, P. & Manocha, L. M. (2010). Enhancement of microporosity through physical activation. **Journal of Pure and Applied Sciences**. 18: 106-109.

- Mi, F.I., Shyu, S.S., Wong, T.B., Jang, S.F., Lee, S.T., Lu, K.T. (1999). Chitosan-polyelectrolyte complexation for the preparation of gel beads and controlled release of anticancer drug II, effect of pH-dependent ionic crosslinking or interpolymer complex using triphosphate or polyphosphate as reagent. **Journal of Applied Polymer Science**. 74: 1093-1107.
- Michael E. Aulton, Kevin Taylor. (2013). **Aulton's Pharmaceuticals: The Design and Manufacture of Medicines**. Elsevier Health Sciences. pp. 459-461.
- MicroMath Scientist Handbook Rev. 7EEF (1995). **MicroMath**: Salt Lake City. 467.
- Miller, Clarence. A., Neogi, P. (ed.). (2008). **Fundamentals of Interfacial Tension, Chap. 1, in: Interfacial Phenomena - Equilibrium and Dynamics Effects** (Second Edition), CRC Press.
- Mishra, M.K. (1987). Solution properties of shellac, 4. Solubility parameter of shellac. **Die Angewandte Makromolekulare Chemie**. 147 (1): 107-112.
- Moseson, D., Mulcrone, R., Levine, S.A., Kirkland, N., Smith, T.L. (2008). **Aqueous shellac coatings with effective taste masking and stable release properties**. AAPS Annual Meeting and Exposition, Atlanta, Georgia, USA.
- Motto, F., Gailloud, P. (2000). *In-vitro* assessment of new embolic liquids prepared from preformed polymers and water miscible solvents aneurysm treatment. **Biomaterials**. 21: 803-811.
- Muhr, A.H., Blanshard, J.M.V. (1982). Diffusion in gels. **Polymer**. 23: 1012-1026.
- Naidong, W., Geelen, S., Roets, E., Hoogmartens, J. (1990). Assay and purity control of oxytetracycline and doxycycline by thinlayer chromatography – a comparison with liquid chromatography. **Journal of Pharmaceutical and Biomedical Analysis**. 8: 891-898.
- Nanjwade, V.K., Katare, O.P., Manvi, F.V., Nanjwade, B.K. (2013). Lipid nanoemulsions as drug delivery carriers for poorly water soluble drug. **International Journal of Drug Development and Research**. 5 (1): 333-338.
- Naveed, S., Qamar, H., Jawaid, W., Bokhair, U. (2014). Degradation study of six different brands of doxycycline using UV spectrophotometer. **World Journal of Pharmaceutical Sciences**. 3: 1978-84.
- Nazzal, S., Nutan, M., Palamakula, A., Shah, R., Zaghoul, A.A., Khan, M.A. (2002). Optimization of a self-nanoemulsified tablet dosage form of ubiquinone using response surface methodology: Effect of formulation ingredients. **International Journal of Pharmaceutics**. 240 (1–2): 103-14.
- Nirmal, H.B., Bakliwal, S.R., Pawar, S.P. (2010). *In-Situ* gel: new trends in controlled and sustained drug delivery system. **International Journal of Pharmaceutics**. 2: 1398-1408.

- Núñez, L., Gómez-Barreiro, S., Gracia-Fernández, C.A. (2005). Study of the influence of isomerism on the curing properties of the epoxy system DGEBA (n=0)/1, 2-DCH by rheology. **Rheologica Acta**. 45: 184-191.
- Okamoto, M.Y., Ibanez, P.S. (1986). Final report on the safety assessment of shellac. **International Journal of Toxicology**. 5: 309-327.
- Ortiz-Cruz, A., Santolalla, C., Moreno, E., de los Reyes-Heredia, J.A., Alvarez-Ramirez, J. (2012). Fractal analysis of powder X-ray diffraction patterns. **Physica**. A 391: 1642-1651.
- Osswald, T.A., and G.Menges. (2003). **Materials Science of Polymers for Engineers: Chapter 2 Mechanical behavior of polymer**. Hanser Publishers. Munich. 28-41.
- Owen, R.W., Giacosa, A., Hull, W.E., Haubner, R., Würtele, G., Spiegelhalder, B., Bartsch, H. (2000). Oliveoil consumption and health: the possible role of antioxidants. **The Lancet Oncology**. 1: 107-112.
- Özkaya, N., Nordin, M., Goldsheyder, D., Leger, D (2012). **Fundamentals of Biomechanics: Equilibrium, Motion, and Deformation**. Springer Science, Business Media, LLC.
- Packhaeuser, C.B., Schnieders, J., Oster, C.G., Kissel, T. (2004). *In situ* forming parenteral drug delivery systems: an overview. **European Journal of Pharmaceutics and Biopharmaceutics**. 58: 445-455.
- Pahwa, R., Piplani, M., Garg, V.K., Rao, R., Lamba, H.S., (2011). Formulation and evaluation of orally disintegrating tablets: comparison of natural and synthetic superdisintegrants. **Der Pharmacia Lettre Journal**. 3 (2): 407-418.
- Paiva, J. M. F., Frollini, E. (2006). Unmodified and modified surface sisal fibers as reinforcement of phenolic and lignophenolic matrices composites: thermal analyses of fibers and composites. **Macromolecular Materials and Engineering**. 291: 417.
- Pal, R. (1997). Viscosity and storage/loss moduli for mixtures of fine and coarse emulsions. **Chemical Engineering Journal**. 67: 37.
- Pandit, N.K. (2007). **Introduction to the Pharmaceutical Sciences: Basic principles**. Lippincott Williams & Wilkins. 18.
- Parent, M., Nouvel, C., Koerber, M., Sapin, A., Maincent, P., Boudier, A. (2013). PLGA *in situ* implant formed by phase inversion: critical physicochemical parameters to modulate drug release. **Journal of Controlled Release**. 172: 292-304.
- Patel, H.R., Patel, R.B., Patel, G.N., Patel, M.M. (2010). The influence and compatibility of vegetable oils and other additives on release of ketoprofen from transdermal films. **East and Central African Journal of Pharmaceutical Sciences**. 13: 19-24
- Patil, H.M., Sawant, D.K., Bhavsar, D.S., Patil, J.H., Girase, K.D. (2012). FTIR and thermal studies on gel grown neodymium tartrate crystals. **Journal of Thermal Analysis and Calorimetry**. 107: 1031-1037.



- Perioli, L., Ambrogi, V., Rubini, D., Giovagnoli, S., Ricci, M., Blasi, P., Rossi, C. (2004). Novel mucoadhesive buccal formulation containing metronidazole for the treatment of periodontal disease. **Journal of Controlled Release**. 95 (3): 521-533.
- Petrucci, R.H., Herring, F.G., Madura, J.D., Bissonnette, C. (2007). **General Chemistry: Principles & Modern Applications**. 9th ed. Upper Saddle River, New Jersey. Pearson/Prentice Hall.
- Phaechamud, T., Mahadlek, J. (2015). Solvent exchange-induced *in situ* forming gel comprising ethyl cellulose-antimicrobial drugs. **International Journal of Pharmaceutics**. 494: 381-392.
- Phaechamud, T., Mahadlek, J., Chuenbarn, T. (2016). *In situ* forming gel comprising bleached shellac loaded with antimicrobial drugs for periodontitis treatment. **Materials & design**. 89: 294-303.
- Pichot R. (2010). **Stability and characterisation of emulsions in the presence of colloidal particles and surfactants**. A thesis submitted to The University of Birmingham for the degree of doctor of philosophy. 219.
- Pihlstrom, B. (2001). Periodontal risk assessment, diagnosis and treatment planning. **Journal of Periodontology**. 25: 37-58.
- Polson, A.M., Garrett, S., Stoller, G.H., Bandit, C.L., Hanes, P.J. et al. (2008). Multi-center comparative evaluation of sublingually delivered sanguinarine and doxycycline in the treatment of periodontitis II. Clinical results. **Journal of Periodontology**. 68: 119-126.
- Pragati, S, Ashok, S., Kuldeep, S. (2009). Review recent advances in periodontal drug delivery systems. **International Journal of Drug Delivery**. 1: 1-14
- Questel, J.Y.L., Laurence, C., Lachkar, A., Helbert, M., Berthelot, M. (1992). Hydrogen-bond basicity of secondary and tertiary amides, carbamates, ureas and lactams. **Journal of the Chemical Society, Perkin Transactions**. 2: 2091-2094.
- Rachakonda, V.K., Terramsetty, K.M., Madihally, S.V., Robinson, R.L., Gasem, K.A. (2008). Screening of chemical penetration enhancers for transdermal drug delivery using electrical resistance of skin. **Pharmaceutical Research**. 25: 2697-2704.
- Ramesh, P.J., Basavaiah, K., Tharpa, K., Vinay, K.B., Revanasiddappa, H.D. (2010). Development and validation of RP-HPLC method for the determination of doxycycline hyclate in spiked human urine and pharmaceuticals. **Journal of Pre-Clinical and Clinical Research**. 4: 101-107.
- Ravve, A. (2012). **Principles of Polymer Chemistry, Second Edition: Degradation in polymer**. Springer Science & Business Media. 9: 581-618.
- Renvert, S., Lessem, J., Dahle, N.G., Lindahl, C., Svensson, M. (2006). Topical minocycline microspheres versus topical chlorhexidine gel as an adjunct to mechanical debridement of incipient periimplant infections: a randomized clinical trial. **Journal of Clinical Periodontology**. 33: 362-369.

- Reynolds, J.E.F. (2007). **Martindale the Extra Pharmacopoeia**. 35th ed. London: Pharmaceutical Press.
- Riesen, R., Schawe, J.E.K. (2000). DSC curves: dynamic measurement. **Journal of Thermal Analysis and Calorimetry**. 59: 337-358.
- Roda, A., Magliulo, Mo., Nanni, P., Baraldini, M., Poda, G., et al. (2007). A new oral formulation for the release of sodium butyrate in the illeo-cecal region and colon. **World Journal of Gastroenterology**. 13: 1079-1084.
- Rovi Pharmaceuticals. (2011). **Prolonged release injectable formulations**. [Homepage on the internet]. [Http://www.rovi.es/id\\_formulaciones\\_english.html](http://www.rovi.es/id_formulaciones_english.html). Accessed 10 April 2016.
- Royals, M.A., Fujita, S.M., Yewey, G.L., Rodriguez, J., Chultheiss, P.C., Dunn, R.L. (1999). Biocompatibility of biodegradable *in situ* forming implant system in rhesus monkeys. **Journal of Biomedical Materials Research**. 45: 231-239.
- Rungseevijitprapa, W., Bodmeier, R. (2009). Injectability of bidegradable *in situ* forming microparticle systems (ISM). **European Journal of Pharmaceutical Sciences**. 36 (4-5): 524-531.
- Saltzman, W.M. (2001). **Drug Delivery: Engineering Principles for Drug Therapy; Controlled drug delivery system**. Oxford University Press. 384.
- Samprovalaki, K., Robbins, P.T., Fryer, P.J. (2012). Investigation of the diffusion of dyes in agar gels. **Journal of Food Engineering**. 111: 537-545.
- Sander, C., Holm, P. (2009). Porous magnesium aluminometasilicate tablets as carrier of a cyclosporine self-emulsifying formulation. **AAPS PharmSciTech**. 10 (4): 1388-95.
- Sanghvi, R., Narazaki, R., Machatha, S.G., Yalkowsky, S.H. (2008). Solubility improvement of drugs using N-methyl pyrrolidone. **AAPS PharmSciTech**. 9: 366-376.
- Sangster, J. (1997). **Octanol-Water Partition Coefficients: Fundamentals and Physical Chemistry**. John Wiley & Sons, Inc. United State.
- Sasaki, H., Kojima, M., Mori, Y., Nakamura, J., Shibasaki, J. (1988). Enhancing effect of pyrrolidone derivatives on transdermal delivery. **International Journal of Pharmaceutics**. 44 (1-2): 15-42.
- Sasaki, H., Kojima, M., Nakamura, J., Shibasaki, J. (1990). Acute toxicity and skin irritation of pyrrolidone deivatives as transdermal penetration enhancers. **Chemical and Pharmaceutical Bulletin**. 38 (8): 2308-2310.
- Sato, Y., Oba, T., Watanabe, N., Danjo, K. (2012). Development of formulation device for periodontal disease. **Drug Development and Industrial Pharmacy**. 38 (1): 32-39.

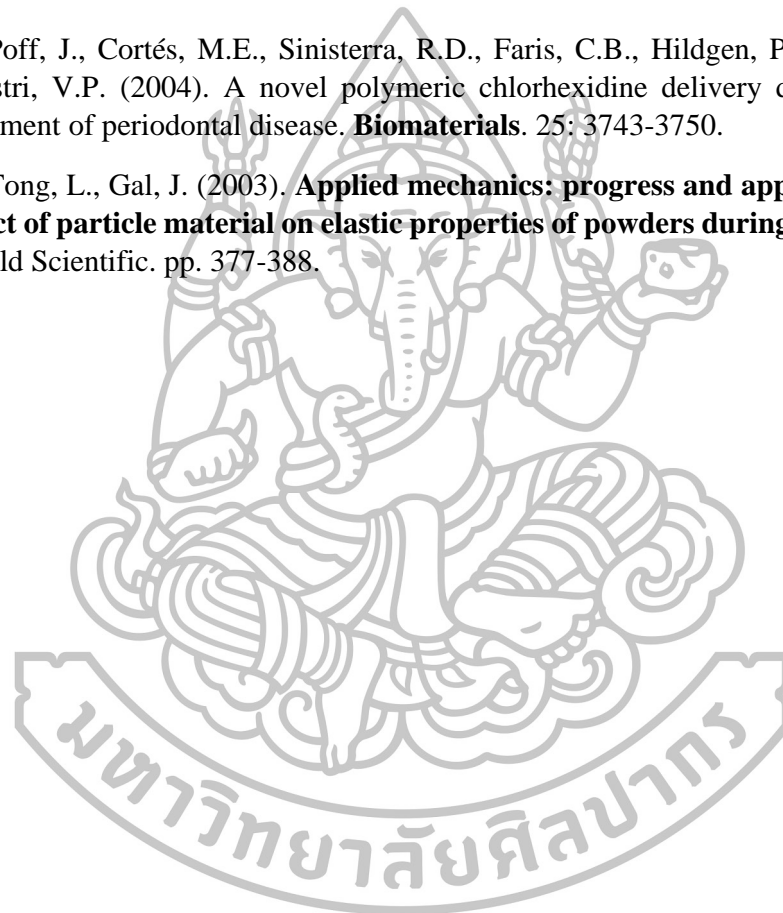
- Sbordone, L., Ramaglia, L., Gulletta, J. (1990). Recolonization of subgingival microflora after scaling and root planning in human periodontitis. **Journal of Periodontology**. 61: 579-584.
- Scheirs, J. (2000). **Compositional and Failure Analysis of Polymers: A Practical Approach; Practical polymer analysis**. John Wiley & Sons. 122.
- Schwach-Abdellaoui, K., Vivien-Casioni, N., Gurny, R. (2000). Local delivery of antimicrobial agents for the treatment of periodontal disease. **European Journal of Pharmaceutics and Biopharmaceutics**. 50: 83-99.
- Setthajindalert, O. (2013). **Preparation of *in situ* forming microparticles and gels as drug controlled release system for periodontitis treatment**. Master thesis. Pharmaceutical sciences, Graduate school, Silpakorn University.
- Seymour, R.A., Heasman, P.A. (1995). Tetracyclines in the management of periodontal diseases. A review. **Journal of Clinical Periodontology**. 22 (1): 22-35.
- Seymour, R.A., Heasman, P.A. (1995). Pharmacological control of periodontal disease. II. Antimicrobial agents. **Journal of Dentistry**. 23: 5-14.
- Shariati, S., Yamini, Y., Esrafil, A. (2009). Carrier mediated hollow fiber liquid phase microextraction combined with HPLC-UV for preconcentration and determination of some tetracycline antibiotics. **Journal of Chromatography B**. 877: 393-400.
- Sherman, P. (1983). **In Encyclopedia of Emulsion Technology**. P. Becher, ed. Marcel Dekker Inc., NY. 405-437.
- Shoaib, H.M., Tazeen, J., Merchant, A.H., Yousuf, I.R. (2006). Evaluation of drug release kinetics from ibuprofen matrix tablets using HPMC. **Pakistan Journal of Pharmaceutical Sciences**. 19: 119-24.
- Siepmann, J., Siepmann, F. (2008). Mathematical modeling of drug delivery. **International Journal of Pharmaceutics**. 364: 328-343.
- Silva-Boghossian, C.M., Neves, A.B., Resende, F.a.R. (2013). A.P.V. Colombo, suppuration associated bacteria in patients with chronic and aggressive periodontitis. **Journal of Periodontology**. 84: e9-e16.
- Silvina, A., Bravo, M., Lamas, C., Claudio, J. (2002). *In-vitro* studies of diclofenac sodium controlled-release from biopolymeric hydrophilic matrices. **Journal of Pharmaceutical Sciences**. 5: 213-19.
- Singhvi, G., Singh M. (2011). Review: *in-vitro* drug release characterization models. **International Journal of Pharmaceutical Sciences and Drug Research**. 2: 77-84.
- Sjoblom, J. (2005). **Emulsions and Emulsion Stability**. CRC Press. 13: 688.
- Skoog, D.A., Holler, F.J., Nieman, T. (1998). **Principles of Instrumental Analysis** (5 ed.). New York. 805–808.

- Skúlason, S., Ingólfsson, E., Kristmundsdóttir, T. (2003). Development of a simple HPLC method for separation of doxycycline and its degradation products. **Journal of Pharmaceutical and Biomedical Analysis**. 33: 667-672.
- Slots, J., Ting, M. (2000). Systemic antibiotics in the treatment of periodontal disease. **Journal of Periodontology**. 106–176.
- Soboyejo, W. (2005). **Mechanical Properties of Engineered Material: overview of mechanical properties and behaviors**. CRC Press. 1: 1-21.
- Souza M.P.R. (2009). Modeling the thixotropic behavior of structured fluids. **Journal of Non-Newtonian Fluid Mechanics**. 164: 66–75.
- Srichan, T., Phaeamud, T. (2016). Designing solvent exchange-induced *in situ* forming gel from aqueous insoluble polymers as matrix base for periodontitis treatment. **AAPS PharmSciTech**. 1-8.
- Stickley, R.G. (2004). Solubilizing excipients in oral and injectable formulations. **Pharmaceutical Research**. 21: 201-230.
- Stippler, E. (2004). **Biorelevant dissolution test methods to assess bioequivalence of drug products**. Doctoral Thesis, Johann Wolfgang Goethe University, Frankfurt am Main, Germany.
- Stone, L.A., Lorenz, K. (1984). The starch of Amaranthus--Physicochemical properties and functional characteristics. **Starch**. 36:232.
- Tan, C.P., Che, M.Y.B. (2002). Differential scanning calorimetric analysis of palm oil, palm oil based products and coconut oil: effects of scanning rate variation. **Food Chemistry**. 76: 89-102.
- Tcholakova, S., Denkov, N. D., Ivanov, I.B., Campbell, B. (2002). Coalescence in  $\beta$ -lactoglobulin-stabilized emulsions: effects of protein adsorption and drop size. **Langmuir**. 18 (23): 8960-8971.
- Tetteh, G., Khan, A.S., Delaine-Smith, R.M., Reilly, G.C., Rehman, I.U. (2014). Electrospun polyurethane/hydroxyapatite bioactive scaffolds for bone tissue engineering: the role of solvent and hydroxyapatite particles. **Journal of the Mechanical Behavior of Biomedical Materials**. 39: 95-110.
- Thakur, R.R.S., Mcmillan, H.L., Jones, D.S. (2014). Solvent induced phase inversion-based *in situ* forming controlled release drug delivery implants. **Journal of Controlled Release**. 176: 8-23
- Tomasi, C., Jan, L.W. (2004). Locally delivered doxycycline improves the healing following non-surgical periodontal therapy in smokers. **Journal of Clinical Periodontology**. 31: 589-595.
- Valenze, G., Veihelmann, S., Peplies, J., Tichy, D., Roldan-Pareja, M.C., Schlagenhaul, U., Vogel, U. (2009). Microbial changes in periodontitis successfully treated by mechanical plaque removal and systemic amoxicillin and metronidazole. **International Journal of Medical Microbiology**. 299: 427-38.

- Van Oss, C.J., Absolom, D.R., Neumann, A.W. (1980). Applications of net repulsive van der Waals forces between different particles, macromolecules, or biological cells in liquids. **Colloids and Surfaces**. 1 (1): 45–56.
- Vaughan, C. D. (1985). Using solubility parameters in cosmetics formulation. **Journal of the Society of Cosmetic Chemists**. 36: 319-333.
- Vincent, J. (2012). **Structural Biomaterials**. 3rd Ed, Princeton University Press.
- Vintiloui, A., Leroux, J.C. (2008). Organogels and their use in drug delivery-a review. **Journal of Controlled Release**. 125: 179-192.
- Visioli, F., Poli, A., Gall, C. (2002). Antioxidant and other biological activities of phenols from olives and olive oil. **Medicinal Research Reviews**. 22: 65-75.
- Voigt, M. (2011). **Biodegradable Non-aqueous *in situ* Forming Microparticle Drug Delivery Systems**. Doctoral thesis. Fachbereich Biologie, Chemie, Pharmazie der Freien Universität Berlin.
- Voigt, M., Koerber, M., Bodmeier, R. (2012). Improve physical stability and injectability of non-aqueous *in situ* PLGA microparticle forming emulsions. **International Journal of Pharmaceutics**. 434: 251-256.
- Vyas, S.P., Sihorkar V., Mishra, V. (2005). Controlled and targeted drug delivery strategies towards intraperiodontal pocket diseases. **Journal of Clinical Pharmacy and Therapeutics**. 25: 21–42.
- Wahrburg, U., Kratz, M., Cullen, P. (2002). Mediterranean diet, olive oil and health. **European Journal of Lipid Science and Technology**. 104: 698-705.
- Walstra, P. (1993). Principles of emulsion formation. **Chemical Engineering Science**. 48 (2): 333-349.
- Wang, L., Wang, A., Zhao, X., Liu, X., Wang, D. et al. (2012). Design of a long-term antipsychotic *in situ* forming implant and its release control method and mechanism. **International Journal of Pharmaceutics**. 427: 284-292.
- Wang, X., Sui, S., Yan, Y., Zhang, R. (2004). Drug release from injectable depots: two different *in vitro* mechanisms. **Journal of Controlled Release**. 99: 207-216.
- Wang, X., Yu, D.G., Li, X.Y., Bligh, S.W., Williams, G.R. (2015) Electrospun medicated shellac nanofibers for colon-targeted drug delivery. **International Journal of Pharmaceutics**. 490 (1-2): 384-90.
- Wang, Y.X., Chen, L. Y. (2011). Impacts of nanowhisker on formation kinetics and properties of all-cellulose composite gels. **Carbohydrate Polymers**. 83 (4): 1937-1946.
- Ward, M.I., Sweeney, J. (2004). **An introduction to the mechanical properties of solid polymers**. 2nd Ed, John Wiley & Sons.

- Webb, A.N., Hardy, P., Peterkin, M., Lee, O., Shalley, H., Croft, K., *et al.* (2008). Tolerability and safety of olive oil-based lipid emulsion in critically ill neonates: A blinded randomized trial. **Nutrition**. 24: 1057-1064.
- Westrin, B.A. (1991). Diffusion in gels containing immobilised gels. **Biotechnology and Bioengineering**. 38: 439-446.
- Widlak, H. (1999). Physical Properties of Fats, Oils, and Emulsifiers. **The American Oil Chemists Society**. 260.
- William, D., Callister, Jr. (2004). **Materials Science and Engineering – An introduction**. Sixth edition, John Wiley & Sons, Inc.
- Winter, H.H. (1987). Can the gel point of a cross-linking polymer be detected by the  $G'$  -  $G''$  crossover? **Polymer Engineering & Science**. 27: 1698-1702.
- Wischke, C.H., Schwendeman, S.P. (2008). Principles of encapsulating hydrophobic drugs in PLA/PLGA microparticles. **International Journal of Pharmaceutics**. 364: 298-327.
- Witt, C. (2001). Morphological characterization of microspheres, films and implants prepared from poly (lactide-co-glycolide) and ABA triblock copolymers: Is the erosion controlled by degradation, swelling or diffusion? **European Journal of Pharmaceutics and Biopharmaceutics**. 51: 171-181.
- Wolff, L., Dahlen, G., Aeppli, D. Bacteria as risk markers for periodontitis. **Journal of Periodontology**. 65: 498-510.
- Wypych, G. (2004). Handbook of plasticizer; Plasticizer motion and diffusion. **ChemTec Publishing**. 7: 151-152.
- Wyss, H.M., Larsen, R.J., Weitz, D.A. (2007). Oscillatory rheology measuring the viscoelastic behaviour of soft materials. **G.I.T. Laboratory Journal**. 3(4): 68-70.
- Yamada, P., Azrrouk, M., Kawasaki, K., Isoda, H. (2008). Inhibitory effect of various Tunisian olive oils on chemical mediator release and cytokine production by basophilic cells. **Journal of Ethology**. 226 (2): 279-287.
- Yang, H., Nguyen, Q.T., Ding, Y., Long, Y., Ping, Z. (2000). Investigation of poly (dimethyl siloxane) (PDMS)–solvent interactions by DSC. **Journal of Membrane Science**. 164: 37-43.
- Yang, X., Liu, Q., Chen, X., Yu, F., Zhu, Z. (2012). Investigation of PVA/ws-chitosan hydrogels prepared by combined gamma radiation and freeze-thawing. **Carbohydrate Polymers**. 73 (3): 401-408.
- Yi, J.Z., Gao, Y.X., Lee, P.D., Flower, H.M., Lindley, T.C. (2003). Scatter in fatigue life due to effects of porosity in cast A356-T6 aluminum–silicon alloys. **Metallurgical and Materials Transactions**. A 34: 1879-1890.

- Yoe, I.C., Poff, J., Cortes, M.E., Sinisterra, R.D., Faris, C.B., Hildgen, P., Langer, R., Shastri, V.P. (2004). A novel polymeric chlorhexidine device for treatment of periodontal disease. **Biomaterials**. 25 (17): 3743-3750.
- Young, T.H., Chen, L.W. (1995). Pore formation mechanism of membranes from phase inversion process. **Desalination**. 103: 233-247.
- Yu, Z., Ramamurthy, N.S., Leung, M., Chang, K.M., McNamara, T.F., Golub, G.M. (1993). Chemically-modified tetracycline normalizes collagen metabolism in diabetic rat: a dose-response study. **Journal of Periodontal Research**. 28 (6): 420-428.
- Yue, I.C., Poff, J., Cortés, M.E., Sinisterra, R.D., Faris, C.B., Hildgen, P., Langer, R., Shastri, V.P. (2004). A novel polymeric chlorhexidine delivery device for the treatment of periodontal disease. **Biomaterials**. 25: 3743-3750.
- Zhang, L., Tong, L., Gal, J. (2003). **Applied mechanics: progress and applications, the effect of particle material on elastic properties of powders during compaction**. World Scientific. pp. 377-388.





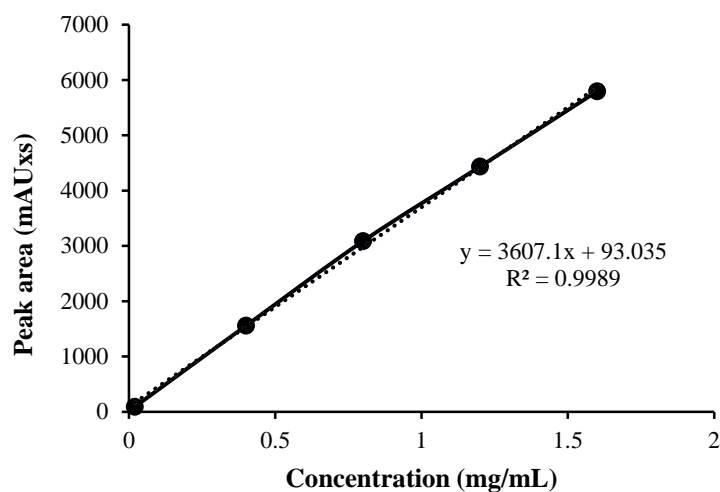
**Appendices**



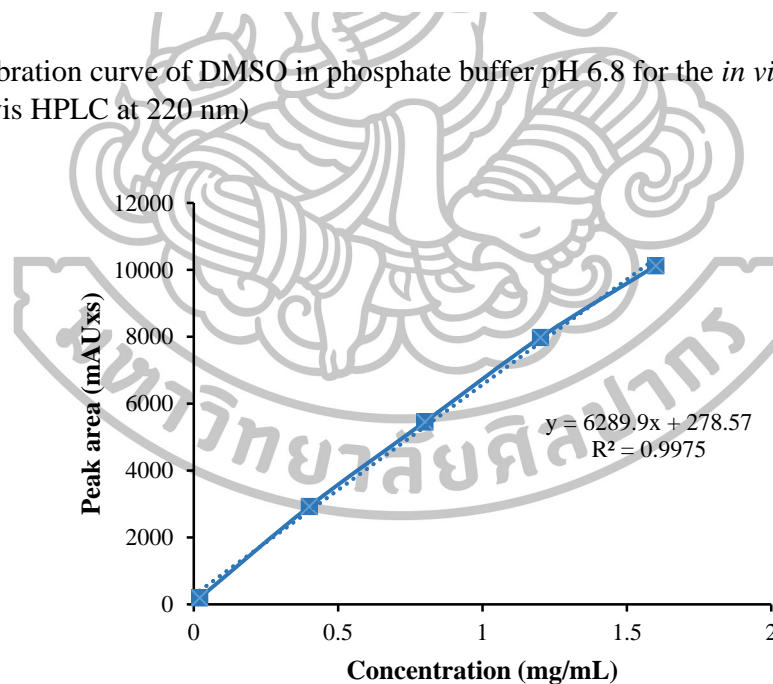
## Appendix I

### HPLC calibration curve for the *in vitro* release study

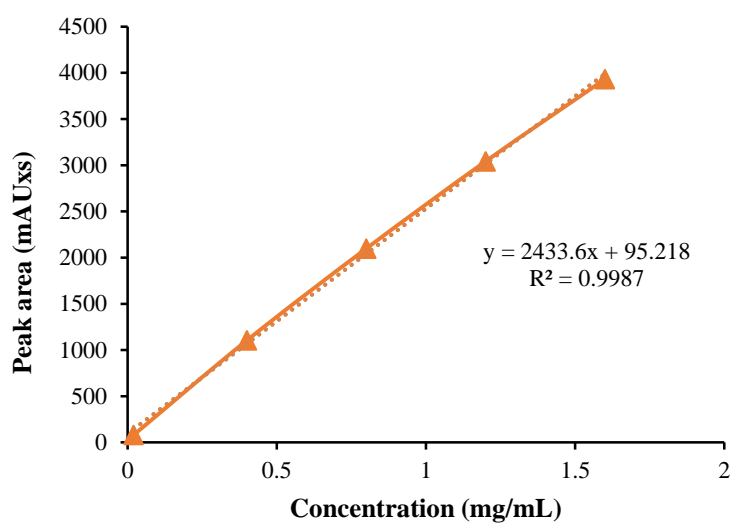
#### 1. Determination of the amount of solvent release



**Fig. 86** Calibration curve of DMSO in phosphate buffer pH 6.8 for the *in vitro* release study (UV-vis HPLC at 220 nm)

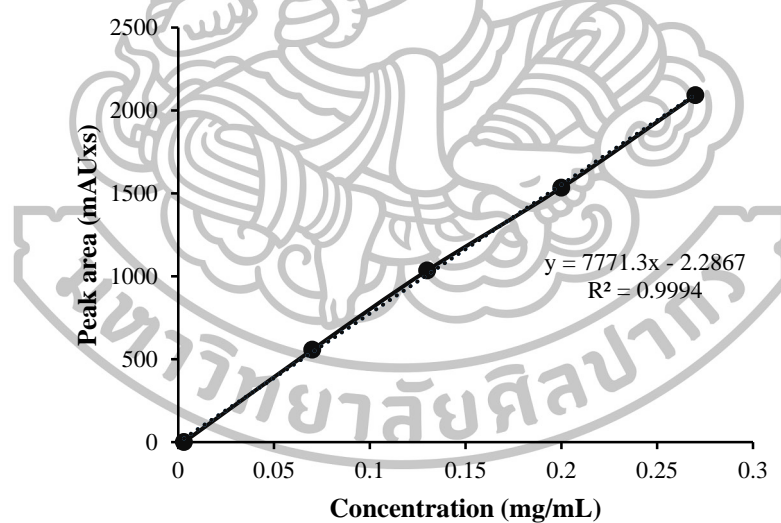


**Fig. 87** Calibration curve of NMP in phosphate buffer pH 6.8 for the *in vitro* release study (UV-vis HPLC at 220 nm)

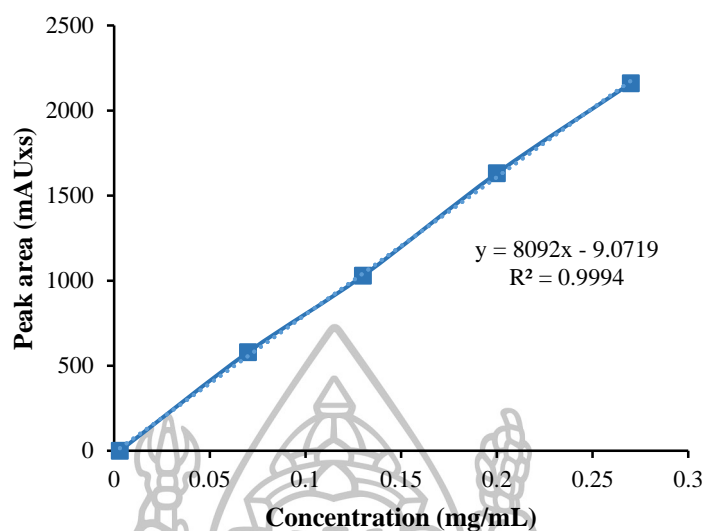


**Fig. 88** Calibration curve of PYR in phosphate buffer pH 6.8 for the *in vitro* release study (UV-vis HPLC at 220 nm)

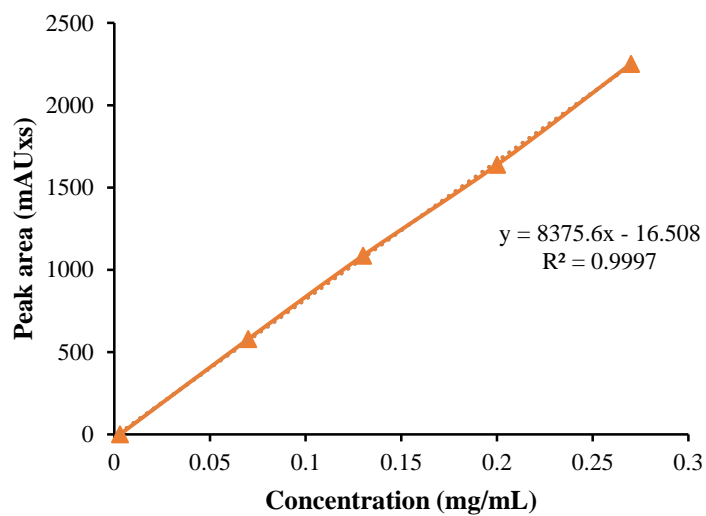
## 2. Determination of the amount of doxycycline release



**Fig. 89** Calibration curve of doxycycline hyclate in DMSO and phosphate buffer pH 6.8 for the *in vitro* release study (UV-vis HPLC at 273 nm)



**Fig. 90** Calibration curve of doxycycline hyclate in NMP and phosphate buffer pH 6.8 for the *in vitro* release study (UV-vis HPLC at 273 nm)



**Fig. 91** Calibration curve of doxycycline hyclate in PYR and phosphate buffer pH 6.8 for the *in vitro* release study (UV-vis HPLC at 273 nm)

## Appendix II

### Evaluation of formulation composition

#### 1. Density

**Table 17** Density of liquid compositions at 25°C (n=3)

Substance	density (g/mL)	
	mean	SD
Water	1.0210	0.0088
Olive oil	0.9398	0.0049
5% GMS / olive oil	0.9406	0.0047
DMSO	1.1332	0.0040
NMP	1.0568	0.0028
PYR	1.1243	0.0090
30% Shellac / DMSO	1.1603	0.0083
30% Shellac / NMP	1.0980	0.0075
30% shellac / PYR	1.1633	0.0019

#### 2. Surface and interfacial tension

**Table 18** Surface tension of different solvents, olive oil and GMS-dispersed olive oil at 25°C (n=3)

Substance	Surface tension (m N/m)	
	mean	SD
Water	72.44	0.56
Olive oil	33.18	0.52
5% GMS / olive oil	33.61	0.09
DMSO	43.71	0.75
NMP	42.00	0.02
PYR	46.57	0.34

**Table 19** Interfacial tension of different solvents in olive oil at 25°C (n=3)

Substance	Interfacial tension (mN/m)	
	mean	SD
Water	15.12	0.20
DMSO	9.56	0.60
NMP	3.08	0.09
PYR	5.03	0.04

### 3. Rate of macroscopic phase separation of emulsion composition

**Table 20** Volume of solvent separation during 24 h at 25°C (n=3)

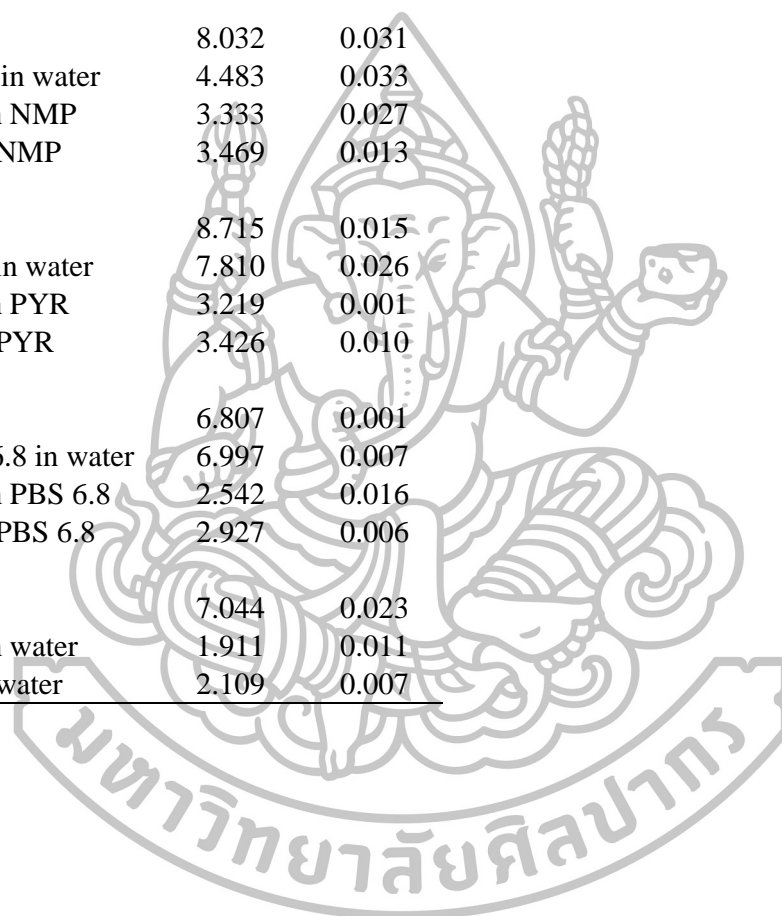
Time (min)	Volume of solvent separation (mL)					
	DMSO : Olive oil		NMP : Olive oil		PYR : Olive	
	mean	SD	mean	SD	mean	SD
0	10.00	0.00	10.00	0.00	10.00	0.00
5	8.07	1.36	3.20	0.00	9.90	0.00
10	7.47	1.75	3.20	0.00	9.87	0.06
15	6.87	2.01	3.20	0.00	9.77	0.06
20	6.60	2.03	3.20	0.00	9.73	0.12
30	6.33	1.72	3.20	0.00	9.60	0.17
40	6.20	1.64	3.20	0.00	9.47	0.23
50	5.93	1.33	3.20	0.00	9.37	0.23
60	5.50	0.70	3.20	0.00	9.27	0.23
90	5.20	0.40	3.20	0.00	9.10	0.26
120	4.87	0.12	3.20	0.00	8.93	0.31
180	4.87	0.12	3.20	0.00	8.40	0.35
240	4.87	0.12	3.20	0.00	7.97	0.40
300	4.87	0.12	3.20	0.00	7.53	0.46
360	4.87	0.12	3.20	0.00	7.07	0.49
480	4.87	0.12	3.20	0.00	6.20	0.61
600	4.87	0.12	3.20	0.00	5.07	0.49
720	4.87	0.12	3.20	0.00	4.50	0.10
1440	4.87	0.12	3.20	0.00	4.50	0.10



#### 4. pH

**Table 21** pH of organic solvents, PBS 6.8, DI water and their solutions at 25°C (n=3)

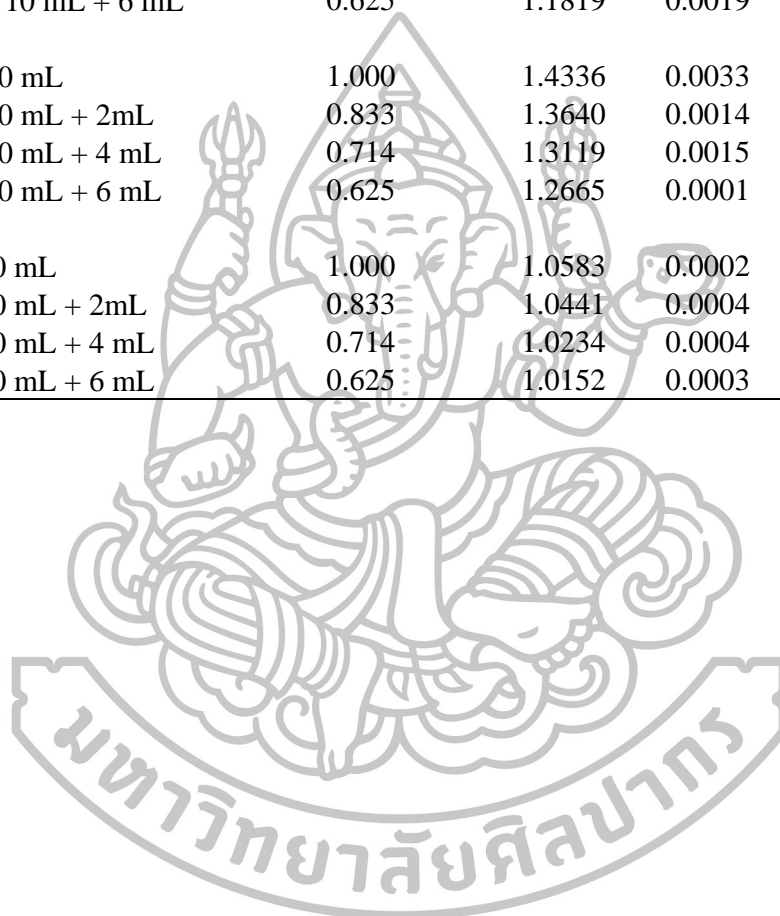
Substance	pH	
	mean	SD
DMSO	6.531	0.019
10% DMSO in water	6.519	0.055
10% DX in DMSO	3.229	0.011
5% DX in DMSO	3.396	0.004
NMP	8.032	0.031
10% NMP in water	4.483	0.033
10% DX in NMP	3.333	0.027
5% DX in NMP	3.469	0.013
PYR	8.715	0.015
10% PYR in water	7.810	0.026
10% DX in PYR	3.219	0.001
5% DX in PYR	3.426	0.010
PBS 6.8	6.807	0.001
10% PBS 6.8 in water	6.997	0.007
10% DX in PBS 6.8	2.542	0.016
5% DX in PBS 6.8	2.927	0.006
water	7.044	0.023
10% DX in water	1.911	0.011
5% DX in water	2.109	0.007



## 5. Relative viscosity

**Table 22** Relative viscosities of diluted bleached shellac (BS) solution in different solvents (n=3)

Substance	Conc. (% g/ml)	Relative viscosities	
		mean	SD
BS-DMSO 10 mL	1.000	1.2925	0.0018
BS-DMSO 10 mL + 2mL	0.833	1.2346	0.0025
BS-DMSO 10 mL + 4 mL	0.714	1.2137	0.0022
BS-DMSO 10 mL + 6 mL	0.625	1.1819	0.0019
BS-NMP 10 mL	1.000	1.4336	0.0033
BS-NMP 10 mL + 2mL	0.833	1.3640	0.0014
BS-NMP 10 mL + 4 mL	0.714	1.3119	0.0015
BS-NMP 10 mL + 6 mL	0.625	1.2665	0.0001
BS-PYR 10 mL	1.000	1.0583	0.0002
BS-PYR 10 mL + 2mL	0.833	1.0441	0.0004
BS-PYR 10 mL + 4 mL	0.714	1.0234	0.0004
BS-PYR 10 mL + 6 mL	0.625	1.0152	0.0003



### Appendix III

#### Evaluation of *in situ* forming systems before exposure to solvent exchange

#### 1. Size of o/o emulsion

**Table 23** Droplet size of o/o emulsion with various concentrations of GMS at phase ratio 1:1 (n=3)

GMS conc. (% w/w)	Droplet size ( $\mu\text{m}$ )	
	mean	SD
0.00	117.86	35.3901
1.25	98.11	21.5220
2.50	84.11	25.8686
3.75	80.31	23.1362
5.00	64.91	16.0881

**Table 24** Droplet size of o/o emulsion at various phase ratios (n=3)

External phase : internal phase	Droplet size ( $\mu\text{m}$ )	
	mean	SD
5:5	95.17	2.1969
6:4	57.24	4.8907
7:3	56.78	2.8533
8:2	31.63	0.9769
9:1	21.27	2.8082

**Table 25** Droplet size of o/o emulsion with constant GMS concentration at various phase ratios (n=3)

External phase : internal phase	Droplet size ( $\mu\text{m}$ )	
	mean	SD
4.75:5	95.25	6.6018
5.75:4	60.28	4.0729
6.75:3	54.43	0.6318
7.75:2	47.33	3.0358
8.75:1	32.07	2.0009



## 2. Appearance viscosity and rheological behavior

### 2.1 Appearance viscosity

**Table 26** Appearance viscosity of solvents at 25°C (n=3)

Substance	Viscosity (cps)	
	mean	SD
DMSO	3.02	0.08
NMP	3.44	0.11
PYR	14.03	0.13
Olive oil	76.05	0.95
GMS dispersion	135.75	0.61

**Table 27** Appearance viscosity of bleached shellac solutions at 25°C (n=3)

<i>In situ</i> forming gels	Viscosity (cps)	
	mean	SD
DMSO gel	124.36	4.00
NMP gel	108.48	2.00
PYR gel	275.43	7.06
DXDM gel	1281.78	35.64
DXN gel	515.94	15.90
DXP gel	3192.68	19.22

**Table 28** Appearance viscosity of ISMs at 25°C (n=3)

ISM	Viscosity (cps)	
	mean	SD
DMSO ism	184.42	2.42
PYR ism	236.54	4.83
DXDM ism	346.34	14.30
DXP ism	363.01	4.51

## Appendix VI

### Evaluation of *in situ* forming systems during exposure to solvent exchange

#### 1. *In vitro* solvent and drug release

##### 1.1 *In vitro* solvent release

**Table 29** Release of DMSO, NMP and PYR from *in situ* forming gels in PBS pH 6.8 within 21 days (n=3)

Time (day)	Solvent release (%)					
	DMSO		NMP		PYR	
	mean	SD	mean	SD	mean	SD
0	4.89	2.37	3.20	1.58	2.52	0.18
0.01	23.89	1.84	8.15	2.43	4.30	0.18
0.02	32.82	4.07	11.63	1.76	6.26	0.61
0.04	38.29	6.58	14.15	1.55	8.11	2.20
0.08	51.11	7.22	21.68	1.38	13.08	2.91
0.17	60.48	5.39	31.09	2.22	19.60	6.54
0.25	65.05	8.84	47.28	9.75	27.28	2.31
0.33	66.62	8.17	59.50	13.62	30.98	3.20
1	81.24	1.69	84.88	1.62	65.02	9.75
2	87.22	2.87	90.44	1.57	88.55	11.33
3	92.82	1.51	93.70	2.46	89.81	4.71
5	96.77	0.44	97.07	5.03	93.35	2.70
7	100.00	0.95	98.21	4.29	96.58	1.01
14	100.00	2.08	100.00	1.88	99.31	1.69
21	100.00	2.81	100.00	1.97	100.00	0.69
28	100.00	2.49	100.00	2.52	100.00	5.17
35	100.00	2.79	100.00	1.58	100.00	6.27

**Table 30** Release of DMSO, NMP and PYR from *in situ* forming microparticles in PBS pH 6.8 within 21 days (n=3)

Time (day)	Solvent release (%)			
	DMSO		PYR	
	mean	SD	mean	SD
0	2.14	0.37	2.20	0.65
0.01	14.86	0.91	5.73	2.25
0.02	19.16	0.50	7.52	1.21
0.04	22.87	1.05	13.76	4.12
0.08	28.40	1.13	15.36	6.68
0.17	33.42	1.57	28.94	6.86
0.25	40.88	3.75	34.10	6.01
0.33	45.37	4.21	41.33	6.75
1	68.53	7.45	64.94	1.65
2	79.35	10.67	82.17	8.22
3	85.41	9.75	89.16	7.79
5	91.61	10.69	93.65	9.05
7	96.31	11.06	96.95	10.78
14	100.00	9.89	100.00	9.14
21	100.00	7.24	100.00	2.54
28	100.00	7.59	100.00	3.04
35	100.00	7.29	100.00	5.93



## 1.2 *In vitro* drug release

**Table 31** Drug release from *in situ* forming gels in PBS pH 6.8 within 21 days

Time (day)	Drug release (%)					
	DMSO		NMP		PYR	
	mean	SD	mean	SD	mean	SD
0	1.55	0.75	0.57	0.08	0.88	0.10
0.01	7.17	0.55	2.30	0.39	2.09	0.11
0.02	11.29	1.47	3.36	0.31	2.45	0.18
0.04	18.72	2.18	4.10	0.33	2.68	0.25
0.08	30.18	1.63	11.51	0.79	3.83	0.48
0.17	42.68	0.52	15.20	0.75	5.27	0.82
0.25	53.41	5.19	23.48	2.82	7.70	1.07
0.33	54.54	2.78	33.31	5.11	9.44	1.06
1	73.25	2.20	63.84	3.25	34.52	3.89
2	78.37	4.69	68.11	3.03	67.99	11.10
3	78.77	3.31	69.31	3.29	80.92	7.19
5	78.77	1.96	69.31	1.64	81.44	4.37
7	78.77	1.29	69.31	2.21	81.44	1.17
14	78.77	1.54	69.31	6.26	81.44	2.43
21	78.77	1.62	69.31	3.03	81.44	2.45
28	78.77	3.18	69.31	1.42	81.44	2.02
35	78.77	9.06	69.31	2.12	81.44	2.08



**Table 32** Drug release from *in situ* forming microparticles in PBS pH 6.8 within 21 days (n=3)

Time (day)	Drug release (%)			
	DMSO		PYR	
	mean	SD	mean	SD
0	1.89	0.37	1.80	0.44
0.01	7.22	0.91	4.60	0.47
0.02	10.43	0.50	4.78	0.56
0.04	16.90	1.05	6.62	1.00
0.08	20.89	1.13	9.37	2.06
0.17	24.26	1.57	15.89	2.38
0.25	31.12	3.75	16.05	2.99
0.33	35.20	4.21	19.61	2.78
1	54.39	7.45	36.01	3.23
2	66.32	10.67	52.47	3.92
3	73.75	9.75	62.74	5.45
5	84.21	10.69	76.96	7.12
7	90.82	11.06	86.95	8.41
14	100.00	9.89	98.18	6.70
21	100.00	7.24	100.00	4.08
28	100.00	7.59	100.00	3.12
35	100.00	7.29	100.00	2.51

## 2. *In vitro* degradability

**Table 33** Dynamic change in total mass of *in situ* forming gels (n=3)

Time (day)	Total mass loss (%)					
	DXDM gel		DXN gel		DXP gel	
	mean	SD	mean	SD	mean	SD
0	0.00	0.00	0.00	0.00	0.00	0.00
1	56.53	0.61	53.97	1.80	47.36	2.79
2	59.24	1.84	58.34	2.47	56.28	3.36
3	65.11	2.67	64.92	2.83	70.80	1.25
5	69.54	0.99	68.29	3.04	73.68	4.26
7	71.18	0.44	71.38	0.80	77.03	2.78
14	73.79	1.15	77.00	2.25	84.46	3.68
45	75.77	1.61	80.19	1.01	93.54	1.50

**Table 34** Dynamic change in mass of bleached shellac from *in situ* forming gels (n=3)

Time (day)	BS mass loss (%)					
	DXDM gel		DXN gel		DXP gel	
	mean	SD	mean	SD	mean	SD
0	0.00	0.00	0.00	0.00	0.00	0.00
1	0.26	0.12	0.79	0.21	5.73	1.60
2	0.38	0.08	1.34	0.36	7.17	0.33
3	0.43	0.43	2.56	0.28	26.47	2.42
5	0.66	0.26	3.59	0.12	39.79	5.34
7	1.44	0.20	4.81	0.24	61.10	4.73
14	9.45	1.39	15.07	0.37	71.63	2.68
45	27.99	1.91	35.19	1.54	83.31	2.66

**Table 35** Dynamic change in water content of *in situ* forming gels (n=3)

Time (day)	Water content (%)					
	DXDM gel		DXN gel		DXP gel	
	mean	SD	mean	SD	mean	SD
0	0.00	0.00	0.00	0.00	0.00	0.00
1	145.89	12.73	173.09	11.15	203.14	11.10
2	196.51	7.61	220.49	3.28	238.38	15.01
3	229.98	13.15	258.31	12.81	358.24	13.60
5	281.04	18.62	375.04	10.24	563.38	20.24
7	330.36	18.42	429.04	22.80	733.24	23.32
14	417.70	14.55	524.27	17.26	911.18	17.68
45	645.61	8.76	724.84	10.57	1531.84	25.57

**Table 36** Dynamic change in total mass of *in situ* forming microparticles (n=3)

Time (day)	Total mass loss (%)			
	DXDM ism		DXP ism	
	mean	SD	mean	SD
0	0.00	0.00	0.00	0.00
1	18.88	1.34	15.14	0.89
2	22.81	1.53	17.34	2.25
3	27.85	1.84	23.14	2.69
5	30.52	0.69	28.01	1.57
7	32.25	1.82	37.19	3.50
14	36.54	2.54	48.05	0.84
45	58.10	2.20	75.78	4.54

**Table 37** Dynamic change in mass of bleached shellac from *in situ* forming microparticles (n=3)

Time (day)	BS mass loss (%)			
	DXDM ism		DXP ism	
	mean	SD	mean	SD
0	0.00	0.00	0.00	0.00
1	0.00	0.00	1.87	0.69
2	1.34	0.11	5.02	1.92
3	2.57	1.15	32.20	1.34
5	5.08	1.21	44.45	1.51
7	9.29	1.11	53.45	3.22
14	14.55	2.37	57.22	2.62
45	23.94	1.49	71.58	2.16

**Table 38** Dynamic change in water content of *in situ* forming microparticles (n=3)

Time (day)	Water content (%)			
	DXDM ism		DXP ism	
	mean	SD	mean	SD
0	0.00	0.00	0.00	0.00
1	143.56	11.04	177.27	26.71
2	167.01	30.63	243.30	38.49
3	190.48	49.42	252.89	53.52
5	230.80	26.62	284.80	9.64
7	264.35	6.14	323.07	40.59
14	315.62	11.75	429.69	35.11
45	379.43	31.22	558.03	28.37

### 3. Rate of water diffusion into *in situ* forming systems

**Table 39** Water diffusion of *in situ* forming gels (n=3)

Time (day)	Water font (mm)					
	DMSO gel		NMP gel		PYR gel	
	mean	SD	mean	SD	mean	SD
0	0.00	0.00	0.00	0.00	0.00	0.00
0.01	0.83	0.29	0.53	0.45	0.23	0.12
0.02	1.27	0.25	0.53	0.45	0.23	0.12
0.04	1.67	0.29	0.53	0.45	0.37	0.12
0.08	2.17	0.29	0.60	0.36	0.60	0.36
0.17	3.17	0.76	1.17	0.76	0.67	0.29
0.33	4.00	1.00	2.00	1.00	1.17	0.29
1	8.00	0.00	4.67	0.58	3.67	1.15
2	18.00	1.00	9.67	1.53	5.67	1.15
3	27.00	1.73	16.00	1.00	8.67	1.15
4	30.00	0.00	24.00	1.00	11.00	0.87
5	30.00	0.00	30.00	0.00	11.50	0.50

Time (day)	Water font (mm)					
	DXDM gel		DXN gel		DXP gel	
	mean	SD	mean	SD	mean	SD
0	0.00	0.00	0.00	0.00	0.00	0.00
0.01	0.50	0.00	0.23	0.23	0.10	0.00
0.02	0.67	0.29	0.50	0.00	0.43	0.12
0.04	1.00	0.00	0.67	0.29	0.50	0.00
0.08	1.33	0.29	0.67	0.29	0.50	0.00
0.17	1.83	0.29	1.00	0.00	0.50	0.00
0.33	2.00	0.00	1.50	0.00	0.70	0.00
1	3.00	0.00	2.00	0.00	1.00	0.00
2	5.00	0.00	4.33	0.58	2.67	0.58
3	7.00	1.00	6.00	1.00	4.33	0.58
4	8.67	0.58	7.00	1.00	5.00	0.87
5	8.67	0.58	7.00	1.00	5.00	0.87



**Table 40** Water diffusion of *in situ* forming microparticles (n=3)

Time (day)	Water font (mm)							
	DMSO ism		PYR ism		DXDM ism		DXP ism	
	mean	SD	mean	SD	mean	SD	mean	SD
0	0.00	0.00	0.00	0.00	0.00	0.00	0.00	0.00
0.01	0.17	0.29	0.00	0.00	0.00	0.00	0.00	0.00
0.02	0.50	0.00	0.33	0.29	0.00	0.00	0.00	0.00
0.04	1.00	0.00	1.00	0.00	0.10	0.00	0.03	0.06
0.08	2.33	0.58	1.67	0.58	0.57	0.40	0.07	0.06
0.17	3.67	0.58	2.67	1.53	1.33	0.58	0.10	0.00
0.33	5.67	0.58	4.00	1.00	2.17	0.29	0.50	0.00
1	8.67	1.53	5.67	1.53	4.67	1.53	2.33	0.58
2	11.67	1.53	8.00	1.00	6.33	2.08	2.33	0.58
3	17.00	1.00	9.33	1.15	8.00	2.65	3.33	0.58
4	20.00	1.00	10.50	1.50	10.00	2.65	4.17	0.76
5	21.00	2.65	11.00	1.73	10.00	2.65	4.17	0.76

#### 4. Solvent diffusion

**Table 41** Solvent diffusion distance of *in situ* forming gels prepared with different solvents (n=3)

Time (min)	Solvent font (mm)					
	DMSO gel		NMP gel		PYR gel	
	mean	SD	mean	SD	mean	SD
5	0.98	0.10	0.91	0.12	0.83	0.20
10	1.37	0.14	1.26	0.14	1.23	0.29
15	1.68	0.13	1.54	0.18	1.47	0.36
20	1.96	0.12	1.78	0.22	1.69	0.37
25	2.11	0.19	1.95	0.23	1.91	0.37
30	2.32	0.20	2.14	0.20	2.09	0.47

**Table 42** Solvent diffusion rate of *in situ* forming gels prepared with different solvents (n=3)

Time (min)	Diffusion rate (mm/min)					
	DMSO gel		NMP gel		PYR gel	
	mean	SD	mean	SD	mean	SD
5	0.20	0.02	0.18	0.02	0.17	0.04
10	0.14	0.01	0.13	0.01	0.12	0.03
15	0.11	0.01	0.10	0.01	0.10	0.02
20	0.10	0.01	0.09	0.01	0.08	0.02
25	0.08	0.01	0.08	0.01	0.08	0.01
30	0.08	0.01	0.07	0.01	0.07	0.02

**Table 43** Solvent diffusion distance of *in situ* forming microparticles prepared with different solvents (n=3)

Time (min)	Solvent font (mm)			
	DMSO ism		PYR ism	
	mean	SD	mean	SD
5	1.11	0.21	1.08	0.15
10	1.57	0.23	1.37	0.13
15	1.84	0.15	1.72	0.00
20	2.07	0.17	1.89	0.05
25	2.33	0.16	2.06	0.07
30	2.55	0.15	2.19	0.05

**Table 44** Solvent diffusion rate of *in situ* forming microparticles prepared with different solvents (n=3)

Time (min)	Diffusion rate (mm/min)			
	DMSO ism		PYR ism	
	mean	SD	mean	SD
5	0.22	0.04	0.22	0.03
10	0.16	0.02	0.14	0.01
15	0.12	0.01	0.11	0.00
20	0.10	0.01	0.09	0.00
25	0.09	0.01	0.08	0.00
30	0.08	0.00	0.07	0.00



## Appendix V

### Evaluation of *in situ* forming systems after exposure to solvent exchange

#### 1. Mechanical property studies

**Table 45** Maximum deformation force or hardness of *in situ* forming gels (n=6)

<i>In situ</i> forming gel	Hardness (N)	
	mean	SD
DMSO gel	2.632	0.211
NMP gel	3.091	0.439
PYR gel	4.925	0.783
DXDM gel	4.014	0.915
DXN gel	3.961	0.315
DXP gel	0.000	0.000

**Table 46** Ratio of remaining force/maximum deformation force or ratio of elasticity/plasticity of *in situ* forming gels (n=6)

<i>In situ</i> forming gel	F remaining / F max deformation	
	mean	SD
DMSO gel	0.030	0.007
NMP gel	0.043	0.036
PYR gel	0.678	0.052
DXDM gel	0.527	0.111
DXN gel	0.317	0.086
DXP gel	0.000	0.000

**Table 47** Maximum deformation force or hardness of *in situ* forming microparticles (n=6)

ISM	Hardness (N)	
	mean	SD
DMSO ism	0.219	0.075
PYR ism	1.732	0.428
DXDM ism	0.217	0.067
DXP ism	0.000	0.000

**Table 48** Ratio of remaining force/maximum deformation force or ratio of elasticity/plasticity of *in situ* forming microparticles (n=6)

ISM	F remaining / F max deformation	
	mean	SD
DMSO ism	0.169	0.058
PYR ism	0.852	0.240
DXDM ism	0.137	0.023
DXP ism	0.000	0.000

## Biography

**Name** Pitsiree Praphanwittaya, Miss

**Date of Birth** March 26, 1990

**Place of Birth** Ratchaburi, Thailand

**Nationality/Religion** Thai/Buddhism

**E-mail address** [barondesperado@hotmail.com](mailto:barondesperado@hotmail.com)

### Education

- |           |   |
|-----------|---|
| 2013-2016 | Master of Pharmacy, Pharmaceutical Sciences<br>Silpakorn Univeristy, Thailand |
| 2008-2012 | Bachelor of Pharmacy<br>Silpakorn University, Thailand                        |

### Publications

1. **Pitsiree Praphanwittaya** and Thawatchai Phaechemud. 2015. Bleached Shellac as Potential Polymeric Matrix for *In Situ* Microparticle (ISM). *Key engineering materials*. 659: 8-12.

### Presentation (Oral)

1. **Pitsiree Praphanwittaya** and Thawatchai Phaechemud. 2014. Bleached Shellac as Potential Polymeric Matrix for *In Situ* Microparticle (ISM). *The 8th International Conference on Materials Science and Technology (MSAT-8)*, National Metal and Materials Technology Center (MTEC), Swissotel Le Concorde, Bangkok, Thailand, 15-16 December 2014. (oral)